Dissertation

Quarklets: Construction and Application in Adaptive Frame Methods

Philipp Keding

2018

Quarklets: Construction and Application in Adaptive Frame Methods

Dissertation
zur
Erlangung des Doktorgrades
der Naturwissenschaften
(Dr. rer. nat.)

dem
Fachbereich Mathematik und Informatik
der Philipps-Universität Marburg
vorgelegt von

M. Sc. Philipp Keding
aus Marburg

Marburg 2018

Vom Fachbereich Mathematik und Informatik
der Philipps-Universität Marburg (Hochschulkennziffer 1180)
als Dissertation angenommen am: 27.08.2018

Erstgutachter: Prof. Dr. Stephan Dahlke, Philipps-Universität Marburg

Zweitgutachter: Prof. Dr. Thorsten Raasch, Universität Siegen

Tag der Einreichung: 29.06.2018
Tag der mündlichen Prüfung: 24.09.2018

Acknowledgements

I would like to express my deep gratitude to my advisor, Prof Dr. Stephan Dahlke, for giving me the opportunity to become a PhD student in his work group. I thank him for his guidance, plenty of useful advices and his continuous support. That he encouraged me to attend various conferences, get in touch with some of the world leading experts in their respective fields and present my work there was of great benefit for me. In particular, I am very thankful that he paved the way for me to a scholarship from the Philipps-University Marburg.

I would also like to thank Prof Dr. Thorsten Raasch for being the second referee and his cooperation. Thanks a lot for inviting me to Mainz to work on the finalization of the first paper.

Furthermore, I would like to thank Dr. Ulrich Friedrich for his willingness to collaborate and to provide his valuable expertise.

Moreover, I am grateful to all of my former and current colleagues in the AG Numerik. Thank you for the nice and friendly atmosphere, the many diverting conversations during daily lunch and coffee breaks and the occasional joint cultural activities. Especially, I would like to thank Alexander Sieber for numerous hours of working together on the further development of quarklets and the open source code. His great ideas contributed a lot to the project.

In addition, I would like to express my thankfulness to my family and friends who always supported me and kept me distracted from mathematics whenever necessary.

Last but not least, I would like to thank you, Bärbel, for all your love and support and for making my life so wonderful.

Zusammenfassung

Die Modellierung von vielen bekannten Problemen der Naturwissenschaften und auch anderer Wissenschaftszweige führt auf *partielle Differentialgleichungen*. Diese lassen sich auch als Operatorgleichungen

$$\mathcal{L}u = f$$

formulieren und unter funktionalanalytischen Gesichtspunkten betrachten. Da eine exakte Lösung von Operatorgleichungen oft nicht zu realisieren ist, besteht der Bedarf nach praktikablen numerischen Verfahren zur näherungsweisen Lösung selbiger. In den letzten Jahren und Jahrzehnten gab es ein ganzes Füllhorn von Neuentwicklungen immer ausgefeilterer Algorithmen, welche, begünstigt durch die Rechenkraft und Speicherkapazität von modernen Computern, in die Praxis umgesetzt werden konnten. Unter mathematischen Gesichtspunkten spielt die theoretische Untersuchung, das heißt der Nachweis von Konvergenz und Konvergenzraten der Algorithmen, eine ebenso große Rolle wie die praktische Realisierung. In dieser Arbeit beschäftigen wir uns mit der Konstruktion von Quarklet-Frames und deren Anwendung zur numerischen Lösung von Operatorgleichungen. Hierbei beschränken wir uns auf die Klasse *elliptischer* Operatorgleichungen, das heißt wir gehen davon aus, dass für den Operator $\mathcal{L} : H \to H'$ von einem Hilbertraum H in seinen Dualraum H' die Elliptizitätsbedingung $C_1||v||_H \leq ||\mathcal{L}v||_{H'} \leq C_2||v||_H$, $v \in H$, mit Konstanten $C_1, C_2 > 0$, erfüllt ist. Dies garantiert eine eindeutige Lösung der Operatorgleichung. In der Regel ist H hierbei ein *Sobolevraum* auf einem Gebiet $\Omega \subset \mathbb{R}^d$ oder einer Mannigfaltigkeit.

Um den Nutzen und die Vorteile von Quarklets gegenüber anderen Verfahren im praktischen Einsatz sowie in der theoretischen Betrachtung zu verstehen, gehen wir an dieser Stelle zunächst auf gängige numerische Lösungsverfahren ein. *Finite-Elemente-Verfahren* beruhen auf einer Diskretisierung des kontinuierlichen Problems durch ein endliches Gitter, welches das Gebiet überspannt. Auf den verschiedenen Abschnitten des Gitters wird nun versucht, die Lösung der Operatorgleichung durch lokale Funktionen zu approximieren. Je feiner das Gitter gewählt wird, desto besser werden die Approximationen. Bei der Wahl der Gitter gibt es natürlich eine Vielzahl von Optionen und Verfeinerungsstrategien. Beginnt man mit einem Gitter gleichmäßiger Weite und verfeinert dies in den sukzessiven Approximationsschritten gleichmäßig, spricht man von einem *uniformen* Verfahren. Der Vorteil besteht in einem Algorithmus, der einfach zu implementieren und nachzuvollziehen ist. Verfahren dieser Art berücksichtigen allerdings nicht die Struktur der Lösung. So spielt es keine Rolle, ob die lokale Approximation im aktuellen Iterationsschritt der tatsächlichen Lösung auf diesem

Gebiet schon recht nahe kommt oder nicht. Weist die exakte Lösung lokale Singularitäten auf, ist der Approximationsfehler von uniformen Verfahren in den Bereichen der Singularitäten aber zumeist viel größer als im restlichen Gebiet. Dieses Phänomen taucht in der Praxis insbesondere bei polygonalen Gebieten oder nichtglatten rechten Seiten f auf. In diesen Fällen erscheint es sinnvoll, die exakte Lösung, dort wo sie glatt ist, mit relativ wenig Aufwand zu approximieren und nur dort, wo sie lokale Singularitäten aufweist, zusätzliche Freiheitsgrade zur genaueren Approximation zu verwenden. Verfahren, die dies realisieren, nennt man *adaptiv*. Da im allgemeinen die Struktur der Lösung unbekannt ist, verlangt man, dass adaptive Verfahren ohne a-priori Informationen über die exakte Lösung die Verfeinerungsstrategie ausführen. Lediglich Informationen, die das Verfahren im Verlauf der Iterationen, also a posteriori, gewinnt, dürfen dazu verwendet werden. Adaptive Finite-Elemente-Verfahren finden in der Praxis regen Einsatz. Der theoretische Nachweis der Konvergenz und von Konvergenzraten ließ aber lange auf sich warten. In einigen Fällen gibt es mittlerweile theoretische Resultate, siehe [13, 86, 87, 99]. Nichtsdestotrotz führte diese Lücke zwischen Theorie und Praxis zu alternativen adaptiven Ansätzen, welche aufgrund stärkerer analytischer Eigenschaften erfolgversprechender im Bezug auf die theoretische Untersuchung erscheinen.

Eine Möglichkeit ist die Verwendung von *Wavelets* in adaptiven Verfahren. Wavelets entstehen durch Dilatieren, Translatieren und Skalieren weniger oder sogar nur einer einzigen Funktion. Die Gesamtheit der Wavelets bildet eine Basis eines Funktionenraums. Anwendung fanden Wavelets zunächst in den Bereichen Signal- und Bildverarbeitung sowie Zeit-Frequenz-Analyse. Die Konstruktion von speziellen Waveletbasen erlaubte aber auch den Einsatz von Wavelets zum numerischen Lösen von Operatorgleichungen. Die Wavelets, die hier zum Einsatz kamen und kommen, vereinen einige wünschenswerte Eigenschaften, die sie zum Einsatz in adaptiven Verfahren prädestinieren. Zum einen ermöglichen sie die Charakterisierung spezieller Glattheitsräume wie Sobolev- und *Besovräume*. Zum anderen sind sie stückweise glatt, kompakt getragen und besitzen verschwindende Momente. Konstruktionen dieser Art sind beispielsweise zu finden in [17,54,56,90,91]. Dadurch können diese Wavelets zur Diskretisierung von Operatorgleichungen verwendet werden und es ist möglich, Singularitäten mit wenigen Wavelets darzustellen. In den bahnbrechenden Arbeiten [31, 32] konnten aufbauend auf Wavelets adaptive numerische Verfahren mit beweisbarer Konvergenz entwickelt werden, welche darüber hinaus *asymptotisch optimal* sind, das heißt sie realisieren die selbe Approximationsrate wie die bestmögliche Approximation der exakten Lösung durch eine gewichtete Summe aus maximal N Wavelets. Speziell für Funktionen, welche Singularitäten aufweisen, konnte in zahlreichen Arbeiten nachgewiesen werden, dass diese Rate höher ist als die Rate von uniformen Verfahren, siehe hierzu etwa [29, 36, 40, 51, 67].

Die Konstruktion von geeigneten Waveletbasen, insbesondere auf komplizierteren Gebieten, stellt eine der größten Schwierigkeiten da. Die Entwicklung von sogenannten *Frames* gestaltet sich oft einfacher. Dies sind Repräsentantensysteme, welche im Gegensatz zu Basen Redundanzen erlauben. In [97] wurde die Konvergenz und asymptotische Optimalität eines adaptiven Verfahrens nachgewiesen, welches auf Waveletframes basiert.

Alle bisher vorgestellten Verfahren haben eines gemeinsam: Um eine bessere Approximation zu erhalten, wird mit einer Verfeinerung im Raum gearbeitet. Während Finite-Elemente-Verfahren dies durch feinere Gitter realisieren, greift man bei Wavelet-Verfahren auf Wavelets mit höherem Dilatationslevel zurück. Methoden dieser Art bezeichnet man in der Literatur häufig als h-Methoden. Im Bereich der Finite-Elemente-Methoden gibt es ein weiteres Paradigma. Ausgehend von einem festen Gitter erreicht man bessere Approximationen durch eine Anreicherung der lokalen Ansatzfunktionen mit Polynomen. Verfahren, welche hierauf basieren, nennt man p-Methoden. Für glatte exakte Lösungen kann man hierbei mit exponentiellen Konvergenzraten rechnen, siehe etwa [5, 7, 95].

Kombinationen von Raumverfeinerung und Anreicherung mit Polynomen sind ebenfalls möglich und kommen in sogenannten hp-Methoden zum Einsatz. Das Kalkül dahinter ist folgendes: Anreicherung mit Polynomen führt zu einer effizienten Darstellung des glatten Anteils einer Funktion durch wenige Funktionen, während eine Verfeinerung im Raum dazu genutzt wird, Singularitäten darzustellen. In der Praxis ist eine hohe Effizienz von adaptiven hp-Finite-Elemente-Methoden festzustellen. Selbst für nicht glatte Funktionen erreicht man bisweilen exponentielle Konvergenzraten, siehe etwa [4, 63, 95]. Der theoretische Nachweis von Konvergenz und Konvergenzraten gestaltet sich dagegen äußerst schwierig. Erst kürzlich konnten hierzu erste Resultate für elliptische Gleichungen zweiter Ordnung bewiesen werden. Wir verweisen hierbei auf die Arbeiten [11, 12, 14–16].

Eine natürliche Frage, die sich stellt, ist: Ist es möglich, hp-Methoden auf Wavelets zu übertragen? Und falls ja, lassen sich die starken analytischen Eigenschaften von Wavelets nutzen um auf lange Sicht die hohen Konvergenzraten von hp-Methoden, welche in der Praxis beobachtet werden, theoretisch nachzuweisen?

Ein Ansatz, der nicht direkt auf Wavelets basiert, sondern auf Funktionen, welche eine Partition der Eins bilden, wurde in [104] vorgeschlagen und in [50] weiter untersucht. Dilatation, Translation und eine Anreicherung mit Polynomen einer Partition der Eins führten hierbei zu einem hoch redundanten Frame, welcher Sobolev- und Besovräume charakterisiert. Übliche Zerlegungen durch Basen werden häufig als atomar bezeichnet. Dementsprechend kann man in diesem Zusammenhang von dem redundanten System als subatomarer, beziehungsweise *quarkonialer* Zerlegung sprechen. Nachteilhaft wirken sich beim quarkonialen Ansatz die fehlenden verschwindenden Momente einer Partition der Eins aus. Diese sind essentiell für ein effizientes adaptives Verfahren und damit auch den Nachweis von Konvergenz und asymptotischer Optimalität.

Das Ziel dieser Arbeit ist einerseits die Konstruktion einer neuen Klasse von Funktionen, den *Quarklets*, welche den quarkonialen Ansatz mit Ideen und Konzepten der Wavelet-Konstruktion vereint. Andererseits wollen wir aufbauend auf Quarklets ein adaptives Frame-Verfahren entwickeln, welches theoretisch nachweisbar konvergent und asymptotisch optimal ist. Diese theoretischen Resultate wollen wir durch numerische Experimente in der Praxis überprüfen.

Zur Vorbereitung der Entwicklung von Quarklets wiederholen wir zunächst ausführlich die wichtigsten Konstruktionsprinzipien von eindimensionalen Wavelets auf der reellen Achse sowie auf dem Einheitsintervall. Daraufhin betrachten wir die Wavelets aus [34] und [90] als jeweilige Realisierung. Diese dienen als Grundlage zur Konstruktion von eindimensionalen Quarklets. Verschwindende Momente der Wavelets bleiben dabei erhalten. Insbesondere die Konstruktion von geeigneten, dem Rand angepassten Quarklets erfordert eine sorgfältige Analyse. Mit den auf dies Weise konstruierten Quarklets lassen sich daraufhin sowohl Frames für Lebesgue- als auch Sobolevräume bilden.

Nachdem die univariate Theorie abgeschlossen ist, verwenden wir einen Tensoransatz um Quarklets auf dem Einheitskubus zu erhalten. Hier ist es nötig die Theorie von Tensorbasen auf Tensorframes zu erweitern. Um vom Einheitskubus zu allgemeinen Gebieten zu gelangen, greifen wir auf *nichtüberlappende Gebietszerlegungen* zurück. Wir setzen sozusagen das gesamte Gebiet aus einzelnen Kuben beziehungsweise parametrisierten Bildern von Kuben zusammen. Besonderes Augenmerk liegt hierbei auf der Konstruktion von geeigneten Fortsetzungsoperatoren an den Rändern der jeweiligen Kuben. Die Redundanz der Frames muss dabei in die Überlegungen einbezogen werden und erfordert einige Anpassungen im Vergleich zum Basisfall.

Um Quarklets in der Praxis zu verwenden, betrachten wir das in [97] propagierte adaptive Richardson-Verfahren für Frames und zeigen, dass es sich auch auf Quarklets anwenden lässt. Hierzu ist es unerlässlich, dass die Steifigkeitsmatrix bezüglich der Quarklets und der jeweiligen Operatorgleichung eine gewisse *Kompressibilität* aufweist. Grob gesagt verstehen wir darunter, dass sich die Steifigkeitsmatrix effizient durch dünnbesetzte Matrizen approximieren lässt. Dies weisen wir exemplarisch für die Poisson-Gleichung nach. Verglichen mit dem Waveletfall gestaltet sich der Beweis der Kompressibilität für Quarklets, bedingt durch deren polynomiale Anreicherung, deutlich aufwendiger.

Das in der Arbeit entwickelte adaptive Quarklet-Verfahren wird an verschiedenen Beispielen getestet. Die Beispiele sind so gewählt, dass durch die Gebietsstruktur beziehungsweise durch die Struktur der rechten Seite der Operatorgleichung Singularitäten in der exakten Lösung entstehen.

Abschließend geben wir einen Ausblick auf mögliche zukünftige Weiterentwicklungen des Quarkletansatzes.

Contents

Introduction

In several fields of natural and social sciences such as chemistry, biology, physics or economics, one main task is to describe and approximate observations made in reality with a mathematical model. In this context, partial differential equations (PDEs) are very well suited for a wide variety of phenomena, for example, electrostatics, cell biology or mathematical finance, just to name a few. Using a weak formulation argument, PDEs can be formulated in a functional analytic setting as an operator equation

$$\mathcal{L}u = f. \tag{0.1}$$

In this thesis, we solely deal with linear operators $\mathcal{L} : H \to H'$ from a Hilbert space H into its normed dual H', where we assume $\mathcal{L}$ to be *elliptic*, i.e., there exist constants $C_1, C_2 > 0$ such that $C_1||v||_H \leq ||\mathcal{L}v||_{H'} \leq C_2||v||_H$ for all $v \in H$. The standard example which fits into this framework is the *Poisson equation* with *Dirichlet boundary conditions* on a bounded domain $\Omega \subset \mathbb{R}^d$

$$-\Delta u = g \text{ in } \Omega, \quad u = 0 \text{ on } \partial\Omega.$$

Albeit not part of this thesis, let us mention that also *integral equations* can be treated in the fashion of (0.1).

If $\mathcal{L}$ is a linear elliptic operator, it is followed by an application of the Lax-Milgram theorem that (0.1) has a unique solution. However, in many cases, it is not possible to find this solution in an analytical way. Therefore, in numerical analysis, one is concerned with the development and analysis of algorithms that provide approximate solutions of operator equations.

A very popular approach is, for example, a uniform finite element method (FEM). The basic idea is a discretization with respect to some equidistant finite grid for the domain Ω. Then, on every subdomain several ansatz functions are used to deliver approximations to the exact solutions. To improve the approximations, one refines the grid uniformly. The refinement is repeated until a desired accuracy is reached.

The theory behind the latter approach is well-understood and the implementation is rather simple. However, a uniform refinement strategy is not always the best choice to obtain a good approximation in a short amount of time. Think of a scenario where at one stage of the approximation process the solution is very well approximated in some regions of the domain whereas in other parts of the region the approximation is far apart from the exact solution. This actually happens if singularities occur in the exact solution. They are usually induced by singularities of the right-hand side

f of (0.1) or the shape of the domain Ω. For example, singularities appear in regions around a non-smooth boundary of the domain, e.g., a reentrant corner. See [60,71,72] for details.

In this case, a more flexible non-uniform scheme, which focuses on refinements in regions where it really pays off, is more efficient. In many applications, the exact solution is not known beforehand. Hence, it is necessary that the scheme detects the eligible regions on its own without any a priori information about the exact solution. Therefore, a non-uniform scheme heavily relies on good local a posteriori error estimators. Schemes that combine a posteriori error estimators with non-uniform refinement are called *adaptive methods*. They allow for a higher resolution in singular regions of the solution and a coarser resolution on smooth parts. Compared to a uniform scheme, an adaptive method is more involved. However, due to the advantages we have just explained, it can lead to higher *convergence rates*, which can be described as the trade-off between the approximation error and the spent amount of degrees of freedom. In the finite element setting, results about convergence rates can be found, e.g., in [13,86,87,99]. For a comprehensive introduction and overview about adaptive finite element methods, see [88, 108]. Since it took a long while from the practical realization of adaptive finite element methods to theoretical convergence rate results, other approaches to adaptivity have been made.

Adaptive wavelet algorithms

Due to their strong analytical properties, *wavelets*, which had their early applications in signal/image processing (cf. [82]) and time-frequency analysis (cf. [25, Chapter 3]), came into focus. There are plenty of examples where wavelets have been applied in adaptive methods until today [9,21,31–33,38,39,42,45,46,49,52,68,69,98,109].

The general idea behind wavelets is to use one single function ψ, called *mother wavelet*, and obtain all other wavelets via dilation, translation and scaling of ψ, i.e., the wavelets are the functions

$$\psi_{j,k} = 2^{j/2}\psi(2^j \cdot -k), \quad j,k \in \mathbb{Z}.$$

The family of wavelets $\Psi_{L_2(\mathbb{R})} = \{\psi_{j,k} : j,k \in \mathbb{Z}\}$ builds an orthonormal basis for $L_2(\mathbb{R})$ or at least a Riesz basis in a less restrictive version. Even if a construction of wavelets is possible without it (cf. [74, 102]), the multiresolution analysis (MRA) introduced by S. Mallat and Y. Meyer in [81, 84] has become the predominant tool in this context. The MRA is generated by a single function φ, called the *scaling function* or *generator*. With this special function at hand the mother wavelet arises via a *two-scale equation*

$$\psi = \sum_{k\in\mathbb{Z}} b_k \varphi(2 \cdot -k),$$

with a mask $\mathbf{b} = \{b_k\}_{k\in\mathbb{Z}}$. For a detailed introduction to wavelets and their construction principles, we refer, e.g., to [30, 58, 82, 110].

In this thesis, the generator φ is always compactly supported and the mask $\mathbf{b}$ is *finite*, i.e., it has only finitely many entries which are not zero. Hence, also the mother wavelet is compactly supported. Therefore, if one wants to analyse a signal, small perturbations will only influence coefficients related to wavelets in the neighbourhood of the perturbations. With increasing level j, the support of the wavelets becomes smaller and smaller such that detail information can be resolved. In other words, the motion from a low to a high scale can be seen as some kind of zoom. Further important properties of wavelets, which make them especially suitable for the adaptive numerical treatment of operator equations, are:

- Weighted sequence norms of wavelet coefficients characterize certain smoothness spaces like Sobolev, Hölder or Besov spaces.

- Wavelets have vanishing moments, which lead to a cancellation of smooth parts of a function.

- Wavelets can be chosen arbitrarily smooth.

The cancellation property together with the zoom to higher scales make it possible to represent functions that exhibit singularities with very few wavelet coefficients. Moreover, the characterization of function spaces allows the construction of a stable wavelet basis for a Sobolev space by a simple rescaling of the original basis for $L_2(\mathbb{R})$.

For the treatment of operator equations on bounded domains some adjustments have to be made. First of all, an adaptation for the wavelets at the boundary is necessary. This can be done in a way that basic properties of wavelets as described above are preserved. Univariate wavelet Riesz basis constructions that are in a certain sense tailor-made for the treatment of operator equations can be found in [17, 54, 56, 90, 91]. These bases, however, can be used to derive bases on cubes or parametric images of cubes. If one needs stable systems for bounded domains that can not be characterized as a parametric image of a cube, two principles are predominant. On the one hand, there are *overlapping domain decompositions* (cf. [41–43,49,97]). As the name suggests, the target domain is decomposed into overlapping subdomains that are parametric images of the cube. In this way, you end up with a stable system which, however, is not a wavelet basis any more but a wavelet *frame*. Roughly speaking, a frame is a generating system which allows for redundancies. For more information on this topic, we refer to [23, 24].

On the other hand, one can try to decompose the domain into parametric images of the cube that do *not* overlap. This procedure is denoted as a *non-overlapping domain decomposition*. Here, the main difficulty lies in the process of piecing together the bases on the respective subdomains along the interfaces. If this is done correctly, you will end up with a wavelet basis on the whole domain. Constructions and applications of non-overlapping domain decompositions can be found, e.g., in [17, 18, 20, 57].

For both decomposition approaches, the characterization of smoothness spaces is still feasible. In particular, for Sobolev spaces on bounded domains. Since in the weak formulation (0.1) the operator $\mathcal{L}$ maps from a Sobolev space into its dual space, weighted wavelet systems on a bounded domain which characterize certain Sobolev spaces can be utilized for the discretization of the operator. In so doing, the operator equation can be transferred into an infinite linear equation system

$$\mathbf{A}\mathbf{u} = \mathbf{f}. \tag{0.2}$$

In order to treat (0.2) numerically, e.g., with an iterative scheme, matrix-vector multiplications with the *stiffness matrix* $\mathbf{A}$ have to be performed. Since $\mathbf{A}$ is biinfinite and in general *not sparse*, i.e., there exist columns or vectors in $\mathbf{A}$ with (infinitely) many non-zero entries, an exact multiplication in a reasonable amount of time is not achievable. Therefore, the matrix-vector multiplication has to be substituted with an inexact version. For this to be done efficiently with a manageable approximation error, it is necessary that the matrix $\mathbf{A}$ exhibits at least a *quasi-sparse* or *compressible* structure, i.e., it can be well approximated by sparse biinfinite matrices. The latter are usually constructed through a *coarsening* of the matrix $\mathbf{A}$, which means that small entries of the matrix are replaced by zeros. In order to do this efficiently, the design of a proper coarsening strategy is mandatory.

Thanks to the locality and the cancellation properties of the wavelets, quasi-sparsity could be verified for a large class of differential and integral operators in wavelet coordinates, cf. [53]. This property was used, e.g., in [8,31,32,97] to design a method

$$\mathbf{APPLY}[\mathbf{A}, \mathbf{v}, \varepsilon] \to \mathbf{w}_\varepsilon$$

which executes the inexact matrix-vector multiplication of $\mathbf{A}$ with a finitely supported vector $\mathbf{v}$ under a maximal error $\varepsilon > 0$ measured in the ℓ_2-norm. The calculation steps within the method are adapted to the modulus of the entries of $\mathbf{v}$ and the error tolerance ε. Hence, we call a wavelet method adaptive whenever an **APPLY** routine is used in it. The progress in this field culminated when in [31] a first adaptive wavelet Galerkin method for elliptic operator equations and shortly after in [32] an adaptive Richardson method were introduced. For both algorithms the convergence and the *asymptotical optimality* could be proven. The latter means that for a stable wavelet system $\Psi = \{\psi_\lambda : \lambda \in \Lambda\}$ for H the solution u of (0.1) is approximated by the algorithm with functions $u_i = \sum_{\lambda \in \Lambda_i} \mathbf{u}_\lambda \psi_\lambda$, $\#\Lambda_i < \infty$ with an optimal relation between the degrees of freedom $\#\Lambda_i$ and the accuracy $||u - u_i||_H$. We speak of an optimal relation whenever $||u - u_i||_H \leq C(\#\Lambda_i)^{-s}$, with the largest possible $s > 0$ and a constant $C > 0$ depending on u. The optimal convergence rate s is predestined by the decay rate of the *best N-term approximation error*

$$\sigma_N(u) = \inf\{||u - v||_H : v = \sum_{\lambda \in \mathcal{I}} \mathbf{v}_\lambda \psi_\lambda, \#\mathcal{I} \leq N, \mathcal{I} \subset \Lambda\}$$

with respect to the wavelet system Ψ. However, the optimal convergence rate s with respect to wavelets depends on the smoothness of u in scales of Besov spaces, cf. [64].

It has turned out that for many operator equations the Besov smoothness is much higher than the regularity measured in Sobolev scales, which in turn is related to the convergence rate of uniform methods. Particularly, this is the case for solutions with local singularities, which turn up on domains with corners or due to singularities of the right-hand side. Verifications of the latter fact for several types of operator equation can be found, e.g., in [29, 36, 40, 51, 67].

At first, the just described algorithms were solely applied to discretizations via wavelet bases. Since the overlapping domain decomposition led to wavelet frames, the natural question was if the algorithms could be assigned to this setting. For the Galerkin methods, the answer is negative. The reason for this is the redundancy of the frame, which leads to submatrices of the stiffness matrix $\mathbf{A}$ that are ill-conditioned or even singular. Therefore, the uniform well-posedness of the finite-dimensional Galerkin subproblems would not be guaranteed without spending additional effort. However, in [97], a generalization of the adaptive Richardson iteration of [32] to wavelet frames was constructed. Moreover, the asymptotic optimality of this algorithm could be verified assuming that the redundancy of the frame could be controlled in a certain way. Further adaptive algorithms based on wavelet frames were constructed and analysed, e.g., in [41, 42, 80, 92, 101, 109]. For a general overview about wavelet methods for operator equations, we refer to [53, 100, 107].

hp-methods

Uniform FEM, adaptive FEM, adaptive wavelet methods: so far, all of the presented algorithms have one thing in common – to improve the accuracy of the approximation, they work with a refinement of the space. In literature, those kind of schemes are sometimes called *h-methods*. In the realm of FEMs, there exists another well-known approach. Instead of refining the space, one fixes the finite element mesh and aims for a polynomial enrichment of the ansatz functions. In that case, one speaks of a *p-method*. In fact, adaptive p finite element methods can be very powerful. Particularly for smooth solutions, exponential convergence rates are possible, cf. [5, 7, 95]. For a theoretical foundation of p-FEMs, we refer to [6].

Also a combination of both space-refinement and polynomial enrichment is possible, leading to *hp-methods*. The reasoning behind this approach is that, on the one hand, a polynomial enrichment of the ansatz functions allows for a sparse approximation of the smooth part of the solution and, on the other hand, the space-refinement serves to render the singularities. An *hp*-FEM was first mentioned in [2, 3]. In practice it is observed that adaptive hp-FEMs are very efficient; sometimes they even have exponential convergence rates for solutions with singularities, cf. [4, 63, 95]. However, rigorous convergence and complexity proofs of *hp*-FEMs could be derived only recently. In the last years, some results have been obtained for *hp*-FEMs of second-order elliptic equations. Let us mention the timely reviews [14–16] and the algorithm proposed in [11, 12].

A natural question that arises is: is it possible to construct wavelet versions of adaptive *hp*-methods? And if so, can this, due to the strong analytical properties of wavelets, pave the way to new convergence proofs for *hp*-methods in the long run? A predecessor approach not directly based on wavelets but on a *partition of unity*, i.e., a function f with the property

$$\sum_{k\in\mathbb{Z}} f(\cdot - k) \equiv 1,$$

was proposed in [104] and further investigated in [50]. Via a polynomial enrichment, dilation and translation of the partition of unity function, highly redundant frames for Sobolev and Besov spaces were derived. These frames can be interpreted as subatomic, i.e., *quarkonial* decompositions, and this concept is of course very close to the idea of an *hp*-finite element system.

However, to design an adaptive numerical scheme directly based on these quarkonial decompositions is highly non-trivial since the frame elements do not possess vanishing moments. As mentioned above, the vanishing moment property is essential for the design of an **APPLY** routine and, therefore, for the convergence and optimality of adaptive wavelet schemes. This thesis is hence focused on another approach, where a wavelet-type modulation of the quarkonial system leads to a family of functions, called *quarklets*, which enables an effective numerical treatment of operator equations.

Main objectives

The first task of this thesis can be summarized as follows:

(T1) The construction of quarklet frames first on the real line and then on quite general bounded domains $\Omega \subset \mathbb{R}^d$. Since the quarklets should be used for the solution of linear elliptic operator equations, they need to fulfil the following characteristics:

  (i) The characterization of the function spaces required for the discretization of the operator equations.

  (ii) Some amount of vanishing moments such that the stiffness matrix of the corresponding operator equation exhibits a quasi-sparse structure.

The construction on the real line is executed by a a polynomial enrichment of the generators of a biorthogonal wavelet basis. The quarklets then arise through a two-scale equation similar to the wavelet case. In this way, the quarklets inherit the polynomial degree of the enriched generators. It turns out that the resulting highly redundant system has the frame property in scales of Sobolev spaces. For this purpose, the verification of certain *Jackson* and *Bernstein* estimates is crucial. Moreover, the whole construction is designed in such a way that the vanishing moments of the underlying wavelet basis are preserved.

The construction of stable systems for quite general domains contained in $\mathbb{R}^d$ is a non-trivial task even in the classical wavelet setting. As mentioned above, this is usually accomplished by some kind of domain decomposition. For instance, one could use an overlapping domain decomposition approach as outlined in [43]. Indeed, it is possible to construct wavelet frames in this way. Moreover, it has been shown that the latter can be applied in adaptive wavelet frame schemes that converge with optimal order. However, in practice, one is often faced with non-trivial quadrature problems that hamper the overall performance of the scheme. Therefore, we proceed in a different way and use a non-overlapping domain decomposition similarly to the earlier work [57]. It was shown in [20] that this approach gives rise to generalised tensor product wavelet bases on quadranglelizable domains. In general, tensor product wavelets can be interpreted as a wavelet version of sparse grids. Therefore, related approximation schemes can attain dimension-independent convergence rates. In [20], it was shown that these properties carry over to the case of more general domains. In this thesis, we show that a combination of these ideas with quarkonial decompositions indeed works and gives rise to a generalized tensor product quarklet frame on domains which can be quadrangulated.

To carry out this program, several steps have to be performed. First of all, the quarklet frame construction on the real line has to be adapted to problems on bounded intervals. In particular, Dirichlet boundary conditions have to be incorporated. Once this is done, a quarklet frame on unit cubes can be designed by taking tensor products. Then, one has to make sure that the new systems are again stable in scales of Sobolev spaces. This is by no means obvious because the underlying Sobolev spaces are usually not of tensor product type. Finally, this construction has to be generalized to arbitrary domains by using non-overlapping domain decomposition strategies and suitable extension operators. In this thesis, we show that all these steps can indeed be carried out. Moreover, we prove that several very important properties such as vanishing moments are preserved, which again implies that the basic building blocks of adaptive algorithms can still be derived.

Once the quarklet frames are constructed, the next task is their application in numerical schemes:

(T2) Based on the constructed quarklet frames we want to design a convergent adaptive scheme for certain linear elliptic operator equations. Furthermore, we want to prove the optimal complexity of the algorithm under certain assumptions. In order to do this, several building blocks have to be established. In particular, the construction of an efficient **APPLY** method is a challenging task. To derive such a method, the careful analysis of a convenient coarsening strategy is mandatory.

As described above, the application of a Galerkin scheme to a frame system runs into stability problems. Therefore, in this thesis the design of an adaptive method is based on a direct iterative scheme. In [97], it was already described how a Richardson iteration could be applied to wavelet frames. We adapt this method in a way that it also works for quarklet frames. Special emphasis lies on a coarsening strategy, which takes both the level and the polynomial degree of the quarklets into account.

The final task is the practical realization of the derived schemes:

(T3) The implementation and numerical experiments in one and two spatial dimensions with representative test problems to verify the convergence and to study the convergence rate for certain linear elliptic problems.

Since *hp*-methods are tailor-made for problems with singularities at some points and a smooth structure elsewhere, we investigate in operator equations where the solutions are of this kind. These characteristics of the solution can be achieved, on the one hand, by the given right-hand side of the operator equation and, on the other hand, by the shape of the domain. For example, we study a test problem on the L-shaped domain, which induces a singularity in the solution due to its reentrant corner.

With slight theoretical adjustments, this thesis summarizes the results of the papers [44, 47] in a uniform display complemented by a detailed foundation, further theoretical insights and extended numerical tests. In particular, the structure of it is organized as follows.

Layout

In **Chapter 1**, we introduce linear elliptic operator equations as the problems that we want to approximately solve with a numerical scheme. We show how linear elliptic boundary value problems on certain kinds of domains, which are also specified in this chapter, fit into this framework. For this purpose, we recall the concept of the weak formulation of boundary value problems. In this context, Sobolev spaces play a central role and are therefore introduced at this point. Finally, we discuss some typical examples that can be treated in the just presented fashion.

Chapter 2 is dedicated to the presentation of frames and Riesz bases for Hilbert spaces. At first, we review the frames and the slightly weaker concept of Bessel systems and collect some of their basic properties. Then, we introduce Riesz bases and shed some light on the connection between them and frames. Afterwards, we show a couple of statements about the interaction of certain operators with the various types of function systems. With *Gelfand frames*, we introduce a specific class of frames in Section 2.4. On the one hand, they serve as stable systems for Lebesgue spaces and, on the other hand, they give rise to frames for a scale of Sobolev spaces via a proper rescaling. Thereupon, we explain in Section 2.5 how these Gelfand frames can be utilized for the discretization of operator equations, which is a crucial step into the direction of a numerical treatment of the latter.

The rather abstract concept of Riesz bases is filled with life in **Chapter 3**, where we are concerned with biorthogonal wavelet Riesz bases. In Section 3.1, we outline how an MRA is used as a construction tool for wavelet Riesz bases on the real line. As a specific example, we take a look at the *Cohen-Daubechies-Feaveau (CDF) wavelets* of [34]. In Section 3.2 we observe which adaptations have to be made to construct wavelet Riesz bases on the interval in a way that certain boundary conditions are fulfilled. In this context, the concept of stable completion is introduced. Moreover, we see in an abstract manner how characterizations of Sobolev spaces can be derived via Jackson and Bernstein estimates. To conclude, we present the *Primbs wavelets* as a realization of boundary adapted wavelets.

Chapter 4 is the first of three consecutive chapters that is devoted to Task (T1), the construction of quarklets. Here, the realization of quarklet frames on the real line is at the centre of our attention. In order to do this, we initially define quarks as polynomially enriched cardinal B-splines and derive necessary estimates for the former, in particular the above mentioned estimates of Jackson and Bernstein-type. Subsequently, we design quarklets in Section 4.2 as linear combinations of translated and dilated quarks. As it turns out, the quarklets inherit the vanishing moments of the underlying wavelet basis, which in fact is the CDF wavelet basis of Section 3.1. Furthermore, we are able to prove the frame property of the quarklet system for the Lebesgue space $L_2(\mathbb{R})$ and for scales of Sobolev spaces $H^s(\mathbb{R})$.

In **Chapter 5**, we show that the construction of quarklets can be adapted to bounded intervals in such a way that, e.g., Dirichlet boundary conditions can be incorporated. For that purpose, we use the generators of the Primbs wavelets of Section 3.2 as a starting point to attain boundary adapted quarks again through a polynomial enrichment. It turns out that only the quarks at the boundaries of the interval differ from the real line quarks. Therefore, for our intentions, it is sufficient to proceed with the verification of certain desirable properties of these boundary quarks. Afterwards, we define quarklets on the unit interval once more via a refinement equation. To secure that the vanishing moment property of the underlying Primbs wavelet basis is not destroyed, we have to pay particular attention to the selection of appropriate coefficients for the *refinement mask*. Once this is done, we derive frame properties in a similar fashion as in the real line case. Finally, as a prearrangement for Section 7.3, where the verification of the quasi-sparsity of stiffness matrices for specific operators is addressed, we analyse certain cancellation properties of the quarklets and their derivatives.

In **Chapter 6**, we generalize the frame construction to bounded domains contained in $\mathbb{R}^d$. In Section 6.1, we start with the design of quarklet frames on unit cubes. We show that by tensorizing quarkonial frames on intervals, one obtains frames for the Sobolev spaces $H^s((0,1)^d)$. In contrast to the basis case, this does not follow by general arguments; it seems that additional conditions on the interval frames are necessary. Fortunately, these conditions are satisfied in our case. Then, the construction on quadranglelizable domains is studied. We show that, with given reference frames on the unit cube, these frames can be extended to the whole domain in such a way that their union once again provides a frame for scales of Sobolev spaces. Finally, we display that with small adaptations, Gelfand frames for very general domains are obtained. This the main result for the construction of quarklet frames.

Having shown this, in **Chapter 7**, we approach Task (T2), the design of an adaptive quarklet scheme. In principle, one can run the machinery of adaptive frame algorithms as outlined in [43]. In Section 7.1, we present an adaptive Richardson iteration in a very general fashion and show its optimality under certain conditions. The construction of the indispensable subroutines **APPLY**, **RHS** and **COARSE** are outlined in Section 7.2. Moreover, we go into detail how quarklet frames can be applied in an adaptive scheme. For the **APPLY** routine to work efficiently, it is necessary that the infinite stiffness matrix in quarklet coordinates is quasi-sparse. Therefore, we provide a compression result for the latter in Section 7.3.

Finally, in **Chapter 8**, we turn to Task (T3) and conduct some numerical experiments of the developed adaptive quarklet algorithm in one and two spatial dimensions. In essence, the Poisson equation on various domains is studied. It turns out that for natural test examples, adaptive quarklet schemes outperform the well-established wavelet (frame) methods. Therefore, the higher redundancy induced by the polynomial enrichment really pays off in practice.

Chapter 1

Elliptic Operator Equations

In this thesis, we construct a new class of functions called quarklets and use them to solve operator equations of the form

$$\mathcal{L}u = f. \tag{1.0.1}$$

Usually, $\mathcal{L}$ is a linear mapping from a Hilbert space H into its dual H'. In addition, we assume the operator $\mathcal{L}$ to be *elliptic*, i.e.,

$$||\mathcal{L}v||_{H'} \sim ||v||_H, \quad \text{for all } v \in H. \tag{1.0.2}$$

This condition is sufficient to guarantee the existence and uniqueness of u, which continuously depends on f, see [75, Theorem 6.5.9]. In this chapter, we describe how linear partial differential equations (PDEs) with boundary values fit into the framework of operator equations. In order to do this, we introduce Sobolev spaces on domains and use them to achieve a weak formulation of the boundary value problems.

1.1 Domains

A *bounded domain* $\Omega \subset \mathbb{R}^d$ is a bounded, connected and open subset of $\mathbb{R}^d$. Recall the *Hölder spaces* $\mathcal{C}^{k,\gamma}(\overline{\Omega})$, $k \in \mathbb{N}_0$, $0 < \gamma \leq 1$ as the set of k-times continuously differentiable functions such that the k-th partial derivative is *Hölder continuous with exponent* γ, i.e.,

$$\sup_{x \neq y \in \Omega} \frac{|\mathrm{D}^\alpha x - \mathrm{D}^\alpha y|}{|x-y|^\gamma} < \infty, \quad \text{for all } |\alpha| \leq k. \tag{1.1.1}$$

Definition 1.1. Let Ω be a bounded domain. We say the boundary $\partial\Omega$ of Ω is k-times Hölder continuous, $k \in \mathbb{N}_0$, if for every $x \in \partial\Omega$ there exists a neighbourhood $M \subset \mathbb{R}^d$ and an invertible function $\phi : M \to B_1(0) := \{y \in \mathbb{R}^d : |y| < 1\}$ such that

$$\phi \in \mathcal{C}^{k,1}(\overline{M}), \quad \phi^{-1} \in \mathcal{C}^{k,1}(\overline{B_1(0)}), \tag{1.1.2}$$

$$\phi(M \cap \Omega) = \{y \in B_1(0), y_d > 0\}, \tag{1.1.3}$$

$$\phi(M \cap \partial\Omega) = \{y \in B_1(0), y_d = 0\}, \tag{1.1.4}$$

$$\phi(M \backslash \overline{\Omega}) = \{y \in B_1(0), y_d < 0\}. \tag{1.1.5}$$

If $k = 0$, the domain Ω is called *Lipschitz domain.*

The prototypical boundary value problem in this thesis is an elliptic PDE on a Lipschitz domain.

1.2 Elliptic boundary value problems

For $k \in \mathbb{N}$, we denote the space of all k-times continuously differentiable functions over a set $\emptyset \neq M \subset \mathbb{R}^d$ by $\mathcal{C}^k(M)$. In addition, let $\mathcal{C}^\infty(M) := \cap_{k\in\mathbb{N}} \mathcal{C}^k(M)$. The space $\mathcal{C}(M)$ contains all continuous functions over M. Note that if M is compact, then, the just defined spaces consist of bounded functions with bounded derivatives up to some order. Let $\Omega \in \mathbb{R}^d$ be a bounded domain. A general linear partial differential operator $L : \mathcal{C}^{2t}(\Omega) \mapsto \mathcal{C}(\Omega)$ of order $2t \in \mathbb{N}$ on Ω in its divergence form is written as

$$L := \sum_{\alpha \leq t} \sum_{\beta \leq t} (-1)^{|\beta|} \mathrm{D}^\beta \left(a_{\alpha,\beta}(x) \mathrm{D}^\alpha \right), \tag{1.2.1}$$

with sufficiently smooth $a_{\alpha,\beta} : \Omega \mapsto \mathbb{R}$. With

$$\mathrm{D}^\alpha := \frac{\partial^{|\alpha|}}{\partial x_1^{\alpha_1} \cdots \partial x_d^{\alpha_d}} \tag{1.2.2}$$

we denote the partial differential operator of order $|\alpha| := \alpha_1 + ... + \alpha_d$ for any multi-index $\alpha := (\alpha_1, ..., \alpha_d) \in \mathbb{N}_0^d$. We assume the coefficients $a_{\alpha,\beta}$ to be symmetric, $a_{\alpha,\beta} = a_{\beta,\alpha}$, and the operator L to be *uniformly elliptic* in Ω, i.e., there exists a function $c : \Omega \mapsto \mathbb{R}$ with $\inf_{x\in\Omega} c(x) > 0$ so that

$$\sum_{|\alpha|=|\beta|=t} a_{\alpha,\beta}(x) \xi^{\alpha+\beta} \geq c(x)|\xi|^{2t}, \quad \text{for all } x \in \Omega, \xi \in \mathbb{R}^d, \tag{1.2.3}$$

where $\xi^\alpha := \xi_1^{\alpha_1} \cdots \xi_d^{\alpha_d}$. We are interested in solving elliptic boundary value problems of the form

$$Lu = g \qquad \text{in } \Omega, \tag{1.2.4}$$

$$\frac{\partial^k u}{\partial n^k} = \varphi_k \quad \text{on } \partial\Omega, \quad k = 0, \ldots, t-1, \tag{1.2.5}$$

with *Dirichlet boundary conditions* and a continuous functions φ_k on the boundary $\partial\Omega$. The first order normal derivative on $\partial\Omega$ is defined as

$$\frac{\partial u}{\partial n}(x) := \langle n(x), \nabla u(x) \rangle = \sum_{i=1}^d n_i(x) \frac{\partial u}{\partial x_i}(x), \quad x \in \partial\Omega, \tag{1.2.6}$$

with the outer normal vector field $n(x) = (n_1(x), \ldots, n_d(x))^T$, $x \in \partial\Omega$ and gradient $\nabla u := \left(\frac{\partial u}{\partial x_1}, \ldots, \frac{\partial u}{\partial x_d} \right)^T$. Of course, the boundary $\partial\Omega$ needs to be sufficiently smooth in order that (1.2.5) is well-defined. In this thesis, we always assume *homogeneous Dirichlet boundary conditions*, i.e,

$$\frac{\partial^k u}{\partial n^k} = 0 \quad \text{on } \partial\Omega, \quad k = 0, \ldots, t-1. \tag{1.2.7}$$

A function $u \in \mathcal{C}^{2t}(\Omega) \cap \mathcal{C}^{t-1}(\overline{\Omega})$ solving the problem (1.2.4), (1.2.7) is called a *classical solution*. If the right-hand side g or the domain Ω is not sufficiently smooth, it can happen that no classical solution to (1.2.4), (1.2.7) exists. To circumvent this problem, it is necessary to mitigate the regularity assumptions on the solution u. By doing so, we see that we can transfer (1.2.4), (1.2.7) into an elliptic operator equation (1.0.1). For this purpose, we need to collect some functional analytic concepts in the next section.

1.3 Sobolev spaces

Our aim is to reformulate (1.2.4), (1.2.7) in a weak sense, which guarantees existence and uniqueness of the solution. In this section, we introduce *Sobolev spaces*, which play a crucial role in this process. A more detailed presentation of Sobolev spaces can be found in [1, 76, 103].

Let $\Omega = \mathbb{R}^d$ or a bounded domain in $\mathbb{R}^d$. For $0 < p \leq \infty$ the *Lebesgue spaces* $L_p(\Omega)$ are defined as the spaces of all equivalence classes of measurable functions $f : \Omega \to \mathbb{C}$ for which

$$||f||_{L_p(\Omega)} := \begin{cases} \left(\int\limits_{\Omega} |f(x)|^p \,\mathrm{d}x \right)^{1/p} &, \quad 0 < p < \infty, \\ \text{ess sup}_{x\in\Omega} |f(x)| &, \quad p = \infty \end{cases} \tag{1.3.1}$$

is finite. For $1 \leq p \leq \infty$ the spaces $(L_p(\Omega), ||\cdot||_{L_p(\Omega)})$ are Banach spaces. The space $L_2(\Omega)$ is even a Hilbert space with the inner product

$$\langle f, g \rangle_{L_2(\Omega)} := \int\limits_{\Omega} f(x)\overline{g(x)} \,\mathrm{d}x. \tag{1.3.2}$$

For $0 < p < 1$, the $L_p(\Omega)$-spaces are only quasi-Banach spaces, i.e., the triangle inequality is only true up to a constant

$$||f + g||_{L_p(\Omega)} \lesssim ||f||_{L_p(\Omega)} + ||g||_{L_p(\Omega)}.$$

We say that $U \subset\subset \Omega$, if U is bounded in $\mathbb{R}^d$ and $\overline{U} \subset \Omega$. We define $L_{p,loc}(\Omega)$ as the space of functions contained in $L_p(U)$ for all $U \subset\subset \Omega$. We call

$$\operatorname{supp} f := \overline{\{x \in \Omega : f(x) \neq 0\}} \tag{1.3.3}$$

the *support* of $f \in \mathcal{C}(\Omega)$. With $\mathcal{C}_0^k(\Omega)$ we denote the space of all functions $f \in \mathcal{C}^k(\Omega)$ with $\operatorname{supp} f \subset\subset \Omega$ and analogously

$$\mathcal{C}_0^\infty(\Omega) := \{f \in \mathcal{C}^\infty(\Omega) : \operatorname{supp} f \subset\subset \Omega\}, \tag{1.3.4}$$

which is called the *space of test functions.* We say a function $f \in L_{1,loc}(\Omega)$ has a *weak derivative* of order $\alpha \in \mathbb{N}_0^d$ if there exists another function $f_\alpha \in L_{1,loc}(\Omega)$ for which it holds that

$$\int_\Omega f(x) \mathrm{D}^\alpha \varphi(x)\,\mathrm{d}x = (-1)^{|\alpha|} \int_\Omega f_\alpha(x)\varphi(x)\,\mathrm{d}x, \quad \text{for all } \varphi \in \mathcal{C}_0^\infty(\Omega), \tag{1.3.5}$$

with $|\alpha| := \sum_{i=1}^d \alpha_i$. The weak derivative is unique up to sets of measure zero. If $f \in \mathcal{C}^k(\Omega)$, $k \in \mathbb{N}$ the classical derivative of f is contained in the equivalence class of weak derivatives. Thus, weak derivatives can be seen as a consistent extension of the classical derivatives. Consequently, we shall not distinguish between the two and write $\mathrm{D}^\alpha f := f_\alpha$.

For $k \in \mathbb{N}_0$ and $1 \le p \le \infty$ we define the *Sobolev spaces of integer order*

$$W_p^k(\Omega) := \{f \in L_p(\Omega) : \mathrm{D}^\alpha f \in L_p(\Omega), |\alpha| \le k\}, \tag{1.3.6}$$

as the spaces of all functions in $L_p(\Omega)$ with weak derivatives up to order k in $L_p(\Omega)$. Equipped with the norms

$$||f||_{W_p^k(\Omega)} := \begin{cases} \left(\sum_{|\alpha| \le k} ||\mathrm{D}^\alpha f||_{L_p(\Omega)}^p \right)^{1/p} & , \quad 1 \le p < \infty, \\ \max_{|\alpha| \le k} ||\mathrm{D}^\alpha f||_{L_\infty(\Omega)} & , \quad p = \infty \end{cases}, \tag{1.3.7}$$

the Sobolev spaces become Banach spaces, see [1, Theorem 3.3]. They are separable if $1 \le p < \infty$ and reflexive if $1 < p < \infty$, see [1, Theorem 3.6]. For the special case $p = 2$ we even obtain a separable Hilbert space

$$H^k(\Omega) := W_2^k(\Omega), \tag{1.3.8}$$

with inner product

$$\langle f, g \rangle_{H^k(\Omega)} = \sum_{|\alpha| \le k} \langle \mathrm{D}^\alpha f, \mathrm{D}^\alpha g \rangle_{L_2(\Omega)}. \tag{1.3.9}$$

Up to this point we have defined Sobolev spaces only for $k \in \mathbb{N}_0$. To define *Sobolev spaces of fractional order* $s \in \mathbb{R}^+ \backslash \mathbb{N}$, we split $s = k + \sigma$ with $k \in \mathbb{N}_0$ and $0 < \sigma < 1$. Then, for $1 \le p < \infty$, the spaces $W_p^s(\Omega)$ are the set of all functions in $L_p(\Omega)$, for which the norm

$$||f||_{W_p^s(\Omega)} := \left(||f||_{W_p^k(\Omega)}^p + \sum_{|\alpha| = k} \int_\Omega \int_\Omega \frac{|\mathrm{D}^\alpha f(x) - \mathrm{D}^\alpha f(y)|^p}{|x - y|^{d + p\sigma}}\,\mathrm{d}x\,\mathrm{d}y \right)^{1/p} \tag{1.3.10}$$

is finite. In the literature they are also sometimes referred to as *Sobolev-Slobodeckij spaces*. Again, these spaces are Banach spaces (cf. [1, Chapter 7]) and $H^s(\Omega) := W_2^s(\Omega)$ is a Hilbert space with inner product

$$\langle f, g\rangle_{H^s(\Omega)} := \langle f, g\rangle_{H^k(\Omega)} + \sum_{|\alpha|=k} \int_\Omega \int_\Omega \frac{(\mathrm{D}^\alpha f(x) - \mathrm{D}^\alpha f(y))\overline{(\mathrm{D}^\alpha g(x) - \mathrm{D}^\alpha g(y))}}{|x-y|^{d+2\sigma}} \,\mathrm{d}x \,\mathrm{d}y. \tag{1.3.11}$$

Since we would like to use Sobolev spaces as an approach to solve boundary value problems we have to state what we mean by a restriction $f_{|\partial\Omega}$ of a function $f \in W_p^s(\Omega)$ to the boundary $\partial\Omega$ for a bounded domain Ω. This is not directly clear, because functions in Sobolev spaces are only unique up to sets of Lebesgue measure zero. One way to deal with it, is to define $W_{0,p}^s(\Omega)$, for $s \geq 0$ and $1 \leq p \leq \infty$, as the closure of all test functions in $W_p^s(\Omega)$ and set $H_0^s(\Omega) := W_{0,p}^s(\Omega)$. We write the dual of $H_0^s(\Omega)$ as $H^{-s}(\Omega) := (H_0^s(\Omega))'$. Note that these spaces consist of distributions. If the boundary $\partial\Omega$ is k-times Hölder continuous, $k \in \mathbb{N}_0$, $1 < p < \infty$, $\frac{1}{p} < s \leq k+1$ and $s - \frac{1}{p}$ is not an integer, then we can make use of the continuous *trace operator*

$$\mathrm{Tr} : W_p^s(\Omega) \to W_p^{s-1/p}(\partial\Omega), \tag{1.3.12}$$

which is defined as the unique extension from $C^\infty(\overline{\Omega})$ to $W_p^s(\Omega)$ of the restriction operator $f \mapsto f_{|\partial\Omega}$ (see [72, Theorem 1.5.1.2] for existence and uniqueness). For more details about Sobolev spaces on surfaces, we refer to [72, Subsection 1.3.3] and [75, Subsection 6.2.5]. The trace operator leads to the alternative characterization

$$W_{0,p}^s(\Omega) = \{f \in W_p^s(\Omega) : \mathrm{Tr}(\mathrm{D}^\alpha f) = 0,\ |\alpha| \leq \lfloor s - 1/p \rfloor\}, \tag{1.3.13}$$

see [72, Corollary 1.5.1.6].

There are cases, where we want to consider zero boundary conditions only on subsets of the boundary $\partial\Omega$. Therefore, we define for $\Gamma \subset \partial\Omega$ and $s > 0$ the spaces

$$W_{\Gamma,p}^s(\Omega) := \mathrm{clos}_{W_p^s(\Omega)}\{f \in W_p^s(\Omega) \cap C^\infty(\Omega) : \operatorname{supp} f \cap \Gamma = \emptyset\}. \tag{1.3.14}$$

If the boundary $\partial\Omega$ consists solely of discrete points $b_1, \ldots, b_r$, $r \in \mathbb{N}$, e.g. in the case of an interval domain, and $\Gamma \subset \{b_1, \ldots, b_r\}$, we slightly adapt the notation in (1.3.14). For $s \in [0, \infty) \setminus (\mathbb{N}_0 + \{\frac{1}{2}\})$, $\vec{\sigma} = (\sigma_1, \ldots, \sigma_r) \in \{0, \lfloor s + 1 - \frac{1}{p} \rfloor\}^r$ and $\sigma_i = \lfloor s + 1 - \frac{1}{p} \rfloor$ if and only if $b_i \in \Gamma$, we define

$$W_{\vec{\sigma},p}^s(\Omega) := W_{\Gamma,p}^s(\Omega). \tag{1.3.15}$$

For the case $p = 2$ we use the notations $H_\Gamma^s(\Omega) := W_{\Gamma,2}^s(\Omega)$ and $H_{\vec{\sigma}}^s(\Omega) := W_{\vec{\sigma},2}^s(\Omega)$.

Since $\mathcal{C}_0^\infty(\Omega)$ is continuously and densely embedded in $L_p(\Omega)$, $1 \leq p < \infty$, it is obvious that $H_0^s(\Omega)$ is continuously and densely embedded in $L_2(\Omega)$. Identifying $L_2(\Omega)$ with $(L_2(\Omega))'$ via the Riesz isomorphism leads to the triple

$$H_0^s(\Omega) \subset L_2(\Omega) \subset H^{-s}(\Omega) \tag{1.3.16}$$

of continuously and densely embedded subsets. Such a structure consisting of Banach spaces H, H' at the left and right and a Hilbert space $\mathcal{V}$ in the middle is called *Gelfand triple*, written as $(H, \mathcal{V}, H')$. It is crucial for the discretization of boundary value problems. Note that in this thesis H is always a Hilbert space. The distributional space $H^{-s}(\Omega)$ is equipped with the norm

$$||g||_{H^{-s}(\Omega)} := \sup\left\{\frac{|\langle g, f\rangle_{H^{-s}(\Omega)\times H_0^s(\Omega)}|}{||f||_{H^s(\Omega)}} : 0 \neq f \in H_0^s(\Omega)\right\}, \tag{1.3.17}$$

where the dual form $\langle\cdot,\cdot\rangle_{H^{-s}(\Omega)\times H_0^s(\Omega)}$ is the unique continuous extension of the inner product $\langle\cdot,\cdot\rangle_{L_2(\Omega)}$.

1.4 Weak formulation

In this section, we reconsider the boundary value problem (1.2.4), (1.2.7) and show how to derive at a *weak formulation*. We roughly follow [75, Section 7.2].

By (1.3.13) for $p = 2$ and $s = t$ we see that every classical solution u of (1.2.4), (1.2.7) lies in $\mathcal{C}^{2t}(\Omega) \cap H_0^t(\Omega)$. To obtain a weak formulation, we integrate Lu against a test function $v \in \mathcal{C}_0^\infty(\Omega)$ and use partial integration to arrive at

$$\begin{aligned}\langle Lu, v\rangle_{L_2(\Omega)} &= \sum_{|\alpha|\le t}\sum_{|\beta|\le t}(-1)^{|\beta|}\int_\Omega \mathrm{D}^\beta\left(a_{\alpha,\beta}(x)\mathrm{D}^\alpha u(x)\right)v(x)\,\mathrm{d}x\\ &= \sum_{|\alpha|\le t}\sum_{|\beta|\le t}\int_\Omega a_{\alpha,\beta}(x)\mathrm{D}^\alpha u(x)\mathrm{D}^\beta v(x)\,\mathrm{d}x =: a(u,v).\end{aligned} \tag{1.4.1}$$

The afore defined $a(\cdot,\cdot)$ is a bilinear form on $H_0^t(\Omega)\times\mathcal{C}_0^\infty(\Omega)$. For coefficients $a_{\alpha,\beta} \in L_\infty(\Omega)$, the bilinear form $a(\cdot,\cdot)$ is bounded and since $\mathcal{C}_0^\infty(\Omega)$ is dense in $H_0^t(\Omega)$ it has a unique and continuous extension in $H_0^t(\Omega)\times H_0^t(\Omega)$, cf. [75, Theorem 7.2.2]. From now on, we mean this extension if we talk about $a(\cdot,\cdot)$. This leads to the estimate

$$a(u,v) \le C_a||u||_{H^t(\Omega)}||v||_{H^t(\Omega)}, \quad \text{for all } u, v \in H_0^t(\Omega), \tag{1.4.2}$$

with a constant $C_a > 0$. If we assume $g \in L_2(\Omega)$, the expression

$$f(v) := \int_\Omega g(x)v(x)\,\mathrm{d}x \tag{1.4.3}$$

is well-defined for $v \in H_0^t(\Omega)$. The weak or *variational* formulation of (1.2.4), (1.2.7) can now be expressed as:

$$\text{Find a } u \in H_0^t(\Omega) \text{ such that } a(u,v) = f(v) \text{ for all } v \in H_0^t(\Omega). \tag{1.4.4}$$

There exists a unique Operator $\mathcal{L} : H_0^t(\Omega) \to H^{-t}(\Omega)$ defined by $\mathcal{L}u := a(u,\cdot)$ for all $u \in H_0^t(\Omega)$. This makes it possible to rewrite (1.4.4) as an operator equation

$$\mathcal{L}u = f, \tag{1.4.5}$$

where $f \in H^{-t}(\Omega)$. Note that in (1.4.5) it is not necessary any more that the distribution f is induced by an element of $L_2(\Omega)$. If we assume the bounded bilinear form $a(\cdot,\cdot)$ to be $H_0^t(\Omega)$-elliptic, i.e., there exists a constant $c_a > 0$ such that

$$a(v,v) \geq c_a ||v||_{H^t(\Omega)}^2, \quad \text{for all } v \in H_0^t(\Omega), \tag{1.4.6}$$

we derive together with (1.4.2) at

$$c_a ||v||_{H^t(\Omega)} \leq ||\mathcal{L}v||_{H^{-t}(\Omega)} \leq C_a ||v||_{H^t(\Omega)}, \quad \text{for all } v \in H_0^t(\Omega).$$

Hence $\mathcal{L}$ is an elliptic operator, cf. (1.0.2). Consequently, the elliptic operator equation (1.4.5) has a unique solution $u \in H_0^t(\Omega)$ with $||u||_{H_0^t(\Omega)} \leq C_E^{-1} ||f||_{H^{-t}(\Omega)}$. The following theorem gives a sufficient condition for the bilinear form $a(\cdot,\cdot)$ to be $H_0^t(\Omega)$-elliptic.

Theorem 1.2. *[75, Theorem 7.2.7] Let $a_{\alpha,\beta}$ be constant for $|\alpha| = |\beta| = t$. Furthermore, let $a_{\alpha,\beta} \equiv 0$ for $0 < |\alpha| + |\beta| \leq 2t - 1$ and $a_{0,0}(x) \geq 0$ for all $x \in \Omega$. Assume that the operator L is uniformly elliptic in the sense of (1.2.3). Then, the bilinear form $a(\cdot,\cdot)$ is $H_0^t(\Omega)$-elliptic.*

For the existence of a weak solution it is sufficient to demand $a(\cdot,\cdot)$ to be $H_0^t(\Omega)$-*coercive*, i.e., there exist constants $C_1 > 0$ and $C_2 \in \mathbb{R}$ such that

$$a(v,v) \geq C_1 ||v||_{H^t(\Omega)}^2 - C_2 ||v||_{L_2(\Omega)}^2, \quad \text{for all } v \in H_0^t(\Omega). \tag{1.4.7}$$

For details we refer to [75, Sections 6.5, 7.2]. Nevertheless, in this thesis we assume $a(\cdot,\cdot)$ to be $H_0^t(\Omega)$-elliptic. To close the first chapter, let us give examples of some common linear elliptic partial differential equations and examine how they fit in the setting presented in this section.

Example 1.3 (Poisson equation)**.** *The Poisson equation with homogeneous boundary conditions is perhaps the most basic and often-quoted example of a linear elliptic boundary value problem. It is given by*

$$\begin{aligned} -\Delta u &= f \quad \text{in } \Omega, \\ u &= 0 \quad \text{on } \partial\Omega. \end{aligned} \tag{1.4.8}$$

The Laplace operator, which reads as $\Delta := \sum_{i=1}^d \frac{\partial^2}{\partial x_i^2}$, is a general linear partial differential operator of order 2 and $-\Delta$ can be written in divergence form (1.2.1) with non-trivial coefficients $a_{\alpha,\beta} \equiv 1$ when $\alpha = \beta$ and $|\alpha| = 1$. Obviously the negative Laplace Operator is uniformly elliptic in the sense of (1.2.3). Hence the associated bilinear form

$$a(u,v) = \int_\Omega \langle \nabla u(x), \nabla v(x) \rangle \, \mathrm{d}x \tag{1.4.9}$$

is $H_0^1(\Omega)$-elliptic, see Theorem 1.2.

Example 1.4. *Another linear elliptic boundary value problem of order 2 is given by the Helmholtz equation with homogeneous boundary conditions:*

$$\begin{aligned} -\Delta u + u &= f \quad \text{in } \Omega, \\ u &= 0 \quad \text{on } \partial\Omega. \end{aligned} \tag{1.4.10}$$

The non-trivial coefficients of $-\Delta u + u$ in divergence form are $a_{\alpha,\beta} \equiv 1$ when $\alpha = \beta$ and $|\alpha| = 1$ as well as $a_{0,0} \equiv 1$. The uniform ellipticity and the assumptions in Theorem 1.2 are fulfilled, which assures the $H_0^1(\Omega)$-ellipticity of the corresponding bilinear form

$$a(u, v) = \int_\Omega \langle \nabla u(x), \nabla v(x) \rangle + u(x)v(x)\, \mathrm{d}x. \tag{1.4.11}$$

Example 1.5. *The biharmonic equation with homogeneous boundary condition reads as*

$$\begin{aligned} \Delta^2 u &= f \quad \text{in } \Omega, \\ u = \tfrac{\partial u}{\partial n} &= 0 \quad \text{on } \partial\Omega. \end{aligned} \tag{1.4.12}$$

The operator Δ^2 of order 4 can be written in divergence form with non-trivial coefficients $a_{\alpha,\beta} \equiv 1$ when $\alpha = \beta$ and $|\alpha| = 2$. Analogue to Example 1.3, we obtain a $H_0^2(\Omega)$-elliptic bilinear form

$$a(u, v) = \int_\Omega \Delta u(x) \Delta v(x)\, \mathrm{d}x. \tag{1.4.13}$$

Chapter 2

Frames and Riesz Bases

In this chapter, we introduce frames and Riesz bases and their basic properties in an abstract fashion. Furthermore, with Gelfand frames, we present a special class of frames and show how they are used to obtain a discretization of operator equations. For further information on frames and Riesz bases we refer to [23, 24].

In the following sections, we assume $\mathcal{I}$ to be a countable index set and H a separable Hilbert space with inner product $\langle\cdot,\cdot\rangle_H$ and induced norm $\|\cdot\|_H := \langle\cdot,\cdot\rangle_H^{1/2}$. Let us recall that the sequence spaces $\ell_p(\mathcal{I})$, $0 < p \leq \infty$ are defined as the spaces of all real- or complex-valued sequences $\mathbf{c} := \{c_\lambda\}_{\lambda\in\mathcal{I}}$ such that

$$\|\mathbf{c}\|_{\ell_p(\mathcal{I})} := \begin{cases} \Big(\sum\limits_{\lambda\in\mathcal{I}} |c_\lambda|^p\Big)^{1/p} & , \quad 0 < p < \infty, \\ \sup\limits_{\lambda\in\mathcal{I}} |c_\lambda| & , \quad p = \infty \end{cases} \tag{2.0.1}$$

is finite. Throughout this thesis, we assume the sequences to be real-valued. For $p \geq 1$, the spaces are Banach spaces whereas they are quasi-Banach spaces for $0 < p < 1$. In the special case $p = 2$, we even get a Hilbert space with inner product $\langle\mathbf{c},\mathbf{d}\rangle_{\ell_2(\mathcal{I})} := \sum_{\lambda\in\mathcal{I}} c_\lambda d_\lambda$.

2.1 Frames for Hilbert spaces

Before we introduce the concept of a frame, we roll out the weaker concept of a *Bessel system* for H, i.e., a system $\mathcal{F} = \{f_\lambda\}_{\lambda\in\mathcal{I}} \subset H$ satisfying the condition

$$\|\left\{\langle g, f_\lambda\rangle_{H'\times H}\right\}_{\lambda\in\mathcal{I}}\|_{\ell_2(\mathcal{I})}^2 \leq B\|g\|_{H'}^2 \tag{2.1.1}$$

for a constant $B > 0$ and all $g \in H'$. One can show that $\mathcal{F}$ is a Bessel system if and only if its *synthesis operator*

$$F_{\mathcal{F}} : \ell_2(\mathcal{I}) \to H, \quad \mathbf{c} \mapsto \sum_{\lambda\in\mathcal{I}} c_\lambda f_\lambda \tag{2.1.2}$$

is well-defined and bounded. In the course of this thesis, we drop the subscript $\mathcal{F}$ in (2.1.2) whenever it is clear from the context to which Bessel system the synthesis operator belongs. Actually, it is enough to require the synthesis operator to be well-defined, as the boundedness follows by an application of the Banach-Steinhaus theorem, see Section 3.2 in [24] for details. The synthesis operator F of a Bessel system does not need to be surjective. Hence, it is possible that there exist $f \in H$ without any series representation in terms of $\mathcal{F}$. Due to that, we introduce the fundamental concept of frames for Hilbert spaces.

Definition 2.1. A system $\mathcal{F} = \{f_\lambda\}_{\lambda\in\mathcal{I}} \subset H$ is a (Hilbert) frame for H if there exist constants $A, B > 0$ such that

$$A\|g\|_{H'}^2 \leq \| \{\langle g, f_\lambda\rangle_{H'\times H}\}_{\lambda\in\mathcal{I}} \|_{\ell_2(\mathcal{I})}^2 \leq B\|g\|_{H'}^2 \tag{2.1.3}$$

holds for all $g \in H'$.

The constants A and B are called *frame bounds*. Obviously, they are not unique. The *optimal lower frame bound* is the supremum over all lower frame bounds whereas the *optimal upper frame bound* is the infimum over all upper frame bounds. If they coincide, we call the frame *tight*. Let us mention that the optimal bounds are actually frame bounds. The aforementioned characterization via the operator F can be shown.

Theorem 2.2. *[24, Theorem 5.5.1] A system $\mathcal{F} = \{f_\lambda\}_{\lambda\in\mathcal{I}} \subset H$ is a frame for H if and only if the synthesis operator F is well-defined and surjective.*

If $\mathcal{F}$ is a frame for H, Theorem 2.2 states that every $f \in H$ has a series representation $\sum_{\lambda\in\mathcal{I}} c_\lambda f_\lambda$. However, the synthesis operator of a frame is not necessarily injective, hence, the representation of an element in H as a linear combination of frame elements is not unique in general. If we consider the expansion coefficients with the smallest possible ℓ_2-norm, we end up with another characterization of frames.

Proposition 2.3. *[109, Proposition 2.2] A system $\mathcal{F} = \{f_\lambda\}_{\lambda\in\mathcal{I}} \subset H$ is a frame for H if and only if*

(i) $\operatorname{clos}_H(\operatorname{span}(\mathcal{F})) = H$ *and*

(ii) $B^{-1}\|f\|_H^2 \leq \inf_{\{\mathbf{c}\in\ell_2(\mathcal{I}),\ F\mathbf{c}=f\}} \|\mathbf{c}\|_{\ell_2(\mathcal{I})}^2 \leq A^{-1}\|f\|_H^2,$ *for all $f \in H$.*

Our next aim is to establish a *frame decomposition* for elements in H. For that purpose, we introduce the adjoint operator of F, which is called *analysis operator* and is given by

$$F_{\mathcal{F}}^* : H' \to \ell_2(\mathcal{I}), \quad g \mapsto \{\langle g, f_\lambda\rangle_{H'\times H}\}_{\lambda\in\mathcal{I}}. \tag{2.1.4}$$

For a frame $\mathcal{F}$ the analysis operator is bounded and injective. We obtain the *frame operator* S by composing F and F^*:

$$S_{\mathcal{F}} : H' \to H, \quad g \mapsto S_{\mathcal{F}}g := F_{\mathcal{F}}F_{\mathcal{F}}^*g = \sum_{\lambda\in\mathcal{I}} \langle g, f_\lambda\rangle_{H'\times H} f_\lambda. \tag{2.1.5}$$

Again, the subscript $\mathcal{F}$ in (2.1.4) and (2.1.5) is dropped if it is appropriate.

Remark 2.4. In some cases, it is appropriate to identify a Hilbert space H with its dual Hilbert space H' via the Riesz mapping. Then, (2.1.3) becomes

$$A\|f\|_H^2 \le \| \{\langle f, f_\lambda\rangle_H\}_{\lambda\in\mathcal{I}} \|_{\ell_2(\mathcal{I})}^2 \le B\|f\|_H^2 \tag{2.1.6}$$

for all $f \in H$. Moreover, the analysis and frame operator become

$$F^* : H \to \ell_2(\mathcal{I}),\ f \mapsto \{\langle f, f_\lambda\rangle_H\}_{\lambda\in\mathcal{I}}, \quad S : H \to H,\ f \mapsto \sum_{\lambda\in\mathcal{I}} \langle f, f_\lambda\rangle_H f_\lambda, \tag{2.1.7}$$

respectively.

The importance of the frame operator becomes clear in the following lemma and theorem:

Lemma 2.5. *[24, Lemma 5.1.5] Let $\mathcal{F} = \{f_\lambda\}_{\lambda\in\mathcal{I}}$ be a frame for H with frame operator S and frame bounds A, B. Then, the following hold:*

(i) The frame operator S is boundedly invertible, self-adjoint and positive definite.

(ii) The system $S^{-1}\mathcal{F} = \{S^{-1}f_\lambda\}_{\lambda\in\mathcal{I}}$ is a frame for H' with frame bounds B^{-1}, A^{-1} and frame operator S^{-1}. It is called the canonical dual frame *of $\mathcal{F}$.*

Since the operator S^{-1} is self-adjoint we obtain the very important frame decomposition:

Theorem 2.6. *[24, Theorem 5.1.6] Let $\mathcal{F} = \{f_\lambda\}_{\lambda\in\mathcal{I}}$ be a frame for H with frame operator S. Then*

$$f = \sum_{\lambda\in\mathcal{I}} \langle S^{-1}f_\lambda, f\rangle_{H'\times H}\, f_\lambda, \quad \textit{for all } f \in H, \tag{2.1.8}$$

and

$$g = \sum_{\lambda\in\mathcal{I}} \langle g, f_\lambda\rangle_{H'\times H} S^{-1} f_\lambda, \quad \textit{for all } g \in H'. \tag{2.1.9}$$

As mentioned before, the coefficients in (2.1.8) are not unique in general. If there exist other decompositions than (2.1.8), we denote the frame $\mathcal{F}$ as *redundant* or *overcomplete*. Frames $\tilde{\mathcal{F}} = \{\tilde{f}_\lambda\}_{\lambda\in\mathcal{I}} \neq S^{-1}\mathcal{F}$ in H', for which

$$f = \sum_{\lambda\in\mathcal{I}} \langle \tilde{f}_\lambda, f\rangle_{H'\times H}\, f_\lambda, \quad \text{for all } f \in H, \tag{2.1.10}$$

are called *non-canonical dual frames* or just *dual frames* of $\mathcal{F}$. Obviously, for dual frames of $\mathcal{F}$, the relation

$$g = \sum_{\lambda\in\mathcal{I}} \langle g, f_\lambda\rangle_{H'\times H} \tilde{f}_\lambda, \quad \text{for all } g \in H', \tag{2.1.11}$$

holds as well. Let $\tilde{F}$ and $\tilde{F}^*$ be the synthesis and the analysis operator of $\tilde{\mathcal{F}}$, respectively. Then, (2.1.10) and (2.1.11) can be expressed in operator form as

$$F\tilde{F}^* = \mathrm{id}_H, \quad F^*\tilde{F} = \mathrm{id}_{H'}, \tag{2.1.12}$$

respectively. A characterization of all dual frames is possible.

Proposition 2.7. *[24, Theorem 6.3.7] Let $\mathcal{F} = \{f_\lambda\}_{\lambda\in\mathcal{I}}$ be a frame for H. The dual frames of $\mathcal{F}$ are precisely the families*

$$\{\tilde{f}_\lambda\}_{\lambda\in\mathcal{I}} = \left\{ S^{-1}f_\lambda + h_\lambda - \sum_{\mu\in\mathcal{I}} \langle S^{-1}f_\lambda, f_\mu\rangle_{H'\times H}\, h_\mu \right\}_{\lambda\in\mathcal{I}}, \tag{2.1.13}$$

where $\{h_\lambda\}_{\lambda\in\mathcal{I}}$ are Bessel systems in H'.

If it is hard to get access to the canonical dual frame , one way out is to look for other dual frames which are easier to find or have better properties for our purposes. One characteristic feature of the canonical dual frame is, that the correspondent frame coefficients $\{\langle S^{-1}f_\lambda, f\rangle_{H'\times H}\}_{\lambda\in\mathcal{I}}$ have minimal $\ell_2(\mathcal{I})$-norm among all sequences satisfying (2.1.10). This becomes obviously clear since for all $\{c_\lambda\}_{\lambda\in\mathcal{I}} \in \ell_2(\mathcal{I})$ with $f = \sum_{\lambda\in\mathcal{I}} c_\lambda f_\lambda$ it holds

$$\sum_{\lambda\in\mathcal{I}} |c_\lambda|^2 = \sum_{\lambda\in\mathcal{I}} |\langle S^{-1}f_\lambda, f\rangle_{H'\times H}|^2 + \sum_{\lambda\in\mathcal{I}} |c_\lambda - \langle S^{-1}f_\lambda, f\rangle_{H'\times H}|^2. \tag{2.1.14}$$

For a proof of (2.1.14) see [24, Lemma 5.4.2]. While in this sense the canonical dual frame can be seen as the most economical among all distinct dual frames, maybe one is interested in other features, e.g., wavelet structure of the dual frame or maximal sparsity of the frame coefficients. For these purposes, it is possible that better weapons of choice than the canonical dual frame are available. In practical applications, it is often difficult to determine the operator S^{-1} and, in addition, there is no warranty that the canonical dual frame $S^{-1}\mathcal{F}$ inherits any properties of the frame $\mathcal{F}$. For example, there exist frames consisting of functions in $\mathcal{C}^k(\mathbb{R})$ where the canonical dual frame elements are not even continuous, cf. [58, Sections 3.3]. Examples where non-canonical dual frames are comparably easy to find are given in [24, Sections 12.5, 18.8]. In the following proposition, we see that a projection can be built out of the synthesis, inverse frame and analysis operator. Among other things, we need this projector in Section 2.5 to describe the solution set of discretized versions of operator equations.

Proposition 2.8. *Let $\mathcal{F} = \{f_\lambda\}_{\lambda\in\mathcal{I}}$ be a frame for a Hilbert space H. Then, the operator*

$$\mathbf{Q} := F^*S^{-1}F : \ell_2(\mathcal{I}) \mapsto \ell_2(\mathcal{I}) \tag{2.1.15}$$

is the orthogonal projection onto $\mathrm{ran}(F^*)$*, i.e.,* $\ker(\mathbf{Q}) = \ker(F)$ *and* $\mathrm{ran}(\mathbf{Q}) = \mathrm{ran}(F^*)$.

Proof. As a composition of bounded operators $F : \ell_2(\mathcal{I}) \mapsto H$, $S^{-1} : H \to H'$ and $F^* : H' \mapsto \ell_2(\mathcal{I})$, the operator $\mathbf{Q}$ is bounded from $\ell_2(\mathcal{I})$ to $\ell_2(\mathcal{I})$. From (2.1.5) we infer that

$$(F^*S^{-1}F)(F^*S^{-1}F) = (F^*S^{-1})(FF^*S^{-1})F = F^*S^{-1}F.$$

Hence, $\mathbf{Q}$ is a projector. Since F^* and S^{-1} are injective we have $\ker(\mathbf{Q}) = \ker(F)$. The surjectivity of F and S^{-1} gives $\operatorname{ran}(\mathbf{Q}) = \operatorname{ran}(F^*)$. Since $\ell_2(\mathcal{I}) = \ker(F) \oplus^\perp \operatorname{ran}(F^*)$ is an orthogonal decomposition of $\ell_2(\mathcal{I})$, the claim follows. □

Frames are still a topic of research and have a lot of applications in different fields of mathematics. Some prominent examples are wavelet frames on $\mathbb{R}^d$ (see [58, Section 3.3], [24, Chapter 18]) or bounded domains (see [109]), or *Gabor frames* (see [24, Chapter 12], [73, Chapter 5]).

2.2 Riesz bases

We now introduce a subclass of frames which is also numerically stable but allows for unique representations in terms of series expansions for every function $f \in H$.

Definition 2.9. A system $\mathcal{F} = \{f_\lambda\}_{\lambda\in\mathcal{I}} \subset H$ is a Riesz basis for H if

$$\operatorname{clos}_H(\operatorname{span}(\mathcal{F})) = H$$

and there exist constants $A, B > 0$ such that

$$A||\mathbf{c}||^2_{\ell_2(\mathcal{I})} \leq ||\sum_{\lambda\in\mathcal{I}} c_\lambda f_\lambda||^2_H \leq B||\mathbf{c}||^2_{\ell_2(\mathcal{I})} \tag{2.2.1}$$

holds for all $\mathbf{c} = \{c_\lambda\}_{\lambda\in\mathcal{I}} \in \ell_2(\mathcal{I})$.

The constants A, B are called *Riesz bounds*. Similar to the frame bounds, they are not unique. *Optimal Riesz bounds* are defined analogously to the frame case. Specifics about the relations between Riesz bases and frames can be found in [24, Section 5.4, Chapter 7]. The first important result, which is not totally obvious by looking at the definitions, is that indeed every Riesz basis is a frame.

Proposition 2.10. *A Riesz basis $\mathcal{F} = \{f_\lambda\}_{\lambda\in\mathcal{I}}$ for H is also a frame for H, and the optimal Riesz bounds coincide with the optimal frame bounds.*

For a proof of the latter see [24, Theorem 5.4.1]. The other way round, not every frame is a Riesz basis. However, one can give some equivalent conditions for a frame to be a Riesz basis, cf. [24, Theorem 7.1.1].

Theorem 2.11. *Let $\mathcal{F} = \{f_\lambda\}_{\lambda\in\mathcal{I}}$ be a frame for H. Then, $\mathcal{F}$ is also a Riesz basis for H if one of the following conditions hold:*

(i) $\ker F = \{0\}$.

(ii) There exists a biorthogonal sequence $\tilde{\mathcal{F}} = \{\tilde{f}_\lambda\}_{\lambda\in\mathcal{I}} \in H'$, *i.e.*, $\langle \tilde{f}_\lambda, f_\mu\rangle_{H'\times H} = \delta_{\lambda,\mu}$ *for all* $\lambda, \mu \in \mathcal{I}$.

(iii) For each $f \in H$ there exists a unique sequence $\mathbf{c}(f) = \{c_\lambda(f)\}_{\lambda\in\mathcal{I}} \in \ell_2(\mathcal{I})$, *such that* $f = \sum_{\lambda\in\mathcal{I}} c_\lambda(f) f_\lambda$.

A system satisfying Theorem 2.11 (iii) is called a *Schauder basis*. Via the following well-known statement about Schauder bases, we see how part (ii) and (iii) of Theorem 2.11 are connected.

Theorem 2.12. *[24, Theorem 3.3.2] Let $\mathcal{F} = \{f_\lambda\}_{\lambda\in\mathcal{I}}$ be a Schauder basis for H. Then, there exists a unique system $\tilde{\mathcal{F}} = \{\tilde{f}_\lambda\}_{\lambda\in\mathcal{I}} \in H'$ for which*

$$f = \sum_{\lambda\in\mathcal{I}} \langle \tilde{f}_\lambda, f\rangle_{H'\times H} f_\lambda, \quad \text{for all } f \in H. \tag{2.2.2}$$

The system $\tilde{\mathcal{F}}$ is a Schauder basis for H', and $\mathcal{F}$ and $\tilde{\mathcal{F}}$ are biorthogonal sequences.

Since every Riesz basis is a frame, we gather from (2.1.8) and (2.2.2) that the system $\tilde{\mathcal{F}}$ in Theorem 2.11 (ii) is given through $\{S^{-1}f_\lambda\}_{\lambda\in\mathcal{I}}$. It is a Riesz basis for H' and is called the *dual Riesz basis*. Accordingly, the biorthogonal sequence $\mathbf{c}(f)$ in Theorem 2.11 (iii) is $\{\langle S^{-1}f_\lambda, f\rangle\}_{H'\times H}$. Summarizing, we can state that Riesz bases are exactly the frames which are non-redundant and therefore allow for unique representations. In Chapter 3, we present wavelet Riesz bases as a special kind of Riesz bases.

2.3 Function systems and operators

In this section, we are going to collect some basic facts about Bessel systems, frames and Riesz bases and their interaction with operators on Hilbert spaces. The results of this section will be of particular interest in Chapter 6, where we are going to construct quarklet frames on general bounded domains.

The following proposition deals with unions of Bessel systems, frames and Riesz bases.

Proposition 2.13. *Let H be a Hilbert space. Then, it holds:*

(i) The disjoint union of finitely many Bessel systems for H is a Bessel system for H.

(ii) A frame for H disjointedly united with a Bessel system for H is a frame for H.

(iii) A Bessel system for H which includes a Riesz basis for H is a frame for H.

Proof. Let $g \in H'$. To prove (i), we assume $\mathcal{B}_i = \{b_\lambda\}_{\lambda\in\mathcal{I}_i} \subset H$, $i = 1, \dots, n$, to be disjoint Bessel systems for H with Bessel bounds $B_i > 0$, $i = 1, \dots, n$. Let $\mathcal{B} = \dot{\bigcup}_{i=1}^n \mathcal{B}_i$ and $\mathcal{I} = \dot{\bigcup}_{i=1}^n \mathcal{I}_i$. Then, we have

$$\| \{\langle g, b_\lambda\rangle_{H'\times H}\}_{\lambda\in\mathcal{I}} \|_{\ell_2(\mathcal{I})}^2 = \sum_{i=1}^n \| \{\langle g, b_\lambda\rangle_{H'\times H}\}_{\lambda\in\mathcal{I}_i} \|_{\ell_2(\mathcal{I}_i)}^2 \le \sum_{i=1}^n B_i \|g\|_{H'}^2. \tag{2.3.1}$$

For (ii), we assume $\mathcal{F} = \{f_\lambda\}_{\lambda\in\mathcal{I}_1}$ and $\mathcal{B} = \{f_\lambda\}_{\lambda\in\mathcal{I}_2}$ to be disjoint and a frame respectively a Bessel system for H. As every frame is a Bessel system, the right-hand inequality of (2.1.3) follows immediately from (i). For the left-hand inequality we write

$$\| \{\langle g, f_\lambda\rangle_{H'\times H}\}_{\lambda\in\mathcal{I}_1\dot\cup\mathcal{I}_2} \|^2_{\ell_2(\mathcal{I}_1\dot\cup\mathcal{I}_2)} \geq \| \{\langle g, f_\lambda\rangle_{H'\times H}\}_{\lambda\in\mathcal{I}_1} \|^2_{\ell_2(\mathcal{I}_1)} \geq A\|g\|^2_{H'},$$

with $A > 0$ a lower frame bound of $\mathcal{F}$. For the proof of part (iii), we consider a countable index set $\mathcal{I}_R \subset \mathcal{I}$ and a Bessel system $\mathcal{B} = \{b_\lambda\}_{\lambda\in\mathcal{I}}$ for H which contains a Riesz basis $\mathcal{R} = \{b_\lambda\}_{\lambda\in\mathcal{I}_R}$ for H. We only have to show the left-hand inequality in (2.1.3). We write

$$\| \{\langle g, b_\lambda\rangle_{H'\times H}\}_{\lambda\in\mathcal{I}} \|^2_{\ell_2(\mathcal{I})} \geq \| \{\langle g, b_\lambda\rangle_{H'\times H}\}_{\lambda\in\mathcal{I}_R} \|^2_{\ell_2(\mathcal{I}_R)} \geq A\|g\|^2_{H'\times H},$$

with $A > 0$ a lower Riesz bound of $\mathcal{R}$. To perform the last estimate, we have used the fact that every Riesz basis is also a frame. □

To conclude this section, we state a proposition which considers the image of frames, Bessel systems and Riesz bases under certain operators.

Proposition 2.14. *Let H_1 and H_2 be Hilbert spaces and $U : H_1 \mapsto H_2$ a linear operator. Then, it holds:*

(i) If $\mathcal{B}$ is a Bessel system for H_1 and U is bounded, then $U\mathcal{B}$ is a Bessel system for H_2.

(ii) If $\mathcal{F}$ is a frame for H_1 and U is bounded and surjective, then $U\mathcal{F}$ is a frame for H_2.

(iii) If $\mathcal{R}$ is a Riesz bases for H_1 and U is bounded and invertible, then $U\mathcal{R}$ is a Riesz basis for H_2.

Proof. At first, we assume that U is bounded and $\mathcal{B} = \{b_\lambda\}_{\lambda\in\mathcal{I}}$ is a Bessel system for H_1. For $g \in H_2$, it is

$$\begin{aligned}\| \{\langle g, Ub_\lambda\rangle_{H_2}\}_{\lambda\in\mathcal{I}} \|^2_{\ell_2(\mathcal{I})} &= \| \{\langle U^*g, b_\lambda\rangle_{H_1}\}_{\lambda\in\mathcal{I}} \|^2_{\ell_2(\mathcal{I})}\\ &\leq B\|U^*g\|^2_{H_1}\\ &\leq B\|U\|^2_{H_1\mapsto H_2}\|g\|^2_{H_2}.\end{aligned}$$

For the last inequality we used $\|U\|_{H_1\mapsto H_2} = \|U^*\|_{H_2\mapsto H_1}$. For a proof of part (ii) we refer to [24, Corollary 5.3.2]. To show (iii), we use the fact that a system $\mathcal{R} = \{r_\lambda\}_{\lambda\in\mathcal{I}}$ is a Riesz basis for a Hilbert space H if and only if there exists a Hilbert space G with an orthonormal basis $\{e_\lambda\}_{\lambda\in\mathcal{I}}$ and a bounded and invertible operator $V : G \mapsto H$, such that $\mathcal{R} = \{Ve_\lambda\}_{\lambda\in\mathcal{I}}$, cf. [24, Definition 3.6.1]. So let $\mathcal{R} = \{r_\lambda\}_{\lambda\in\mathcal{I}}$ be a Riesz basis for H_1 and U bounded and invertible. As mentioned above, $\mathcal{R}$ can be written as $\{Ve_\lambda\}_{\lambda\in\mathcal{I}}$, with $V : G \mapsto H_1$ bounded and invertible. The composition $UV : G \mapsto H_2$ is bounded and invertible as well. Thus, the system $U\mathcal{R} = \{UVe_\lambda\}_{\lambda\in\mathcal{I}}$ is a Riesz basis for H_2. □

2.4 Gelfand frames

As described in Chapter 3, wavelet Riesz bases are often constructed in $L_2(\Omega)$ first. In a second step, smoothness and approximation results allow us to characterize certain smoothness spaces with properly scaled versions of the wavelet Riesz bases. This strategy can be generalized to the case of frames. For this purpose, we introduce a special class of frames for a Hilbert space V which properly scaled are frames for another Hilbert space H. Moreover, we require that a properly scaled version of a certain dual frame is a frame for the dual Hilbert space H'.

The quarklet frames we construct in Chapter 6 possess this kind of structure, where the spaces V and H can be replaced by $L_2(\Omega)$ and $H^s(\Omega)$, respectively.

Definition 2.15. Let (H, V, H') be a Gelfand triple of Hilbert spaces. A frame $\mathcal{F} = \{f_\lambda\}_{\lambda\in\mathcal{I}} \subset V$ for V with a dual frame $\tilde{\mathcal{F}} = \{\tilde{f}_\lambda\}_{\lambda\in\mathcal{I}} \subset V'$ is called a Gelfand frame for the Gelfand triple (H, V, H'), if $\mathcal{F} \subset H$ and $\tilde{\mathcal{F}} \subset H'$ and there exists another Gelfand triple $(h, \ell_2(\mathcal{I}), h')$ of sequence spaces over $\mathcal{I}$ such that

$$\begin{aligned} &T := F_{\mathcal{F}}|_h : h \to H, \quad \mathbf{c} \mapsto \sum_{\lambda\in\mathcal{I}} c_\lambda f_\lambda, \\ &\tilde{T}^* : H \to h, \quad f \mapsto \{\langle \tilde{f}_\lambda, f\rangle_{H'\times H}\}_{\lambda\in\mathcal{I}} \end{aligned} \tag{2.4.1}$$

are bounded operators. Furthermore, we require the existence of an isomorphism $D : h \to \ell_2(\mathcal{I})$ such that its adjoint $D^* : \ell_2(\mathcal{I}) \to h'$ is also an isomorphism.

One can show that the adjoint operators corresponding to (2.4.1) are

$$\begin{aligned} &T^* : H' \to h', \quad g \mapsto \{\langle g, f_\lambda\rangle_{H'\times H}\}_{\lambda\in\mathcal{I}}, \\ &\tilde{T} : h' \to H', \quad \mathbf{c} \mapsto \sum_{\lambda\in\mathcal{I}} c_\lambda \tilde{f}_\lambda, \end{aligned} \tag{2.4.2}$$

respectively. Note the slight difference of the operators in (2.4.1) and (2.4.2) in contrast to the synthesis and analysis operator of $\mathcal{F}$ and $\tilde{\mathcal{F}}$, as defined in (2.1.2) and (2.1.4), respectively.

In our applications, the isomorphisms in Definition 2.15 are *weight matrices* $D := \operatorname{diag}(d_\lambda)_{\lambda\in\mathcal{I}}$. Hence, it is $D = D^*$. Moreover, the spaces h are weighted sequence spaces $\ell_{2,D}(\mathcal{I})$. By that, we mean the sets of all sequences $\mathbf{c} = \{c_\lambda\}_{\lambda\in\mathcal{I}}$ for which

$$||\mathbf{c}||_{\ell_{2,D}(\mathcal{I})} := ||D\mathbf{c}||_{\ell_2(\mathcal{I})} \tag{2.4.3}$$

is finite. The next important result shows that properly scaled versions of a Gelfand frame for (H, V, H') constitute frames for H and H'. For a proof we refer to [109, Proposition 2.9].

Proposition 2.16. *Let $\mathcal{F} = \{f_\lambda\}_{\lambda\in\mathcal{I}} \subset V$ be a Gelfand frame for (H, V, H'). If the corresponding sequence spaces are given by $(\ell_{2,D}(\mathcal{I}), \ell_2(\mathcal{I}), \ell_{2,D^{-1}}(\mathcal{I}))$ with the weight matrix $D = \operatorname{diag}(d_\lambda)_{\lambda\in\mathcal{I}}$, then the sets $\mathcal{G} := D^{-1}\mathcal{F} = \{d_\lambda^{-1} f_\lambda\}_{\lambda\in\mathcal{I}}$ and $\tilde{\mathcal{G}} := D\tilde{\mathcal{F}} = \{d_\lambda \tilde{f}_\lambda\}_{\lambda\in\mathcal{I}}$ constitute frames for H and H', respectively.*

Remark 2.17. It is easy to show that the synthesis and analysis operator of $\mathcal{G}$ are given by

$$F_{\mathcal{G}} = TD^{-1} : \ell_2(\mathcal{I}) \to H,\ \mathbf{c} \mapsto \sum_{\lambda \in \mathcal{I}} c_\lambda d_\lambda^{-1} f_\lambda \tag{2.4.4}$$

and

$$F_{\mathcal{G}}^* = (D^*)^{-1}T^* : H' \to \ell_2(\mathcal{I}),\ g \mapsto \{\langle g, d_\lambda^{-1} f_\lambda \rangle_{H' \times H}\}_{\lambda \in \mathcal{I}}, \tag{2.4.5}$$

respectively.

In Figure 2.1, the relations of the involved operators in a Gelfand frame become clearer.

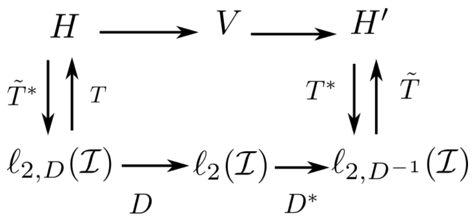

Figure 2.1: Diagram of the interaction of the operators for a Gelfand frame $\mathcal{F}$.

2.5 Discretization of operator equations

For a separable Hilbert space H we want to discretize the operator equation

$$\mathcal{L}u = f, \tag{2.5.1}$$

with $\mathcal{L} : H \to H'$, $u \in H$, $f \in H'$. We assume to have available a Gelfand triple (H, V, H') and a Gelfand frame $\mathcal{F} = \{f_\lambda\}_{\lambda \in \mathcal{I}}$ for (H, V, H'). The corresponding Gelfand triple of sequence spaces over $\mathcal{I}$ shall be given by $(\ell_{2,D}(\mathcal{I}), \ell_2(\mathcal{I}), \ell_{2,D^{-1}}(\mathcal{I}))$, with a weight matrix $D = \{d_\lambda\}_{\lambda \in \mathcal{I}}$. It follows by Proposition 2.16 that $\mathcal{G} = D^{-1}\mathcal{F}$ is a frame for H. From Section 2.1 we recall that its analysis operator $F_{\mathcal{G}}^* = (D^*)^{-1}T^*$ is injective from H' to $\ell_2(\mathcal{I})$. Therefore, we can multiply Equation (2.5.1) from the left with $(D^*)^{-1}T^*$. This leads to

$$(D^*)^{-1}T^*\mathcal{L}u = (D^*)^{-1}T^*f. \tag{2.5.2}$$

Moreover, we deduce from Theorem 2.2 that the synthesis operator $F_{\mathcal{G}} = TD^{-1}$ of $\mathcal{G}$ is onto from $\ell_2(\mathcal{I})$ to H. Hence, for every $u \in H$ there is a $\mathbf{u} \in \ell_2(\mathcal{I})$ such that $TD^{-1}\mathbf{u} = u$. Applying this in (2.5.2), we get an equation in $\ell_2(\mathcal{I})$, namely

$$(D^*)^{-1}T^*\mathcal{L}TD^{-1}\mathbf{u} = (D^*)^{-1}T^*f. \tag{2.5.3}$$

The latter can also be written as

$$\mathbf{Au} = \mathbf{f}, \tag{2.5.4}$$

with

$$\mathbf{A} := (D^*)^{-1}T^*\mathcal{L}TD^{-1} : \ell_2(\mathcal{I}) \to \ell_2(\mathcal{I}) \tag{2.5.5}$$

the discrete version of the operator $\mathcal{L}$ and

$$\mathbf{f} := (D^*)^{-1}T^*f \in \ell_2(\mathcal{I}) \tag{2.5.6}$$

the discrete right-hand side. If $\mathcal{L}$ is a symmetric, positive definite operator, i.e., $\mathcal{L} = \mathcal{L}^*$ and $\langle \mathcal{L}v, v\rangle_{H'\times H} > 0$ for all $v \neq 0$, we deduce the relation

$$\langle (D^*)^{-1}T^*\mathcal{L}TD^{-1}\mathbf{v}, \mathbf{v}\rangle_{\ell_2(\mathcal{I})} = \langle \mathbf{v}, (D^*)^{-1}T^*\mathcal{L}TD^{-1}\mathbf{v}\rangle_{\ell_2(\mathcal{I})}, \quad \mathbf{v} \in \ell_2(\mathcal{I}).$$

Hence, $\mathbf{A}$ is symmetric as well. Moreover, we have

$$\langle (D^*)^{-1}T^*\mathcal{L}TD^{-1}\mathbf{v}, \mathbf{v}\rangle_{\ell_2(\mathcal{I})} = \langle \mathcal{L}TD^{-1}\mathbf{v}, TD^{-1}\mathbf{v}\rangle_{H'\times H}, \quad \mathbf{v} \in \ell_2(\mathcal{I}). \tag{2.5.7}$$

Since TD^{-1} is not necessarily injective, the positive definiteness of $\mathcal{L}$ does not carry over to $\mathbf{A}$ in general. Anyway, $\mathbf{A}$ is at least positive semidefinite. There is one more thing we can deduce from (2.5.7). For $\lambda \in \mathcal{I}$, let $\mathbf{e}_\lambda := \{\delta_{\lambda,\nu}\}_{\nu\in\mathcal{I}} \in \ell_2(\mathcal{I})$. Then, it is

$$\mathbf{e}_\lambda^T \mathbf{A} \mathbf{e}_\mu = \langle \mathcal{L}(d_\mu^{-1}f_\mu), d_\lambda^{-1}f_\lambda\rangle_{H'\times H} = (\mathcal{L}(d_\mu^{-1}f_\mu))(d_\lambda^{-1}f_\lambda) = a(d_\mu^{-1}f_\mu, d_\lambda^{-1}f_\lambda).$$

Therefore, the operator $\mathbf{A}$ can also be seen as a biinfinite matrix with entries $\mathbf{A}_{\lambda,\mu} := a(d_\mu^{-1}f_\mu, d_\lambda^{-1}f_\lambda)$, $\lambda, \mu \in \mathcal{I}$. It is called *stiffness matrix*. In the following lemma, some properties of $\mathbf{A}$ are summarized.

Lemma 2.18. *The operator* $\mathbf{A}$ *is bounded from* $\ell_2(\mathcal{I})$ *to* $\ell_2(\mathcal{I})$. *Moreover,*

$$\mathbf{A}|_{\operatorname{ran}(\mathbf{A})} : \operatorname{ran}(\mathbf{A}) \to \operatorname{ran}(\mathbf{A}) \tag{2.5.8}$$

is boundedly invertible and $\ker(\mathbf{A}) = \ker(TD^{-1})$, *whereas* $\operatorname{ran}(\mathbf{A}) = \operatorname{ran}((D^*)^{-1}T^*)$.

Proof. As a composition of bounded operators $D^{-1} : \ell_2(\mathcal{I}) \to \ell_{2,D}(\mathcal{I})$, $T : \ell_{2,D}(\mathcal{I}) \to H$, $\mathcal{L} : H \to H'$, $T : H' \to \ell_{2,D^{-1}}(\mathcal{I})$, $(D^*)^{-1} : \ell_{2,D^{-1}}(\mathcal{I}) \to \ell_2(\mathcal{I})$, the operator $\mathbf{A}$ is bounded from $\ell_2(\mathcal{I})$ to $\ell_2(\mathcal{I})$. From the injectivity of $(D^*)^{-1}T^*$ and $\mathcal{L}$ we conclude $\ker(\mathbf{A}) = \ker(TD^{-1})$. Since TD^{-1} and $\mathcal{L}$ are onto it is $\operatorname{ran}(\mathbf{A}) = \operatorname{ran}((D^*)^{-1}T^*)$. With $S_\mathcal{G} = TD^{-1}(D^*)^{-1}T^*$ the frame operator of $\mathcal{G}$, we define $\mathbf{B} := F_\mathcal{G}^* S_\mathcal{G}^{-1}\mathcal{L}^{-1}S_\mathcal{G}^{-1}F_\mathcal{G}$. The operator $\mathbf{B}$ is a composition of bounded operators, thus bounded. The composition of $\mathbf{A}$ and $\mathbf{B}$ leads to

$$\mathbf{AB} = \mathbf{BA} = F_\mathcal{G}^* S_\mathcal{G}^{-1} F_\mathcal{G}.$$

We recall from Proposition 2.8 that $F_\mathcal{G}^* S_\mathcal{G}^{-1} F_\mathcal{G}$ is the orthogonal projection $\mathbf{Q}$ onto $\operatorname{ran}(F_\mathcal{G}^*) = \operatorname{ran}((D^*)^{-1}T^*)$. Hence, together with the previous part of this proof we infer that $\mathbf{AB} = \mathbf{BA}$ is the projection onto $\operatorname{ran}(\mathbf{A})$. Therefore, $\mathbf{B}$ is the inverse of $\mathbf{A}$ on its range, what proves the claim. □

We have already seen that the solutions of the operator equation (2.5.1) and the discrete equation (2.5.4) are related via $TD^{-1}\mathbf{u} = u$. From Lemma 2.18, we know that the solution of (2.5.4) is unique on its range. It remains to state how the set of all solutions of (2.5.4) can be characterized. For a proof of the following lemma we refer to [109, Proposition 2.12].

Lemma 2.19. *Let* $\mathbf{u}$ *be an arbitrary solution of* (2.5.1) *and* $\mathbf{Q} := F_{\mathcal{G}}^* S_{\mathcal{G}}^{-1} F_{\mathcal{G}}$ *the orthogonal projection onto* $\mathrm{ran}(\mathbf{A})$. *Then,* $\mathbf{Qu}$ *is the unique solution of* (2.5.1) *in* $\mathrm{ran}(\mathbf{A})$. *The set of all solutions of* (2.5.1) *can be written as* $\mathbf{Qu} + \ker(TD^{-1})$.

Remark 2.20. It is possible to perform the discretization of the operator equation (2.5.1) directly with a frame for H as it is done in [97]. This direct and more general approach can be applied to a broader class of frames, e.g., Gabor frames, which do not allow for the construction of Gelfand frames. However, in the wavelet as well as in the quarklet setting it seems natural to utilize the Gelfand frame approach. The big advantage of Gelfand frames is that in combination with certain smoothness and approximation results they lead to powerful and easy to handle norm-equivalences. With the latter, one can describe certain smoothness spaces by ℓ_2-norms of weighted expansion coefficients with respect to the particular Gelfand frame $\mathcal{F}$.

In this section, we have seen that linear elliptic operator equations can be transferred via a Gelfand frame into a matrix-vector equation. The natural way to proceed is to solve this matrix-vector equation with some iterative method. However, before we do this, we have to make sure that the multiplication of the biinfinite matrix $\mathbf{A}$ with a vector $\mathbf{v}$ can be efficiently approximated in a numerically stable way. For that, a certain quasi-sparse structure of the matrix $\mathbf{A}$ is necessary. Throughout the following of this thesis, we see that our frames of choice, the quarklet frames on general domains, which are constructed in Chapter 6, do allow for quasi-sparse stiffness matrices. However, the verification of this statement is given in Chapter 7.

Chapter 3

Wavelet Riesz Bases

In this chapter, we introduce wavelets. It is outlined how to construct wavelets on the real line and on the unit interval. In both cases, we give a concrete example. These examples serve as the building blocks for the construction of quarklets, which is the topic of the Chapters 4-6.

Let us stress that Jackson and Bernstein estimates play a key role in this context. These approximation and regularity results pave the way for wavelet Riesz bases not only in L_2 but also in scales of Sobolev spaces H^s. For further information on wavelets, we refer to [25, 58, 84, 110].

Throughout this chapter, we identify $L_2(\mathbb{R})$ with its dual space, such that dual Riesz bases are also contained in $L_2(\mathbb{R})$.

3.1 Wavelets on the real line

In this section, it is outlined how to construct wavelets on the real line via a pair of biorthogonal multiresolution analyses. Moreover, we give a concrete realization of a wavelet Riesz basis resting upon spline functions which was initially introduced in [34].

3.1.1 Construction principles on the real line

As the definition of wavelets differ in various sources, let us at first fix what we understand by a wavelet.

Definition 3.1. Let $\psi \in L_2(\mathbb{R})$ and $\psi_{j,k} := 2^{j/2}\psi(2^j \cdot -k)$, $j, k \in \mathbb{Z}$. The function ψ is called a *(mother) wavelet* if

(i) the family $\{\psi_{j,k} : j, k \in \mathbb{Z}\}$ is a Riesz basis for $L_2(\mathbb{R})$ and

(ii) the dual Riesz basis is also generated by a single function $\tilde{\psi} \in L_2(\mathbb{R})$.

The duality relation reads as

$$\langle \psi_{j,k}, \tilde{\psi}_{j',k'} \rangle_{L_2(\mathbb{R})} = \delta_{j,j'}\delta_{k,k'}.$$

The functions ψ, $\tilde{\psi}$ are called biorthogonal. If $\psi = \tilde{\psi}$, the family $\{\psi_{j,k} : j, k \in \mathbb{Z}\}$ is an orthonormal basis for $L_2(\mathbb{R})$ and ψ is called an orthogonal wavelet.

The most simple example for a wavelet is the so-called *Haar wavelet*

$$\psi(x) = \begin{cases} 1, & x \in [0, \frac{1}{2}), \\ -1, & x \in [\frac{1}{2}, 1), \\ 0, & \text{else}, \end{cases} \tag{3.1.1}$$

first mentioned in [74]. It is even an orthogonal wavelet. However, the Haar wavelet is not even continuous. To construct symmetric wavelets with higher smoothness and compact support, it is necessary to give up the orthonormality, see, e.g., [58, Section 8.3].

The principle tool to construct wavelet bases is the concept of multiresolution analysis (MRA). It was brought up first by S. Mallat in [81].

Definition 3.2. Let $\varphi \in L_2(\mathbb{R})$ and $\varphi_{j,k} := 2^{j/2}\varphi(2^j \cdot -k)$, $j, k \in \mathbb{Z}$. The sequence of function spaces $\mathcal{V} = \{V_j\}_{j\in\mathbb{Z}}$ with

$$V_j = \operatorname{clos}_{L_2(\mathbb{R})} \operatorname{span}\{\varphi_{j,k} : k \in \mathbb{Z}\}$$

is called a *multiresolution analysis (MRA)* for $L_2(\mathbb{R})$ if

(i) $V_j \subset V_{j+1}$ for all $j \in \mathbb{Z}$,

(ii) $\operatorname{clos}_{L_2(\mathbb{R})} \bigcup_{j\in\mathbb{Z}} V_j = L_2(\mathbb{R})$,

(iii) $\bigcap_{j\in\mathbb{Z}} V_j = \{0\}$, and

(iv) the family $\{\varphi_{0,k} : k \in \mathbb{Z}\}$ is a Riesz basis for V_0.

The function φ is called *generator* of the MRA $\mathcal{V}$.

From Definition 3.2 (iv) and $||\varphi_{j,k}||_{L_2(\mathbb{R})} = ||\varphi||_{L_2(\mathbb{R})}$, we conclude that the set $\{\varphi_{j,k} : j, k \in \mathbb{Z}\}$ is a Riesz basis for V_j for all $j \in \mathbb{Z}$, with Riesz constants that do not depend on the level j. Furthermore, with a *refinement mask* $\mathbf{a} := \{a_k\}_{k\in\mathbb{Z}} \in \ell_2(\mathbb{Z})$, it holds a *two-scale relation* of the form

$$\varphi = \sum_{k\in\mathbb{Z}} a_k \varphi(2 \cdot -k). \tag{3.1.2}$$

For the construction of biorthogonal wavelets we need two MRAs which are biorthogonal to each other.

Definition 3.3. Two MRAs $\mathcal{V} = \{V_j\}_{j\in\mathbb{Z}}$ and $\tilde{\mathcal{V}} = \{\tilde{V}_j\}_{j\in\mathbb{Z}}$ with respective generators $\varphi, \tilde{\varphi} \in L_2(\mathbb{R})$ are called a pair of *biorthogonal MRAs* for $L_2(\mathbb{R})$ if it holds

$$\langle \varphi, \tilde{\varphi}(\cdot - k)\rangle_{L_2(\mathbb{R})} = \delta_{0,k}, \quad k \in \mathbb{Z}. \tag{3.1.3}$$

The generators are called a pair of *biorthogonal generators* for $L_2(\mathbb{R})$.

In the following, we denote $\mathcal{V}$ and $\tilde{\mathcal{V}}$ as the primal and the dual MRA, respectively. The same applies for the generators φ and $\tilde{\varphi}$, which are called primal and dual generator, respectively. We assume that φ is a *partition of unity*, i.e.,

$$\sum_{k\in\mathbb{Z}} \varphi_{0,k} \equiv 1, \quad \text{almost everywhere.}$$

If the partition of unity property of φ and (3.1.3) hold, it is possible to normalize φ and $\tilde{\varphi}$, such that

$$\int_{\mathbb{R}} \varphi(x)\,\mathrm{d}x = \int_{\mathbb{R}} \tilde{\varphi}(x)\,\mathrm{d}x = 1.$$

To construct biorthogonal wavelets with the help of biorthogonal MRAs, we use the relations $V_j \subset V_{j+1}$ and $\tilde{V}_j \subset \tilde{V}_{j+1}$ to define the complement spaces W_j of V_j and $\tilde{W}_j$ of $\tilde{V}_j$ via

$$V_{j+1} = V_j \oplus W_j, \quad \tilde{V}_{j+1} = \tilde{V}_j \oplus \tilde{W}_j, \tag{3.1.4}$$

and the biorthogonality conditions

$$V_j \perp \tilde{W}_j, \quad \tilde{V}_j \perp W_j, \tag{3.1.5}$$

for all $j \in \mathbb{Z}$. In other words W_j and $\tilde{W}_j$ are the spaces that describe the informations that lead from coarser scales V_j, $\tilde{V}_j$ to finer scales V_{j+1}, $\tilde{V}_{j+1}$, respectively. Furthermore, from (3.1.4), (3.1.5) and Definition 3.7 (ii), (iii) one can deduce the decomposition formulas

$$L_2(\mathbb{R}) = \bigoplus_{j=-\infty}^{\infty} W_j = V_{j_0} \oplus \left(\bigoplus_{j=j_0}^{\infty} W_j \right) \tag{3.1.6}$$

for all $j_0 \in \mathbb{Z}$. The next step is to construct functions ψ, $\tilde{\psi} \in L_2(\mathbb{R})$ such that

$$\langle \psi, \tilde{\psi}(\cdot - k)\rangle_{L_2(\mathbb{R})} = \delta_{0,k}, \quad k \in \mathbb{Z},$$

and

$$W_j = \operatorname{clos}_{L_2(\mathbb{R})} \operatorname{span}\{\psi_{j,k} : k \in \mathbb{Z}\}, \quad \tilde{W}_j = \operatorname{clos}_{L_2(\mathbb{R})} \operatorname{span}\{\tilde{\psi}_{j,k} : k \in \mathbb{Z}\},$$

for all $j \in \mathbb{Z}$, where $\psi_{j,k} := 2^{j/2}\psi(2^j \cdot -k)$, $\tilde{\psi}_{j,k} := 2^{j/2}\tilde{\psi}(2^j \cdot -k)$, $j, k \in \mathbb{Z}$. Assuming the two scale relations

$$\varphi = \sum_{k\in\mathbb{Z}} a_k \varphi(2 \cdot -k), \quad \tilde{\varphi} = \sum_{k\in\mathbb{Z}} \tilde{a}_k \tilde{\varphi}(2 \cdot -k)$$

with the refinement masks $\mathbf{a} = \{a_k\}_{k\in\mathbb{Z}}$, $\tilde{\mathbf{a}} := \{\tilde{a}_k\}_{k\in\mathbb{Z}} \in \ell_2(\mathbb{Z})$, it was shown in [34] that

$$\psi = \sum_{k\in\mathbb{Z}} b_k \varphi(2\cdot -k), \quad \tilde{\psi} = \sum_{k\in\mathbb{Z}} \tilde{b}_k \tilde{\varphi}(2\cdot -k), \tag{3.1.7}$$

with

$$b_k := (-1)^{k+1}\tilde{a}_{1-k-2\ell}, \quad \tilde{b}_k := (-1)^{k+1} a_{1-k-2\ell}, \quad k \in \mathbb{Z}, \tag{3.1.8}$$

where the parameter $\ell \in \mathbb{Z}$ can be chosen arbitrarily, fulfil the requirements. In the orthonormal case $\psi = \tilde{\psi}$, it follows immediately that $\{\psi_{j,k} : j,k \in \mathbb{Z}\}$ is an orthonormal basis for $L_2(\mathbb{R})$. In the general case, it requires further properties of the spaces V_j and $\tilde{V}_j$, e.g., the availability of Jackson and Bernstein estimates, to conclude that $\{\psi_{j,k} : j,k \in \mathbb{Z}\}$ is a Riesz basis for $L_2(\mathbb{R})$. For details, see [30, 34]. If $\{\psi_{j,k} : j,k \in \mathbb{Z}\}$ is a Riesz basis for $L_2(\mathbb{R})$, then it follows by (3.1.6) with $j_0 = 0$ that the family

$$\Psi^B_{L_2(\mathbb{R})} := \{\varphi_{0,k}, \psi_{j,k} : (j,k) \in \Lambda^B\}, \quad \Lambda^B := \{(j,k) : j \in \mathbb{N}_0, k \in \mathbb{Z}\} \tag{3.1.9}$$

is also a Riesz basis for $L_2(\mathbb{R})$. Moreover,

$$\tilde{\Psi}^B_{L_2(\mathbb{R})} := \{\tilde{\varphi}_{0,k}, \tilde{\psi}_{j,k} : (j,k) \in \Lambda^B\} \tag{3.1.10}$$

is the dual Riesz basis of $\tilde{\Psi}^B_{L_2(\mathbb{R})}$.

Throughout this thesis, we solely deal with generators φ and $\tilde{\varphi}$ that have compact support. In this case, the corresponding refinement masks only have finitely many non-trivial entries. It immediately follows by (3.1.7) and (3.1.8) that also the primal and dual wavelets have compact support.

For further reading on wavelet constructions via biorthogonal MRAs we refer to [19, 52].

3.1.2 The Cohen-Daubechies-Feveau wavelets

In this subsection, we present the class of spline wavelets constructed in [34]. In the following, they are denoted as CDF wavelets. They are a realization of the biorthogonal wavelets presented in the last subsection and serve as the starting point for two further constructions presented in this thesis. On the one hand, boundary adaptations of CDF wavelets lead to wavelet Riesz bases on the interval $[0,1]$. This is outlined in Subsection 3.2.2. On the other hand, polynomial enrichment of the CDF wavelets enables the construction of quarklets on the real axis, which is the topic of Chapter 4.

For fixed $m \in \mathbb{N}$, let N_m be the *cardinal B-spline* of order m. One way to construct cardinal B-splines is to use recursive convolution, i.e.,

$$N_1 := \chi_{[0,1)}, \quad N_m := N_{m-1} * N_1 := \int_{\mathbb{R}} N_{m-1}(\cdot - y) N_1(y)\,\mathrm{d}y, \; m > 1. \tag{3.1.11}$$

In the next proposition, we collect several well-known facts about cardinal B-splines. For a proof we refer to [25, Theorem 4.3].

Proposition 3.4. *The cardinal B-spline N_m satisfies the following properties:*

(i) *N_m has compact support. Particularly, it is* $\operatorname{supp} N_m = [0, m]$*.*

(ii) *The cardinal B-spline is a partition of unity, i.e.,* $\sum_{k\in\mathbb{Z}} N_m(\cdot - k) \equiv 1$*.*

(iii) $\int_{\mathbb{R}} N_m(x)\,\mathrm{d}x = 1$*.*

(iv) *For $m > 1$ it holds*

$$N'_m = N_{m-1} - N_{m-1}(\cdot - 1). \tag{3.1.12}$$

(v) *For $m > 1$ the cardinal B-splines N_m and N_{m-1} are related by the recursion formula*

$$N_m = \frac{\cdot}{m-1} N_{m-1} + \frac{m - \cdot}{m-1} N_{m-1}(\cdot - 1). \tag{3.1.13}$$

(vi) *N_m is refinable with the two-scale relation*

$$N_m = \sum_{k=0}^{m} 2^{-m+1} \binom{m}{k} N_m(2 \cdot -k). \tag{3.1.14}$$

(vii) *The spaces* $\operatorname{clos}_{L_2(\mathbb{R})} \operatorname{span}\{2^{j/2} N_m(2^j \cdot -k) : k \in \mathbb{Z}\}$ *with $j \in \mathbb{Z}$ are an MRA for $L_2(\mathbb{R})$.*

(viii) *$N_m \in H^s(\mathbb{R})$, for $0 \le s < m - \frac{1}{2}$.*

(ix) *N_m is symmetric around the axis at $x = \frac{m}{2}$.*

(x) *The explicit formula*

$$N_m = \frac{1}{(m-1)!}(m - \cdot)^{m-1} \tag{3.1.15}$$

holds on the interval $[m-1, m]$.

For further information on cardinal B-splines, see [25, 62, 94].

Since all requirements of Subsection 3.1.1 are fulfilled by N_m, it is reasonable to define the primal generator $\varphi := N_m$. From now on, let us fix $\tilde{m} \in \mathbb{N}$, with the properties that $\frac{\tilde{m}}{m}$ is sufficiently big and $m + \tilde{m}$ is even. In [34], it was shown that there exist a dual generator to φ with properties that are collected in the following proposition.

Proposition 3.5. *There exists a dual generator $\tilde{\varphi} \in L_2(\mathbb{R})$ to $\varphi = N_m$ with the following properties:*

(i) $\tilde{\varphi}$ *has compact support. Particularly, it is*

$$\operatorname{supp}\tilde{\varphi} = [-\tilde{m}+1, \tilde{m}+m-1] \supset \operatorname{supp}\varphi.$$

(ii) $\tilde{\varphi}$ *is refinable with a refinement mask* $\tilde{\mathbf{a}} = \{\tilde{a}_k\}_{k\in\mathbb{Z}}$*,* $\tilde{a}_k = 0$ *for* $k < -\tilde{m}+1 \vee k > \tilde{m}+m-1$*. Therefore, the two-scale relation is given by*

$$\tilde{\varphi} = \sum_{k=-\tilde{m}+1}^{\tilde{m}+m-1} \tilde{a}_k \tilde{\varphi}(2\cdot -k).$$

(iii) $\int_{\mathbb{R}} \tilde{\varphi}(x)\,\mathrm{d}x = 1.$

(iv) $\tilde{\varphi}$ *is symmetric around* $\frac{m}{2}$*.*

We choose $\ell := 0$ as the parameter in (3.1.8). Then, by the relations (3.1.7), (3.1.8) the primal and dual wavelets arise immediately and the whole basis is given by $\{\varphi_{0,k}, \psi_{j,k} : (j,k) \in \Lambda^B\}$, cf (3.1.9). We have $\operatorname{supp}\psi = [1-\frac{m+\tilde{m}}{2}, \frac{m+\tilde{m}}{2}]$, and ψ is symmetric around $\frac{1}{2}$ if m is even and antisymmetric around $\frac{1}{2}$ if m is odd. See [58] for details. As a linear combination of dilations and translations of φ, we conclude by Proposition 3.4 (viii) that ψ is contained in $H^s(\mathbb{R})$, $0 \le s < m - \frac{1}{2}$. Furthermore, ψ has $\tilde{m}$ *vanishing moments*, i.e,

$$\int_{\mathbb{R}} x^r \psi(x)\,\mathrm{d}x = 0, \quad r = 0, \dots, \tilde{m}-1.$$

An illustration of the generators for $m = 2, 3, 4$ is given in Figure 3.1. Mother wavelets for certain combinations of m and $\tilde{m}$ can be viewed in Figure 3.2.

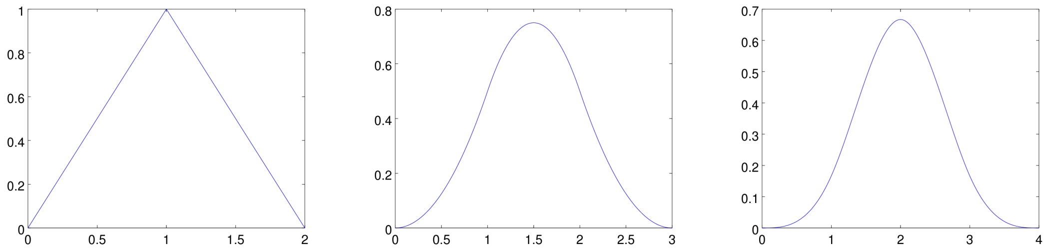

Figure 3.1: Primal CDF generators $\varphi = N_m$ for $m = 2, 3, 4$.

Remark 3.6. Actually, the construction in [34] starts with translated versions of cardinal B-splines as generators. They are centred around 0 for m even and around $\frac{1}{2}$ for m odd, what corresponds to an integer shift of $\lfloor \frac{m}{2} \rfloor$ to the left compared to our approach. The dual generators are shifted analogously. Moreover, there are cases, e.g., $m = \tilde{m} = 2$, where the wavelets in [34] are a reflection along the X-axis of the wavelets described in here. The reason for this is a slight difference in the formulas for the refinement masks $\mathbf{b} = \{b_k\}_{k\in\mathbb{Z}}$, cf. (3.1.8). Nevertheless, up to this reflection, both constructions lead to the same Riesz bases.

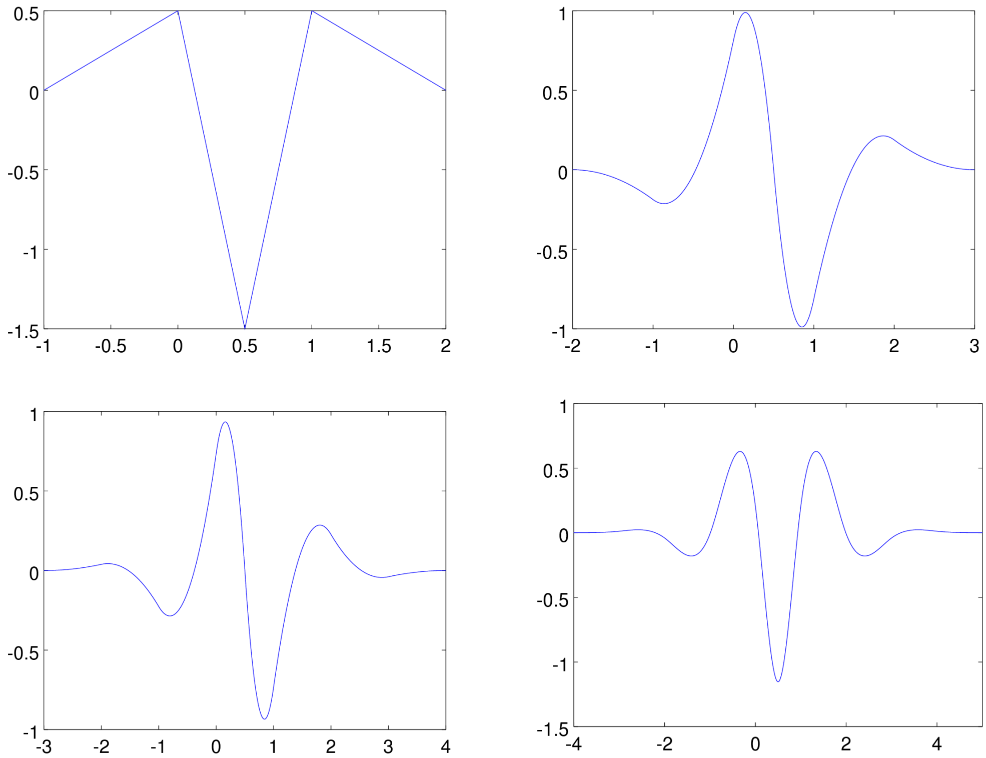

Figure 3.2: Primal CDF mother wavelets ψ for ($m = 2$, $\tilde{m} = 2$), ($m = 3$, $\tilde{m} = 3$), ($m = 3$, $\tilde{m} = 5$) and ($m = 4$, $\tilde{m} = 6$).

3.2 Wavelets on the interval

To construct wavelets on the interval, an adaptation of the concepts on the real axis is necessary. In particular, one has to form boundary near functions that, on the one hand, preserve the stability of the system and, on the other hand, are appropriate to describe spaces with certain boundary conditions. Moreover, for the numerical application, it is crucial to preserve the vanishing moments of the wavelets. In Subsection 3.2.1, we introduce a general concept for the construction of wavelet bases on the interval by roughly following the lines of [54, 90, 91]. In Subsection 3.2.2, we recall a realization of a wavelet basis on the interval constructed in [90, 91]. Other possible wavelet constructions on the interval are mentioned in [54, 56].

3.2.1 Construction principles on the interval

At first, we adapt the concept of MRAs to the interval case.

Definition 3.7. Let $j_0 \in \mathbb{N}_0$ and $\Delta_j \subset \mathbb{Z}$ be finite index sets for $\mathbb{N} \ni j \geq j_0$. Let

$$\Phi_j^B := \{\varphi_{j,k} : \varphi_{j,k} \in L_2(0,1), k \in \Delta_j\}$$

be a set of linear independent functions. The sequence of function spaces $\mathcal{V} = \{V_j\}_{j \geq j_0}$ with

$$V_j = \mathrm{clos}_{L_2(0,1)} \operatorname{span} \Phi_j^B$$

is called a multiresolution analysis (MRA) for $L_2(0,1)$ if

(i) $V_j \subset V_{j+1}$ for all $j \geq j_0$,

(ii) $\mathrm{clos}_{L_2(0,1)} \bigcup_{j \geq j_0} V_j = L_2(0,1)$, and

(iii) the sequence of sets $\Phi^B := \{\Phi_j^B\}_{j \geq j_0}$ is *uniformly stable*, i.e., there exist constants $0 < C_1 \leq C_2 < \infty$, that can be chosen independently from j, such that

$$C_1 ||\mathbf{c}||_{\ell_2(\Delta_j)} \leq || \sum_{k \in \Delta_j} c_k \varphi_{j,k} ||_{L_2(0,1)} \leq C_2 ||\mathbf{c}||_{\ell_2(\Delta_j)} \tag{3.2.1}$$

for all $\mathbf{c} = \{c_k\}_{k \in \Delta_j} \in \ell_2(\Delta_j)$.

The functions $\varphi_{j,k}$ $j \geq j_0$, $k \in \Delta_j$ are called (primal) generator functions.

Remark 3.8. It is possible to incorporate boundary conditions into the construction of MRAs. Independently of these boundary conditions, every MRA we use leads to $L_2(0,1)$ Riesz bases. The importance of it lies in the aspect that, depending on the boundary conditions of the MRA, scaled versions of the Riesz bases lead to Sobolev spaces $H^s_{\vec{\sigma}}(0,1)$ with different boundary conditions $\vec{\sigma} = (\sigma_0, \sigma_1) \in \{0, \lfloor s + \frac{1}{2} \rfloor\}^2$. For reasons of clarity and comprehensibility, we spare the indication with $\vec{\sigma}$ up to a point where it seems reasonable.

The main difference to the real axis case is that we no longer assume that the functions $\varphi_{j,k}$ are dilated and translated versions of a single function φ. While this property in fact can be sustained for functions away from the boundary, for functions at the boundary modifications are necessary. Moreover, we fix a *coarsest level* $j_0 \in \mathbb{N}_0$. By doing this, we make sure that the supports of all involved functions fit into the interval.

Similar to the real axis case, we work with a pair of dual MRAs. The dual MRA is also built by a finite set of functions

$$\tilde{\Phi}_j^B := \{\tilde{\varphi}_{j,k} : \tilde{\varphi}_{j,k} \in L_2(0,1), k \in \Delta_j\}.$$

Note that we have the same index sets Δ_j as in the primal case. Likewise, the same coarsest level $j_0 \in \mathbb{N}_0$ is fixed. The biorthogonality condition can be expressed as

$$\langle \Phi_j^B, \tilde{\Phi}_j^B \rangle := \{\langle \varphi_{j,k}, \tilde{\varphi}_{j,k'} \rangle_{L_2(0,1)}\}_{k,k' \in \Delta_j} = \mathbf{I}_{\Delta_j}, \tag{3.2.2}$$

for all $j \geq j_0$.

Since every basis of a finite dimensional space is also a Riesz basis, it is no surprise that an equation of the kind (3.2.1) holds for all $\mathbf{c} \in \ell_2(\Delta_j)$, $j \geq j_0$. The crucial point is the independence of j of the Riesz constants C_1, C_2 in (3.2.1), which is key for the construction of stable bases in $L_2(0,1)$. In the following lemma, we give a criterion for uniform stability.

Lemma 3.9. *[54, Lemma 2.1(i)] Let $\mathcal{V}$, $\tilde{\mathcal{V}}$ be a pair of biorthogonal MRAs for $L_2(0,1)$. If the primal and dual generator functions are* uniformly bounded*,*

$$||\varphi_{j,k}||, ||\tilde{\varphi}_{j,k}|| \lesssim 1, \quad \text{for all } j \geq j_0, k \in \Delta_j,$$

and locally finite*, i.e.,*

$$\#\{k' \in \Delta_j : \operatorname{supp} \varphi_{j,k'} \cap \operatorname{supp} \varphi_{j,k} \neq \emptyset\}, \#\{k' \in \Delta_j : \operatorname{supp} \tilde{\varphi}_{j,k'} \cap \operatorname{supp} \tilde{\varphi}_{j,k} \neq \emptyset\} \lesssim 1$$

for all $j \geq j_0$, $k \in \Delta_j$, then Φ^B and $\tilde{\Phi}^B$ are uniformly stable.

Because the spaces V_j and $\tilde{V}_j$ are nested, there exist two-scale relations for all $j \geq j_0$ which can be expressed as

$$\Phi_j^B = \mathbf{M}_{j,0}^T \Phi_{j+1}^B, \quad \tilde{\Phi}_j^B = \tilde{\mathbf{M}}_{j,0}^T \tilde{\Phi}_{j+1}^B, \tag{3.2.3}$$

with *refinement matrices* $\mathbf{M}_{j,0}, \tilde{\mathbf{M}}_{j,0} \in \mathbb{R}^{\Delta_{j+1}^B \times \Delta_j^B}$, $j \geq j_0$. In this context Φ_j^B, $\tilde{\Phi}_j^B$ are interpreted as column vectors. In contrast to the two-scale relation (3.1.7) on the real line, now, the two-scale relation depends explicitly on the level j. Since Φ_j^B are Riesz bases for their span with uniformly bounded constants, the matrices $\mathbf{M}_{j,0}$, $\tilde{\mathbf{M}}_{j,0}$ are uniformly bounded in j as well, i.e.,

$$||\mathbf{M}_{j,0}||_{\ell_2(\Delta_j)\to\ell_2(\Delta_{j+1})} = \mathcal{O}(1), \quad ||\tilde{\mathbf{M}}_{j,0}||_{\ell_2(\Delta_j)\to\ell_2(\Delta_{j+1})} = \mathcal{O}(1),$$

for all $j \geq j_0$. The aim now is to find sequences of complementary spaces $\{W_j\}_{j \geq j_0}$, $\{\tilde{W}_j\}_{j \geq j_0}$ such that

$$V_{j+1} = V_j \oplus W_j, \quad \tilde{V}_{j+1} = \tilde{V}_j \oplus \tilde{W}_j \tag{3.2.4}$$

and

$$V_j \perp \tilde{W}_j, \quad \tilde{V}_j \perp W_j \tag{3.2.5}$$

for all $j \geq j_0$. Additionally, for finite index sets $\nabla_j \subset \mathbb{Z}$, we want to construct bases $\Psi_j^B := \{\psi_{j,k} : \psi_{j,k} \in L_2(0,1), k \in \nabla_j\}$, $\tilde{\Psi}_j^B := \{\tilde{\psi}_{j,k} : \tilde{\psi}_{j,k} \in L_2(0,1), k \in \nabla_j\}$ for W_j, $\tilde{W}_j$, respectively, such that

$$\Psi_{L_2(0,1)}^B := \Phi_{j_0}^B \cup \bigcup_{j \geq j_0} \Psi_j^B, \qquad \tilde{\Psi}_{L_2(0,1)}^B := \tilde{\Phi}_{j_0}^B \cup \bigcup_{j \geq j_0} \tilde{\Psi}_j^B$$

are a pair of dual Riesz bases for $L_2(0,1)$. We denote $\Psi_{L_2(0,1)}^B$ and $\tilde{\Psi}_{L_2(0,1)}^B$ as *(biorthogonal) wavelet bases* for $L_2(0,1)$ or alternatively as *bases of wavelet-type*.
Let us fix the notations $\nabla_{j_0-1} := \Delta_j$ and $\Psi_{j_0-1}^B := \Phi_{j_0}^B$, $\tilde{\Psi}_{j_0-1}^B := \tilde{\Phi}_{j_0}^B$ as well as $\psi_{j_0-1,k} := \varphi_{j_0,k}$, $\tilde{\psi}_{j_0-1,k} := \tilde{\varphi}_{j_0,k}$ for all $k \in \nabla_{j_0-1}$. The whole index set shall be defined as

$$\nabla^B := \{(j,k) : j \geq j_0 - 1, k \in \nabla_j\}. \tag{3.2.6}$$

This leads to the neatly arranged notations

$$\Psi^B_{L_2(0,1)} = \bigcup_{j\geq j_0-1} \Psi^B_j = \{\psi_{j,k} : (j,k) \in \nabla^B\},$$
$$\tilde{\Psi}^B_{L_2(0,1)} = \bigcup_{j\geq j_0-1} \tilde{\Psi}^B_j = \{\tilde{\psi}_{j,k} : (j,k) \in \nabla^B\},$$

for the wavelet bases.

A general idea to construct wavelet bases is the method of stable completion, see, e.g., [19, 54, 55], which is outlined in the following.

Definition 3.10. Matrices $\mathbf{M}_{j,1} \in \mathbb{R}^{\Delta_{j+1}\times\nabla_j}$, $j \geq j_0$ are called a *stable completion* of $\mathbf{M}_{j,0}$ if

$$\mathbf{M}_j := (\mathbf{M}_{j,0}, \mathbf{M}_{j,1}) \in \mathbb{R}^{\Delta_{j+1}\times\Delta_{j+1}} \tag{3.2.7}$$

are invertible for all $j \geq j_0$ and $\mathbf{M}_j$ as well as $\mathbf{M}_j^{-1}$ are uniformly bounded in j, i.e.,

$$||\mathbf{M}_j||_{\mathscr{L}(\ell_2(\Delta_{j+1}))} = \mathcal{O}(1), \quad ||\mathbf{M}_j^{-1}||_{\mathscr{L}(\ell_2(\Delta_{j+1}))} = \mathcal{O}(1), \tag{3.2.8}$$

for all $j \geq j_0$.

The following proposition clarifies how stable completions $\mathbf{M}_{j,1}$ can be linked with the construction of wavelet bases for $L_2(0,1)$.

Proposition 3.11. *[19, Corollary 2.1] Let Φ^B be uniformly stable with refinement matrices $\mathbf{M}_{j,0}$. Then, the sequence of sets $\{\Phi^B_j \cup \Psi^B_j\}_{j\geq j_0}$ is uniformly stable if and only if $\Psi^B_j = \mathbf{M}^T_{j,1}\Phi^B_{j+1}$ for all $j \geq j_0$ with $\mathbf{M}_{j,1}$ a stable completion of $\mathbf{M}_{j,0}$.*

Stable completions are not unique. Actually, in [19, Subsection 3.1] it has been shown that every stable completion can be written as a linear transformation of some initial stable completion. In the following proposition, we see how to extract a stable completion that fits to our purpose of constructing biorthogonal wavelet bases.

Proposition 3.12. *[19, Corollary 3.1] Let Φ^B, $\tilde{\Phi}^B$ be uniformly stable with refinement matrices $\mathbf{M}_{j,0}$, $\tilde{\mathbf{M}}_{j,0}$. Assume that $\breve{\mathbf{M}}_{j,1}$ is some stable completion of $\mathbf{M}_{j,0}$ and that $\breve{\mathbf{G}}^T_j = \begin{pmatrix}\breve{\mathbf{G}}^T_{j,0}\\ \breve{\mathbf{G}}^T_{j,1}\end{pmatrix}$ is the inverse of $\mathbf{M}_j$. Then, there exists a stable completion $\mathbf{M}_{j,1}$ of $\mathbf{M}_{j,0}$ given by*

$$\mathbf{M}_{j,1} := (\mathbf{I}_{\Delta_{j+1}} - \mathbf{M}_{j,0}\tilde{\mathbf{M}}^T_{j,0})\breve{\mathbf{M}}_{j,1} \tag{3.2.9}$$

such that the inverse of $\mathbf{M}_j$ is given by $\mathbf{G}^T_j = \begin{pmatrix}\tilde{\mathbf{M}}^T_{j,0}\\ \breve{\mathbf{G}}^T_{j,1}\end{pmatrix}$. The collections

$$\Psi^B_j = \mathbf{M}^T_{j,1}\Phi^B_{j+1}, \quad \tilde{\Psi}^B_j = \breve{\mathbf{G}}^T_{j,1}\tilde{\Phi}^B_{j+1} \tag{3.2.10}$$

form biorthogonal systems

$$\langle \Psi_j^B, \tilde{\Psi}_j^B \rangle = \mathbf{I}_{\nabla_j} \quad \langle \Psi_j^B, \tilde{\Phi}_j^B \rangle = \langle \Phi_j^B, \tilde{\Psi}_j^B \rangle = \mathbf{0},$$

so that

$$\langle \Psi_{L_2(0,1)}^B, \tilde{\Psi}_{L_2(0,1)}^B \rangle = \mathbf{I}_{\nabla^B}.$$

Proposition 3.11 guarantees the uniform stability of $\{\Phi_j^B \cup \Psi_j^B\}_{j \geq j_0}$, whereas Proposition 3.12 shows how to ensure the biorthogonality of the systems $\Psi_{L_2(0,1)}^B$ and $\tilde{\Psi}_{L_2(0,1)}^B$. But it is still to discuss if $\Psi_{L_2(0,1)}^B$ and $\tilde{\Psi}_{L_2(0,1)}^B$ provide biorthogonal Riesz bases for $L_2(0,1)$. In other words, we need to check if the whole collections are L_2-stable over all levels. For this purpose, we introduce some notation. For all $j \geq j_0$, we denote with

$$Q_j : L_2(0,1) \to V_j, \; Q_j f := \sum_{k \in \Delta_j^B} \langle f, \tilde{\varphi}_{j,k} \rangle \varphi_{j,k}, \tag{3.2.11}$$

$$Q_j^* : L_2(0,1) \to \tilde{V}_j, \; Q_j^* f := \sum_{k \in \Delta_j^B} \langle f, \varphi_{j,k} \rangle \tilde{\varphi}_{j,k} \tag{3.2.12}$$

the projectors onto V_j and $\tilde{V}_j$. By setting $Q_{j_0-1} := 0$, any $f \in L_2(0,1)$ can be written as

$$f = \sum_{j \geq j_0 - 1} (Q_{j+1} - Q_j) f,$$

with convergence of the sum in $L_2(0,1)$. In particular, the difference $(Q_{j+1} - Q_j)f$ is the projection of f onto the complement spaces W_j. In the following theorem, we see that certain *direct* and *inverse* estimates give rise to norm equivalences not only in $L_2(0,1)$ but also in a range of Sobolev spaces. To the direct estimates we often refer to as *Jackson* estimates, whereas inverse estimates are called *Bernstein* estimates.

Theorem 3.13. *[53, Theorem 5.8] Let Φ^B and $\tilde{\Phi}^B$ be uniformly stable and the projections Q_j be defined as in (3.2.11). Assume that for $\mathcal{S} \in \{\mathcal{V}, \tilde{\mathcal{V}}\}$ a* Jackson estimate

$$\inf_{v_j \in \mathcal{S}_j} ||f - v_j||_{L_2(0,1)} \lesssim 2^{-sj} ||f||_{H^s(0,1)}, \quad f \in H^s(0,1), \; s \leq \sigma_{\mathcal{S}}, \tag{3.2.13}$$

and a Bernstein estimate

$$||v_j||_{H^s(0,1)} \lesssim 2^{sj} ||v_j||_{L_2(0,1)}, \quad v_j \in \mathcal{S}_j, \; s \leq \mu_{\mathcal{S}}, \tag{3.2.14}$$

hold. Let $\gamma := \min\{\sigma_{\mathcal{V}}, \mu_{\mathcal{V}}\}$ and $\tilde{\gamma} := \min\{\sigma_{\tilde{\mathcal{V}}}, \mu_{\tilde{\mathcal{V}}}\}$. Then, we have the norm equivalence

$$||f||_{H^s(0,1)} \eqsim \left(\sum_{j \geq j_0 - 1} 2^{2sj} ||(Q_{j+1} - Q_j) f||_{L_2(0,1)}^2 \right)^{1/2}, \quad s \in (-\tilde{\gamma}, \gamma). \tag{3.2.15}$$

Exceptionally, in (3.2.15), $H^s(0,1)$ for $s < 0$ is to be read as the dual space of $H^{-s}(0,1)$. An abstract *basis free* version of Theorem 3.13 can be found in [52, Theorem 3.2].

Since for all $j \geq j_0$, Ψ_j^B is a Riesz basis for W_j with the biorthogonal set $\tilde{\Psi}_j^B$ and Riesz constants independent of j, (3.2.15) leads to the norm equivalence

$$||f||_{H^s(0,1)} \eqsim \left(\sum_{j \geq j_0 - 1} \sum_{k \in \nabla_j^B} 2^{2sj} |\langle f, \tilde{\psi}_{j,k} \rangle|^2 \right)^{1/2}, \quad s \in (-\tilde{\gamma}, \gamma). \tag{3.2.16}$$

For $s = 0$, (3.2.16) states that $\tilde{\Psi}^B_{L_2(0,1)}$ is a frame for $L_2(0,1)$. Since it has a biorthogonal sequence $\Psi^B_{L_2(0,1)}$ in $L_2(0,1)$, both $\tilde{\Psi}^B_{L_2(0,1)}$ and $\Psi^B_{L_2(0,1)}$ are Riesz basis for $L_2(0,1)$. As (3.2.16) holds for a whole range of Sobolev spaces, the Riesz basis property carries over to these spaces through a simple scaling of $\Psi^B_{L_2(0,1)}$. For this purpose, let us introduce the *scaling matrix*

$$\mathbf{D}^B := \operatorname{diag}(2^{js})_{\lambda \in \nabla^B}, \quad \lambda = (j,k) \in \nabla^B, \tag{3.2.17}$$

for a fixed $s \in [0, \gamma)$. The scaled versions of $\Psi^B_{L_2(0,1)}$ are then defined through

$$\Psi^B_{H^s_{\vec{\sigma}}(0,1)} := (\mathbf{D}^B)^{-1} \Psi^B_{L_2(0,1)} = \{2^{-js} \psi_{\lambda,\vec{\sigma}} : \lambda = (j,k) \in \nabla^B_{\vec{\sigma}}\}, \tag{3.2.18}$$

where $\vec{\sigma} \in \{0, \lfloor s + \frac{1}{2} \rfloor\}^2$ depends on the incorporated boundary conditions of the MRA, cf. Remark 3.8. In the following proposition, it is stated that these scaled collections of wavelets are indeed Riesz bases for $H^s_{\vec{\sigma}}(0,1)$, cf. (1.3.15).

Proposition 3.14. *[109, Proposition 2.6] Under the same conditions as in Theorem 3.13 and for $s \in [0, \gamma)$, $\vec{\sigma} \in \{0, \lfloor s + \frac{1}{2} \rfloor\}^2$, the family $\Psi^B_{H^s_{\vec{\sigma}}(0,1)}$ as defined in* (3.2.18), *is a Riesz basis for $H^s_{\vec{\sigma}}(0,1)$.*

Through a biorthogonality argument, it is easy to see that the dual Riesz bases of $\Psi^B_{H^s_0(0,1)}$ for $H^{-s}(0,1)$, $s \in [0, \gamma)$, are

$$\tilde{\Psi}^B_{H^{-s}(0,1)} := \mathbf{D}^B \tilde{\Psi}^B_{L_2(0,1)} = \{2^{js} \tilde{\psi}_\lambda : \lambda = (j,k) \in \nabla^B\}.$$

In the next subsection, we see how the wavelets constructed in [90, 91] perfectly fit into the just introduced framework.

3.2.2 The Primbs wavelets

In this subsection, we reproduce the construction of the Primbs wavelets as outlined in [90,91]. It is a realization of wavelets that is based on splines as generator functions. Therefore, it belongs to the class of spline wavelet bases. For a comprehensive theory of spline wavelet bases, we refer to [25–28]. Another construction of biorthogonal wavelets on the interval can be found in [54]. For the orthogonal case, we refer to [35] for a detailed overview.

For a fixed degree $m \geq 2$ and $j \in \mathbb{N}$, we consider the knot sequence $T_{m,j} := \{t_{j,k}\}_{k=-m+1}^{2^j+m-1}$ of equidistant dyadic knots with multiplicity m on the boundary,

$$t_{j,k} := \begin{cases} 0 & , \quad k = -m+1, \ldots, 0, \\ 2^{-j}k & , \quad k = 1, \ldots, 2^j - 1, \\ 1 & , \quad k = 2^j \ldots, 2^j + m - 1 \end{cases},$$

and the *Schoenberg B-splines*

$$B_{m,j,k} := (t_{j,k+m} - t_{j,k})[t_{j,k}, \ldots, t_{j,k+m}; \max\{0, t - \cdot\}^{m-1}], \tag{3.2.19}$$

for $k = -m+1, \ldots, 2^j - 1$. The *divided difference*

$$[t_0, \ldots, t_n; f(t)]$$

of a knot sequence $\{t_k\}_{k=0}^n$ and an arbitrary function f is defined as the unique leading coefficient of the interpolation polynomial to the points $(t_k, f(t_k))$, $k = 0, \ldots, n$. The generators on level $j \in \mathbb{N}$ are then defined as

$$\begin{aligned} \Phi_j^B &= \{\varphi_{j,k} : k \in \Delta_j\} := \{2^{j/2} B_{m,j,k} : k \in \Delta_j\}, \\ \Delta_j &:= \{-m+1, \ldots, 2^j - 1\}. \end{aligned} \tag{3.2.20}$$

Let us fix a coarsest level $j_0 \in \mathbb{N}_0$ and assume that $\mathbb{N}_0 \ni j \geq j_0$. The generators have compact support in $[t_{j,k}, t_{j,k+m}]$,

$$\operatorname{supp} \varphi_{j,k} = \begin{cases} [0, 2^{-j}(m+k)], & k = -m+1, \ldots, -1, \\ [2^{-j}k, 2^{-j}(m+k)], & k = 0, \ldots, 2^j - m, \\ [2^{-j}k, 1], & k = 2^j - m, \ldots, 2^j - 1. \end{cases} \tag{3.2.21}$$

The *inner generators*

$$\Phi_j^{B,(I)} := \{\varphi_{j,k} : k \in \Delta_j^{(I)}\}, \quad \Delta_j^{(I)} := \{0, \ldots, 2^j - m\}, \tag{3.2.22}$$

are dilated and translated versions of a cardinal B-spline. To be more precise, we have $\varphi_{j,k} = N_m(2^j \cdot -k)$, for $k \in \Delta_j^{(I)}$. The *right boundary generators*

$$\Phi_j^{B,(R)} := \{\varphi_{j,k} : k \in \Delta_j^{(R)}\}, \quad \Delta_j^{(R)} := \{2^j - m + 1, \ldots, 2^j - 1\}, \tag{3.2.23}$$

are reflected versions of the *left boundary generators*

$$\Phi_j^{B,(L)} := \{\varphi_{j,k} : k \in \Delta_j^{(L)}\}, \quad \Delta_j^{(L)} := \{-m+1, \ldots, -1\}, \tag{3.2.24}$$

i.e., $\varphi_{j,k} = \varphi_{j,2^j-m-k}(1 - \cdot)$, for $k \in \Delta_j^{(L)}$. Moreover, the generators suffice the simple relation $\varphi_{j+1,k} = \sqrt{2}\,\varphi_{j,k}(2\cdot)$, $k \in \Delta_j^{(L)} \cup \Delta_j^{(I)}$. We refer to [94] for a proof of the latter facts. We further mention that only the outermost generators on the left-hand and the right-hand side do not vanish at the boundaries. This can be recognized well in Figure 3.3 for the case $m = 3$:

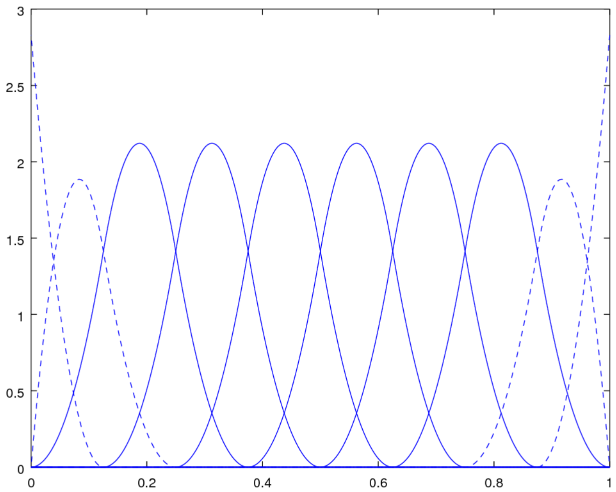

Figure 3.3: Generators $\varphi_{j,k}$ for the Primbs wavelets with free boundary conditions of order $m = 3$ with $\tilde{m} = 3$ vanishing moments on the coarsest level $j_0 = 3$. The dotted lines indicate the boundary generators whereas functions with solid lines are inner generators.

The sequence of function spaces $\mathcal{V} = \{V_j\}_{j \geq j_0} = \operatorname{clos}_{L_2(0,1)} \operatorname{span} \Phi_j^B$ is an MRA for $L_2(0,1)$ with order m of *polynomial exactness*, i.e., the space Π_{m-1} of polynomials with degree at most $m-1$ is contained in V_j for all $j \geq j_0$. It is possible to construct a biorthogonal MRA $\tilde{\mathcal{V}}$ with polynomial exactness $\tilde{m} \in \mathbb{N}$ if $\frac{\tilde{m}}{m}$ is large enough and $m + \tilde{m}$ is even. We skip the details here since the construction is very technical and the dual side is not explicitly used in our applications. However, it can be shown that the pair of biorthogonal MRAs fulfil Jackson and Bernstein estimates in the fashion of (3.2.13), (3.2.14).

We obtain the wavelets through stable completion as described in the last subsection. The bases of the complement spaces W_j, $j \geq j_0$ then look like

$$\Psi_j^B = \{\psi_{j,k} : k \in \nabla_j\}, \quad \nabla_j := \{0, \ldots, 2^j - 1\}. \tag{3.2.25}$$

As in the generator case, we differ between *boundary* and *inner wavelets*. Therefore, we introduce the notations

$$\Psi_j^{B,(\text{loc})} := \{\psi_{j,k} : k \in \nabla_j^{(\text{loc})}\}, \quad \text{loc} \in \{L, I, R\},$$

with

$$\begin{aligned}\nabla_j^{(L)} &:= \left\{0, \dots, \frac{m+\tilde{m}-4}{2}\right\},\\ \nabla_j^{(I)} &:= \left\{\frac{m+\tilde{m}-2}{2}, \dots, 2^j - \frac{m+\tilde{m}}{2}\right\},\\ \nabla_j^{(R)} &:= \left\{2^j - \frac{m+\tilde{m}}{2} + 1, \dots, 2^j - 1\right\}.\end{aligned} \tag{3.2.26}$$

Similar to the generators, the wavelets fulfil the relation $\psi_{j+1,k} = \sqrt{2}\,\psi_{j,k}(2\cdot)$, $k \in \nabla_j^{(L)} \cup \nabla_j^{(I)}$. Moreover, they are compactly supported with

$$\operatorname{supp}\psi_{j,k} = \begin{cases}[0, 2^{-j}(m+\tilde{m}-2)], & k \in \nabla_j^{(L)},\\ [2^{-j}(-\frac{m+\tilde{m}-2}{2}+k), 2^{-j}(\frac{m+\tilde{m}}{2}+k)], & k \in \nabla_j^{(I)},\\ [1-2^{-j}(m+\tilde{m}-2), 1], & k \in \nabla_j^{(R)}.\end{cases}$$

Up to a scaling factor and a translation, the inner wavelets $\Psi_j^{B,(I)}$ match the spline wavelets on the interval constructed in Subsection 3.1.2. In total analogy to the generators, for every level $j \geq j_0$, only the outermost boundary functions on the left-hand and the right-hand side do not vanish at the boundary. These properties can be observed in Figure 3.4. The whole wavelet collection

$$\Psi^B_{L_2(0,1)} = \{\psi_\lambda : \lambda \in \nabla^B\}, \quad \nabla^B = \{(j,k) : \mathbb{N}_0 \ni j \geq j_0 - 1, k \in \nabla_j\}, \tag{3.2.27}$$

is a Riesz basis for $L_2(0,1)$ and since all the requirements of Proposition 3.14 are fulfilled, $\Psi^B_{H^s(0,1)} = \mathbf{D}^{-1}\Psi^B_{L_2(0,1)}$ is a Riesz basis for $H^s(0,1)$ for $s \in [0, m-\frac{1}{2})$. Furthermore, all wavelets have vanishing moments up to order $\tilde{m}$,

$$\int_0^1 x^r \psi_{j,k}(x)\,\mathrm{d}x = 0, \quad r = 0, \dots, \tilde{m}-1,\ (j,k) \in \nabla^B.$$

The latter follows directly by the polynomial exactness of order $\tilde{m}$ of the dual MRA and $\langle \tilde{\Phi}_j^B, \Psi_j^B \rangle = \mathbf{0}$. This property is crucial for compression results, which in turn are necessary to show the optimal convergence of adaptive numerical schemes, cf. Chapter 7. Therefore, one main task for the construction of quarklets is to inherit the vanishing moments of the wavelets.

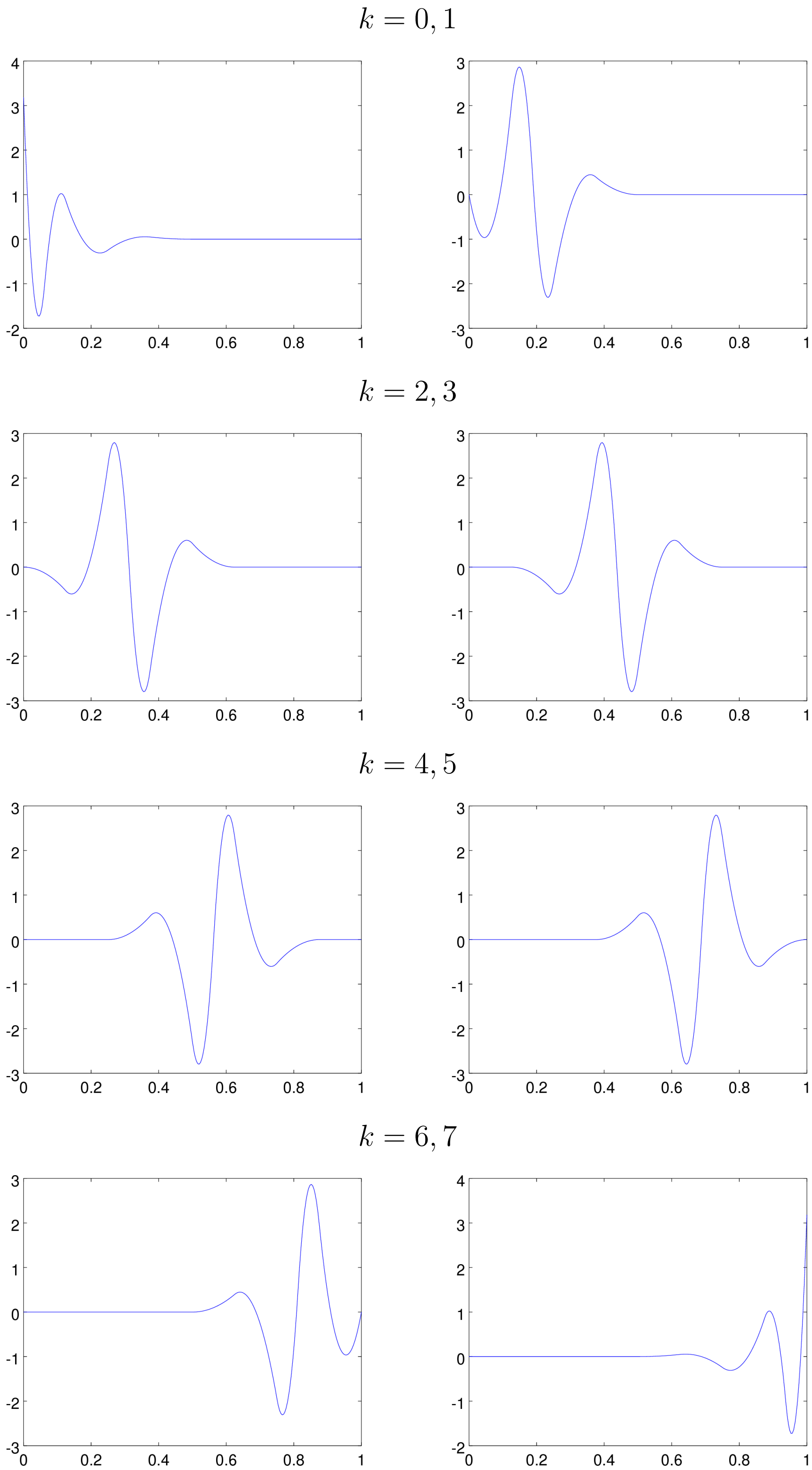

Figure 3.4: Primbs wavelets $\psi_{j,k}$ with free boundary conditions of order $m = 3$ with $\tilde{m} = 3$ vanishing moments on the coarsest level $j_0 = 3$.

Remark 3.15. To incorporate Dirichlet boundary conditions on both sides, we cancel the outermost functions of the primal MRA, which are the only ones that do not vanish at the boundary. As a result, we receive the adapted index set $\Delta_{j,\vec{\sigma}} = \{-m+2,\ldots,2^j-2\}$, with $\vec{\sigma} = (\lfloor s+\frac{1}{2}\rfloor, \lfloor s+\frac{1}{2}\rfloor)$. Obviously, $\mathcal{V}$ does not reproduce the constant polynomials any more. To keep the dimensions on the primal and dual side equal, we have to adapt the dual MRA as well. In contrast to the primal MRA, this can be done without cancelling out all the functions that with positive absolute value at the boundary. Thus, we conserve the polynomial exactness of order $\tilde{m}$ on the dual side. If the boundary adaptation is made in this fashion, we speak of *complementary boundary conditions*. Induced by the adaptation of the dual MRA, the primal wavelets at the boundary change (cf. Figure 3.5), although the index sets for the primal wavelets stay the same.

It is also possible to impose Dirichlet boundary conditions only on one side of the boundary. Then, with the respective $\vec{\sigma}$ the index sets $\Delta_{j,\vec{\sigma}}$ become $\{-m+2,\ldots,2^j-1\}$ or $\{-m+1,\ldots,2^j-2\}$ for Dirichlet boundary conditions at the left-hand and the right-hand side, respectively. A detailed description of adaptations to certain boundary conditions can be found in [91, Subsection 5.3].

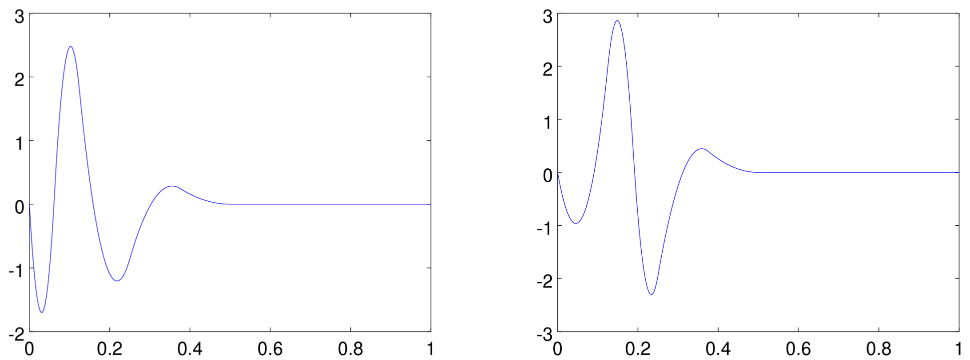

Figure 3.5: Left boundary Primbs wavelets for complementary boundary conditions of order $m=3$ and $\tilde{m}=3$ vanishing moments on the coarsest level $j_0=3$.

The refinement matrices, cf. Definition 3.10, are of the form

$$\mathbf{M}_{j,0} = \begin{pmatrix} \mathbf{M}_0^L & & \\ & \mathbf{M}_{j,0}^I & \\ & & \mathbf{M}_0^R \end{pmatrix}, \qquad \mathbf{M}_{j,1} = \begin{pmatrix} \mathbf{M}_1^L & & \\ & \mathbf{M}_{j,1}^I & \\ & & \mathbf{M}_1^R \end{pmatrix}, \tag{3.2.28}$$

with $\mathbf{M}^I_{j,0} \in \mathbb{R}^{\#\Delta^{(I)}_{j+1} \times \#\Delta^{(I)}_j}$, $\mathbf{M}^I_{j,1} \in \mathbb{R}^{\#\Delta^{(I)}_{j+1} \times \#\nabla^{(I)}_j}$, $\mathbf{M}^{\mathrm{loc}}_0 \in \mathbb{R}^{(2m-2) \times \#\Delta^{(\mathrm{loc})}_j}$ and $\mathbf{M}^{\mathrm{loc}}_1 \in \mathbb{R}^{(2m+2\tilde{m}-4) \times \#\nabla^{(\mathrm{loc})}_j}$, for loc $\in \{L, R\}$. As an example, for the case $m = 3$, $\tilde{m} = 3$ we have the primal refinement submatrices

$$\mathbf{M}^L_0 = \frac{1}{\sqrt{2}} \begin{pmatrix} 1 & 0 \\ 1/2 & 1/2 \\ 0 & 3/4 \\ 0 & 1/4 \end{pmatrix}, \quad \mathbf{M}^I_{3,0} = \frac{1}{\sqrt{2}} \begin{pmatrix} 1/4 & 0 & 0 & 0 & 0 & 0 \\ 3/4 & 0 & 0 & 0 & 0 & 0 \\ 3/4 & 1/4 & 0 & 0 & 0 & 0 \\ 1/4 & 3/4 & 0 & 0 & 0 & 0 \\ 0 & 3/4 & 1/4 & 0 & 0 & 0 \\ 0 & 1/4 & 3/4 & 0 & 0 & 0 \\ 0 & 0 & 3/4 & 1/4 & 0 & 0 \\ 0 & 0 & 1/4 & 3/4 & 0 & 0 \\ 0 & 0 & 0 & 3/4 & 1/4 & 0 \\ 0 & 0 & 0 & 1/4 & 3/4 & 0 \\ 0 & 0 & 0 & 0 & 3/4 & 1/4 \\ 0 & 0 & 0 & 0 & 1/4 & 3/4 \\ 0 & 0 & 0 & 0 & 0 & 3/4 \\ 0 & 0 & 0 & 0 & 0 & 1/4 \end{pmatrix},$$

and

$$\mathbf{M}^L_1 = \frac{1}{\sqrt{2}} \begin{pmatrix} 9/8 & 0 \\ -327/256 & 15/32 \\ 577/1024 & -15/128 \\ 51/1024 & 195/128 \\ -75/512 & -75/64 \\ -13/512 & -13/64 \\ 27/1024 & 27/128 \\ 9/1024 & 9/128 \end{pmatrix},$$

$$\mathbf{M}^I_{3,1} = \frac{1}{\sqrt{2}} \begin{pmatrix} -3/32 & 0 & 0 & 0 \\ -9/32 & 0 & 0 & 0 \\ 7/32 & -3/32 & 0 & 0 \\ 45/32 & -9/32 & 0 & 0 \\ -45/32 & 7/32 & 3/32 & 0 \\ -7/32 & 45/32 & 9/32 & 0 \\ 9/32 & -45/32 & -7/32 & 3/32 \\ 3/32 & -7/32 & -45/32 & 9/32 \\ 0 & 9/32 & 45/32 & -7/32 \\ 0 & 3/32 & 7/32 & -45/32 \\ 0 & 0 & -9/32 & 45/32 \\ 0 & 0 & -3/32 & 7/32 \\ 0 & 0 & 0 & -9/32 \\ 0 & 0 & 0 & -3/32 \end{pmatrix}.$$

Chapter 4

Quarklet Frames on the Real Line

This chapter is dedicated to the development of quarklets on the real line. The purpose of the construction is twofold. On the one hand, real line quarklets serve for theoretical inspections. With them, it is possible to characterize the Lebesgue space $L_2(\mathbb{R})$ as well as a range of Sobolev spaces $H^s(\mathbb{R})$. Furthermore, it should be theoretically feasible to characterize other smoothness spaces like Besov and Triebel-Lizorkin spaces on the real line, just to name a few. On the other hand, they serve as the groundwork for quarklet frame constructions on bounded domains as outlined in the Chapters 5 and 6.

In Section 4.1, we introduce quarks, which serve as the generator functions for quarklets, and establish some important estimates. Thereupon, we define shift-invariant quarklets in Section 4.2. Moreover, with vanishing moments, the frame property and compressibility, we prove several crucial properties of the quarklets.

The ideas for the construction of real line quarklets were developed in [47]. In this chapter, we slightly adapt the concept to derive quarklets which are symmetric independently of their order.

4.1 Construction and properties of quarks

In this section, we see how quarks emerge out of a multiplication of polynomials with generators. Moreover, some crucial estimates, which pave the way to show stability properties of the quarklet systems in Section 4.2, are established.

4.1.1 From generators to quarks

Let $m \in \mathbb{N}$. Given the generator $\varphi = N_m$, cf. (3.1.11), we define *(B-spline) quarks* by

$$\varphi_p := \left(\frac{\cdot - m/2}{m/2}\right)^p \varphi, \quad \text{for all } p \in \mathbb{N}_0. \tag{4.1.1}$$

Note the slightly different definition of the quarks in comparison to [47, Section 2].

For the support of the quarks φ_p, it holds $\operatorname{supp} \varphi_p = [0, m]$, $p \in \mathbb{N}_0$ since they obviously have the same support as the cardinal B-splines N_m, cf. Proposition 3.4

(i). By the symmetry properties of N_m, cf. Proposition 3.4 (ix), we have

$$\varphi\left(x+\frac{m}{2}\right)=\varphi\left(-x+\frac{m}{2}\right),\quad x\in\mathbb{R}.$$

For the polynomials it holds

$$\left(\frac{(x+m/2)-m/2}{m/2}\right)^p=(-1)^p\left(\frac{(-x+m/2)-m/2}{m/2}\right)^p,\quad x\in\mathbb{R}.$$

Combining both equations leads to

$$\varphi_p\left(x+\frac{m}{2}\right)=(-1)^p\varphi_p\left(-x+\frac{m}{2}\right),\quad x\in\mathbb{R}.$$

Hence, φ_p is symmetric around the axis at $x=\frac{m}{2}$ for p even and antisymmetric around the axis at $x=\frac{m}{2}$ for p odd. In Figure 4.1, this symmetry can be observed well.

Similar to the generator case, we define dilated and translated versions

$$\varphi_{p,j,k}:=2^{j/2}\varphi_p(2^j\cdot-k)=\left(\frac{2^j\cdot-k-m/2}{m/2}\right)^p\varphi_{j,k},\quad\text{for all } p,j\in\mathbb{N}_0,k\in\mathbb{Z}.\tag{4.1.2}$$

For given $p,j\in\mathbb{N}_0$, we shall consider the closed subspaces

$$V_{p,j}=\operatorname{clos}_{L_2(\mathbb{R})}\operatorname{span}\{\varphi_{i,j,k}:i=0,\dots,p,\ k\in\mathbb{Z}\}.\tag{4.1.3}$$

The spaces $V_{p,j}=\{f(2^j\cdot):f\in V_{0,p}\}$ are closely related to certain polynomial spline spaces. In fact, it obviously holds that $V_{0,p}\subset\operatorname{clos}_{L_2(\mathbb{R})}S^{m-2}_{m+p}$, where S^r_n is the polynomial spline space of order n and regularity r with respect to integer nodes of multiplicity $n-r-1$,

$$S^r_n:=\left\{f\in L_2(\mathbb{R}):f|_{[k,k+1)}\in\Pi_{n-1},k\in\mathbb{Z}\right\}\cap C^r(\mathbb{R}).$$

However, for $m\geq 2$, S^{m-2}_{m+p} is strictly larger than $\operatorname{span}\{\varphi_i(\cdot-k):i=0,\dots,p,\ k\in\mathbb{Z}\}$. A simple counterexample for $m=2$ is the quadratic B-spline with respect to double integer knots, $r(x)=\max\{0,1-|1-x|\}^2$. Although r is contained $\in S^0_3$, it does not have a finite linear expansion with respect to the integer translates of $N_2(x)$ and $(x-1)N_2(x)$.

In the following subsections, it is our aim to verify certain estimates. First, we prove a Jackson estimate of the form

$$\|f\|^2_{L_2(\mathbb{R})}+\sum_{j=0}^{\infty}2^{2js}E_{p,j}(f)^2\leq C\|f\|^2_{H^s(\mathbb{R})},\tag{4.1.4}$$

for all $f\in H^s(\mathbb{R})$, $0<s<m-\frac{1}{2}$, $p\in\mathbb{N}_0$, where $E_{p,j}(f):=\inf_{v\in V_{p,j}}\|f-v\|_{L_2(\mathbb{R})}$ is the error of the best $L_2(\mathbb{R})$ approximation from $V_{p,j}$ and $C>0$. Second, we establish a norm estimate of the quarks

$$\|\varphi_p\|_{L_q(\mathbb{R})}\simeq(p+1)^{-(m-1+1/q)},\quad\text{for all } p\geq(m-1)^2,p\in\mathbb{N}_0,1\leq q\leq\infty.\tag{4.1.5}$$

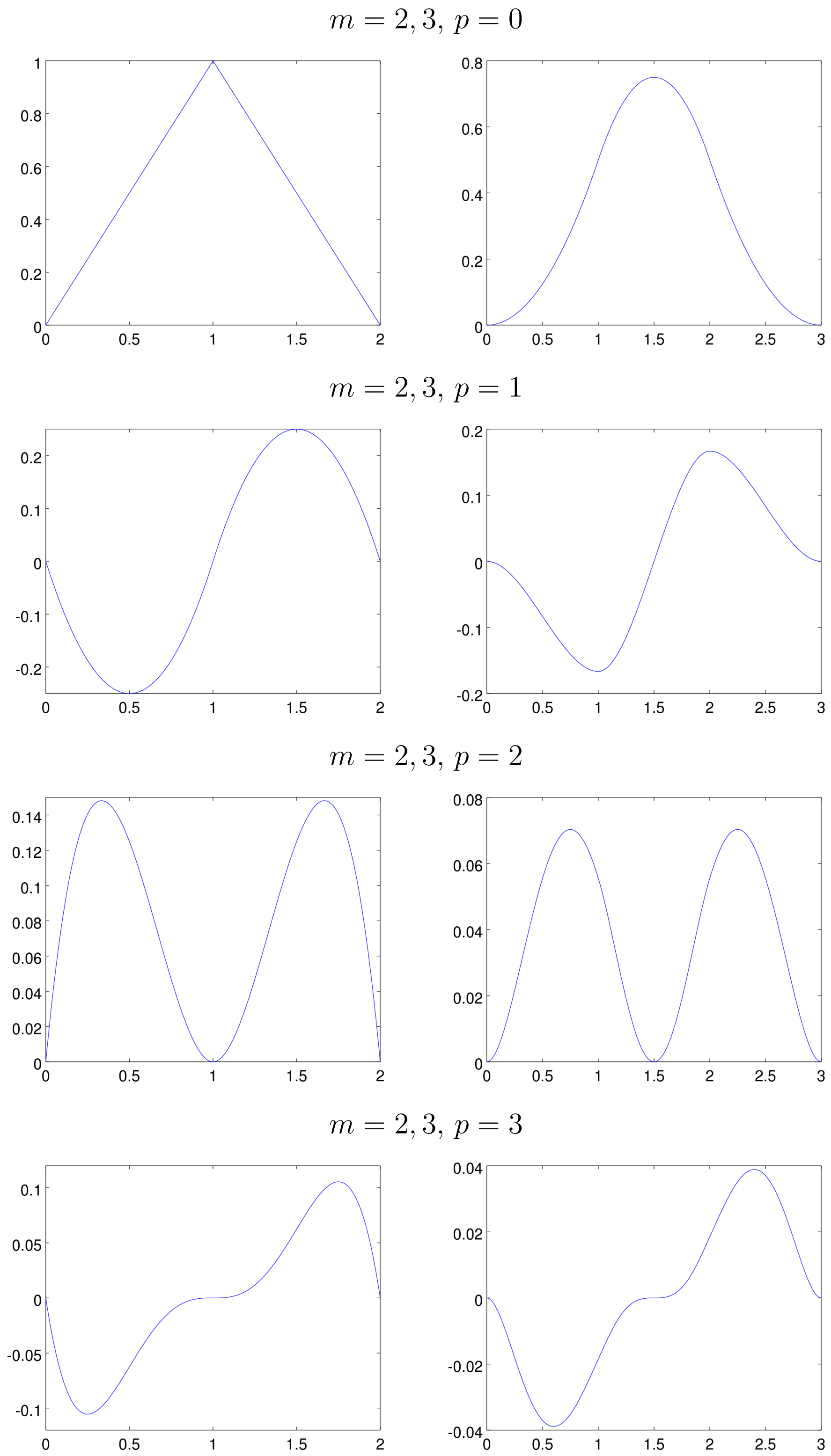

Figure 4.1: B-spline quarks φ_p of orders $m = 2, 3$ and polynomial degrees $p = 0, 1, 2, 3$.

Third, we show a Bernstein estimate,

$$\|g\|_{H^s(\mathbb{R})} \leq B_{s,p} 2^{js} \|g\|_{L_2(\mathbb{R})}, \quad \text{for all } g \in V_{p,j}, 0 < s < m - \frac{1}{2}, p \in \mathbb{N}_0, \tag{4.1.6}$$

with $B_{s,p} > 0$. The conditions (4.1.4), (4.1.5) and (4.1.6), are the main ingredients to show the stability of a properly weighted system of dilates and translates of the quarklets ψ_p, $p \in \mathbb{N}_0$, which we introduce in Section 4.2.

4.1.2 Direct estimates

We shall first derive direct estimates for the approximation spaces $V_{p,j}$ from (4.1.3). They are closely related to known results from spline theory.

Proposition 4.1. *There exists $C = C(m) > 0$, such that*

$$(p+1)^{2s} \sum_{j=0}^{\infty} 2^{2js} E_{p,j}(f)^2 \leq C \|f\|^2_{H^s(\mathbb{R})}, \tag{4.1.7}$$

for all $f \in H^s(\mathbb{R})$, $0 \leq s \leq m$, $p \in \mathbb{N}_0$. In particular, it holds that

$$E_{p,j}(f) \leq C^{1/2} (p+1)^{-s} 2^{-js} \|f\|_{H^s(\mathbb{R})}, \tag{4.1.8}$$

for all $f \in H^s(\mathbb{R})$, $0 \leq s \leq m$, $p, j \in \mathbb{N}_0$.

Proof. Let $p, j \in \mathbb{N}_0$ and $f \in L_2(\mathbb{R})$ be fixed. In view of (4.1.1), (4.1.2) and (4.1.3), $V_{p,j}$ contains at least all $v \in L_2(\mathbb{R})$ of the form

$$v = \sum_{k \in \mathbb{Z}} p_k \varphi(2^j \cdot -k), \tag{4.1.9}$$

where $p_k \in \Pi_p$ are polynomials of degree at most p, for all $k \in \mathbb{Z}$, and the sum converges in $L_2(\mathbb{R})$. From the partition of unity property $\sum_{k \in \mathbb{Z}} \varphi(\cdot - k) \equiv 1$, and from (4.1.9), we can deduce that

$$f - v = \sum_{k \in \mathbb{Z}} \big(f - p_k\big) \varphi(2^j \cdot -k).$$

Define $I_{j,l} := 2^{-j}[l, l+1]$ and $S_{j,k} := \operatorname{supp} \varphi(2^j \cdot -k)$, for all $l, k \in \mathbb{Z}$. By the compact support of φ, $\#\{k \in \mathbb{Z} : S_{j,k} \cap I_{j,l} \neq \emptyset\}$ is uniformly bounded in $l \in \mathbb{Z}$ and $j \in \mathbb{N}_0$. For any $f \in L_2(\mathbb{R})$, we can therefore estimate

$$\begin{aligned}
\|f - v\|^2_{L_2(\mathbb{R})} &= \sum_{l \in \mathbb{Z}} \int_{I_{j,l}} \Big(\sum_{k \in \mathbb{Z}} \big(f(x) - p_k(x)\big) \varphi(2^j x - k) \Big)^2 \,\mathrm{d}x \\
&\leq C_1 \sum_{k \in \mathbb{Z}} \sum_{l \in \mathbb{Z}} \int_{I_{j,l}} \big(f(x) - p_k(x)\big)^2 \varphi(2^j x - k)^2 \,\mathrm{d}x \\
&= C_1 \sum_{k \in \mathbb{Z}} \int_{S_{j,k}} \big(f(x) - p_k(x)\big)^2 \varphi(2^j x - k)^2 \,\mathrm{d}x \\
&\leq C_1 \|\varphi\|^2_{L_\infty(\mathbb{R})} \sum_{k \in \mathbb{Z}} \big\|f - p_k\big\|^2_{L_2(S_{j,k})},
\end{aligned}$$

with $C_1 = C_1(m) > 0$.

Now let $f \in H^m(\mathbb{R})$ and let $p_k \in \Pi_{p+1}$ be the orthogonal projection of $f|_{S_{j,k}}$ onto Π_{p+1} in $L_2(S_{j,k})$. It follows that $\|p_k\|_{L_2(S_{j,k})} \le \|f\|_{L_2(S_{j,k})}$ and due to $\varphi \in L_\infty(\mathbb{R})$, the sum (4.1.9) really converges in $L_2(\mathbb{R})$, so that this particular v is contained in $V_{p,j}$. Moreover, standard results from polynomial approximation tell us that

$$\|f - p_k\|_{L_2(S_{j,k})} \le C_2(p+1)^{-m}2^{-jm}|f|_{H^m(S_{j,k})},$$

where $C_2 = C_2(m) > 0$ is independent of j, k and p, see [95, Corollary 3.12]. We deduce that with $C_3 = C_3(m) > 0$,

$$E_{p,j}(f) \le \|f - v\|_{L_2(\mathbb{R})} \le C_3(p+1)^{-m}2^{-jm}|f|_{H^m(\mathbb{R})}, \tag{4.1.10}$$

where we used that the sets $S_{j,k}$ have uniformly bounded overlap in $j \in \mathbb{N}_0$.

For arbitrary $f \in L_2(\mathbb{R})$, using the triangle inequality and (4.1.10), we see that for each $g \in H^m(\mathbb{R})$, we have

$$E_{p,j}(f) \le \|f - g\|_{L_2(\mathbb{R})} + E_{p,j}(g) \le \|f - g\|_{L_2(\mathbb{R})} + C_3(p+1)^{-m}2^{-jm}|g|_{H^m(\mathbb{R})}.$$

By consequence, taking the infimum over $g \in H^m(\mathbb{R})$, $E_{p,j}(f)$ can be estimated by values of the K functional $K(f,t) := \inf_{g\in H^m(\mathbb{R})} \|f - g\|_{L_2(\mathbb{R})} + t|g|_{H^m(\mathbb{R})}$,

$$E_{p,j}(f) \le C_3 K\Big(f, (p+1)^{-m}2^{-jm}\Big). \tag{4.1.11}$$

Now, we use the fact that for $0 < s \le m$, an equivalent norm on $H^s(\mathbb{R})$ is given by

$$\|f\|_{[L_2(\mathbb{R}),H^m(\mathbb{R})]_{s/m,2}} = \|f\|_{L_2(\mathbb{R})} + \bigg(\int_0^\infty \Big(t^{-s/m}K(f,t)\Big)^2 \frac{\mathrm{d}t}{t}\bigg)^{1/2},$$

with constants in the norm equivalence only depending on m, see [10] for details. Similar to [10, Lemma 3.1.3], we can replace the latter integral by a discrete sum, losing constants that only depend on m. In fact, for $(p+1)^{-m}2^{-jm} \le t \le (p+1)^{-m}2^{-(j-1)m}$, it follows from the monotonicity property $K(f,as) \le \max\{1,a\}K(f,s)$ of the K functional that

$$\begin{aligned} 2^{-s}(p+1)^s 2^{js} K\Big(f, (p+1)^{-m}2^{-jm}\Big) &\le t^{-s/m}K(f,t) \\ &\le 2^m (p+1)^s 2^{js} K\Big(f, (p+1)^{-m}2^{-jm}\Big). \end{aligned}$$

We can therefore estimate

$$\int_0^\infty \Big(t^{-s/m}K(f,t)\Big)^2 \frac{\mathrm{d}t}{t} = \sum_{j\in\mathbb{Z}} \int_{(p+1)^{-m}2^{-jm}}^{(p+1)^{-m}2^{-(j-1)m}} \Big(t^{-s/m}K(f,t)\Big)^2 \frac{\mathrm{d}t}{t}$$

$$\begin{cases} \le 2^{2m}(\log 2^m)(p+1)^{2s} \sum_{j\in\mathbb{Z}} 2^{2js} K\Big(f, (p+1)^{-m}2^{-jm}\Big)^2 \\ \ge 2^{-2s}(\log 2^m)(p+1)^{2s} \sum_{j\in\mathbb{Z}} 2^{2js} K\Big(f, (p+1)^{-m}2^{-jm}\Big)^2 \end{cases},$$

so that the claim follows from (4.1.11) and summation over $j \in \mathbb{N}_0$. □

Remark 4.2. The properties of N_m that we used in the proof of Proposition 4.1 were the compact support, the partition of unity property and $N_m \in L_\infty(\mathbb{R})$. Hence, a Jackson estimate in the fashion of (4.1.7) holds for all spaces $V_{p,j}$ for which φ fulfils the above-mentioned requirements, cf. Subsection 4.1.1.

4.1.3 Norm estimates

Now, we establish sharp bounds for the L_q norms of single B-spline quarks, as $p \to \infty$. In view of $\varphi \in L_\infty(\mathbb{R})$, (4.1.1) and the identity

$$\left\|\left(\tfrac{\cdot - m/2}{m/2}\right)^p\right\|_{L_q(0,m)} = \left(\frac{2}{pq+1}\right)^{1/q}, \quad \text{for all } p \in \mathbb{N}_0,\ 0 < q < \infty,$$

we obtain the simple estimate

$$\|\varphi_p\|_{L_q(\mathbb{R})} \leq \left(\tfrac{2}{pq+1}\right)^{1/q} \|\varphi\|_{L_\infty(\mathbb{R})}, \quad \text{for all } p \in \mathbb{N}_0,\ 0 < q < \infty. \tag{4.1.12}$$

These asymptotics in p are already sharp, e.g., if φ is the step function $\chi_{[0,1)}$, with

$$\|\varphi_p\|_{L_q(\mathbb{R})} = (pq+1)^{-1/q}, \quad \text{for all } p \in \mathbb{N}_0,\ 0 < q < \infty. \tag{4.1.13}$$

In case that φ has higher regularity in $L_\infty(\mathbb{R})$, the L_q norms of φ_p decay even faster with p. The aim is to establish sharp bounds for the L_q norms of the B-spline quarks φ_p, as $p \to \infty$. We start with an auxiliary result on the location of the extrema of φ_p for sufficiently large values of p.

Lemma 4.3. *Let $2 \leq m \in \mathbb{N}$, $\varphi = N_m$ and φ_p be given by* (4.1.1)*. Then,*

$$\|\varphi_p\|_{L_\infty(\mathbb{R})} = \left|\varphi_p(\hat{x})\right|, \quad \hat{x} := \frac{2pm + m^2 - m}{2(p+m-1)}, \quad \textit{for all } p \geq (\tfrac{m}{2}-1)(m-1). \tag{4.1.14}$$

Proof. Let $2 \leq m \in \mathbb{N}$ be fixed. Let $p \in \mathbb{N}_0$ with $p \geq (\frac{m}{2}-1)(m-1)$ be fixed. The case $p = 0$ can only occur if $m = 2$. Then, the extremum of φ_0 is obviously at $x = 1$, which coincides with $\hat{x}$ for $p = 0$, $m = 2$. Hence, from now on, we can assume that $p > 0$.

It is sufficient to determine the extrema of φ_p in $[\frac{m}{2}, m)$, because $\varphi_p\left(x + \frac{m}{2}\right) = (-1)^p \varphi_p\left(-x + \frac{m}{2}\right)$ for all $x \in \mathbb{R}$. We prove that φ_p is non-decreasing on $[\frac{m}{2}, m-1]$. For $m = 2$, there is nothing to prove. For $m \geq 3$, φ_p is continuously differentiable. Let $x \in [\frac{m}{2}, m-1]$. A simple estimate leads to

$$\begin{aligned}(\tfrac{m}{2})^p \varphi_p'(x) &= (x - \tfrac{m}{2})^{p-1}\Big(pN_m(x) + (x - \tfrac{m}{2})N_m'(x)\Big) \\ &\geq (x - \tfrac{m}{2})^{p-1}\Big(pN_m(x) - (\tfrac{m}{2} - 1)\left|N_m'(x)\right|\Big).\end{aligned}$$

By applying (3.1.12) we further derive

$$\begin{aligned}(\tfrac{m}{2})^p\varphi_p'(x) &\geq (x-\tfrac{m}{2})^{p-1}\Big(pN_m(x)-(\tfrac{m}{2}-1)\Big|N_{m-1}(x)-N_{m-1}(x-1)\Big|\Big)\\ &\geq (x-\tfrac{m}{2})^{p-1}\Big(pN_m(x)-(\tfrac{m}{2}-1)\Big(N_{m-1}(x)+N_{m-1}(x-1)\Big)\Big).\end{aligned}$$

For all $x\in[\frac{m}{2},m-1]$, we have $\min\{x,m-x\}\geq 1$ and thus

$$\begin{aligned}(\tfrac{m}{2})^p\varphi_p'(x) &\geq (x-\tfrac{m}{2})^{p-1}\\ &\quad\cdot\Big(pN_m(x)-(\tfrac{m}{2}-1)\Big(xN_{m-1}(x)+(m-x)N_{m-1}(x-1)\Big)\Big).\end{aligned}$$

An application of (3.1.13) gives

$$(\tfrac{m}{2})^p\varphi_p'(x)\geq (x-\tfrac{m}{2})^{p-1}\Big(p-(\tfrac{m}{2}-1)(m-1)\Big)N_m(x),$$

which is non-negative because $p\geq(\frac{m}{2}-1)(m-1)$. Therefore, all local maxima of φ_p are located in $[m-1,m]$, whenever $p\geq(\frac{m}{2}-1)(m-1)$. On $[m-1,m]$, we have $N_m(x)=\frac{1}{(m-1)!}(m-x)^{m-1}$, cf. (3.1.15), so that from

$$\begin{aligned}(\tfrac{m}{2})^p(m-1)!\varphi_p'(x) &= p(x-\tfrac{m}{2})^{p-1}(m-x)^{m-1}-(m-1)(x-\tfrac{m}{2})^p(m-x)^{m-2}\\ &= (x-\tfrac{m}{2})^{p-1}(m-x)^{m-2}\Big(pm+\tfrac{m^2}{2}-\tfrac{m}{2}-(p+m-1)x\Big),\end{aligned}$$

we obtain the critical points m and $\hat{x}:=\frac{2pm+m^2-m}{2(p+m-1)}$. Using that $p\geq(\frac{m}{2}-1)(m-1)$, we observe that indeed $\hat{x}\in[m-1,m]$, since

$$m-1=m-\tfrac{m(m-1)/2}{(m/2-1)(m-1)+m-1}\leq m-\tfrac{m(m-1)/2}{p+m-1}=\hat{x}\leq m.$$

Due to $\varphi_p(m)=0$, the symmetry of φ_p and the fact that φ_p is positive for $x\in[\frac{m}{2},m]$, the global maximum of φ_p is attained in $[m-1,m]$, so that the unique local maximum $\hat{x}$ is also global.

□

From Figure 4.2, it can be observed that the location of the extrema of φ_p is very near to the boundary of the support for a high polynomial degree p. This underpins Lemma 4.3, wherein we just have shown that an extrema occurs at $\hat{x}=\frac{2pm+m^2-m}{2(p+m-1)}\underset{p\to\infty}{\longrightarrow} m$.

Now that we know the location of the quarks' global extrema, we are ready to prove a norm estimate.

Proposition 4.4. *Let $2\leq m\in\mathbb{N}$, $\varphi=N_m$ and φ_p be given by (4.1.1). For each $1\leq q\leq\infty$, there exist $c=c(m,q),C=C(m,q)>0$ such that*

$$c(p+1)^{-(m-1+1/q)}\leq\|\varphi_p\|_{L_q(\mathbb{R})}\leq C(p+1)^{-(m-1+1/q)}, \tag{4.1.15}$$

for all $p\geq(m-1)^2$, $p\in\mathbb{N}_0$.

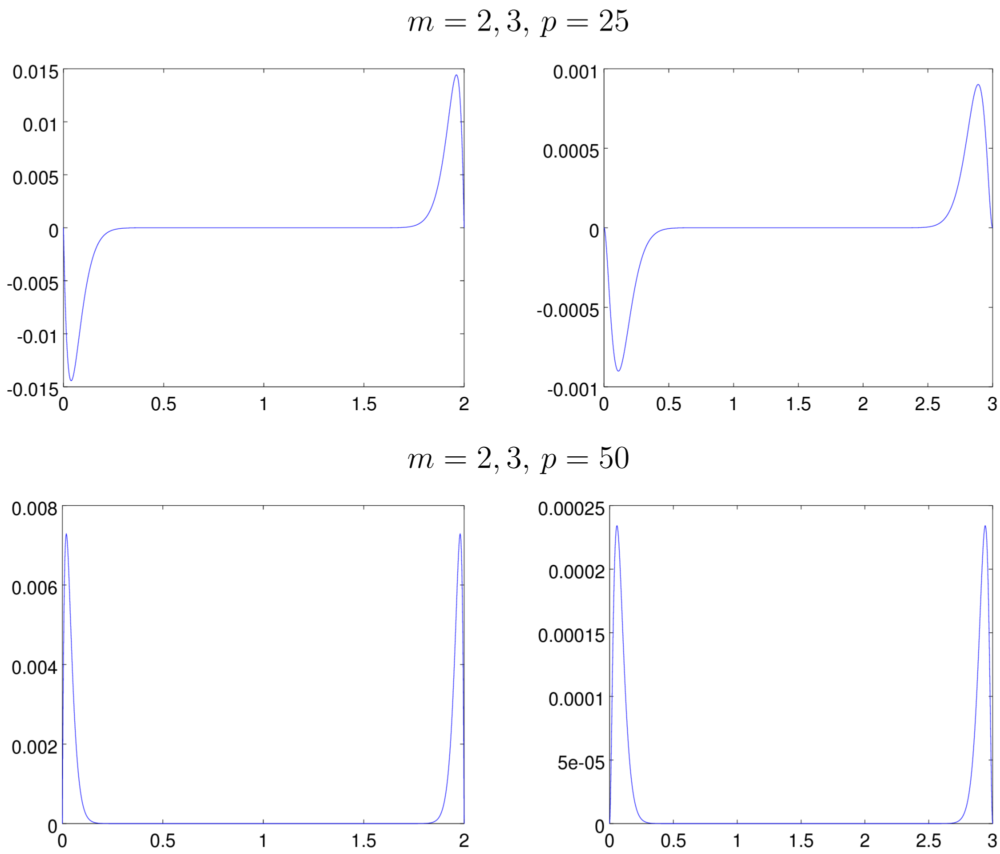

Figure 4.2: B-spline quarks φ_p of orders $m = 2, 3$ and polynomial degrees $p = 25, 50$.

Proof. The special case $m = 1$ is already covered by (4.1.13), so we can assume that $m \geq 2$, without loss of generality, and hence $p \geq (m-1)^2 \geq 1$.

In order to show the upper bound in (4.1.15), we study the extremal values $q \in \{1, \infty\}$ and conclude by an application of Hölder's inequality. For $q = 1$, we exploit that for any $g \in C^m[0, m]$,

$$\int_0^m g^{(m)}(x) N_m(x) \, \mathrm{d}x = \sum_{k=0}^{m} (-1)^{m-k} \binom{m}{k} g(k).$$

In the case that p is even, we can use $g := \frac{1}{(p+m)\cdots(p+1)} (\cdot - \frac{m}{2})^{p+m}$ and the non-negativity of φ_p to infer that with $C_1 = C_1(m) := \sum_{k=0}^{m} \binom{m}{k} |k - \frac{m}{2}|^m$,

$$\begin{aligned} \|\varphi_p\|_{L_1(\mathbb{R})} &= \left(\frac{2}{m}\right)^p \int_0^m (x - \tfrac{m}{2})^p N_m(x)\ \mathrm{d}x \\ &= \left(\frac{2}{m}\right)^p \sum_{k=0}^{m} \frac{(-1)^{m-k}\binom{m}{k}(k-\frac{m}{2})^{p+m}}{(p+m)\cdots(p+1)} \\ &\leq C_1(p+1)^{-m}. \end{aligned} \tag{4.1.16}$$

If $p \geq 1$ is odd, the estimate $\left|\frac{x-m/2}{m/2}\right| \leq 1$ for all $x \in \operatorname{supp}\varphi_p$ yields

$$\|\varphi_p\|_{L_1(\mathbb{R})} \leq \|\varphi_{p-1}\|_{L_1(\mathbb{R})} \leq C_1 p^{-m} \leq C_1 2^m (p+1)^{-m}. \tag{4.1.17}$$

For $q = \infty$, Lemma 4.3 tells us that for all $p \geq (\frac{m}{2} - 1)(m-1)$ and $\hat{x} := \frac{2pm+m^2-m}{2(p+m-1)}$,

$$\|\varphi_p\|_{L_\infty(\mathbb{R})} = \left(\frac{2\hat{x}-m}{m}\right)^p N_m(\hat{x}).$$

Since $\hat{x} \in [m-1, m]$, we can use the representation formula (3.1.15) to derive

$$\begin{aligned} \|\varphi_p\|_{L_\infty(\mathbb{R})} &= \frac{1}{(m-1)!}\left(\frac{2\hat{x}-m}{m}\right)^p (m-\hat{x})^{m-1} \\ &= \frac{1}{(m-1)!}\left(\frac{p}{p+m-1}\right)^p \left(\frac{m(m-1)}{2(p+m-1)}\right)^{m-1}. \end{aligned} \tag{4.1.18}$$

The latter, we estimate from above by

$$\|\varphi_p\|_{L_\infty(\mathbb{R})} \leq \frac{1}{(m-1)!}\left(\frac{m(m-1)}{2}\right)^{m-1} (p+1)^{-(m-1)}, \tag{4.1.19}$$

Thus, we already proved the lower estimate in (4.1.15) for $q = \infty$.

Finally, let $1 < q < \infty$ and $p \geq (m-1)^2$. By an application of Hölder's inequality for $\varphi_p \in L_1(\mathbb{R}) \cap L_\infty(\mathbb{R})$, we obtain from (4.1.16), (4.1.17) and (4.1.19) the upper estimate in (4.1.15),

$$\|\varphi_p\|_{L_q(\mathbb{R})} \leq \|\varphi_p\|_{L_1(\mathbb{R})}^{1/q} \|\varphi_p\|_{L_\infty(\mathbb{R})}^{1-1/q} \leq C_2(p+1)^{-(m-1+1/q)},$$

where $C_2 = C_2(m,q) > 0$.

It remains to show the lower estimate in (4.1.15) for $1 \leq q \leq \infty$. If $q = \infty$, we use the representation (4.1.18) to estimate from below by

$$\|\varphi_p\|_{L_\infty(\mathbb{R})} \geq \frac{1}{(m-1)!} e^{1-m} \left(\frac{m}{2}\right)^{m-1} (p+1)^{-(m-1)}. \tag{4.1.20}$$

Now, let us consider the case $q \in \mathbb{N}$. We use again (3.1.15) to estimate

$$\begin{aligned}
\|\varphi_p\|^q_{L_q(\mathbb{R})} \geq \int_{m-1}^{m} \varphi_p(x)^q \,\mathrm{d}x &= \frac{1}{\big((m-1)!\big)^q} \int_{m-1}^{m} (\tfrac{2x-m}{m})^{pq}(m-x)^{(m-1)q} \,\mathrm{d}x \\
&= \frac{1}{\big((m-1)!\big)^q} \int_0^1 (1-\tfrac{2y}{m})^{pq} y^{(m-1)q} \,\mathrm{d}y \\
&\geq \frac{1}{\big((m-1)!\big)^q} \int_0^1 (1-y)^{pq} y^{(m-1)q} \,\mathrm{d}y.
\end{aligned}$$

Due to $q \in \mathbb{N}$, the latter integral can be computed explicitly, by means of $(m-1)q$ times partial integration, and with $C_3(m,q) > 0$ we obtain

$$\begin{aligned}
\int_0^1 (1-y)^{pq} y^{(m-1)q} \,\mathrm{d}y &= \frac{\big((m-1)q\big)!}{(pq+1)\cdots\big(pq+(m-1)q\big)} \int_0^1 (1-y)^{(p+m-1)q} \,\mathrm{d}y \\
&= \frac{\big((m-1)q\big)!}{(pq+1)\cdots\big(pq+(m-1)q+1\big)} \\
&\geq C_3(p+1)^{-(m-1)q-1},
\end{aligned}$$

from which the lower estimate in (4.1.15) immediately follows. Finally, let $1 \leq q < \infty$ be arbitrary. If $1 \leq q \leq 2$, Hölder's inequality tells us that

$$\|\varphi_p\|_{L_2(\mathbb{R})} \leq \|\varphi_p\|^{q/2}_{L_q(\mathbb{R})} \|\varphi_p\|^{1-q/2}_{L_\infty(\mathbb{R})}.$$

With $C_3 = C_3(m,q) > 0$, isolating $\|\varphi_p\|_{L_q(\mathbb{R})}$ and an application of (4.1.15) for the L_2 and L_∞ case yields

$$\begin{aligned}
\|\varphi_p\|_{L_q(\mathbb{R})} &\geq \|\varphi_p\|^{2/q}_{L_2(\mathbb{R})} \|\varphi_p\|^{1-2/q}_{L_\infty(\mathbb{R})} \\
&\geq C_3(p+1)^{-2(m-1/2)/q}(p+1)^{-(m-1)(1-2/q)} \\
&= C_3(p+1)^{-(m-1+1/q)}.
\end{aligned}$$

Analogously, if $2 \leq q < \infty$, Hölder's inequality tells us that

$$\|\varphi_p\|_{L_2(\mathbb{R})} \leq \|\varphi_p\|^{1-1/(2(1-1/q))}_{L_1(\mathbb{R})} \|\varphi_p\|^{1/(2(1-1/q))}_{L_q(\mathbb{R})},$$

so that isolation of $\|\varphi_p\|_{L_q(\mathbb{R})}$ and an application of (4.1.15) for L_1 and L_2 prove the claim,

$$\begin{aligned}
\|\varphi_p\|_{L_q(\mathbb{R})} &\geq \|\varphi_p\|^{2-2/q}_{L_2(\mathbb{R})} \|\varphi_p\|^{2/q-1}_{L_1(\mathbb{R})} \\
&\geq C_4(p+1)^{-(m-1/2)(2-2/q)}(p+1)^{-m(2/q-1)} \\
&= C_4(p+1)^{-(m-1+1/q)},
\end{aligned}$$

with $C_4 = C_4(m,q) > 0$. □

4.1.4 Inverse estimates

This subsection is concerned with the derivation of certain Bernstein-type estimates. All three statements (4.1.21)-(4.1.23) look alike in regard that a norm of some kind of derivative on the left-hand side is estimated by a norm of the actual function multiplied with a weight on the right-hand side. However, every single statement in its special form is needed in the course of this chapter.

Proposition 4.5. *Let $m \in \mathbb{N}$, $\varphi = N_m$ and let $V_{p,j}$ be given by* (4.1.3). *Then for $1 \le q \le \infty$, there exists $C = C(m) > 0$, such that for all $f \in V_{p,j}$,*

$$\omega_m(f,t)_{L_q(\mathbb{R})} \le C \min\left\{1, (p+1)^2 2^j t\right\}^{m-1+1/q} \|f\|_{L_q(\mathbb{R})}. \tag{4.1.21}$$

Proof. Let $f = \sum_{0 \le i \le p} \sum_{k \in \mathbb{Z}} c_{i,k} \varphi_{i,j,k} \in V_{p,j}$. If $t \ge (p+1)^{-2} 2^{-j}$, we simply use

$$\omega_m(f,t)_{L_q(\mathbb{R})} \le 2^m \|f\|_{L_q(\mathbb{R})} = 2^m \min\{1, (p+1)^2 2^j t\}^{m-1+1/q} \|f\|_{L_q(\mathbb{R})}.$$

Now let $t < (p+1)^{-2} 2^{-j}$. By using $V_{p,j} \subset W_q^{m-1}(\mathbb{R})$ and standard arithmetics for the moduli of smoothness, see [65, Section 2.7], we see that $\omega_m(f,t)_{L_q(\mathbb{R})} \le t^{m-1} \omega_1(f^{(m-1)}, t)_{L_q(\mathbb{R})}$. But $f^{(m-1)}$ is piecewise polynomial of degree p without continuity assumptions at the nodes $x_l := 2^{-j} l$, $l \in \mathbb{Z}$. We compute for $0 < h \le t \le 2^{-j}$ and $q < \infty$ that

$$\begin{aligned}
&\left\| f^{(m-1)}(\cdot + h) - f^{(m-1)} \right\|_{L_q(\mathbb{R})}^q \\
&= \sum_{l \in \mathbb{Z}} \left\| f^{(m-1)}(\cdot + h) - f^{(m-1)} \right\|_{L_q(x_l, x_{l+1})}^q \\
&= \sum_{l \in \mathbb{Z}} \left(\left\| f^{(m-1)}(\cdot + h) - f^{(m-1)} \right\|_{L_q(x_l, x_{l+1}-h)}^q \right. \\
&\quad \left. + \left\| f^{(m-1)}(\cdot + h) - f^{(m-1)} \right\|_{L_q(x_{l+1}-h, x_{l+1})}^q \right) \\
&\le 2^{1-1/q} \sum_{l \in \mathbb{Z}} \left(h^q \|f^{(m)}\|_{L_q(x_l, x_{l+1})}^q + \|f^{(m-1)}\|_{L_q(x_{l+1}-h, x_{l+1})}^q + \|f^{(m-1)}\|_{L_q(x_l, x_l+h)}^q \right).
\end{aligned}$$

An application of standard estimates for polynomials yields

$$\|f^{(m-1)}\|_{L_q(x_{l+1}-h, x_{l+1})}^q + \|f^{(m-1)}\|_{L_q(x_l, x_l+h)}^q \le C_1 h 2^j p^2 \|f^{(m-1)}\|_{L_q(x_l, x_{l+1})}^q,$$

with $C_1 > 0$ independent of m, p and q. Using the L_q Markov inequality for algebraic polynomials P of degree i on an interval I,

$$\|P'\|_{L_q(I)} \le C_2 \frac{i^2}{|I|} \|P\|_{L_q(I)},$$

with $C_2 = C_2(q) > 0$ independent of i, we end up with

$$\begin{aligned}\omega_m(f,t)^q_{L_q(\mathbb{R})} &\leq t^{(m-1)q} \sup_{|h|\leq t} \left\| f^{(m-1)}(\cdot + h) - f^{(m-1)} \right\|^q_{L_q(\mathbb{R})} \\ &\leq C_3 t^{(m-1)q} \Big(h^q (p+1)^{2mq} 2^{jmq} + h 2^{j(1+(m-1)q)} p^{2+2(m-1)q} \Big) \sum_{l\in\mathbb{Z}} \|f\|^q_{L_q(x_l,x_{l+1})} \\ &\leq C_4 t^{(m-1)q+1} (p+1)^{2(m-1)q+2} 2^{j(1+(m-1)q)} \|f\|^q_{L_q(\mathbb{R})},\end{aligned}$$

where $C_3 = C_3(m,q) > 0$, $C_4 = C_4(m,q) > 0$. The case $q = \infty$ is completely analogous. □

As we have seen in the proof of Proposition 4.5, a Bernstein-type estimate is a statement about the properties of the induced spaces $V_{p,j}$ but not of the quarks φ_p. Hence, a different quarkonial approach that leads to the same refinement spaces $V_{p,j}$ allows for a similar Bernstein-type estimate. This also holds true for the two upcoming estimates.

Corollary 4.6. *Let $m \in \mathbb{N}$, $\varphi = N_m$ and let $V_{p,j}$ be given by (4.1.3). Then, for $1 \leq q \leq \infty$, there exists $C = C(m,q) > 0$, such that for all $f \in V_{p,j}$*

$$\|f^{(k)}\|_{L_q(\mathbb{R})} \leq C(p+1)^{2k} 2^{jk} \|f\|_{L_q(\mathbb{R})}, \quad \textit{for all } k = 0,\ldots,m-1. \tag{4.1.22}$$

Proof. Without loss of generality, let $\mathbb{N} \ni m \geq 2$ and $k = 1,\ldots,m-1$. Note that $V_{p,j} \subset W_q^{m-1}(\mathbb{R})$, so that $f^{(k)}$ is well-defined for each $f \in V_{p,j}$. Let us first consider the case $k = 1$. We can use that for all $f \in W_q^1(\mathbb{R})$, $1 \leq q \leq \infty$,

$$\|f'\|_{L_q(\mathbb{R})} = \lim_{t\to 0} \frac{\omega_1(f,t)_{L_q(\mathbb{R})}}{t},$$

see [78, Proposition 2.4] for the case $q < \infty$. For $q = \infty$, the latter equation can be inferred at least for continuous functions. Using a Marchaud-type inequality

$$\omega_1(f,t)_{L_q(\mathbb{R})} \leq C_1 t \int_t^\infty \frac{\omega_m(f,s)_{L_q(\mathbb{R})}}{s^2} \,\mathrm{d}s,$$

with $C_1 = C_1(m) > 0$, confer [65, Section 2.8] for details, we derive from (4.1.21) that

$$\begin{aligned}\|f'\|_{L_q(\mathbb{R})} &\leq C_1 \limsup_{t\to 0} \int_t^\infty \frac{\omega_m(f,s)_{L_q(\mathbb{R})}}{s^2} \,\mathrm{d}s \\ &= C_1 \Bigg(\limsup_{t\to 0} \int_t^{(p+1)^{-2}2^{-j}} \frac{\omega_m(f,s)_{L_q(\mathbb{R})}}{s^2} \,\mathrm{d}s + \int_{(p+1)^{-2}2^{-j}}^\infty \frac{\omega_m(f,s)_{L_q(\mathbb{R})}}{s^2} \,\mathrm{d}s \Bigg) \\ &\leq C_2 \Bigg(\Big((p+1)^2 2^j \Big)^{m-1+1/q} \int_0^{(p+1)^{-2}2^{-j}} s^{m-3+1/q} \,\mathrm{d}s + \int_{(p+1)^{-2}2^{-j}}^\infty s^{-2} \,\mathrm{d}s \Bigg) \|f\|_{L_q(\mathbb{R})} \\ &= C_2 \left(\frac{1}{m-2+1/q} + 1 \right) (p+1)^2 2^j \|f\|_{L_q(\mathbb{R})},\end{aligned}$$

with $C_2 = C_2(m,q) > 0$. The case of general $k = 2, \dots, m-1$ can be treated by induction over k, repeating the previous Marchaud-type estimate k times. $\square$

Corollary 4.7. *Let $m \in \mathbb{N}$, $\varphi = N_m$ and let $V_{p,j}$ be given by (4.1.3). For each $0 \le s < m - \frac{1}{2}$, there exists $C = C(m,s) > 0$, such that*

$$|f|_{H^s(\mathbb{R})} \le C(p+1)^{2s} 2^{js} \|f\|_{L_2(\mathbb{R})}, \quad \text{for all } p, j \in \mathbb{N}_0, f \in V_{p,j}. \tag{4.1.23}$$

Proof. Let $s > 0$, without loss of generality. In view of the norm estimate

$$|f|_{H^s(\mathbb{R})} \le C_1 \Big(\int_0^\infty \Big(t^{-s} \omega_m(f,t)_{L_2(\mathbb{R})} \Big)^2 \frac{\mathrm{d}t}{t} \Big)^{1/2}, \quad \text{for all } 0 < s < m,$$

where $C_1 = C_1(s) > 0$, we can compute that by (4.1.21),

$$\begin{aligned} |f|^2_{H^s(\mathbb{R})} &\le \Big(C_2 (p+1)^{2(2m-1)} 2^{j(2m-1)} \int_0^{(p+1)^{-2} 2^{-j}} t^{-2s+2m-2} \,\mathrm{d}t \\ &\qquad + C_2 \int_{(p+1)^{-2}2^{-j}}^\infty t^{-(2s+1)} \,\mathrm{d}t \Big) \|f\|^2_{L_2(\mathbb{R})} \\ &\le \Big(\frac{C_2}{2m-1-2s} + \frac{C_2}{2s} \Big) (p+1)^{4s} 2^{2js} \|f\|^2_{L_2(\mathbb{R})}, \quad \text{for all } 0 < s < m - \frac{1}{2}, \end{aligned}$$

with $C_2 = C_2(m,s) > 0$. Due to the fact that (4.1.23) trivially holds for $s = 0$ with $C = 1$, an interpolation argument shows that C does in fact only depend on s as $s \to m - \frac{1}{2}$. $\square$

We note, however, that (4.1.23) is not sharp for single quarks. If $\varphi = N_2$ is the hat function and $s = 1$, one can explicitly compute that

$$\begin{aligned} \|\varphi_p'\|^2_{L_2(\mathbb{R})} &= 2 \int_1^2 (x-1)^{2p-2} \Big(p - (p+1)(x-1) \Big)^2 \,\mathrm{d}x \\ &= 2 \int_0^1 y^{2p-2} \Big(p - (p+1)y \Big)^2 \,\mathrm{d}y \\ &= 2 \Big(p^2 \int_0^1 y^{2p-2} \,\mathrm{d}y - 2p(p+1) \int_0^1 y^{2p-1} \,\mathrm{d}y + (p+1)^2 \int_0^1 y^{2p} \,\mathrm{d}y \Big) \\ &= 2 \frac{p^2(2p+1) - (p+1)(2p-1)(2p+1) + (2p-1)(p+1)^2}{(2p-1)(2p+1)} \\ &= \frac{2p}{4p^2-1}, \end{aligned}$$

i.e., $\|\varphi_p'\|_{L_2(\mathbb{R})} \eqsim (p+1)^{-1/2} \eqsim (p+1)\|\varphi_p\|_{L_2(\mathbb{R})}$, as $p \to \infty$, while (4.1.23) only yields $|\varphi_p|_{H^1(\mathbb{R})} \le C(p+1)^2 \|\varphi_p\|_{L_2(\mathbb{R})}$, as $p \to \infty$.

4.2 Construction and properties of quarklets

In this section, we define quarklets on the real line. They are introduced as linear combinations of quarks. Actually, it is possible to construct stable systems in Lebesgue and Sobolev spaces directly out of quarks as it was shown in [50]. However, due to their lack of vanishing moments, they do not lead to compressible stiffness matrices. Therefore, an application in adaptive schemes for operator equations is not feasible with this quarkonial systems.

In Subsection 4.2.1, we show how a wavelet-type modification of the quark system leads to quarklets with vanishing moments. Moreover, we derive crucial cancellation and compression results, which are a cornerstone for the adaptive schemes of Chapter 7. In Subsection 4.2.2, we expose how to construct quarklet frames in $L_2(\mathbb{R})$ and $H^s(\mathbb{R})$.

4.2.1 Shift-invariant quarklets

Let $m, \tilde{m} \in \mathbb{N}$ with $\frac{\tilde{m}}{m}$ large enough and $m+\tilde{m}$ even be fixed. Throughout this section let $\varphi = N_m$, cf. (3.1.11), be the generator and

$$\psi = \sum_{k\in\mathbb{Z}} b_k \varphi(2\cdot -k), \tag{4.2.1}$$

cf. (3.1.7), the wavelet with $\tilde{m}$ vanishing moments of the Cohen/Daubechies/Feveau construction outlined in Subsection 3.1.2.

Mimicking the definition (4.2.1) of the wavelet ψ, let us consider the following *quarklets* ψ_p,

$$\psi_p := \sum_{k\in\mathbb{Z}} b_k \varphi_p(2\cdot -k), \quad \text{for all } p \in \mathbb{N}_0. \tag{4.2.2}$$

Let us stress that the two-scale coefficients $\mathbf{b} = \{b_k\}_{k\in\mathbb{Z}}$ in (4.2.2) are exactly the same as in (4.2.1). We refer to Figure 4.3 for an illustrative example.

By assumption, $\psi_0 = \psi$ has $\tilde{m}$ vanishing moments. The following lemma shows that the other ψ_p inherit the same property.

Lemma 4.8. *For each $p \in \mathbb{N}_0$, the quarklet ψ_p has $\tilde{m}$ vanishing moments.*

Proof. Let us first prove the auxiliary result that the coefficient sequence $\mathbf{b} = \{b_k\}_{k\in\mathbb{Z}}$ has $\tilde{m}$ discrete moments,

$$\sum_{k\in\mathbb{Z}} k^q b_k = 0, \quad \text{for all } q \in \mathbb{N}_0,\ 0 \le q < \tilde{m}. \tag{4.2.3}$$

We proceed by induction over q. For $q = 0$, $z := \int_{\mathbb{R}} \varphi(x)\,\mathrm{d}x \neq 0$, the compact support of φ and (4.2.1) imply that

$$\sum_{k\in\mathbb{Z}} b_k = \frac{1}{z} \sum_{k\in\mathbb{Z}} b_k \int_{\mathbb{R}} \varphi(x-k)\,\mathrm{d}x = \frac{2}{z} \int_{\mathbb{R}} \psi(x)\,\mathrm{d}x = 0.$$

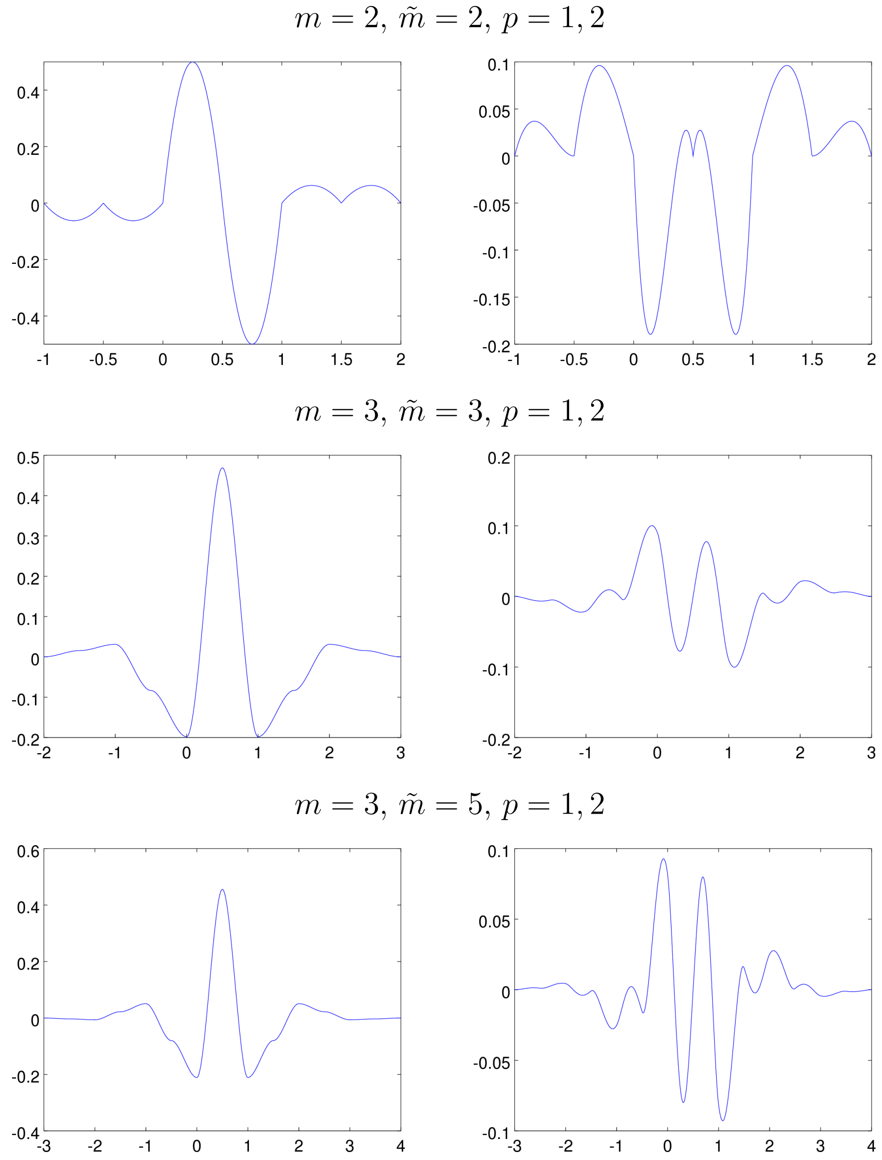

Figure 4.3: B-spline quarklets ψ_p with order and vanishing moments $(m, \tilde{m}) = (2, 2), (3, 3), (3, 5)$ and polynomial degree $p = 1, 2$.

Now assume that (4.2.3) holds for all $0 \leq r \leq q-1$, where $0 \leq q < \tilde{m}$. By the vanishing moment property of ψ, we compute that

$$0 = \int_{\mathbb{R}} x^q \psi(x)\,\mathrm{d}x = \sum_{k\in\mathbb{Z}} b_k \int_{\mathbb{R}} x^q \varphi(2x-k)\,\mathrm{d}x = \frac{1}{2^{q+1}} \sum_{k\in\mathbb{Z}} b_k \int_{\mathbb{R}} (y+k)^q \varphi(y)\,\mathrm{d}y,$$

so that the induction hypothesis yields (4.2.3),

$$\begin{aligned} 0 &= \sum_{k\in\mathbb{Z}} b_k \int_{\mathbb{R}} \sum_{r=0}^{q} \binom{q}{r} k^r y^{q-r} \varphi(y)\,\mathrm{d}y \\ &= \sum_{r=0}^{q} \binom{q}{r} \int_{\mathbb{R}} y^{q-r}\varphi(y)\,\mathrm{d}y \sum_{k\in\mathbb{Z}} k^r b_k \\ &= z \sum_{k\in\mathbb{Z}} k^q b_k. \end{aligned}$$

In view of (4.2.3), the vanishing moment property of ψ_p easily follows from

$$\begin{aligned} \int_{\mathbb{R}} x^q \psi_p(x)\,\mathrm{d}x &= \sum_{k\in\mathbb{Z}} b_k \int_{\mathbb{R}} x^q \varphi_p(2x-k)\,\mathrm{d}x \\ &= \frac{1}{2^{q+1}} \sum_{k\in\mathbb{Z}} b_k \int_{\mathbb{R}} (y+k)^q \varphi_p(y)\,\mathrm{d}y \\ &= \frac{1}{2^{q+1}} \sum_{l=0}^{q} \binom{q}{l} \int_{\mathbb{R}} y^{q-l}\varphi_p(y)\,\mathrm{d}y \sum_{k\in\mathbb{Z}} k^l b_k = 0, \quad \text{for all } 0 \leq q < \tilde{m}. \end{aligned}$$

□

Based on the vanishing moment properties of the quarklets ψ_p, we immediately get the following cancellation estimates for inner products of the $\psi_{p,j,k}$ with smooth functions, using standard techniques from wavelet analysis.

Proposition 4.9. *There exists $C = C(m, \tilde{m}) > 0$, such that for all $f \in W^r_\infty(\mathbb{R})$, $0 \leq r \leq \tilde{m}-1$,*

$$\left|\langle f, \psi_{p,j,k}\rangle_{L_2(\mathbb{R})}\right| \leq C(p+1)^{-m} 2^{-j(r+1/2)} |f|_{W^r_\infty(\operatorname{supp}\psi_{p,j,k})}, \tag{4.2.4}$$

for all $p, j \in \mathbb{N}_0$, $k \in \mathbb{Z}$.

Proof. By Lemma 4.8, each quarklet ψ_p and hence $\psi_{p,j,k}$ has $\tilde{m}$ vanishing moments. Therefore, given some $f \in L_2(\mathbb{R})$, an application of Hölder's inequality implies that

$$\begin{aligned} \left|\langle f, \psi_{p,j,k}\rangle_{L_2(\mathbb{R})}\right| &= \inf_{P\in\mathbb{P}_r} \left|\langle f-P, \psi_{p,j,k}\rangle_{L_2(\mathbb{R})}\right| \\ &\leq \inf_{P\in\mathbb{P}_r} \|f-P\|_{L_\infty(\operatorname{supp}\psi_{p,j,k})} \|\psi_{p,j,k}\|_{L_1(\mathbb{R})}. \end{aligned}$$

A Whitney-type estimate on $\operatorname{supp}\psi_{p,j,k}$, (4.2.2) and (4.1.15) immediately yield (4.2.4),

$$\begin{aligned}\left|\langle f,\psi_{p,j,k}\rangle_{L_2(\mathbb{R})}\right| &\le C_1 2^{-j(r+1/2)}|f|_{W^r_\infty(\operatorname{supp}\psi_{p,j,k})}\|\varphi_p\|_{L_1(\mathbb{R})}\\ &\le C_2(p+1)^{-m}2^{-j(r+1/2)}|f|_{W^r_\infty(\operatorname{supp}\psi_{p,j,k})},\end{aligned}$$

where $C_1 = C_1(m,\tilde{m}) > 0$, $C_2 = C_2(m,\tilde{m}) > 0$. □

In the sequel, we consider the usual dyadic dilates and translates of the quarklets,

$$\psi_{p,j,k} := 2^{j/2}\psi_p(2^j\cdot - k), \quad \text{for all } p,j\in\mathbb{N}_0, k\in\mathbb{Z}. \tag{4.2.5}$$

On this occasion, let us fix the notation

$$\psi_{p,-1,k} := \varphi_p(\cdot - k), \quad \text{for all } p\in\mathbb{N}_0, k\in\mathbb{Z}, \tag{4.2.6}$$

for the quarks and the index set

$$\Lambda := \{(p,j,k) : p\in\mathbb{N}_0, j\in\mathbb{N}_0\cup\{-1\}, k\in\mathbb{Z}\}, \tag{4.2.7}$$

which is an extension of the Riesz basis index set

$$\Lambda^B = \{(j,k) : j\in\mathbb{N}_0\cup\{-1\}, k\in\mathbb{Z}\},$$

cf. (3.1.9).

4.2.2 The frame property in $L_2(\mathbb{R})$ and $H^s(\mathbb{R})$

We shall now study the stability properties of the full quarklet system. In particular, we investigate under which conditions on the weights $w_p \ge 0$, the weighted system

$$\Psi_{L_2(\mathbb{R})} := \left\{w_p\psi_{p,j,k} : (p,j,k)\in\Lambda\right\} \tag{4.2.8}$$

is a frame for $L_2(\mathbb{R})$. Setting $w_0 := 1$, $\Psi_{L_2(\mathbb{R})}$ contains the Riesz basis for $L_2(\mathbb{R})$,

$$\Psi^B_{L_2(\mathbb{R})} = \left\{\varphi(\cdot - k), 2^{j/2}\psi(2^j\cdot - k) : j\in\mathbb{N}_0, k\in\mathbb{Z}\right\},$$

so that we are left with proving the Bessel property of $\Psi_{L_2(\mathbb{R})}$. We have to show that the synthesis operator

$$F : \ell_2(\Lambda) \to L_2(\mathbb{R}), \quad \mathbf{c} \mapsto \sum_{p\ge 0}\sum_{j\ge -1}\sum_{k\in\mathbb{Z}} c_{p,j,k}w_p\psi_{p,j,k}, \tag{4.2.9}$$

of $\Psi_{L_2(\mathbb{R})}$ is well-defined and bounded, cf. (2.1.2). We exploit the following proposition.

Proposition 4.10. *Let $m \geq 2$. There exists $C = C(m, \tilde{m}) > 0$, such that the Gramian matrix*

$$\mathbf{G}_p := \Big(\big\langle \psi_{p,j,k}, \psi_{p,j',k'} \big\rangle_{L_2(\mathbb{R})} \Big)_{(j,k),(j',k') \in \Lambda^B}, \tag{4.2.10}$$

is a bounded operator on $\ell_2(\Lambda^B)$ with

$$\|\mathbf{G}_p\|_{\mathscr{L}(\ell_2(\Lambda^B))} \leq C(p+1)^{-1}, \tag{4.2.11}$$

for all $p \in \mathbb{N}_0$.

Proof. By the Schur lemma, it is sufficient to prove that $\mathbf{G}_p$ is bounded on $\ell_1(\Lambda^B)$ and $\ell_\infty(\Lambda^N)$.. Due to the symmetry of $\mathbf{G}_p$, a norm bound in $\ell_\infty(\Lambda^B)$ is sufficient. Let $(j', k') \in \Lambda^B$, and $\mathbf{c} = \{c_{j,k}\}_{(j,k) \in \Lambda^B} \in \ell_\infty(\Lambda^B)$. We start estimating with

$$\begin{aligned} \Big| (\mathbf{G}_p \mathbf{c})_{(j',k')} \Big| &= \Big| \sum_{j \geq -1} \sum_{k \in \mathbb{Z}} c_{j,k} \langle \psi_{p,j',k'}, \psi_{p,j,k} \rangle_{L_2(\mathbb{R})} \Big| \\ &\leq \|\mathbf{c}\|_{\ell_\infty(\Lambda^B)} \Big(\sum_{j=-1}^{j'-1} \sum_{k \in \mathbb{Z}} \Big| \langle \psi_{p,j',k'}, \psi_{p,j,k} \rangle_{L_2(\mathbb{R})} \Big| + \sum_{j \geq j'} \sum_{k \in \mathbb{Z}} \Big| \langle \psi_{p,j',k'}, \psi_{p,j,k} \rangle_{L_2(\mathbb{R})} \Big| \Big). \end{aligned}$$

Now we want to estimate the inner products. We confine ourselves to the case where both functions are quarklets, and exploit the cancellation property (4.2.4). If quarks are involved an even better estimate is possible. Since these estimates are executed in detail later in Section 7.3, where we achieve compression estimates, we spare this part here.

In the first sum over k, where $j < j'$, we can estimate the non-zero inner products between quarklets by an application of (4.2.4), (4.2.2), (4.1.22) and (4.1.15)

$$\begin{aligned} \Big| \langle \psi_{p,j',k'}, \psi_{p,j,k} \rangle_{L_2(\mathbb{R})} \Big| &\leq C_1 (p+1)^{-m} 2^{-j'(m-1/2)} |\psi_{p,j,k}|_{W^{m-1}(L_\infty(\mathbb{R}))} \\ &\leq C_2 (p+1)^{-m} 2^{-(j'-j)(m-1/2)} \|\psi_p^{(m-1)}\|_{L_\infty(\mathbb{R})} \\ &\leq C_3 (p+1)^{-m} 2^{-(j'-j)(m-1/2)} \|\varphi_p^{(m-1)}\|_{L_\infty(\mathbb{R})} \\ &\leq C_4 (p+1)^{m-2} 2^{-(j'-j)(m-1/2)} \|\varphi_p\|_{L_\infty(\mathbb{R})} \\ &\leq C_5 (p+1)^{-1} 2^{-(j'-j)(m-1/2)}, \end{aligned}$$

where $C_i = C_i(m, \tilde{m}) > 0$, $i = 1, \ldots, 5$. The number of non-zero inner products per j in the first sum is bounded by a constant independent of j and j',

$$\sum_{j=0}^{j'-1} \sum_{k \in \mathbb{Z}} \Big| \langle \psi_{p,j',k'}, \psi_{p,j,k} \rangle_{L_2(\mathbb{R})} \Big| \leq C_5 (p+1)^{-1} \sum_{j=0}^{j'-1} 2^{-(j'-j)(m-1/2)}.$$

In a completely analogous way, using that the number of non-zero inner products per j in the second sum is bounded by a constant multiple of $2^{j-j'}$, the second sum can be estimated by

$$\sum_{j \geq j'} \sum_{k \in \mathbb{Z}} \Big| \langle \psi_{p,j',k'}, \psi_{p,j,k} \rangle_{L_2(\mathbb{R})} \Big| \leq C_6 (p+1)^{-1} \sum_{j \geq j'} 2^{-(j-j')(m-3/2)},$$

with $C_6 = C_6(m, \tilde{m}) > 0$. Therefore, due to $m \geq 2$, we obtain (4.2.11),

$$\left|(\mathbf{G}_p\mathbf{c})_{(j',k')}\right| \leq C_7(m,\psi)\|\mathbf{c}\|_{\ell_\infty(\Lambda^B)}(p+1)^{-1},$$

with $C_7 = C_7(m, \tilde{m}) > 0$. □

In case that the weights w_p decay sufficiently fast, we finally obtain the boundedness of F and hence the L_2 frame property.

Theorem 4.11. *Let $w_p \geq 0$ be chosen such that $w_0 = 1$ and $w_p^2(p+1)^{-1}$ is summable. Then $\Psi_{L_2(\mathbb{R})}$ as defined in (4.2.12) is a frame for $L_2(\mathbb{R})$.*

Proof. For $\mathbf{c} \in \ell_2(\Lambda)$ and $\mathbf{c}_p = (c_{p,j,k})_{(j,k)\in\Lambda^B} \in \ell_2(\Lambda^B)$ the part of $\mathbf{c}$ with fixed $p \in \mathbb{N}_0$, we compute by using the triangle inequality for $L_2(\mathbb{R})$ and the definition of the Gramian matrix $\mathbf{G}_p$ that

$$\begin{aligned}\left\|F\mathbf{c}\right\|_{L_2(\mathbb{R})} &= \Big\|\sum_{p\geq 0}\sum_{j\geq -1}\sum_{k\in\mathbb{Z}} c_{p,j,k}w_p\psi_{p,j,k}\Big\|_{L_2(\mathbb{R})}\\ &\leq \sum_{p\geq 0} w_p\Big\|\sum_{j\geq -1}\sum_{k\in\mathbb{Z}} c_{p,j,k}\psi_{p,j,k}\Big\|_{L_2(\mathbb{R})}\\ &\leq \sum_{p\geq 0} w_p\left(\langle\mathbf{c}_p, \mathbf{G}_p\mathbf{c}_p\rangle_{\ell_2(\Lambda^B)}\right)^{1/2}.\end{aligned}$$

By Proposition 4.10 and a two times application of the Cauchy-Schwarz inequality, we conclude that

$$\begin{aligned}\left\|F\mathbf{c}\right\|_{L_2(\mathbb{R})} &\leq \sum_{p\geq 0} w_p\left(||\mathbf{G}_p||_{\mathscr{L}(\ell_2(\Lambda^B))}||\mathbf{c}_p||^2_{\ell_2(\Lambda^B)}\right)^{1/2}\\ &\leq C\sum_{p\geq 0} w_p(p+1)^{-1/2}||\mathbf{c}_p||_{\ell_2(\Lambda^B)}\\ &\leq C\left(\sum_{p\geq 0} w_p^2(p+1)^{-1}\right)^{1/2}||\mathbf{c}||_{\ell_2(\Lambda)}\end{aligned}$$

with $C = C(m, \tilde{m}) > 0$. □

Remark 4.12. Obviously, the weights in Theorem 4.11 have to be taken sufficiently small to obtain a frame in $L_2(\mathbb{R})$ with reasonable frame bounds. The key is not to take them too small as it leads to very big coefficients in the solution of operator equations. This could destroy the behaviour of a numerical solution scheme involving quarklets. A reasonable choice for w_p is $(p+1)^{-\delta_1/2}$, with $\delta_1 > 0$, guaranteeing the convergence of the series $\sum_{p\geq 0} w_p^2(p+1)^{-1}$. The division by 2 in the exponent becomes clear in Chapter 6, where we transfer quarklets to multiple spatial dimensions.

On account of this, the conditions on the weights in Theorem 4.11 and the upcoming Theorem 4.15 are a huge development compared to previous constructions with exponentially decaying weights [104–106].

During the course of this chapter, we have derived all the necessary building blocks that are needed to construct stable quarklet frames not only for $L_2(\mathbb{R})$ but also for scales of Sobolev spaces $H^s(\mathbb{R})$. In the remainder of this subsection, we show that the weighted system

$$\Psi_{H^s(\mathbb{R})} := \{w_{p,j,s}\psi_{p,j,k} \ : \ (p,j,k) \in \Lambda\}, \tag{4.2.12}$$

with $w_{p,j,s} := 2^{-js}(p+1)^{-2s-\delta_1/2-\delta_2/2}$ for $j \in \mathbb{N}_0$ and $w_{p,-1,s} := w_{p,0,s}$ with $\delta_1 > 0$, $\delta_2 > 1$, has the frame property in $H^s(\mathbb{R}), 0 < s < m - \frac{1}{2}$. Let us mention first that $\Psi_{H^s(\mathbb{R})}$ contains the weighted wavelet system

$$\Psi^B_{H^s(\mathbb{R})} := \{w_{0,j,s}\psi_{0,j,k} \ : \ j \in \mathbb{N}_0 \cup \{-1\}, k \in \mathbb{Z}\}, \tag{4.2.13}$$

with $w_{0,j,s} = 2^{-js}$ for $j \in \mathbb{N}_0$ and $w_{0,-1,s} = w_{0,0,s} = 1$, which is known to be a Riesz basis in $H^s(\mathbb{R})$, $0 < s < m-\frac{1}{2}$ (see [85, Section 6.10] for a proof). So, as in the L_2 case, we are left with proving the Bessel property of $\Psi_{H^s(\mathbb{R})}$. For that purpose, we use some techniques of an abstract axiomatic approach to build multi-scale *hp*-frames (frames build by dyadic dilation, translation and *p*-enrichment) from families of multi-scale *h*-frames (built by dyadic dilation and translation). They can be applied since the quarklets fit into the concept of *hierarchical frame families*. Roughly speaking, this means that a polynomial enrichment of the *h*-frame up to an arbitrary fixed degree already yields a frame for the whole space and not only a frame system for a subspace. We refer to [89, Section 3] for further details.

For $p, j \in \mathbb{N}_0$, we define

$$\begin{aligned} \Psi_{p,j} &:= \{\psi_{i,\ell,k} : (i,\ell,k) \in \Lambda_{p,j}\}, \\ \Lambda_{p,j} &:= \{(i,\ell,k) : i = 0,\dots,p, \ \ell = -1,\dots,j-1, \ k \in \mathbb{Z}\}, \end{aligned} \tag{4.2.14}$$

as the family of quarklets capped at a polynomial degree p and a level $j-1$. The corresponding spaces are denoted as

$$U_{p,j} := \operatorname{clos}_{L_2(\mathbb{R})} \operatorname{span} \Psi_{p,j}. \tag{4.2.15}$$

Then, the sequence of spaces $\mathcal{U} := \{U_{p,j}\}_{p,j\in\mathbb{N}_0}$, satisfies the monotonicity property

$$U_{p,j-1} \subset U_{p,j} \subset U_{p+1,j} \subset H^s(\mathbb{R}), \quad j \in \mathbb{N}, p \in \mathbb{N}_0, \tag{4.2.16}$$

with $0 \le s < m - \frac{1}{2}$. In the following proposition, we prove further properties of $\mathcal{U}_p$, which are important to show the Bessel property of $\Psi_{H^s(\mathbb{R})}$.

Proposition 4.13. *Let $p, j \in \mathbb{N}_0$ be fixed and $\Psi_{p,j}$, $U_{p,j}$ defined as in* (4.2.14), (4.2.15), *respectively. Then, for $0 \le s < m - \frac{1}{2}$, a Bernstein estimate of the form*

$$\|f\|_{H^s(\mathbb{R})} \le C_1(p+1)^{2s}2^{js}\|f\|_{L_2(\mathbb{R})}, \tag{4.2.17}$$

with $C_1 = C_1(m,s) > 0$*, holds for all* $f \in U_{p,j}$*. Furthermore,* $\Psi_{p,j}$ *forms a Bessel sequence for* $U_{p,j}$*, i.e.*

$$B^{-1}\|f\|^2_{L_2(\mathbb{R})} \leq \inf_{\{\mathbf{c}\in\ell_2(\Lambda_{p,j}):F_{\Psi_{p,j}}\mathbf{c}=f\}} \sum_{i=0}^{p}\sum_{\ell=-1}^{j-1}\sum_{k\in\mathbb{Z}} |c_{i,\ell,k}|^2, \quad \text{for all } f \in U_{p,j}, \quad (4.2.18)$$

cf. Proposition 2.3, with Bessel bound of the form $B = C_2(p+1)^{\delta_1}$*, where* $C_2 = C_2(m,\tilde{m},\delta_1) > 0$ *and* $\delta_1 > 0$*.*

To prove (4.2.17), we need a technical refinement result of the sequence $\{V_{p,j}\}_{j\in\mathbb{N}_0}$, $p \in \mathbb{N}_0$.

Lemma 4.14. *For any* $p \in \mathbb{N}_0$*, the vector* $(\varphi_0, \dots, \varphi_p)$ *is* refinable*, i.e., there exist* $(p+1)\times(p+1)$*-matrices* $\mathbf{C}_k$ *such that*

$$\begin{pmatrix} \varphi_0 \\ \vdots \\ \varphi_p \end{pmatrix} = \sum_{k\in\mathbb{Z}} \mathbf{C}_k \begin{pmatrix} \varphi_0(2\cdot -k) \\ \vdots \\ \varphi_p(2\cdot -k) \end{pmatrix}.$$

Consequently, the sequence $\{V_{p,j}\}_{j\in\mathbb{N}_0}$ *as defined in* (4.1.3) *is nested,* $V_{p,j} \subset V_{p,j+1}$ *for* $j \in \mathbb{N}_0$*.*

Proof. By using the definition of φ_p and the refinability of $\varphi = \varphi_0$ we obtain for $x \in \mathbb{R}$:

$$\begin{aligned}
\varphi_i(x) &= x^i\varphi(x) \\
&= \frac{1}{2^q}(2x)^i \sum_{k\in\mathbb{Z}} a_k\varphi(2x-k) \\
&= \frac{1}{2^i}\sum_{k\in\mathbb{Z}} a_k(2x-k+k)^i\varphi(2x-k) \\
&= \frac{1}{2^i}\sum_{k\in\mathbb{Z}} a_k \sum_{l=0}^{i}(2x-k)^l\binom{i}{l}k^{i-l}\varphi(2x-k) \\
&= \sum_{k\in\mathbb{Z}}\frac{1}{2^i}a_k\sum_{l=0}^{i}\binom{i}{l}k^{i-l}\varphi_l(2x-k).
\end{aligned}$$

Setting

$$(\mathbf{C}_k)_{i,l} := \frac{1}{2^i}a_k^i\binom{i}{l}k^{i-l}$$

yields the result. □

Now we are ready to prove Proposition 4.13.

Proof. Because of the two-scale-equation (4.2.2), the function $\psi_{i,\ell,k}$, $(i,\ell,k) \in \Lambda_{p,j}$ is contained in the space $V_{p,\ell+1}$ as defined in (4.1.3). As we have seen in Lemma 4.14, the sequence $\{V_{p,j}\}_{j\in\mathbb{N}_0}$ is nested. Since $\ell+1 \in \{0,\dots,j\}$, we conclude that $V_{p,\ell+1} \subset V_{p,j}$. Consequently, it follows that

$$U_{p,j} \subset V_{p,j}.$$

Therefore, Corollary 4.7 implies (4.2.17). To show (4.2.18) let $f \in U_{p,j}$, $p,j \in \mathbb{N}_0$. For $\delta > 0$ we use the fact that with the weight $w_p := (p+1)^{-\delta_1/2}$ the family

$$\Psi_{L_2(\mathbb{R})} = \{w_p \psi_{p,j,k} \ : \ (p,j,k) \in \Lambda\}$$

is a frame for $L_2(\mathbb{R})$, cf. Theorem 4.11, to estimate

$$\begin{aligned}
\inf_{\{\mathbf{c}\in\ell_2(\Lambda_{p,j}):F_{\Psi_{p,j}}\mathbf{c}=f\}} \sum_{(i,\ell,k)\in\Lambda_{p,j}} |c_{i,\ell,k}|^2 &= w_p^2 \inf_{\{\mathbf{c}\in\ell_2(\Lambda_{p,j}):F_{\Psi_{p,j}}\mathbf{c}=f\}} \sum_{(i,\ell,k)\in\Lambda_{p,j}} |w_p^{-1} c_{i,\ell,k}|^2 \\
&\geq w_p^2 \inf_{\{\mathbf{c}\in\ell_2(\Lambda_{p,j}):F_{\Psi_{p,j}}\mathbf{c}=f\}} \sum_{(i,\ell,k)\in\Lambda_{p,j}} |w_i^{-1} c_{i,\ell,k}|^2 \\
&\geq w_p^2 \inf_{\{\tilde{\mathbf{c}}\in\ell_2(\Lambda):F_{\Psi_{L_2(\mathbb{R})}}\tilde{\mathbf{c}}=f\}} \sum_{(i,\ell,k)\in\Lambda} |\tilde{c}_{i,\ell,k}|^2 \\
&\geq C w_p^2 \|f\|^2_{L_2(\mathbb{R})},
\end{aligned}$$

with $C = C(m,\tilde{m},\delta_1) > 0$ the reciprocal upper frame bound of $\Psi_{L_2(\mathbb{R})}$. □

Since we have all the prerequisites available, we can prove now the first main result of this thesis, namely the frame property of a quarklet system in $H^s(\mathbb{R})$, $0 < s < m - \frac{1}{2}$.

Theorem 4.15. *The system $\Psi_{H^s(\mathbb{R})}$ as defined in (4.2.12) is a frame for $H^s(\mathbb{R})$, $0 < s < m - \frac{1}{2}$.*

Proof. We split the proof into two parts, where we prove in the first part, that for fixed $p \in \mathbb{N}_0$, $0 < s < m - \frac{1}{2}$ the system

$$\begin{aligned}
\Psi_p &:= \bigcup_{j\in\mathbb{N}_0} w_{j,s} \Psi_{p,j} = \{w_{j,s}\psi_{i,j,k} : (i,j,k) \in \Lambda_p\}, \\
\Lambda_p &:= \{(i,j,k) : i = 0,\dots,p, \ j \in \mathbb{N}_0 \cup \{-1\}, \ k \in \mathbb{Z}\},
\end{aligned} \tag{4.2.19}$$

with $w_{j,s} := 2^{-js}$ for $j \in \mathbb{N}_0$ and $w_{-1,s} := w_{0,s} = 1$, constitutes a Bessel sequence for $H^s(\mathbb{R})$, cf. (2.1.1), with Bessel bound dependent on p. In the second part of the proof, we use this statement to prove the Bessel property for the whole system $\Psi_{H^s(\mathbb{R})}$.

Let $f \in H^s(\mathbb{R})$, $0 < s < m - \frac{1}{2}$, $p \in \mathbb{N}_0$ and fix a $\delta_1 > 0$. Since Ψ_p has an underlying $H^s(\mathbb{R})$ Riesz basis $\Psi^B_{H^s(\mathbb{R})}$, cf. (4.2.13), there exists a decomposition

$$f = \sum_{j\geq -1} f_{p,j} := \sum_{(i,j,k)\in\Lambda_p} c_{i,j,k} \left(w_{j,s}\psi_{i,j,k}\right), \tag{4.2.20}$$

where the functions $f_{p,j}$ are contained in $U_{p,j+1}$ for $j \in \mathbb{N}_0 \cup \{-1\}$. Using (4.2.18), this leads us to the estimate

$$\sum_{j\geq -1} w_{j,s}^{-2} ||f_{p,j}||_{L_2(\mathbb{R})}^2 \leq C_1(p+1)^{\delta_1} \sum_{(i,j,k)\in\Lambda_p} |c_{q,j,k}|^2, \tag{4.2.21}$$

with $C_1 = C_1(m, \tilde{m}, \delta_1) > 0$. By exploiting a Cauchy-Schwarz type inequality of the form

$$|\langle g, h\rangle_{H^s(\mathbb{R})}| \leq ||g||_{H^{s+\varepsilon}(\mathbb{R})} ||h||_{H^{s-\varepsilon}(\mathbb{R})}, \qquad g, h \in H^{s+\varepsilon}(\mathbb{R}),$$

for $0 < s - \varepsilon < s + \varepsilon < \gamma$, and (4.2.17) we estimate

$$\begin{aligned}
||f||_{H^s(\mathbb{R})}^2 &= |\langle \sum_{j\geq -1} f_{p,j}, \sum_{\ell\geq 0} f_{p,\ell}\rangle_{H^s(\mathbb{R})}| \\
&\leq 2 \sum_{j\geq -1} \sum_{\ell\geq j} |\langle f_{p,j}, f_{p,\ell}\rangle_{H^s(\mathbb{R})}| \\
&\leq 2 \sum_{j\geq -1} \sum_{\ell\geq j} ||f_{p,j}||_{H^{s+\varepsilon}(\mathbb{R})} ||f_{p,\ell}||_{H^{s-\varepsilon}(\mathbb{R})} \\
&\leq C_2(p+1)^{4s} \sum_{j\geq -1} \sum_{\ell\geq -1} 2^{-\varepsilon|j-\ell|} (w_{j,s}^{-1} ||f_{p,j}||_{L_2(\mathbb{R})})(w_{\ell,s}^{-1} ||f_{p,\ell}||_{L_2(\mathbb{R})}) \\
&\leq C_2 M_\varepsilon (p+1)^{4s} \sum_{j\geq -1} w_{j,s}^{-2} ||f_{p,j}||_{L_2(\mathbb{R})}^2,
\end{aligned} \tag{4.2.22}$$

with $C_2 = C_2(m, s) > 0$ and M_ε the norm of the matrix operator with entries $2^{-\varepsilon|j-\ell|}$ mapping ℓ_2 to ℓ_2. Combining (4.2.22) with (4.2.21) we have

$$||f||_{H^s(\mathbb{R})}^2 \leq C_3 M_\varepsilon (p+1)^{4s+\delta_1} \sum_{(i,j,k)\in\Lambda_p} |c_{q,j,k}|^2,$$

with $C_3 = C_3(m, \tilde{m}, s, \delta_1) > 0$. Taking the infimum shows the first part of the proof. To show the Bessel property for the whole system $\Psi_{H^s(\mathbb{R})}$, we assume

$$\sum_{p\geq 0} f_p := \sum_{(p,j,k)\in\Lambda} c_{p,j,k}\, w_{p,j,s}\, \psi_{p,j,k} = \sum_{(p,j,k)\in\Lambda} \left(c_{p,j,k}\, w_{p,j,s}\, w_{j,s}^{-1}\right) (w_{j,s} \psi_{p,j,k})$$

to be a fixed decomposition of f with the weights $w_{p,j,s} = 2^{-js}(p+1)^{-2s-\delta_1/2-\delta_2/2}$, $\delta_2 > 1$, for $j \geq 0$ and $w_{p,-1,s} = w_{p,0,s}$, as defined in (4.2.12). By using the triangle inequality, the Cauchy-Schwarz inequality and the first part of the proof with the fact that $f_p \in \Psi_p$, $p \in \mathbb{N}_0$, we compute

$$\begin{aligned}
\|f\|^2_{H^s(\mathbb{R})} &= \Big\| \sum_{p\geq 0} f_p \Big\|^2_{H^s(\mathbb{R})} \\
&\leq \Big(\sum_{p\geq 0} \|f_p\|_{H^s(\mathbb{R})} \Big)^2 \\
&= \Big(\sum_{p\geq 0} (p+1)^{-\delta_2/2} (p+1)^{\delta_2/2} \|f_p\|_{H^s(\mathbb{R})} \Big)^2 \\
&\leq \sum_{p'\geq 0} (p'+1)^{-\delta_2} \sum_{p\geq 0} (p+1)^{\delta_2} \|f_p\|^2_{H^s(\mathbb{R})} \\
&\leq C_4 M_\varepsilon \sum_{p\geq 0} (p+1)^{4s+\delta_2+\delta_1} \sum_{j\geq -1} \sum_{k\in\mathbb{Z}} \Big(w_{p,j,s}\, w_{j,s}^{-1} \Big)^2 |c_{p,j,k}|^2,
\end{aligned}$$

with $C_4 = C_4(m, \tilde{m}, s, \delta_1, \delta_2) > 0$ Since $(p+1)^{4s+\delta_1+\delta_2} \Big(w_{p,j,s}\, w_{j,s}^{-1} \Big)^2 = 1$, we obtain

$$\|f\|^2_{H^s(\mathbb{R})} \leq C_4 M_\varepsilon \sum_{p\geq 0} \sum_{j\geq -1} \sum_{k\in\mathbb{Z}} |c_{p,j,k}|^2.$$

Taking the infimum finally shows the Bessel property for the system $\Psi_{H^s(\mathbb{R})}$ and so the claim is proved. □

4.2.3 Compression estimates in one dimension

In this subsection, we prove a compression estimate for the one-dimensional quarklets on the real line as introduced in this chapter and their derivatives, respectively. These results are the foundation for the considerations in Section 7.3, where we show the compressibility of elliptic operators in d spatial dimensions.

Proposition 4.16. *Let $m, \tilde{m} \geq 3$, and $(p, j, k), (p', j', k') \in \Lambda$. Then, the following relations hold:*

(i) There exists $C = C(m, \tilde{m}) > 0$, such that the unweighted quarks and quarklets satisfy

$$\Big| \langle \psi_{p,j,k}, \psi_{p',j',k'} \rangle_{L_2(\mathbb{R})} \Big| \leq C \Big((p+1)(p'+1) \Big)^{m-1} 2^{-|j-j'|(m-1/2)}. \tag{4.2.23}$$

(ii) There exists $C' = C'(m, \tilde{m}) > 0$, such that the derivatives of the unweighted quarks and quarklets satisfy

$$2^{-(j+j')} \Big| \langle \psi'_{p,j,k}, \psi'_{p',j',k'} \rangle_{L_2(\mathbb{R})} \Big| \leq C' \Big((p+1)(p'+1) \Big)^{m-1} 2^{-|j-j'|(m-3/2)}. \tag{4.2.24}$$

Proof. At first, we proof (ii). Note that by $m \geq 3$, φ and hence ψ and ψ_p have $m-1$ weak derivatives in $L_q(\mathbb{R})$, $1 \leq q \leq \infty$. Let us consider the case $j, j' \in \mathbb{N}_0$, where both functions are quarklets. For $j' \geq j$, we use the compact support of ψ and the fact that ψ' has $\tilde{m}+1$ vanishing moments to compute that for each $r = 0, \ldots, \tilde{m}$,

$$\begin{aligned}\left|\langle \psi'_{p,j,k}, \psi'_{p',j',k'}\rangle_{L_2(\mathbb{R})}\right| &= \inf_{P\in\Pi_r} \left|\langle \psi'_{p,j,k} - P, \psi'_{p',j',k'}\rangle_{L_2(\mathbb{R})}\right| \\ &\leq \inf_{P\in\Pi_r} \|\psi'_{p,j,k} - P\|_{L_\infty(\operatorname{supp}\psi_{p',j',k'})}\|\psi'_{p',j',k'}\|_{L_1(\mathbb{R})}.\end{aligned}$$

On the one hand, from (4.2.5), (4.2.2), (4.1.22) and (4.1.15), we obtain that with $C_1 = C_1(m) > 0$ and $C_2 = C_2(m) > 0$

$$\begin{aligned}\|\psi'_{p',j',k'}\|_{L_1(\mathbb{R})} &= 2^{j'/2}\|\psi'_{p'}\|_{L_1(\mathbb{R})} \\ &\leq C_1 2^{j'/2}\|\varphi'_{p'}\|_{L_1(\mathbb{R})} \\ &\leq C_2(p'+1)^{-(m-2)}2^{j'/2}.\end{aligned} \tag{4.2.25}$$

On the other hand, by Whitney's theorem, for each choice of p, j, k, p', j', k', there exists $Q \in \Pi_r$ such that with $C_3 = C_3(r) > 0$ and $C_4 = C_4(r) > 0$,

$$\begin{aligned}\|\psi'_{p,j,k} - Q\|_{L_\infty(\operatorname{supp}\psi_{p',j',k'})} &\leq C_3\omega_{r+1}(\psi'_{p,j,k}, 2^{-j'})_{L_\infty(\mathbb{R})} \\ &\leq C_4 2^{-j'(r+1)}|\psi'_{p,j,k}|_{W^{r+1}_\infty(\mathbb{R})}.\end{aligned}$$

Due to $\psi' \in W^{m-2}_\infty(\mathbb{R})$, the latter norm is finite for all $0 \leq r \leq m-3$. Picking $r = m-3 \geq 0$, an application of (4.2.5), (4.2.2), (4.1.22) and (4.1.15) shows that with $C_5 = C_5(m) > 0$, $C_6 = C_6(m) > 0$ and $C_7 = C_7(m) > 0$

$$\begin{aligned}\inf_{P\in\Pi_{m-3}} \|\psi'_{p,j,k} - P\|_{L_\infty(\operatorname{supp}\psi_{p',j',k'})} &\leq C_5 2^{-j'(m-2)}|\psi'_{p,j,k}|_{W^{m-2}_\infty(\mathbb{R})} \\ &= C_5 2^{-j'(m-2)}2^{j(m-1/2)}\|\psi_p^{(m-1)}\|_{L_\infty(\mathbb{R})} \\ &\leq C_6 2^{-j'(m-2)}2^{j(m-1/2)}\|\varphi_p^{(m-1)}\|_{L_\infty(\mathbb{R})} \\ &\leq C_7(p+1)^{m-1}2^{-j'(m-2)}2^{j(m-1/2)}.\end{aligned} \tag{4.2.26}$$

Combining the previous estimates, we obtain that with $C_8 = C_8(m) > 0$

$$\left|\langle \psi'_{p,j,k}, \psi'_{p',j',k'}\rangle_{L_2(\mathbb{R})}\right| \leq C_8(p+1)^{m-1}(p'+1)^{-(m-2)}2^{j+j'}2^{-(j'-j)(m-3/2)}.$$

If $j' \leq j$, we obtain in a completely analogous way that

$$\left|\langle \psi'_{p,j,k}, \psi'_{p',j',k'}\rangle_{L_2(\mathbb{R})}\right| \leq C_8(p'+1)^{m-1}(p+1)^{-(m-2)}2^{j+j'}2^{-(j-j')(m-3/2)}.$$

In the case that both functions are quarks φ on a fixed level $j_0 \in \mathbb{N}_0$, we estimate

$$\left|\langle \varphi'_{p,j_0,k}, \varphi'_{p',j_0,k'}\rangle_{L_2(\mathbb{R})}\right| \leq 2^{3j_0/2}\left\|\varphi'_p\right\|_{L_\infty(\mathbb{R})} 2^{j_0/2}\left\|\varphi'_{p'}\right\|_{L_1(\mathbb{R})}.$$

Previously in the proof, we have already seen that $||\varphi'_{p'}||_{L_1(\mathbb{R})} \leq C_9(p'+1)^{-(m-2)}$ with $C_9 = C_9(m) > 0$, and from (4.1.15) and (4.1.22) we derive $||\varphi'_p||_{L_\infty(\mathbb{R})} \leq C_{10}(p+1)^{-(m-3)}$ with $C_{10} = C_{10}(m) > 0$. With $C_{11} = C_{11}(m) > 0$, this leads to

$$\left|\langle \varphi'_{p,j_0,k}, \varphi'_{p',j_0,k'} \rangle_{L_2(\mathbb{R})}\right| \leq C_{11}(p+1)^{-(m-3)}(p'+1)^{-(m-2)}2^{2j_0}.$$

If both φ and ψ are involved with $C_{12} = C_{12}(m) > 0$, we obtain similar to the first case

$$\begin{aligned}\left|\langle \varphi'_{p,j_0,k}, \psi'_{p',j',k'} \rangle_{L_2(\mathbb{R})}\right| &= \inf_{P \in \Pi_r} \left|\langle \varphi'_{p,j_0,k} - P, \psi'_{p',j',k'} \rangle_{L_2(\mathbb{R})}\right| \\ &\leq \inf_{P \in \Pi_r} \|\varphi'_{p,j_0,k} - P\|_{L_\infty(\operatorname{supp} \psi_{p',j',k'})} \|\psi'_{p',j',k'}\|_{L_1(\mathbb{R})} \\ &\leq C_{12}(p+1)^{m-1}(p'+1)^{-(m-2)}2^{-(j'-j_0)(m-3/2)}2^{j_0+j'},\end{aligned}$$

and therefore (5.3.5).

The proof of (i) is quite similar. We just give a sketch of the adaptations to be made. Instead of (4.2.25), we obtain the estimate

$$||\psi_{p',j',k'}||_{L_1(\mathbb{R})} \lesssim (p'+1)^{-m}2^{-j'/2}. \tag{4.2.27}$$

Furthermore, we replace the estimate (4.2.26) by

$$\inf_{P \in \Pi_{m-2}} \|\psi_{p,j,k} - P\|_{L_\infty(\operatorname{supp} \psi_{p',j',k'})} \lesssim (p+1)^{m-1}2^{-j'(m-1)}2^{j(m-1/2)}. \tag{4.2.28}$$

Combining (4.2.27) and (4.2.28) yields

$$\left|\langle \psi_{p,j,k}, \psi_{p',j',k'} \rangle_{L_2(\mathbb{R})}\right| \lesssim (p+1)^{m-1}(p'+1)^{-m}2^{(j-j')(m-1/2)}.$$

The analogous result holds with interchanged roles of (p, j, k) and (p', j', k'). The minimum over both estimates and similar adaptations for the case that quarks are involved yield (5.3.4). □

Chapter 5

Quarklet Frames on the Unit Interval

In this chapter, we want to construct quarklets on the interval that again give rise to stable systems for a class of function spaces. Since the inner quarks and quarklets stay the same as in the shift-invariant case on the real line in Chapter 4, for the most part we deal with the adaptation of quarks and quarklets at the boundaries. For the latter, the generators and wavelets of the Primbs wavelet basis, cf. Subsection 3.2.2, are the groundwork of the construction. It turns out, that with the boundary adapted quarklets it is indeed possible to construct frames on the unit interval.

Initially, in Section 5.1, we define quarks on the interval and derive similar estimates as in Chapter 4. Section 5.2 is dedicated to the construction of boundary adapted quarklets. We introduce quarklets as linear combinations of quarks. To preserve the vanishing moments of the Primbs wavelets, we adapt the refinement mask for the boundary quarklets. The new mask coefficients are deduced via a linear equation system. Moreover, cancellation properties of the quarklets and their derivatives are displayed. These results serve as a foundation to derive compression results in the proceeding. Afterwards, in Section 5.3, we show crucial frame properties for the boundary adapted quarklet system, which are the main results of this chapter.

Let us mention that the findings of this chapter were already published in [44, Section 2]. In distinction to [44], we derive symmetric inner quarks for all orders m.

5.1 Boundary adapted quarks

In this section, we construct quarks on the interval and derive crucial Bernstein and norm estimates. Let $m, j \in \mathbb{N}$, $j \geq j_0 \in \mathbb{N}$ and $\varphi_{j,k} = 2^{j/2} B_{m,j,k}$ be the generators of the Primbs basis, cf. (3.2.20). Since the inner Schoenberg splines $B_{m,j,k}$ are dilated and translated copies of the cardinal B-spline N_m, cf. (3.1.11), we may construct the inner quarks similar to the ones constructed in Chapter 4. Hence, all important estimates for the inner quarks are already available and it is sufficient to focus on the boundary quarks as they differ from the construction in Chapter 4.

We define a quark as the product of a generator with a certain monomial. As before, let $p \in \mathbb{N}_0$. Then the *(Schoenberg B-spline) quarks* $\varphi_{p,j,k}$ are defined by

$$\varphi_{p,j,k} := \begin{cases} \left(\frac{2^j\cdot}{k+m}\right)^p \varphi_{j,k}, & k = -m+1,\dots,-1, \\ \left(\frac{2^j\cdot -k-m/2}{m/2}\right)^p \varphi_{j,k}, & k = 0,\dots,2^j-m, \\ \varphi_{p,j,2^j-m-k}(1-\cdot), & k = 2^j-m+1,\dots,2^j-1. \end{cases} \tag{5.1.1}$$

Indeed, the inner quarks, i.e., $\varphi_{p,j,k}$, $k = 0,\dots,2^j-m$, correspond to the real line quarks, cf. (4.1.2). Obviously, for $p = 0$, the functions $\varphi_{0,j,k}$ are the generators of the Primbs wavelets. The shape of the inner quarks for certain m, p could already be observed in Figure 4.1. A couple of left boundary quarks are displayed in Figure 5.1. The boundary quarks on the right hand side are actually reflections of the left boundary quarks.

The quarks form subspaces $V_{p,j}$ of $L_2(0,1)$:

$$\begin{aligned} V_{p,j} &= \operatorname{clos}_{L_2(0,1)} \operatorname{span}\{\varphi_{q,j,k} : q = 0,\dots,p, k \in \Delta_j\}, \\ \Delta_j &= \{-m+1,\dots,2^j-1\}, \end{aligned} \tag{5.1.2}$$

cf. (3.2.20). We shall now investigate some of the interval quarks' basic properties. First, we show a two-scale relation for the boundary quarks similar to Lemma 4.14. This is necessary in Section 5.3 to derive frame properties of boundary adapted quarklet systems. Because of the symmetry, we restrict our discussion to left boundary quarks.

Lemma 5.1. *For every $p \in \mathbb{N}_0$ there exist coefficients $a^j_{q,k,\ell} \in \mathbb{R}$, so that the left boundary quarks fulfil a two-scale relation of the form*

$$\varphi_{p,j,k} = \sum_{\ell=-m+1}^{m-2} \sum_{q=0}^{p} a^j_{q,k,\ell} \varphi_{p,j+1,\ell}, \quad k = -m+1,\dots,-1. \tag{5.1.3}$$

Proof. Let $k \in \{-m+1,\dots,-1\}$ be fixed. We use the corresponding two-scale relation for the Primbs wavelet generators, cf. [91, Lemma 3.3]:

$$\varphi_{j,k} = \sum_{\ell=-m+1}^{m-2} a^j_{k,\ell} \varphi_{j+1,\ell}.$$

Inserting this relation into the definition of the left boundary quarks, we obtain:

$$\begin{aligned} \varphi_{p,j,k} &= \left(\frac{2^j\cdot}{k+m}\right)^p \varphi_{j,k} = \left(\frac{2^j\cdot}{k+m}\right)^p \sum_{\ell=-m+1}^{m-2} a^j_{k,\ell}\varphi_{j+1,\ell} \\ &= \left(\frac{2^j\cdot}{k+m}\right)^p \left(\sum_{\ell=-m+1}^{-1} a^j_{k,\ell}\varphi_{j+1,\ell} + \sum_{\ell=0}^{m-2} a^j_{k,\ell}\varphi_{j+1,\ell}\right). \end{aligned} \tag{5.1.4}$$

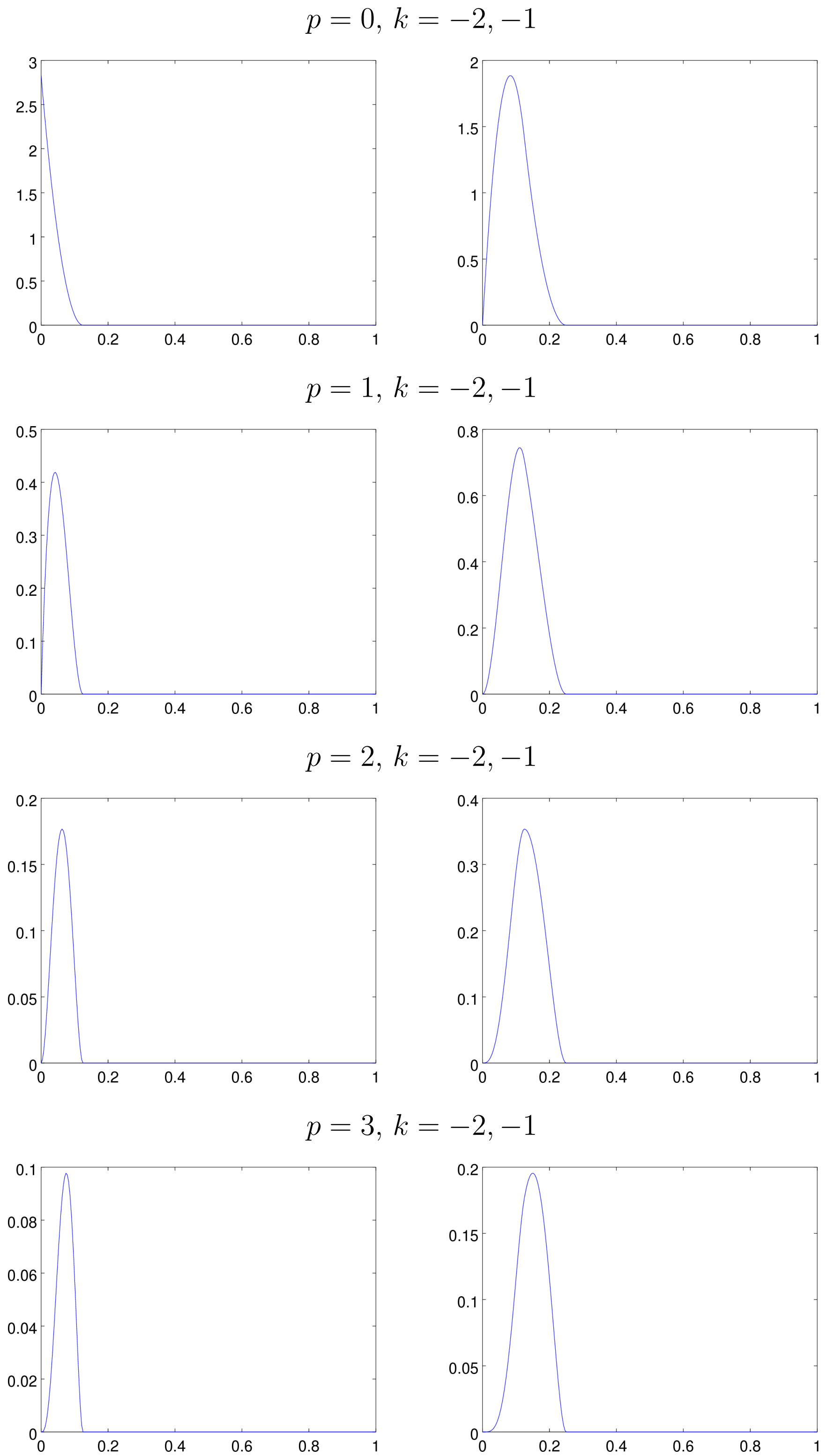

Figure 5.1: Left boundary quarks $\varphi_{p,j_0,k}$ of order $m = 3$ and polynomial degrees $p = 0, 1, 2, 3$.

The first sum can be converted into a sum of left boundary quarks of degree p:

$$\begin{aligned}\left(\frac{2^j\cdot}{k+m}\right)^p \sum_{\ell=-m+1}^{-1} a^j_{k,\ell}\varphi_{j+1,\ell} &= \sum_{\ell=-m+1}^{-1} a^j_{k,\ell}\left(\frac{\ell+m}{2(k+m)}\right)^p (\ell+m)^p \frac{(2^{j+1}\cdot)^p}{(\ell+m)^p}\varphi_{j+1,\ell} \\ &= \sum_{\ell=-m+1}^{-1} a^j_{k,\ell}\left(\frac{\ell+m}{2(k+m)}\right)^p \varphi_{p,j+1,\ell}. \qquad (5.1.5)\end{aligned}$$

For the second sum we obtain by an application of the binomial theorem:

$$\begin{aligned}(2^j\cdot)^p \sum_{\ell=0}^{m-2} a^j_{k,\ell}\varphi_{j+1,\ell} =& 2^{-p}\sum_{\ell=0}^{m-2} a^j_{k,\ell}\left(2^{j+1}\cdot-\ell-\frac{m}{2}+\ell+\frac{m}{2}\right)^p \varphi_{j+1,\ell} \\ =& 2^{-p}\sum_{\ell=0}^{m-2} a^j_{k,\ell}\sum_{q=0}^{p}\binom{p}{q}\left(2^{j+1}\cdot-\ell-\frac{m}{2}\right)^q\left(\ell+\frac{m}{2}\right)^{p-q}\varphi_{j+1,\ell}.\end{aligned}$$

Putting the monomials and wavelet generators together, we get:

$$\begin{aligned}(2^j\cdot)^p \sum_{\ell=0}^{m-2} a^j_{k,\ell}\varphi_{j+1,\ell} &= \sum_{\ell=0}^{m-2}\sum_{q=0}^{p} a^j_{k,\ell}2^{-p}\binom{p}{q}\left(\ell+\frac{m}{2}\right)^{p-q}\left(\frac{m}{2}\right)^q \\ &\quad\cdot\frac{\left(2^{j+1}\cdot-\ell-\frac{m}{2}\right)^q}{\left(\frac{m}{2}\right)^q}\varphi_{j+1,\ell} \\ &= \sum_{\ell=0}^{m-2}\sum_{q=0}^{p} a^j_{k,\ell}2^{-p}\binom{p}{q}\left(\ell+\frac{m}{2}\right)^{p-q}\left(\frac{m}{2}\right)^q\varphi_{q,j+1,\ell}. \qquad (5.1.6)\end{aligned}$$

Combining (5.1.4)-(5.1.6) leads to the coefficients of the two-scale relation

$$a^j_{q,k,\ell} = \begin{cases} a^j_{k,\ell}\left(\frac{\ell+m}{2(k+m)}\right)^p \delta_{p,q}, & \ell=-m+1,\dots,-1, \\ a^j_{k,\ell}\left(\frac{1}{2(k+m)}\right)^p\binom{p}{q}\left(\ell+\frac{m}{2}\right)^{p-q}(\frac{m}{2})^q, & \ell=0,\dots,m-2,\end{cases}$$

what proves the claim. □

In the sequel, it is helpful to study the properties of the quarks independently of the level. For this purpose, we introduce quarks on level zero on the interval $[0,\infty)$:

$$\varphi_{p,0,k} := \begin{cases}\left(\frac{\cdot}{k+m}\right)^p\varphi_{0,k}, & k=-m+1,\dots,-1, \\ \left(\frac{\cdot-k-m/2}{m/2}\right)^p N_m(\cdot-k), & k=0,1,\dots.\end{cases}$$

The left boundary and inner quarks, cf. (5.1.1), are scaled and dilated versions of the quarks on level zero. To be more precise, we have the relation

$$\varphi_{p,j,k} = 2^{j/2}\varphi_{p,0,k}(2^j\cdot), \quad k=-m+1,\dots,2^j-m. \qquad (5.1.7)$$

To be able to show the stability of the quarklet systems, bounds for the L_q-norm of the boundary quarks are necessary. In Proposition 5.2, we formulate such a statement. Analogous properties for the inner quarks have been stated in Proposition 4.4. The quite technical proof of Proposition 5.2 can be found in the appendix.

Proposition 5.2. *Let $k = 1, \dots, m-1$. For every left boundary quark $\varphi_{p,0,-m+k}$, and $1 \leq q \leq \infty$, there exist constants $c = c(m,k,q) > 0$, $C = C(m,k,q) > 0$, such that for all $p \geq (m-1)(k-1)$:*

$$c(p+1)^{-(m-1+1/q)} \leq ||\varphi_{p,0,-m+k}||_{L_q(\mathbb{R})} \leq C(p+1)^{-(m-1+1/q)}. \tag{5.1.8}$$

As already mentioned in the previous chapters, Jackson and Bernstein inequalities play a key role to obtain stable systems not only in $L_2(0,1)$, but also in scales of Sobolev spaces $H^s(0,1)$. Similar to the real line case, it suffices to rely on the Jackson inequalities for $p = 0$, since an inclusion of a Riesz basis in our frame construction assures the lower frame inequality, cf. (2.1.3). Indeed, a result of the type

$$\inf_{v \in V_{0,j}} ||f - v||_{L_2(0,1)} \leq 2^{-js}||f||_{H^s(0,1)}, \quad \text{for all } f \in H^s(0,1),\ 0 \leq s < m, \tag{5.1.9}$$

can be found in [91, Lem. 5.2 (ii)]. The Bernstein inequalities of the shift-invariant quarks directly carry over to boundary adapted quarks. We write down:

Corollary 5.3. *Let $p \in \mathbb{N}_0$, $j \geq j_0$ and the spaces $V_{p,j}$ be given by (5.1.2). Then the following Bernstein inequalities hold true: For $1 \leq q \leq \infty$ and $r \in \mathbb{N}_0$, $r \leq m-1$ there exists a constant $C_1 = C_1(m,q) > 0$, such that for all $f \in V_{p,j}$:*

$$||f^{(r)}||_{L_q(0,1)} \leq C_1(p+1)^{2r}2^{jr}||f||_{L_q(0,1)}. \tag{5.1.10}$$

Moreover, for $0 \leq s < m - \frac{1}{2}$ there exists a constant $C_2 = C_2(m,s) > 0$, such that for all $f \in V_{p,j}$:

$$|f|_{H^s(0,1)} \leq C_2(p+1)^{2s}2^{js}||f||_{L_2(0,1)}. \tag{5.1.11}$$

5.2 Boundary quarklets with vanishing moments

Now, we discuss the construction of quarklets on the interval. Henceforth we consider boundary conditions and assume $\vec{\sigma} = (\sigma_0, \sigma_1) \in \{0, \lfloor s + \frac{1}{2} \rceil\}^2$, $s > 0$ to be fixed. The natural approach would be to proceed similar to the real line case and assign a given wavelet mask also for the definition of quarklets. The interval quarks have been build on the foundation of Primbs generators. Hence, assigning the mask of the Primbs wavelets seems to be the obvious choice. Quite surprisingly, this procedure solely works for inner quarklets. It does *not* work for the boundary quarklets since this would destroy the vanishing moment properties. It turns out that in order to preserve the vanishing moment properties of the underlying Primbs wavelet basis for the full quarklet system, it is necessary to adapt the two-scale relation of the boundary quarklets.

In any event, analogously to the shift-invariant case, cf. Section 4.2, quarklets are defined as linear combinations of quark generators on the next higher level. Let us recall the index sets

$$\Delta_{j,\vec{\sigma}} = \{-m+1+\operatorname{sgn}\sigma_0, \dots, 2^j - 1 - \operatorname{sgn}\sigma_1\}, \quad \nabla_j = \{0, \dots, 2^j - 1\},$$

cf. (3.2.20), (3.2.25), and their separations as in (3.2.22)-(3.2.26). Then, the two-scale relation (4.2.2) for one quarklet becomes

$$\psi^{\vec{\sigma}}_{p,j,\ell} := \sum_{k \in \Delta_{j+1,\vec{\sigma}}} b^{p,j,\vec{\sigma}}_{k,\ell} \varphi_{p,j+1,k}, \quad \ell \in \nabla_j. \tag{5.2.1}$$

We already notice that in contrast to (4.2.2) the coefficients $b^{p,j,\vec{\sigma}}_{k,\ell}$ in (5.2.1) do not only depend on k. Before we proceed with the construction, let us fix some notation. We define the sets

$$\Phi^{\vec{\sigma}}_{p,j} := \{\varphi_{p,j,k} : k \in \Delta_{j,\vec{\sigma}}\}, \quad \Psi^{\vec{\sigma}}_{p,j} := \{\psi^{\vec{\sigma}}_{p,j,k} : k \in \nabla_j\}, \quad p, j \in \mathbb{N}_0, j \geq j_0, \tag{5.2.2}$$

and the refinement matrix

$$\mathbf{M}_{p,j,\vec{\sigma}} := \{(b^{p,j,\vec{\sigma}}_{k,\ell})\}_{(k,\ell) \in \Delta_{j+1,\vec{\sigma}} \times \nabla_{j,\vec{\sigma}}}. \tag{5.2.3}$$

Then, (5.2.1) can be reformulated as

$$\Psi_{p,j,\vec{\sigma}} = \mathbf{M}^T_{p,j,\vec{\sigma}} \Phi_{p,j+1,\vec{\sigma}}. \tag{5.2.4}$$

Now, let us continue with the construction process. At first, we discuss the construction of the inner quarklets. For $p, j \in \mathbb{N}_0$, $j \geq j_0$, $k \in \nabla^{(I)}_{j,\vec{\sigma}}$, the inner wavelets of the Primbs basis are given by $\psi^{\vec{\sigma}}_{j,\ell} = \sum_{k \in \Delta_{j+1,\vec{\sigma}}} b^{j,\vec{\sigma}}_{k,\ell} \varphi_{j+1,k}$, where the coefficients $b^{j,\vec{\sigma}}_{k,\ell}$ are the entries of the stable completion $\mathbf{M}_{j,1}$ of the Primbs basis, cf. (3.2.10). We construct an inner quarklet by keeping these coefficients and inserting them into (5.2.1):

$$b^{p,j,\vec{\sigma}}_{k,\ell} := b^{j,\vec{\sigma}}_{k,\ell}, \quad k \in \Delta_{j+1,\vec{\sigma}}, \ \ell \in \nabla^I_j. \tag{5.2.5}$$

Since the inner Primbs wavelets are cardinal B-splines, the inner quarklets defined above have the same number of vanishing moments, cf. Lemma 4.8.

The next step is to construct boundary quarklets. As already mentioned, the coefficients of the boundary wavelets are not suitable for the boundary quarklets, since in general the vanishing moment properties can not be preserved. A simple counter-example for $m = 2$ is given by

$$\int_{\mathbb{R}} \sum_{k=-1}^{2} b^{2,(0,0)}_{k,0} \varphi_{1,3,k} = \frac{1}{8},$$

where the non-trivial coefficients are $(b_{k,0}^{2,(0,0)})_{k=-1}^{2} = \sqrt{2}(\frac{3}{2}, -\frac{9}{8}, \frac{1}{4}, \frac{1}{8})$.

Therefore, instead of keeping the coefficients, our approach is to modify them in a way that the $\tilde{m}$ equations

$$\int_{\mathbb{R}} x^q \psi_{p,j,\ell}^{\vec{\sigma}}(x)\ \mathrm{d}x = \int_{\mathbb{R}} x^q \sum_{k\in\Delta_{j+1,\vec{\sigma}}} b_{k,\ell}^{p,j,\vec{\sigma}} \varphi_{p,j+1,k}\ \mathrm{d}x = 0, \quad q = 0, ..., \tilde{m}-1 \tag{5.2.6}$$

are fulfilled not only for $p = 0$ but for all $p \in \mathbb{N}_0$. We restrict our discussion to left boundary quarklets, i.e., $\ell \in \nabla_j^{(L)}$, and assume that they are only composed of left boundary and inner quarks. To get at least one non-trivial solution of (5.2.6), we further assume that every boundary quarklet consists of $\tilde{m}+1$ quarks. Furthermore, the ℓ-th quarklets representation should begin at the leftmost but ℓ quark with respect to boundary conditions. For $p > 0$ and a fixed $\ell \in \nabla_j^{(L)}$, this leads to the $\tilde{m} \times (\tilde{m}+1)$ linear system of equations

$$\sum_{k=-m+1+\operatorname{sgn}\sigma_0+\ell}^{-m+1+\operatorname{sgn}\sigma_0+\ell+\tilde{m}} b_{k,\ell}^{p,j,\vec{\sigma}} \int_{\mathbb{R}} x^q \varphi_{p,j+1,k}(x)\ \mathrm{d}x = 0, \quad q = 0, ..., \tilde{m}-1, \tag{5.2.7}$$

to determine the quarklet coefficients for one boundary quarklet $\psi_{p,j,\ell}^{\vec{\sigma}}$. In matrix-vector form, (5.2.7) can be written as

$$\mathbf{X}\mathbf{b} = \mathbf{0}, \quad \mathbf{X} = \left\{ \int_{\mathbb{R}} x^q \varphi_{p,j+1,k}(x)\ \mathrm{d}x \right\}_{\substack{q\in\{0,...,\tilde{m}-1\},\\ k\in\Delta_\ell^*}}, \quad \mathbf{b} = \{b_{k,\ell}^{p,j,\vec{\sigma}}\}_{k\in\Delta_\ell^*}, \tag{5.2.8}$$

where

$$\Delta_\ell^* := \{-m+1+\operatorname{sgn}\sigma_0+\ell, \dots, -m+1+\operatorname{sgn}\sigma_0+\ell+\tilde{m}\}.$$

To solve (5.2.7) or (5.2.8), respectively, we need to calculate the first $\tilde{m}$ moments of the quarks. The following relations hold.

Lemma 5.4. *Let $p, j \in \mathbb{N}_0$, $j \geq j_0$. For the left boundary quarks $\varphi_{p,j+1,k}$, $k \in \Delta_{j,\vec{\sigma}}^{(L)}$, we have*

$$\int_{\mathbb{R}} x^q \varphi_{p,j+1,k}(x)\ \mathrm{d}x = (m-1)! \frac{2^{-(j+1)(q+1/2)}}{(q+p+m)...(q+p+1)} \frac{1}{(k+m)^p(k+m-1)!} \cdot \left(\sum_{i=0}^{k+m} \binom{k+m}{i} (-1)^{k+m-i} i^{q+p+m+k} \right). \tag{5.2.9}$$

For the inner quarks $\varphi_{p,j+1,k}$, $k \in \Delta_{j,\vec{\sigma}}^{(I)}$, it holds

$$\int_{\mathbb{R}} x^q \varphi_{p,j+1,k}(x)\ \mathrm{d}x = 2^{-(j+1)(q+1/2)} \left(\frac{m}{2}\right)^{-p} \sum_{i=0}^{p} \frac{\binom{p}{i}\left(-k-\frac{m}{2}\right)^{p-i}}{(i+q+m)...(i+q+1)} \cdot \left(\sum_{r=0}^{m} \binom{m}{r} (-1)^{m-r} (k+r)^{i+q+m} \right). \tag{5.2.10}$$

Proof. For a proof of these rather technical results we refer to [96, Section 3.4]. □

From Lemma 5.4 we directly conclude that

$$\int_{\mathbb{R}} x^q \varphi_{p,j+1,k}(x)\,\mathrm{d}x = 2^{-(q+1/2)} \int_{\mathbb{R}} x^q \varphi_{p,j,k}(x)\,\mathrm{d}x, \quad k \in \Delta_\ell^*,\ \ell \in \nabla_j^{(L)}.$$

Therefore, the solution $\mathbf{b}$ in (5.2.8) is independent of j. Hence, we can drop the index j for the two-scale coefficients in the case of boundary quarklets. Furthermore, numerical tests indicate that the matrix $\mathbf{X}$ in (5.2.8) has full rank $\tilde{m}$ so that a non-trivial solution $\mathbf{b}$ is unique except for scaling. Hence, we are able to construct quarklets at the boundary with vanishing moments. We scale with respect to the quadratic norm such that $||\mathbf{b}||_2 = 1$. If $0 \neq \mathbf{b}$ solves (5.2.7), the ℓ-th left boundary quarklet is

$$\psi_{p,j,\ell}^{\vec{\sigma}} = \sum_{k=-m+1+\operatorname{sgn}\sigma_0+\ell}^{-m+1+\operatorname{sgn}\sigma_0+\ell+\tilde{m}} b_{k,\ell}^{p,\vec{\sigma}} \varphi_{p,j+1,k}, \quad \ell \in \nabla^{(L)}. \tag{5.2.11}$$

The construction for right boundary quarklets is completely analogue.

To summarize the construction of quarklets on the interval, it is convenient to take a look at the structure of the refinement matrix $\mathbf{M}_{p,j,\vec{\sigma}}$, cf. (5.2.3). It can be written as a block matrix

$\mathbf{M}_{p,j,\vec{\sigma}} =$

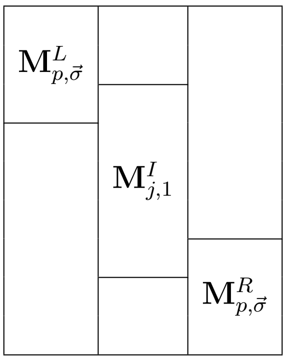

,

with $\mathbf{M}_{j,1}^I \in \mathbb{R}^{\#\Delta_{j+1}^{(I)} \times \#\nabla_j^{(I)}}$, and $\mathbf{M}_{p,\vec{\sigma}}^{\mathrm{loc}} \in \mathbb{R}^{(\#\Delta_0^* + \#\nabla^{(\mathrm{loc})}-1)\times\#\nabla^{(\mathrm{loc})}}$, for $p > 0$, $\mathrm{loc} \in \{L, R\}$. Compared to the case $p > 0$, for $p = 0$, the matrix $\mathbf{M}_{p,\vec{\sigma}}^{\mathrm{loc}}$, $\mathrm{loc} \in \{L, R\}$, has a bigger amount of rows due to the fact that more quarks are involved in the two-scale equation.

For $p = 0$, $\mathbf{M}_{p,j,\vec{\sigma}}$ corresponds to the two-scale matrix of the Primbs wavelets $\mathbf{M}_{j,1}$, cf. (3.2.28). As a consequence, the Primbs wavelet basis is included in the quarklet system. As mentioned earlier in this chapter, this assures the lower frame bound inequality. The inner matrix $\mathbf{M}_{j,1}^I$ represents the two-scale coefficients of the inner quarklets. It is also the inner two-scale matrix of the Primbs wavelets and therefore independent of p but dependent on j. Of course, it is also independent of the imposed boundary condition $\vec{\sigma}$. The left boundary matrix $\mathbf{M}_{p,\vec{\sigma}}^L$ contains the coefficients for the left boundary quarklets. It is dependent on p. Hence, we have to calculate boundary coefficients for every polynomial degree p. Fortunately, it is independent of j, such that a calculation on every level is dispensable. The right boundary matrix $\mathbf{M}^R_{p,\vec{\sigma}}$ has similar properties to $\mathbf{M}^L_{p,\vec{\sigma}}$. As an example, if we indicate all non-zero elements with a $*$, for $p > 0$, $m = 3$, $\tilde{m} = 5$, the matrix $\mathbf{M}^L_{p,\vec{\sigma}}$ has the structure

$$\mathbf{M}^L_{p,\vec{\sigma}} = \begin{bmatrix} * & & \\ * & * & \\ * & * & * \\ * & * & * \\ * & * & * \\ * & * & * \\ & * & * \\ & & * \end{bmatrix}.$$

In the Tables 5.1-5.2 boundary coefficients $b^{p,\vec{\sigma}}_{k,\ell}$ for certain parameters are displayed. Finally, we observe some boundary quarklets in Figure 5.2.

p	$b^{p,\vec{0}}_{-1,0}$	$b^{p,\vec{0}}_{0,0}$	$b^{p,\vec{0}}_{1,0}$
1	0	-0.707	0.707
3	0	-0.707	0.707
5	0	-0.707	0.707
7	0	-0.707	0.707
9	0	-0.707	0.707
11	0	-0.707	0.707
13	0	-0.707	0.707
15	0	-0.707	0.707
17	0	-0.707	0.707
19	0	-0.707	0.707

p	b_{-1}	b_0	b_1
2	-0.808	0.566	-0.162
4	-0.835	0.537	-0.119
6	-0.849	0.519	-0.094
8	-0.858	0.507	-0.078
10	-0.864	0.499	-0.066
12	-0.869	0.492	-0.058
14	-0.872	0.487	-0.051
16	-0.874	0.483	-0.046
18	-0.876	0.48	-0.042
20	-0.879	0.476	-0.037

Table 5.1: Two-scale coefficients for the only left boundary quarklet $\psi^{\vec{0}}_{p,j,0}$ for free boundary conditions and $m = \tilde{m} = 2$.

p	$b^{p,\vec{0}}_{-2,0}$	$b^{p,\vec{0}}_{-1,0}$	$b^{p,\vec{0}}_{0,0}$	$b^{p,\vec{0}}_{1,0}$
1	0.855	-0.285	0.399	-0.171
2	-0.114	0.568	-0.784	0.222
3	0.915	-0.244	0.302	-0.109
4	-0.661	-0.221	0.68	-0.23
5	0.93	-0.236	0.271	-0.084
6	-0.823	-0.067	0.526	-0.203
7	0.935	-0.235	0.255	-0.07
8	-0.869	-0.005	0.456	-0.193
9	0.939	-0.235	0.245	-0.06
10	-0.887	0.028	0.42	-0.19
11	0.941	-0.235	0.238	-0.052
12	-0.896	0.048	0.399	-0.19
13	0.942	-0.236	0.233	-0.047
14	-0.901	0.061	0.384	-0.19
15	0.944	-0.236	0.228	-0.042
16	-0.904	0.071	0.374	-0.191
17	0.945	-0.236	0.225	-0.038
18	0.906	-0.079	-0.368	0.192
19	0.945	-0.236	0.222	-0.035
20	0.909	-0.078	-0.364	0.189

p	$b^{p,\vec{0}}_{-2,1}$	$b^{p,\vec{0}}_{-1,1}$	$b^{p,\vec{0}}_{0,1}$	$b^{p,\vec{0}}_{1,1}$
1	0	0.408	-0.816	0.408
2	-0.522	0.806	-0.279	0.022
3	0	0.408	-0.816	0.408
4	-0.64	0.698	0.245	-0.207
5	0	0.408	-0.816	0.408
6	-0.587	0.421	0.604	-0.335
7	-0	0.408	-0.816	0.408
8	-0.506	0.226	0.745	-0.372
9	-0	0.408	-0.816	0.408
10	0.448	-0.112	-0.801	0.381
11	0	0.408	-0.816	0.408
12	0.409	-0.041	-0.827	0.383
13	-0	0.408	-0.816	0.408
14	0.382	0.005	-0.841	0.383
15	0	0.409	-0.816	0.407
16	0.361	0.04	-0.85	0.382
17	-0.01	0.446	-0.803	0.394
18	0.33	0.052	-0.85	0.407
19	0.046	0.098	-0.803	0.587
20	-0.553	0.831	-0.04	-0.041

Table 5.2: Two-scale coefficients for the left boundary quarklets $\psi^{\vec{0}}_{p,j,0}$, $\psi^{\vec{0}}_{p,j,1}$ for free boundary conditions and $m = \tilde{m} = 3$.

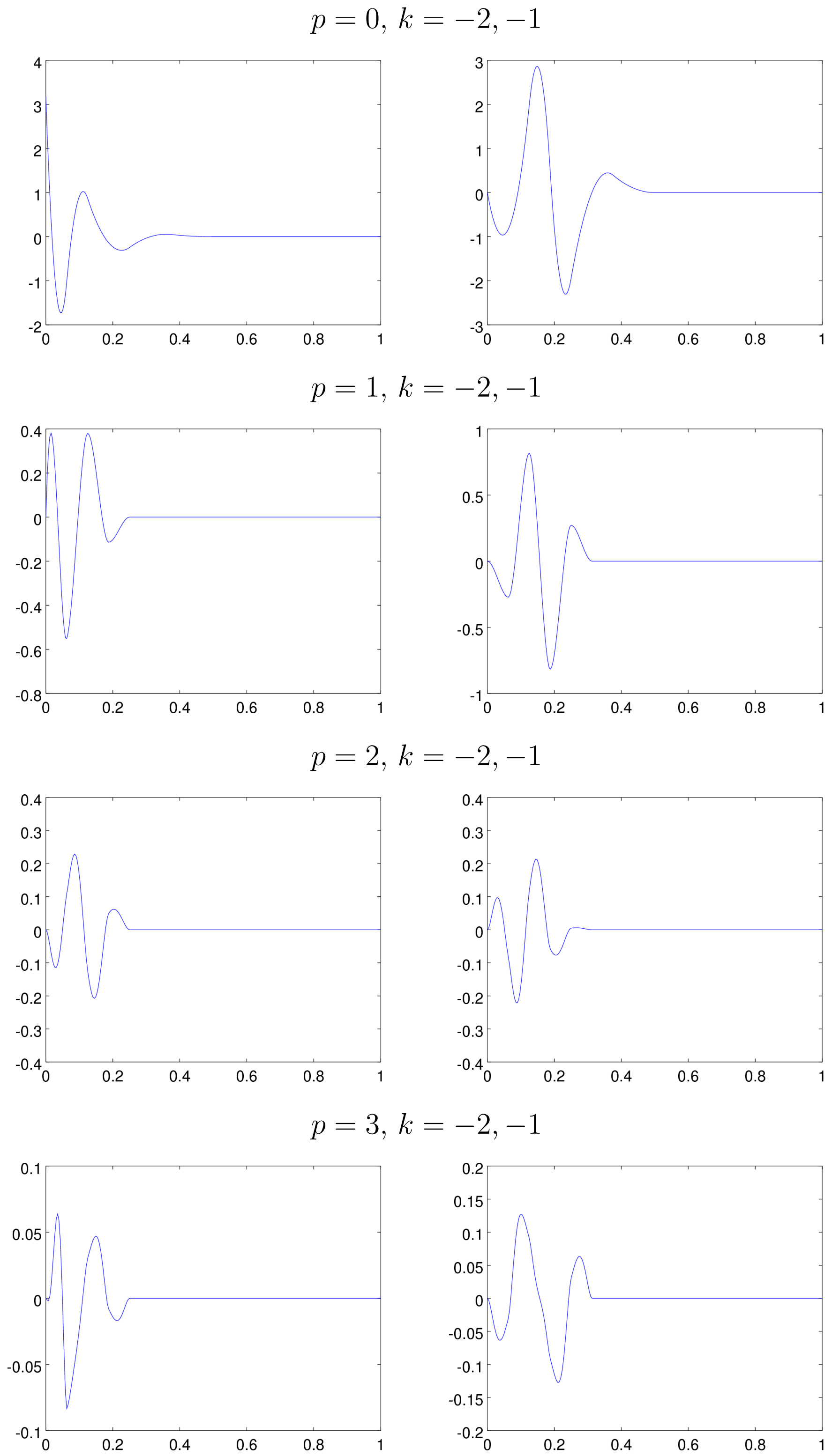

Figure 5.2: Left boundary quarklets $\psi_{p,j_0,k}$ of order $m = 3$ with $\tilde{m} = 3$ vanishing moments, polynomial degrees $p = 0, 1, 2, 3$ and free boundary conditions.

5.3 Quarklet frames for $L_2(0,1)$ and $H^s(0,1)$

Now that the construction of boundary adapted quarklets has been performed in a satisfying way, we proceed similar to Chapter 4 to show frame properties for smoothness spaces on the unit interval. For the sake of completeness, we write down the necessary results. The proofs are similar or equivalent to the proofs of the corresponding statements for the shift-invariant case in Chapter 4.

As an augmentation of the Primbs basis index set $\nabla^B_{\vec{\sigma}}$, cf. (3.2.27), we define the index set for the whole quarklet system by

$$\nabla_{\vec{\sigma}} := \{(p,j,k) : p,j \in \mathbb{N}_0, j \geq j_0 - 1, k \in \nabla_{j,\vec{\sigma}}\}, \tag{5.3.1}$$

with the conventions $\nabla_{j,\vec{\sigma}} := \nabla_j$ for $j \geq j_0$, $\nabla_{j_0-1,\vec{\sigma}} := \Delta_{j_0,\vec{\sigma}}$, cf. (3.2.25) and Remark 3.15, respectively. In this regard we also fix $\psi^{\vec{\sigma}}_{p,j_0-1,k} := \varphi_{p,j_0,k}$ for $(p, j_0-1, k) \in \nabla_{\vec{\sigma}}$.

The vanishing moment property of the quarklets immediately leads to the following cancellation property of the quarklets.

Proposition 5.5. *Let $(p,j,k) \in \nabla_{\vec{\sigma}}$, $j \geq j_0$ and $\psi^{\vec{\sigma}}_{p,j,k}$ a quarklet with $\tilde{m}$ vanishing moments. There exists a constant $C = C(m,\tilde{m}) > 0$, such that for every $r \in \mathbb{N}_0, r \leq \tilde{m}-1$ and $f \in W^r_\infty(\mathbb{R})$:*

$$|\langle f, \psi^{\vec{\sigma}}_{p,j,k}\rangle_{L_2(\mathbb{R})}| \leq C(p+1)^{-m} 2^{-j(r+1/2)} |f|_{W^r_\infty(\mathrm{supp}\,\psi^{\vec{\sigma}}_{p,j,k})}. \tag{5.3.2}$$

Proof. The proof can be performed by following the lines of Proposition 4.9. From the vanishing moments of the quarklets, Hölder's inequality and a Whitney type estimate it follows:

$$|\langle f, \psi^{\vec{\sigma}}_{p,j,k}\rangle_{L_2(\mathbb{R})}| \leq C_1 |\mathrm{supp}\ \psi_{p,j,k}|^r |f|_{W^r_\infty(\mathrm{supp}\ \psi^{\vec{\sigma}}_{p,j,k})} ||\psi^{\vec{\sigma}}_{p,j,k}||_{L_1(\mathrm{supp}\ \psi^{\vec{\sigma}}_{p,j,k})}, \tag{5.3.3}$$

where $C_1 > 0$ only depends on r. W.l.o.g, we assume that only left boundary and inner quarklets occur in (5.3.3). Due to the symmetry of the boundary quarks, the estimates are also valid for right boundary quarklets. To further estimate the L_1-norm expression in (5.3.3), we use (5.2.1) and the relation

$$\varphi_{p,j,k} = 2^{j/2} \varphi_{p,0,k}(2^j \cdot), \quad k = -m+1, \ldots, 2^j - m.$$

Combining this relation and the norm estimate (5.1.8), we obtain

$$||\psi^{\vec{\sigma}}_{p,j,k}||_{L_1(\mathrm{supp}\ \psi^{\vec{\sigma}}_{p,j,k})} \leq C_2 2^{-\frac{j+1}{2}} (p+1)^{-m} \sum_{\ell \in \Delta_{j+1,\vec{\sigma}}} |b^{p,j,\vec{\sigma}}_{k,\ell}|,$$

where $C_2 > 0$ only depends on m. The claim finally follows by estimating the asymptotic behaviour of $|\mathrm{supp}\ \psi^{\vec{\sigma}}_{p,j,k}|$ by 2^{-j}. □

Moreover, the boundary quarklets have all the necessary properties such that compression estimates similar to the ones stated in Proposition 4.16 hold.

Proposition 5.6. *Let $m, \tilde{m} \geq 3$, and $(p,j,k),(p',j',k') \in \nabla_{\vec{\sigma}}$. Then, the following relations hold:*

(i) There exists $C = C(m,\tilde{m})$, such that the unweighted quarks and quarklets satisfy

$$\left|\langle \psi^{\vec{\sigma}}_{p,j,k}, \psi^{\vec{\sigma}}_{p',j',k'} \rangle_{L_2(0,1)}\right| \leq C\Big((p+1)(p'+1)\Big)^{m-1} 2^{-|j-j'|(m-1/2)}. \tag{5.3.4}$$

(ii) There exists $C' = C'(m,\tilde{m}) > 0$, such that the derivatives of the unweighted quarks and quarklets satisfy

$$2^{-(j+j')}\left|\langle (\psi^{\vec{\sigma}}_{p,j,k})', (\psi^{\vec{\sigma}}_{p',j',k'})' \rangle_{L_2(0,1)}\right| \leq C'\Big((p{+}1)(p'{+}1)\Big)^{m-1} 2^{-|j-j'|(m-3/2)}. \tag{5.3.5}$$

Proof. Since the inner quarklets are equivalent to the ones in the shift-invariant case, we only have to consider boundary quarklets. Without loss of generality, due to symmetry arguments, it is sufficient to show the property for left boundary quarklets. The latter are refinable as a linear combination of left boundary and inner quarks with a finite coefficient mask bounded independently of p and j, cf. (5.2.1). The left boundary and inner quarks are scaled and dilated version of quarks on level zero, cf. (5.1.7). Since the latter satisfy the norm estimate (5.2) and the Bernstein estimate (5.1.10), we are able to perform similar steps as in the proof of Proposition 4.16 and therefore the claim holds also for boundary quarklets. □

With the cancellation property (5.3.2) at hand, also the estimates for the Gramian matrices from Section 4.2 can be immediately transferred to the boundary adapted case. This is the last missing ingredient to show the frame property of the quarklet systems in $L_2(0,1)$ and $H^s(0,1)$.

Proposition 5.7. *For fixed $p \in \mathbb{N}_0$, the Gramian matrix*

$$\mathbf{G}_p^{L_2(0,1)} := \Big(\langle \psi^{\vec{\sigma}}_{p,j,k}, \psi^{\vec{\sigma}}_{p,j',k'} \rangle_{L_2(0,1)}\Big)_{(j,k),(j',k') \in \nabla^B_{\vec{\sigma}}} \tag{5.3.6}$$

is a bounded operator on $\ell_2(\nabla^B_{\vec{\sigma}})$, i.e., there exists a constant $C = C(m,\tilde{m}) > 0$, such that

$$||\mathbf{G}_p^{L_2(0,1)}||_{\mathscr{L}(\ell_2(\nabla^B_{\vec{\sigma}}))} \leq C(p+1)^{-1}. \tag{5.3.7}$$

Now, we have finally collected all the necessary building blocks to transfer the frame properties of the shift-invariant quarklets to the case of boundary adapted quarklets. The following two theorems are the main result of this chapter. They state that the construction ideas of frames for Lebesgue spaces and scales of Sobolev spaces in the shift-invariant case, cf. Theorems 4.11, 4.15, respectively, can be carried over to the boundary adapted quarklets. These frames serve as a starting point for the construction of multivariate tensor frames on cubes and more general domains, as it is outlined in Chapter 6. At first, we formulate the frame property in $L_2(0,1)$.

Theorem 5.8. *The weighted quarklet system*

$$\Psi_{L_2(0,1),\vec{\sigma}} := \{(p+1)^{-\delta_1/2}\psi_\lambda^{\vec{\sigma}} : \lambda = (p,j,k) \in \nabla_{\vec{\sigma}}\}, \quad \delta_1 > 0, \tag{5.3.8}$$

is a frame for $L_2(0,1)$.

Choosing suitable weights, we derive frames for Sobolev spaces $H^s_{\vec{\sigma}}(0,1)$, $0 < s < m - \frac{1}{2}$.

Theorem 5.9. *For* $0 \leq s < m - \frac{1}{2}$*, the weighted quarklet system*

$$\Psi_{H^s_{\vec{\sigma}}(0,1)} := \{(p+1)^{-2s-\delta_1/2-\delta_2/2}2^{-sj}\psi_\lambda^{\vec{\sigma}} : \lambda = (p,j,k) \in \nabla_{\vec{\sigma}}\}, \quad \delta_1 > 0,\ \delta_2 > 1, \tag{5.3.9}$$

is a frame for $H^s_{\vec{\sigma}}(0,1)$.

Chapter 6

Quarklet Frames on Bounded Domains

This chapter settles the case of the construction of quarklets. We show how to use the unit interval frames of Chapter 5 to construct quarklet frames on multidimensional domains. In two consecutive steps, we construct quarklet frames on unit cubes and then extent these frames to general domains. The main challenges are to transfer the ideas of tensorization and extension operators, which were used for the construction of wavelet bases, cf. [20], to the case of frames. It turns out that with some additional effort, these ideas can be indeed successfully applied also in this setting.

The course of this chapter is as follows: in Section 6.1, we show how to construct quarklet frames on the unit cube out of tensor products of quarklet frames on the unit interval. For this purpose, we introduce a principle to construct frames for tensor products and intersections of Hilbert spaces in a general manner. Subsequently, we apply this approach to quarklets. In Section 6.2, we extend the unit cube frames to general bounded domains. In order to do this, we introduce the domains of interest as the union of parametric images of the unit cube and recall some ideas of [20] concerning extension operators and isomorphisms between Sobolev spaces on different domains. Thereupon, we describe in a general setting how a combination of frames on cubes, Bessel systems which include the image of an extension operator and simple extensions lead to frames for Sobolev spaces on our target domain $\Omega \subset \mathbb{R}^d$. Finally, we show that the general machinery can be applied to our setting and present explicit constructions. The frame properties of the generalized quarklet frames stated in the consecutive Theorems 6.19 and 6.20 are at the heart of this thesis. On the one hand, they build the conclusion of the construction of quarklets which has started in Chapter 4. On the other hand, they are the foundation for quarklets to be applied in adaptive numerical schemes as it will be outlined in the following chapters.

The construction of quarklet frames on general domains was already outlined in [44, Section 4]. In this chapter, we summarize the findings complemented with visualizations of the frame elements and further insights. In particular, the embedding of the approach into the Gelfand frame setting constitutes an enhancement of the theory.

6.1 Frame constructions on cubes

Before we start with the actual construction of frames on cubes, let us briefly recall the definitions of tensor products and intersections of Hilbert spaces. For additional details on this topic, we refer to [22, 70].

6.1.1 Tensor products and intersections of Hilbert spaces

For two Hilbert spaces G and H we define

$$F(G,H) := \left\{ \sum_{i=1}^{n} \alpha_i (g_i, h_i) : \alpha_j \in \mathbb{R}, (g_i, h_i) \in G \times H, n \in \mathbb{N} \right\}. \tag{6.1.1}$$

Every $f = \sum_{i=1}^{n} \alpha_i (g_i, h_i) \in F(G,H)$ induces an operator $A_f : G' \to H$, given by

$$A_f \phi := \sum_{i=1}^{n} \alpha_i \phi(g_i) h_i, \quad \phi \in G'.$$

For $f, \tilde{f} \in F(G,H)$, we define the equivalence relation

$$f \simeq \tilde{f} \Longleftrightarrow A_f \phi = A_{\tilde{f}} \phi, \quad \text{for all } \phi \in G'.$$

With $T(G,H)$ we denote the quotient space $F(G,H)/\simeq$. For $g \in G$, $h \in H$ the notation $g \otimes h$ is reserved for the equivalence class in $T(G,H)$ containing (g,h). Then, the inner product

$$\langle g_1 \otimes h_1, g_2 \otimes h_2 \rangle_{G \otimes H} := \langle g_1, g_2 \rangle_G \langle h_1, h_2 \rangle_H, \quad g_1, g_2 \in G, h_1, h_2 \in H, \tag{6.1.2}$$

extended by linearity turns $T(G,H)$ into a pre-Hilbert space. The closure of $T(G,H)$ with respect to the induced norm

$$|| \cdot ||_{G \otimes H} := \langle \cdot, \cdot \rangle_{G \otimes H}^{1/2} \tag{6.1.3}$$

is a Hilbert space and is denoted with $G \otimes H$. Moreover, if G and H are function spaces over domains Ω_1 and Ω_2, respectively, the formal tensor expressions have a more immediate meaning. In this case, the tensor product space $G \otimes H$ can be identified as a function space over the Cartesian product domain $\Omega_1 \times \Omega_2$, i.e., for functions $g : \Omega_1 \to \mathbb{R}$, $h : \Omega_2 \to \mathbb{R}$, the tensor product turns into

$$g \otimes h(x,y) := g(x)h(y), \quad x \in \Omega_1, y \in \Omega_2. \tag{6.1.4}$$

The Lebesgue spaces L_2 are of tensor product type and it holds the relation

$$L_2(\Omega_1 \times \Omega_2) = L_2(\Omega_1) \otimes L_2(\Omega_2) \tag{6.1.5}$$

in terms of equivalent norms, cf. [22, Theorem 1.39] for a proof. For Sobolev spaces over Cartesian products the situation is slightly different and it is necessary to introduce intersections of Hilbert spaces to formulate a relation similar to (6.1.5). For two Hilbert spaces G and H the space of functions $f \in G \cap H$ equipped with the norm

$$\|\cdot\|_{G\cap H} := \left(\|\cdot\|_G^2 + \|\cdot\|_H^2\right)^{1/2} \tag{6.1.6}$$

is a Hilbert space itself if it is non-trivial. For $s \in [0,\infty) \setminus (\mathbb{N}_0 + \{\frac{1}{2}\})$ and domains Ω_1 and Ω_2 it holds the relation

$$H_0^s(\Omega_1 \times \Omega_2) = H_0^s(\Omega_1) \otimes L_2(\Omega_2) \cap L_2(\Omega_1) \otimes H_0^s(\Omega_2), \tag{6.1.7}$$

cf. [70]. [61] In this section, the case where Ω_1 and Ω_2 are intervals and as a result $\Omega_1 \times \Omega_2$ is a rectangle is of interest. Tensor product constructions carry over to dimensions $d > 2$. Moreover, formula (6.1.7) holds with more general boundary conditions. Due to the just mentioned facts, it seems reasonable to fix the notation of the generic case of this section. Let $\square := (0,1)^d$ be the d-times unit cube. Furthermore, let $s \in [0,\infty) \setminus (\mathbb{N}_0 + \{\frac{1}{2}\})$ and $\boldsymbol{\sigma} = (\vec{\sigma_1}, \ldots, \vec{\sigma_d})$, $\vec{\sigma_i} = ((\sigma_i)_0, (\sigma_i)_1) \in \{0, \lfloor s + \frac{1}{2} \rfloor\}^2$. We define $\Gamma_{\boldsymbol{\sigma}} \subset \partial\square$ as the union of hyperplanes

$$[0,1]^{i-1} \times \{0\} \times [0,1]^{d-i}, \quad i \in \{1,\ldots,d\},$$

for which $(\sigma_i)_0 = \lfloor s + \frac{1}{2} \rfloor$ and

$$[0,1]^{i-1} \times \{1\} \times [0,1]^{d-i}, \quad i \in \{1,\ldots,d\},$$

for which $(\sigma_i)_1 = \lfloor s + \frac{1}{2} \rfloor$. Then, the relation

$$H^s_{\Gamma_{\boldsymbol{\sigma}}}(\square) = \bigcap_{i=1}^{d} H_i^s(\square) \tag{6.1.8}$$

holds, where

$$H_i^s(\square) := L_2(0,1) \otimes \cdots \otimes L_2(0,1) \otimes H^s_{\vec{\sigma_i}}(0,1) \otimes L_2(0,1) \otimes \cdots \otimes L_2(0,1), \tag{6.1.9}$$

with $H^s_{\vec{\sigma_i}}(0,1)$ at the i-th spot. Cf. (1.3.14) and (1.3.15) for the definitions of Sobolev spaces with certain boundary conditions.

In the following subsection we shed some light on the construction of frames for $H_i^s(\square)$ and $H^s_{\Gamma_{\boldsymbol{\sigma}}}(\square)$.

6.1.2 Tensor and intersection frames

The following two lemmas give rise to the construction of frames on tensor product spaces and on intersections of Hilbert spaces, respectively. They generalize the respective Lemmas 3.1.5 and 3.1.8 of [66] from the case of Riesz bases to the case of frames. They are not only valid for the case of quarklet frames but for a much broader class of frames.

We assume that for a countable index set $\mathcal{J}$, the system $\mathcal{F}_{L_2(0,1)} = \{f_\lambda\}_{\lambda\in\mathcal{J}}$ is a frame for $L_2(0,1)$ with frame bounds $A, B > 0$, such that, for certain scalar weights $w_\lambda > 0$ and an $s \in [0,\infty) \setminus (\mathbb{N}_0 + \{\frac{1}{2}\})$, the set $\{w_\lambda^{-1} f_\lambda\}_{\lambda\in\mathcal{J}}$ is a frame for $H^s_{\vec{\sigma}}(0,1)$, $\vec{\sigma} \in \{0, \lfloor s+\frac{1}{2}\rfloor\}^2$, with frame bounds $A_s, B_s > 0$. In the following lemma, for the sake of a neat notation, we identify $H^s_{\vec{\sigma}}(0,1)$ with its dual. But let us mention that the statement also holds true without an identification of the spaces.

Lemma 6.1. *The system*

$$\mathcal{F}_{H^s_i(\square)} := \left\{ w_{\lambda_i}^{-1} f_{\lambda_1} \otimes \cdots \otimes f_{\lambda_d} \right\}_{\boldsymbol{\lambda}\in\mathcal{J}^d}, \quad \boldsymbol{\lambda} = \{\lambda_1, \ldots, \lambda_d\},$$

is a frame for the tensor product Sobolev space $H^s_i(\square)$ with frame bounds $A_s A^{d-1}$ and $B_s B^{d-1}$, i.e.,

$$A_s A^{d-1} \|f\|^2_{H^s_i(\square)} \leq \sum_{\boldsymbol{\lambda}\in\mathcal{J}^d} \left| \langle f, w_{\lambda_i}^{-1} f_{\lambda_1} \otimes \cdots \otimes f_{\lambda_d} \rangle_{H^s_i(\square)} \right|^2 \leq B_s B^{d-1} \|f\|^2_{H^s_i(\square)}, \quad (6.1.10)$$

for all $f \in H^s_i(\square)$, cf. (2.1.6).

Proof. Without loss of generality, we may assume that $i = 1$. Moreover, it is sufficient to show (6.1.10) on a dense subset of $H^s_1(\square)$, cf. [24, Lemma 5.1.9] , e.g., for all finite sums of tensor product functions like

$$f = \sum_{k=1}^{K} g_k^{(1)} \otimes \cdots \otimes g_k^{(d)}, \quad g_k^{(j)} \in \begin{cases} H^s_{\vec{\sigma_1}}(0,1) & , \ j = 1, \\ L_2(0,1) & , \ 2 \leq j \leq d. \end{cases} \quad (6.1.11)$$

Assume that f has this form, and let $U = \{u_j\}_{j\in\mathbb{N}}$ and $V = \{v_j\}_{j\in\mathbb{N}}$ be orthonormal bases for $H^s(0,1)$ and $L_2(0,1)$, respectively. Then obviously, the system

$$\{u_{j_1} \otimes v_{j_2} \otimes \cdots \otimes v_{j_d}\}_{j_l\in\mathbb{N}, 1\leq l\leq d}$$

is an orthonormal basis for $H^s_1(\square)$. By consequence, an application of the Parseval identity in $H^s_1(\square)$ and in $H^s_{\vec{\sigma_1}}(0,1)$ yields

$$\begin{aligned} \|f\|^2_{H^s_1(\square)} &= \sum_{\substack{j_l\in\mathbb{N}\\1\leq l\leq d}} \left| \langle f, u_{j_1} \otimes v_{j_2} \otimes \cdots \otimes v_{j_d} \rangle_{H^s_1(\square)} \right|^2 \\ &= \sum_{\substack{j_l\in\mathbb{N}\\1\leq l\leq d}} \left| \sum_{k=1}^{K} \langle g_k^{(1)} \otimes \cdots \otimes g_k^{(d)}, u_{j_1} \otimes v_{j_2} \otimes \cdots\cdots \otimes v_{j_d} \rangle_{H^s_1(\square)} \right|^2 \\ &= \sum_{\substack{j_l\in\mathbb{N}\\1\leq l\leq d}} \left| \sum_{k=1}^{K} \langle g_k^{(1)}, u_{j_1} \rangle_{H^s_{\vec{\sigma_1}}(0,1)} \prod_{\nu=2}^{d} \langle g_k^{(\nu)}, v_{j_\nu} \rangle_{L_2(0,1)} \right|^2 \end{aligned}$$

$$= \sum_{\substack{j_l \in \mathbb{N} \\ 2 \le l \le d}} \sum_{j_1 \in \mathbb{N}} \left| \left\langle \sum_{k=1}^{K} \prod_{\nu=2}^{d} \langle g_k^{(\nu)}, v_{j_\nu} \rangle_{L_2(0,1)} g_k^{(1)}, u_{j_1} \right\rangle_{H^s_{\vec{\sigma}_1}(0,1)} \right|^2$$

$$= \sum_{\substack{j_l \in \mathbb{N} \\ 2 \le l \le d}} \left\| \sum_{k=1}^{K} \prod_{\nu=2}^{d} \langle g_k^{(\nu)}, v_{j_\nu} \rangle_{L_2(0,1)} g_k^{(1)} \right\|^2_{H^s_{\vec{\sigma}_1}(0,1)}.$$

The $H^s_{\vec{\sigma}_1}(0,1)$-norms can be estimated from above and from below by using the frame property of $\{w_{\lambda_1}^{-1} f_{\lambda_1}\}_{\lambda_1 \in \mathcal{J}}$ in $H^s_{\vec{\sigma}_1}(0,1)$, resulting in the auxiliary estimate

$$A_s \|f\|^2_{H^s_1(\square)} \le \sum_{\lambda_1 \in \mathcal{J}} w_{\lambda_1}^{-2} \sum_{\substack{j_l \in \mathbb{N} \\ 2 \le l \le d}} \left| \sum_{k=1}^{K} \langle g_k^{(1)}, f_{\lambda_1} \rangle_{H^s_{\vec{\sigma}_1}(0,1)} \prod_{\nu=2}^{d} \langle g_k^{(\nu)}, v_{j_\nu} \rangle_{L_2(0,1)} \right|^2 \le B_s \|f\|^2_{H^s_1(\square)}. \tag{6.1.12}$$

It remains to bound the middle sum in (6.1.12) from above and from below. For fixed $\lambda_1, \dots, \lambda_d \in \mathcal{J}$, we can transform

$$\sum_{k=1}^{K} \langle g_k^{(1)}, f_{\lambda_1} \rangle_{H^s_{\vec{\sigma}_1}(0,1)} \prod_{\nu=2}^{d} \langle g_k^{(\nu)}, v_{j_\nu} \rangle_{L_2(0,1)}$$
$$= \left\langle \sum_{k=1}^{K} \langle g_k^{(1)}, f_{\lambda_1} \rangle_{H^s_{\vec{\sigma}_1}(0,1)} \prod_{\nu=3}^{d} \langle g_k^{(\nu)}, v_{j_\nu} \rangle_{L_2(0,1)} g_k^{(2)}, v_{j_2} \right\rangle_{L_2(0,1)}.$$

By using the Parseval identity in $L_2(0,1)$, we deduce

$$\sum_{j_2 \in \mathcal{J}} \left| \sum_{k=1}^{K} \langle g_k^{(1)}, f_{\lambda_1} \rangle_{H^s_{\vec{\sigma}_1}(0,1)} \prod_{\nu=2}^{d} \langle g_k^{(\nu)}, v_{j_\nu} \rangle_{L_2(0,1)} \right|^2$$
$$= \left\| \sum_{k=1}^{K} \langle g_k^{(1)}, f_{\lambda_1} \rangle_{H^s_{\vec{\sigma}_1}(0,1)} \prod_{\nu=3}^{d} \langle g_k^{(\nu)}, v_{j_\nu} \rangle_{L_2(0,1)} g_k^{(2)} \right\|^2_{L_2(0,1)},$$

so that the frame property of $\mathcal{F}$ in $L_2(0,1)$ yields

$$A \sum_{j_2 \in \mathcal{J}} \left| \sum_{k=1}^{K} \langle g_k^{(1)}, f_{\lambda_1} \rangle_{H^s_{\vec{\sigma}_1}(0,1)} \prod_{\nu=2}^{d} \langle g_k^{(\nu)}, v_{j_\nu} \rangle_{L_2(0,1)} \right|^2$$
$$\le \sum_{\lambda_2 \in \mathcal{J}} \left| \left\langle \sum_{k=1}^{K} \langle g_k^{(1)}, f_{\lambda_1} \rangle_{H^s_{\vec{\sigma}_1}(0,1)} \prod_{\nu=3}^{d} \langle g_k^{(\nu)}, v_{j_\nu} \rangle_{L_2(0,1)} g_k^{(2)}, f_{\lambda_2} \right\rangle_{L_2(0,1)} \right|^2$$
$$\le B \sum_{j_2 \in \mathcal{J}} \left| \sum_{k=1}^{K} \langle g_k^{(1)}, f_{\lambda_1} \rangle_{H^s_{\vec{\sigma}_1}(0,1)} \prod_{\nu=2}^{d} \langle g_k^{(\nu)}, v_{j_\nu} \rangle_{L_2(0,1)} \right|^2.$$

In view of (6.1.12), this implies

$$A_s A\|f\|^2_{H^s_1(\square)} \leq \sum_{\lambda_1,\lambda_2\in\mathcal{J}} w^{-2}_{\lambda_1}$$
$$\cdot \sum_{\substack{j_l\in\mathbb{N}\\ 3\leq l\leq d}} \left| \sum_{k=1}^{K} \langle g^{(1)}_k, f_{\lambda_1}\rangle_{H^s_{\sigma_1}(0,1)} \langle g^{(2)}_k, f_{\lambda_2}\rangle_{L_2(0,1)} \prod_{\nu=3}^{d} \langle g^{(\nu)}_k, v_{j_\nu}\rangle_{L_2(0,1)} \right|^2$$
$$\leq B_s B\|f\|^2_{H^s_1(\square)}.$$

The claim (6.1.10) follows by repeating the aforementioned calculations and estimates in each of the remaining modes $3 \leq \nu \leq d$. □

Remark 6.2. By following the lines of the proof of Lemma 6.1, one can also show that the system $\mathcal{F}_{L_2(\square)} = \left\{f_{\lambda_1}\otimes\cdots\otimes f_{\lambda_d}\right\}_{\boldsymbol{\lambda}\in\mathcal{J}^d}$ is a frame for $L_2(\square)$ with frame bounds A^d, B^d.

Lemma 6.1 provides us with tensor frames for all the spaces $H^s_i(\square)$ defined in (6.1.9) as long as the required frames for $L_2(0,1)$ are available. It remains to check under which conditions the tensor frames also give rise to suitable systems in the intersection space $H^s_{\Gamma_{\boldsymbol{\sigma}}}(\square)$, cf. (6.1.8). Quite surprisingly, to perform our proof, it is not sufficient that the individual system possesses the frame property. In addition, each of the frames must contain a Riesz basis. Although this assumption is in a certain sense restrictive, let us already mention that it is satisfied in the case of quarklets since our quarklet frames by construction contain a wavelet Riesz basis.

Lemma 6.3. *Let $\mathcal{F}_{L_2(\square)} = \{\boldsymbol{f}_{\boldsymbol{\lambda}}\}_{\boldsymbol{\lambda}\in\mathcal{J}^d}$ be a frame for $L_2(\square)$ as in Remark 6.2 and for $i \in \{1,\dots,d\}$ and some non-zero scalars w_{λ_i}, $\boldsymbol{\lambda} = (\lambda_1,\dots,\lambda_d) \in \mathcal{J}^d$, the sets $\mathcal{F}_{H^s_i(\square)} = \{(w_{\lambda_i})^{-1}\boldsymbol{f}_{\boldsymbol{\lambda}}\}_{\boldsymbol{\lambda}\in\mathcal{J}^d}$ form frames for $H^s_i(\square) \subset L_2(\square)$ as in Lemma 6.1. Furthermore, we assume that there exists a Riesz basis $\mathcal{R}_{L_2(\square)} := \{\boldsymbol{f}_{\boldsymbol{\lambda}}\}_{\boldsymbol{\lambda}\in\mathcal{J}^d_{\mathcal{R}}} \subset \mathcal{F}_{L_2(\square)}$ for $L_2(\square)$ such that the sets $\mathcal{R}_{H^s_i(\square)} := \{w^{-1}_{\lambda_i}\boldsymbol{f}_{\boldsymbol{\lambda}}\}_{\boldsymbol{\lambda}\in\mathcal{J}^d_{\mathcal{R}}}$ form Riesz bases for $H^s_i(\square)$. Then, the collection*

$$\left\{\left(\sum_{i=1}^{d} w^2_{\lambda_i}\right)^{-1/2} \boldsymbol{f}_{\boldsymbol{\lambda}}\right\}_{\boldsymbol{\lambda}\in\mathcal{J}^d}$$

is a frame for $H^s_{\Gamma_{\boldsymbol{\sigma}}}(\square)$.

Proof. It is sufficient to prove the lemma for the case $d = 2$. Then, the general result follows by induction. Let $\boldsymbol{f} \in H^s_1(\square)\cap H^s_2(\square)$. Since $\mathcal{R}_{L_2(\square)}$ is a Riesz basis for $L_2(\square)$ we have a unique representation $\boldsymbol{f} = \sum_{\boldsymbol{\lambda}\in\mathcal{J}^2_{\mathcal{R}}} \hat{c}_{\boldsymbol{\lambda}}\boldsymbol{f}_{\boldsymbol{\lambda}}$. Let B_i, $i \in \{1,2\}$ be the optimal upper frame bounds and $B_{\max} := \max\{B_1, B_2\}$. Then, the frame property of $\mathcal{F}_{H^s_i(\square)}$ in $H^s_i(\square)$ implies

$$B^{-1}_{\max}\,\|\boldsymbol{f}\|^2_{H^s_i(\square)} \leq B^{-1}_i\,\|\boldsymbol{f}\|^2_{H_i} \leq \inf_{\boldsymbol{c}^{(i)}\in\ell_2(\mathcal{J}^2):(\boldsymbol{c}^{(i)})^T\mathcal{F}_H=\boldsymbol{f}} \sum_{\boldsymbol{\lambda}\in\mathcal{J}^2} w^2_{\lambda_i}(c^{(i)}_{\boldsymbol{\lambda}})^2. \tag{6.1.13}$$

The definition of $\|\cdot\|_{H_1^s(\square)\cap H_2^s(\square)}$, cf. (6.1.6), and (6.1.13) lead to

$$\begin{aligned} B_{\max}^{-1} \|\boldsymbol{f}\|^2_{H_1^s(\square)\cap H_2^s(\square)} &\leq \inf_{(\boldsymbol{c}^{(1)},\boldsymbol{c}^{(2)})\in(\ell_2(\mathcal{J}^2))^2:(\boldsymbol{c}^{(i)})^T\mathcal{F}_{L_2(\square)}=\boldsymbol{f}} \sum_{\boldsymbol{\lambda}\in\mathcal{J}^2} w_{\lambda_1}^2 (c_{\boldsymbol{\lambda}}^{(1)})^2 + w_{\lambda_2}^2 (c_{\boldsymbol{\lambda}}^{(2)})^2 \\ &\leq \inf_{\boldsymbol{c}\in\ell_2(\mathcal{J}^2):\boldsymbol{c}^T\mathcal{F}_{L_2(\square)}=\boldsymbol{f}} \sum_{\boldsymbol{\lambda}\in\mathcal{J}^2} \left(w_{\lambda_1}^2 + w_{\lambda_2}^2\right) c_{\boldsymbol{\lambda}}^2, \end{aligned} \tag{6.1.14}$$

showing the lower frame inequality, cf. Proposition 2.3. Let $A_i^{\mathcal{R}}$, $i \in \{1,2\}$ be the optimal lower Riesz bounds and $A_{\min}^{\mathcal{R}} = \min\{A_1^{\mathcal{R}}, A_2^{\mathcal{R}}\}$. For the upper frame inequality we use the unique representation and the Riesz basis properties of $\mathcal{R}_{H_i^s(\square)}$ in $H_i^s(\square)$, $i \in \{1,2\}$ to estimate

$$\begin{aligned} \inf_{\boldsymbol{c}\in\ell_2(\mathcal{J}^2):\boldsymbol{c}^T\mathcal{F}_{L_2(\square)}=\boldsymbol{f}} \sum_{\boldsymbol{\lambda}\in\mathcal{J}^2} \left(w_{\lambda_1}^2 + w_{\lambda_2}^2\right) c_{\boldsymbol{\lambda}}^2 &\leq \sum_{\boldsymbol{\lambda}\in\mathcal{J}^2_{\mathcal{R}}} \left(w_{\lambda_1}^2 + w_{\lambda_2}^2\right) \hat{c}_{\boldsymbol{\lambda}}^2 \\ &= \sum_{\boldsymbol{\lambda}\in\mathcal{J}^2_{\mathcal{R}}} w_{\lambda_1}^2 \hat{c}_{\boldsymbol{\lambda}}^2 + \sum_{\boldsymbol{\lambda}\in\mathcal{J}^2_{\mathcal{R}}} w_{\lambda_2}^2 \hat{c}_{\boldsymbol{\lambda}}^2 \\ &\leq (A_1^{\mathcal{R}})^{-1} \|\boldsymbol{f}\|^2_{H_1^s(\square)} + (A_2^{\mathcal{R}})^{-1} \|\boldsymbol{f}\|^2_{H_2^s(\square)} \\ &\leq (A_{\min}^{\mathcal{R}})^{-1} \|\boldsymbol{f}\|^2_{H_1^s(\square)\cap H_2^s(\square)}. \end{aligned} \tag{6.1.15}$$

Combining (6.1.14) and (6.1.15) proves the claim. □

Remark 6.4. From the proof of Lemma 6.3 frame bounds can be easily deduced. An upper frame bound is given by the maximum of all upper frame bounds of the frames $\mathcal{F}_{H_i^s(\square)}$. A lower frame bound is given by the minimum of all lower Riesz bounds of the Riesz bases $\mathcal{R}_{H_i^s(\square)}$.

6.1.3 Quarklet frames on the unit cube

An application of Remark 6.2 and Theorem 5.8 yields the following theorem, which is one of the main results of this thesis.

Theorem 6.5. *Let $\{\Psi_{\lambda_i}^{\vec{\sigma_i}}\}, i = 1,\dots,d$, be a family of univariate boundary adapted quarklet frames of order $m \geq 2$, with $\tilde{m}$ vanishing moments, $\tilde{m} \geq m$, according to Theorem 5.8. Then the family*

$$\boldsymbol{\Psi}_{L_2(\square),\boldsymbol{\sigma}} := \bigotimes_{i=1}^d \Psi_{L_2(0,1),\vec{\sigma_i}} = \left\{ (w_{\boldsymbol{\lambda}}^{L_2})^{-1} \boldsymbol{\psi}_{\boldsymbol{\lambda}}^{\boldsymbol{\sigma}} : \boldsymbol{\lambda} \in \boldsymbol{\nabla}_{\boldsymbol{\sigma}} := \prod_{i=1}^d \nabla_{\vec{\sigma_i}} \right\}, \tag{6.1.16}$$

$$\boldsymbol{\psi}_{\boldsymbol{\lambda}}^{\boldsymbol{\sigma}} := \bigotimes_{i=1}^d \psi_{\lambda_i}^{\vec{\sigma_i}}, \tag{6.1.17}$$

with the weights

$$w_{\boldsymbol{\lambda}}^{L_2} := \prod_{i=1}^d (p_i+1)^{\delta_1/2}, \quad \delta_1 > 0, \tag{6.1.18}$$

is a quarkonial tensor frame for $L_2(\square)$.

By means of Lemma 6.1, Lemma 6.3 and Theorem 5.9 we also obtain quarkonial frames for the Sobolev space $H^s_{\Gamma_{\boldsymbol{\sigma}}}(\square)$, which is another main result.

Theorem 6.6. *Let* $\{\Psi^{\vec{\sigma_i}}_{\lambda_i}\}, i = 1, \ldots, d$*, be a family of univariate boundary adapted quarklet frames according to Theorem 5.8, with order* $m \geq 2$*,* $\tilde{m} \geq 2$ *vanishing moments,* $\frac{\tilde{m}}{m}$ *sufficiently large and* $\tilde{m} + m$ *even. Then, the family*

$$\boldsymbol{\Psi}_{H^s_{\Gamma_{\boldsymbol{\sigma}}}(\square)} := \left\{ (w^{H^s}_{\boldsymbol{\lambda}})^{-1} \boldsymbol{\psi}^{\boldsymbol{\sigma}}_{\boldsymbol{\lambda}} : \boldsymbol{\lambda} \in \boldsymbol{\nabla}_{\boldsymbol{\sigma}} \right\}, \tag{6.1.19}$$

with the weights

$$w^{H^s}_{\boldsymbol{\lambda}} := \left(\sum_{i=1}^{d} (p_i + 1)^{4s+\delta_2} \, 4^{sj_i} \right)^{1/2} \prod_{i=1}^{d} (p_i + 1)^{\delta_1/2}, \quad \boldsymbol{\lambda} = (\boldsymbol{p}, \boldsymbol{j}, \boldsymbol{k}), \delta_1 > 0,\ \delta_2 > 1, \tag{6.1.20}$$

is a frame for $H^s_{\Gamma_{\boldsymbol{\sigma}}}(\square)$*,* $0 \leq s < m - \frac{1}{2}$*,* $s \notin (\mathbb{N}_0 + \{\frac{1}{2}\})$*.*

Examples of quarks and quarklets on the unit cube are visualized in Figures 6.1, 6.2, respectively.

Remark 6.7. Let us also introduce the notation

$$\boldsymbol{\Psi}^B_{L_2(\square),\boldsymbol{\sigma}} := \bigotimes_{i=1}^{d} \Psi^B_{L_2(0,1),\vec{\sigma_i}} = \left\{ \boldsymbol{\psi}^{\boldsymbol{\sigma}}_{\boldsymbol{\lambda}} : \boldsymbol{\lambda} \in \boldsymbol{\nabla}^B_{\boldsymbol{\sigma}} := \prod_{i=1}^{d} \nabla^B_{\vec{\sigma_i}} \right\} \tag{6.1.21}$$

for the $L_2(\square)$ Riesz basis. Accordingly,

$$\boldsymbol{\Psi}^B_{H^s_{\Gamma_{\boldsymbol{\sigma}}}(\square)} := \left\{ \left(\sum_{i=1}^{d} 4^{sj_i} \right)^{-1/2} \boldsymbol{\psi}^{\boldsymbol{\sigma}}_{\boldsymbol{\lambda}} : \boldsymbol{\lambda} \in \boldsymbol{\nabla}^B_{\boldsymbol{\sigma}} \right\} \tag{6.1.22}$$

denotes a Riesz basis for $H^s_{\Gamma_{\boldsymbol{\sigma}}}(\square)$.

$$\boldsymbol{p} = (1,1),\ \boldsymbol{j} = (2,2),\ \boldsymbol{k} = (1,2)$$

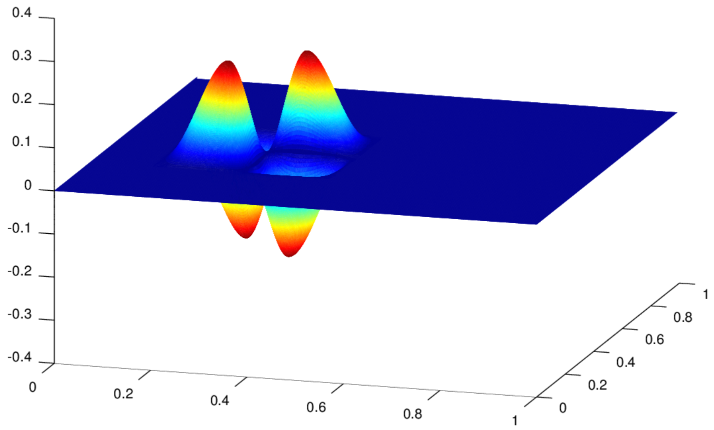

$$\boldsymbol{p} = (2,1),\ \boldsymbol{j} = (2,2),\ \boldsymbol{k} = (1,2)$$

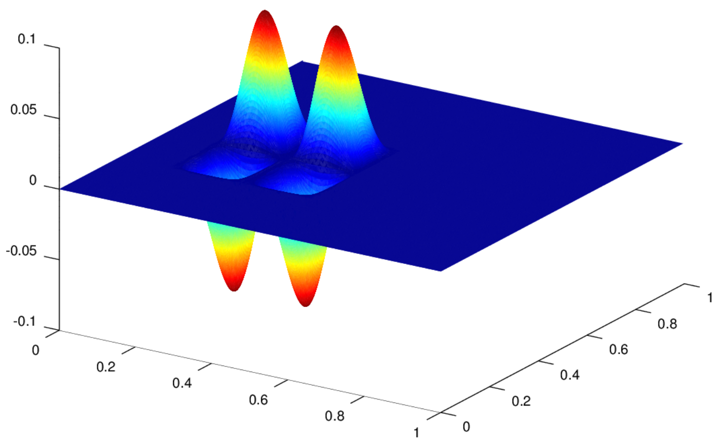

Figure 6.1: Unweighted quarks $\boldsymbol{\psi}_{\lambda}^{\sigma}$ on the two-dimensional unit cube.

$$\boldsymbol{p} = (1,1),\ \boldsymbol{j} = (3,3),\ \boldsymbol{k} = (4,3)$$

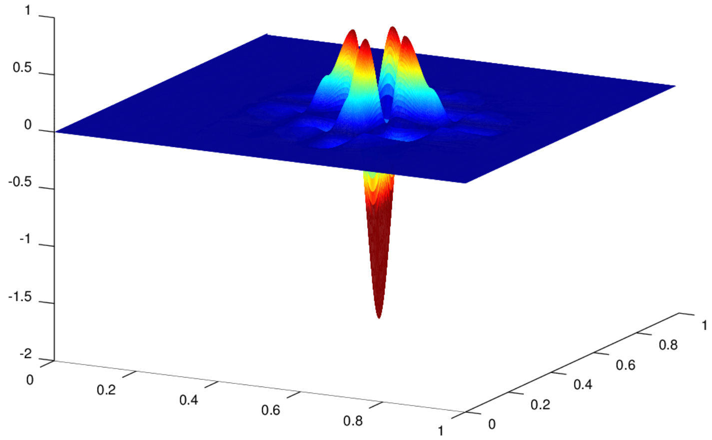

$$\boldsymbol{p} = (1,2),\ \boldsymbol{j} = (3,2),\ \boldsymbol{k} = (5,1)$$

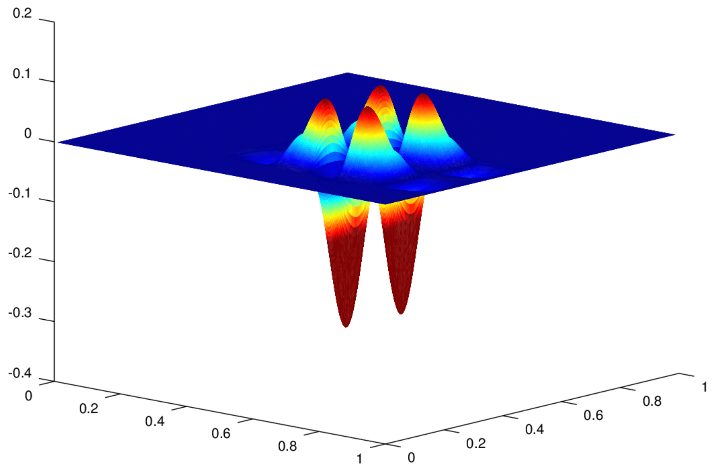

Figure 6.2: Unweighted quarklets $\boldsymbol{\psi}_\lambda^{\boldsymbol{\sigma}}$ on the two-dimensional unit cube.

6.2 From cubes to general bounded domains

In this section, we explain how to use a non-overlapping domain decomposition approach to extend frames from cubes to general bounded domains. Thereupon, we apply the extension to the quarklet frames on cubes from the previous section. In comparison to the non-overlapping extension of Riesz bases, see, e.g., [20], several adaptations have to be made.

6.2.1 The abstract extension process

In this subsection, we collect the basic tools which are needed to extend function systems on cubes to general domains. Further information can be found in [20]. This approach can be used as a starting point of the frame construction on general domains. The final quarklet construction can be found in Subsection 6.2.3.

Let us first describe the types of domains we are concerned with in the sequel. Let $\{\square_0, \dots, \square_N\}$ with $\square_j := \tau_j + \square$, $\tau_j \in \mathbb{Z}^d$, $j = 0, \dots, N$ be a fixed finite set of hypercubes. We assume $\cup_{j=0}^N \square_j \subset \Omega \subset (\cup_{j=0}^N \overline{\square}_j)^{\text{int}}$ and such that $\partial\Omega$ is a union of (closed) facets of the $\square_j$'s. The situation $\Omega \subsetneq (\cup_{j=0}^N \overline{\square}_j)^{\text{int}}$ occurs if Ω has one or more cracks, cf. Figure 6.3.

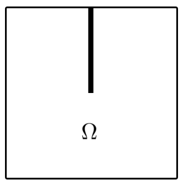

Figure 6.3: The slitdomain is a typical example where $\Omega = (-1,1)^2 \setminus \{0\} \times (0,1)$ is a strict subdomain of $(\cup_{j=0}^3 \overline{\square}_j)^{\text{int}} = (-1,1)^2$.

Later on, we present a construction procedure of frames for Sobolev spaces on Ω that starts with frames for corresponding Sobolev spaces on the subdomains $\square_j$ and makes use of extension operators. These extension operators form a crucial ingredient in the final construction, see again Subsection 6.2.3. The following conditions $(\mathcal{D}_1)$-$(\mathcal{D}_5)$ are taken from [20] and ensure the existence of suitable extension operators.

We set $\Omega_i^{(0)} := \square_i$, $i = 0, \dots, N$ and create a sequence $\{\Omega_i^{(q)} : q \le i \le N\}_{0 \le q \le N}$ of sets of polytopes, where each next entry in this sequence is created by joining two polytopes from the previous entry whose joint interface is part of a hyperplane. More precisely, we assume that for any $1 \le q \le N$, there exists a $q \le \bar{i} = \bar{i}^{(q)} \le N$ and $q - 1 \le i_1 = i_1^{(q)} \ne i_2 = i_2^{(q)} \le N$ such that

$(\mathcal{D}_1)$ $\Omega_{\bar{i}}^{(q)} = \left(\overline{\Omega_{i_1}^{(q-1)} \cup \Omega_{i_2}^{(q-1)}} \setminus \partial\Omega\right)^{\text{int}}$ is connected, and the interface $J := \Omega_{\bar{i}}^{(q)} \setminus (\Omega_{i_1}^{(q-1)} \cup \Omega_{i_2}^{(q-1)})$ is part of a hyperplane,

$(\mathcal{D}_2)$ $\{\Omega_i^{(q)} : q \le i \le N, i \ne \bar{i}\} = \left\{\Omega_i^{(q-1)} : q - 1 \le i \le N, i \ne \{i_1, i_2\}\right\}$,

($\mathcal{D}_3$) $\Omega_N^{(N)} = \Omega$.

By construction, the boundary of each $\Omega_i^{(q)}$ is a union of facets of hypercubes $\square_j$. We define $\mathring{H}^s(\Omega_i^{(q)})$ to be the closure in $H^s(\Omega_i^{(q)})$ of the smooth functions on $\Omega_i^{(q)}$ that vanish on the union of the facets of the $\square_j$ on which homogeneous Dirichlet boundary conditions are imposed, and that are part of $\partial\Omega_i^{(q)}$. Note that $\mathring{H}^s(\Omega_N^{(N)}) = H_0^s(\Omega)$ and for some $\boldsymbol{\sigma}(j) \in (\{0, \lfloor s+1/2 \rfloor\}^2)^d$,

$$\mathring{H}^s(\Omega_j^{(0)}) = \mathring{H}^s(\square_j) = H^s_{\Gamma_{\boldsymbol{\sigma}(j)}}(\square_j).$$

The boundary conditions on the hypercubes that determine the spaces $\mathring{H}^s(\Omega_i^{(q)})$, and the order in which polytopes are joined should be chosen such that

($\mathcal{D}_4$) on the $\Omega_{i_1}^{(q-1)}$ and $\Omega_{i_2}^{(q-1)}$ sides of J, the boundary conditions are of order 0 and $\lfloor s + \frac{1}{2} \rfloor$, respectively,

and, w.l.o.g. assuming that $J = \{0\} \times \breve{J}$ and $(0,1) \times \breve{J} \subset \Omega_{i_1}^{(q-1)}$,

($\mathcal{D}_5$) for any function in $\mathring{H}^s(\Omega_{i_1}^{(q-1)})$ that vanishes near $\{0,1\} \times \breve{J}$, its reflection in $\{0\} \times \mathbb{R}^{d-1}$ (extended with zero, and then restricted to $\Omega_{i_2}^{(q-1)}$) is in $\mathring{H}^s(\Omega_{i_2}^{(q-1)})$.

The condition ($\mathcal{D}_5$) can be formulated by saying that the order of the boundary condition at any subfacet of $\Omega_{i_1}^{(q-1)}$ adjacent to J should not be less than this order at its reflection in J, where in case this reflection is not part of $\partial\Omega_{i_2}^{(q-1)}$, the latter order should be read as the highest possible one $\lfloor s + \frac{1}{2} \rfloor$; and furthermore, that the order of the boundary condition at any subfacet of $\Omega_{i_2}^{(q-1)}$ adjacent to J should not be larger than this order at its reflection in J, where in case this reflection is not part of $\partial\Omega_{i_1}^{(q-1)}$, the latter order should be read as the lowest possible one 0. In the Figures 6.4 and 6.5 we see illustrations, where the conditions ($\mathcal{D}_1$)-($\mathcal{D}_5$) are fulfilled.

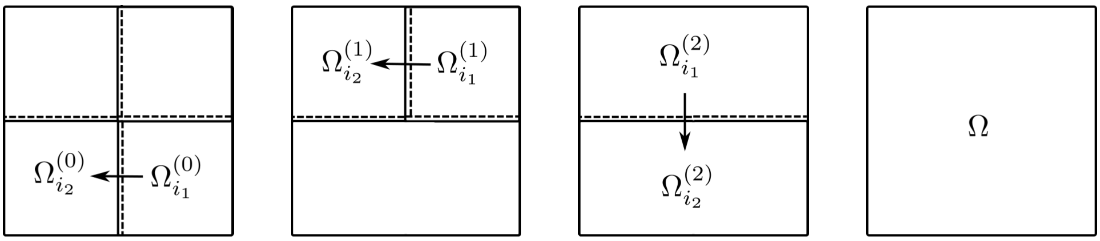

Figure 6.4: First example of a domain decomposition such that ($\mathcal{D}_1$)-($\mathcal{D}_5$) are fulfilled. The arrows indicate the direction of the non-trivial extension. Dotted lines and solid lines indicate free and zero boundary conditions, respectively.

Given $1 \le q \le N$, for $l \in \{1,2\}$, let $R_l^{(q)}$ be the *restriction* of functions on $\Omega_{\bar{i}}^{(q)}$ to $\Omega_{i_l}^{(q-1)}$, let $\eta_2^{(q)}$ be the *extension* of functions on $\Omega_{i_2}^{(q-1)}$ to $\Omega_{\bar{i}}^{(q)}$ by zero, and let $E_1^{(q)}$ be some non-trivial *extension* of functions on $\Omega_{i_1}^{(q-1)}$ to $\Omega_{\bar{i}}^{(q)}$.

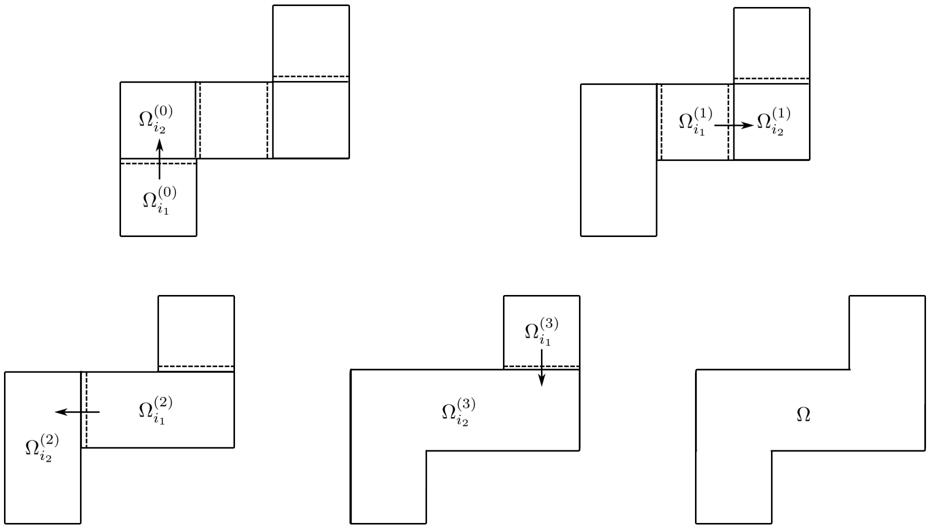

Figure 6.5: Second example of a domain decomposition such that $(\mathcal{D}_1)$-$(\mathcal{D}_5)$ are fulfilled. The arrows indicate the direction of the non-trivial extension. Dotted lines and solid lines indicate free and zero boundary conditions, respectively.

Roughly speaking, in every step of our construction we glue together two adjacent domains. One ingredient in such a step is a bijective operator between Sobolev spaces on those domains. In the following proposition, which is taken from [20, Proposition 2.1], we consider a more general framework and give conditions under which a class of mappings between a Banach space and the Cartesian product of two other Banach spaces consists of isomorphisms. In Proposition 6.9, cf. [20, Proposition 4.2], we apply these statements to our special case.

Proposition 6.8. *For normed linear spaces V and V_i ($i = 1, 2$), let $E_1 \in B(V_1, V)$, $\eta_2 \in B(V_2, V)$, $R_1 \in B(V, V_1)$, and $R_2 \in B(\mathrm{ran}(\eta_2), V_2)$ be such that*

$$R_1 E_1 = \mathrm{Id}, \quad R_2 \eta_2 = \mathrm{Id}, \quad R_1 \eta_2 = 0, \quad \mathrm{ran}(\mathrm{Id} - E_1 R_1) \subset \mathrm{ran}(\eta_2).$$

Then, the operator

$$E = [E_1 \quad \eta_2] \in B(V_1 \times V_2, V)$$

is boundedly invertible, with inverse

$$E^{-1} = \begin{bmatrix} R_1 \\ R_2(\mathrm{Id} - E_1 R_1) \end{bmatrix}.$$

Proposition 6.9. *For $s > 0$, assume that $E_1^{(q)} \in B\left(\mathring{H}^s(\Omega_{i_1}^{(q-1)}), \mathring{H}^s(\Omega_{\bar{i}}^{(q)})\right)$. Then,*

$$E^{(q)} := [E_1^{(q)} \quad \eta_2^{(q)}] \in B\Big(\prod_{l=1}^{2} \mathring{H}^s(\Omega_{i_l}^{(q-1)}), \mathring{H}^s(\Omega_{\bar{i}}^{(q)})\Big)$$

is boundedly invertible.

Proof. This is a direct application of Proposition 6.8 with $V_1 = \mathring{H}^s(\Omega_{i_1}^{(q-1)})$, $V_2 = \mathring{H}^s(\Omega_{i_2}^{(q-1)})$, $V = \mathring{H}^s(\Omega_{\bar{i}}^{(q)})$, $E_1 = E_1^{(q)}$, $\eta_2 = \eta_2^{(q)}$ and $R_l = R_l^{(q)}$, for $l \in \{1, 2\}$. $\square$

Sequential execution of extensions as in Proposition 6.9 induces an isomorphism from the Cartesian product of Sobolev spaces on the cubes $\square_j$ onto the Sobolev spaces on the target domain Ω.

Corollary 6.10. *For U being the composition of the mappings $E^{(q)}$, $q = 1, \ldots, N$, from Proposition 6.9, trivially extended with identity operators in coordinates $i \in \{q-1, \ldots, N\} \setminus \{i_1^{(q)}, i_2^{(q)}\}$, it holds that*

$$U \in B\Big(\prod_{j=0}^{N} \mathring{H}^s(\square_j), H_0^s(\Omega)\Big). \tag{6.2.1}$$

is boundedly invertible.

Remark 6.11. If we apply U to Riesz bases on cubes $\square_j$, we end up with a Riesz basis on Ω. While this is also true for the case of frames, the way for the construction of frames in this thesis is slightly different, mainly to preserve the vanishing moments of the frames on cubes. Nevertheless, the operators $E^{(q)}$ as defined in Proposition 6.9 play an important role in the construction process.

The next proposition provides the link between the extension approach and tensor products. It states that under the conditions $(\mathcal{D}_1)$-$(\mathcal{D}_5)$, the extensions $E_1^{(q)}$ can be constructed (essentially) as tensor products of *univariate extensions* with identity operators in the other Cartesian directions.

Proposition 6.12. *In the setting of $(\mathcal{D}_1)$, w.l.o.g. let $J = \{0\} \times \check{J}$ and $(0,1) \times \check{J} \subset \Omega_{i_1}^{(q-1)}$. Let G_1 be an* extension *operator of functions on $(0,1)$ to functions on $(-1,1)$ such that*

$$G_1 \in B\left(L_2(0,1), L_2(-1,1)\right), \quad G_1 \in B\left(H^s(0,1), H^s_{(\lfloor s+\frac{1}{2}\rfloor,0)}(-1,1)\right).$$

Let $T^{(q)} \in B\left(\mathring{H}^s(\Omega_{i_1}^{(q-1)}), \mathring{H}^s(\Omega_{i_2}^{(q-1)})\right)$ be defined as the composition of the restriction to $(0,1) \times \check{J}$, followed by an application of

$$G_1 \otimes \mathrm{Id} \otimes \cdots \otimes \mathrm{Id},$$

an extension by 0 to $\Omega_{i_2}^{(q-1)} \setminus (-1,0) \times \check{J}$ and a restriction to $\Omega_{i_2}^{(q-1)}$. Then, we define $E_1^{(q)} \in B\left(\mathring{H}^s(\Omega_{i_1}^{(q-1)}), \mathring{H}^s(\Omega_{\bar{i}}^{(q)})\right)$ as the operator which is the identity operator if restricted to $\mathring{H}^s(\Omega_{i_1}^{(q-1)})$ and $T^{(q)}$ if restricted to $\mathring{H}^s(\Omega_{i_2}^{(q-1)})$. By proceeding this way, $E_1^{(q)}$ is well-defined and boundedly invertible as required in Proposition 6.9.

6.2.2 Construction of frames by extension

Based on the setting outlined in the previous subsection, we now describe a general procedure to construct frames for the Sobolev space $H_0^s(\Omega)$, provided that suitable frames and Riesz bases, respectively, on the cubes $\square_j$ are given. That such frames and Riesz bases on cubes are available in the quarklet setting has already been shown in Section 6.1. A combination of the results of Subsections 6.2.1, 6.2.2 and Section 6.1 provides us with the desired quarklet frames on general domains Ω, cf. Subsection 6.2.3.

For $j = 0, \ldots, N$, let $\boldsymbol{\mathcal{F}}_j$ be a frame for $L_2(\square_j)$, that renormalized in $H^s(\square_j)$, is a frame for $\mathring{H}^s(\square_j)$. Furthermore, assume that there exists a Riesz basis $\boldsymbol{\mathcal{R}}_j \subset \boldsymbol{\mathcal{F}}_j$ for $L_2(\square_j)$, that renormalized in $H^s(\square_j)$, is a Riesz basis for $\mathring{H}^s(\square_j)$. Renormalized versions of all sets are indicated with an upper $s \geq 0$ with the conventions $\boldsymbol{\mathcal{R}}_j^s := \boldsymbol{\mathcal{R}}_j$, $\boldsymbol{\mathcal{F}}_j^s := \boldsymbol{\mathcal{F}}_j$ for $s = 0$. For $q = 0, \ldots, N$, $i = q, \ldots, N$ and $s \geq 0$ we define recursively

$$\boldsymbol{\mathcal{R}}_i^{s,(q)} := \begin{cases} \boldsymbol{\mathcal{R}}_i^s, & q = 0, \\ \boldsymbol{\mathcal{R}}_{\hat{i}}^{s,(q-1)}, & 1 \leq q \leq N,\ i \neq \bar{i},\ \Omega_i^{(q)} = \Omega_{\hat{i}}^{(q-1)}, \\ E_1^{(q)}(\boldsymbol{\mathcal{R}}_{i_1}^{s,(q-1)}) \cup \eta_2^{(q)}(\boldsymbol{\mathcal{R}}_{i_2}^{s,(q-1)}), & 1 \leq q \leq N,\ i = \bar{i}, \end{cases} \tag{6.2.2}$$

with $E_1^{(q)}$ defined as in Proposition 6.12. We observe that the set of functions $\boldsymbol{\mathcal{R}}_N^{s,(N)}$ is exactly $U(\boldsymbol{\mathcal{R}}_0^s, \ldots, \boldsymbol{\mathcal{R}}_N^s)$, with U defined as in Corollary 6.10. Thus, it is a Riesz basis for $H_0^s(\Omega)$, cf. Proposition 2.14 (iii). For the frame construction, we have to assume the existence of an additional family $\Xi^{s,(q)}$ which forms a Bessel system for $\mathring{H}^s(\Omega_i^{(q)})$, cf. (2.1.1), and satisfies $E_i^{(q)}(\boldsymbol{\mathcal{R}}_i^{s,(q-1)}) \subset \Xi^{s,(q)}$. Then, for $q = 0, \ldots, N$, $i = q, \ldots, N$ and $s \geq 0$ we set

$$\boldsymbol{\mathcal{F}}_i^{s,(q)} := \begin{cases} \boldsymbol{\mathcal{F}}_i^s, & q = 0, \\ \boldsymbol{\mathcal{F}}_{\hat{i}}^{s,(q-1)}, & 1 \leq q \leq N,\ i \neq \bar{i},\ \Omega_i^{(q)} = \Omega_{\hat{i}}^{(q-1)}, \\ \Xi^{s,(q)} \cup \eta_2^{(q)}(\boldsymbol{\mathcal{F}}_{i_2}^{s,(q-1)}), & 1 \leq q \leq N, i = \bar{i}. \end{cases} \tag{6.2.3}$$

The next proposition implies that, by proceeding this way, we indeed obtain suitable frames for $H_0^s(\Omega)$. For the proof, we make use of some statements about function systems and operators from Section 2.3. Further information concerning the additional Bessel system as well as construction details can be found in Subsection 6.2.3, Remark 6.16.

Proposition 6.13. *For $q = 0, \ldots, N$, $i = q, \ldots, N$ and $s > 0$, let $\boldsymbol{\mathcal{F}}_i^{s,(q)}$ be defined as in (6.2.3). Then, $\boldsymbol{\mathcal{F}}^s := \boldsymbol{\mathcal{F}}_N^{s,(N)}$, is a frame for $H_0^s(\Omega)$.*

Proof. Let $1 \leq q \leq N$. Since $\boldsymbol{\mathcal{F}}_{i_2}^{s,(q-1)}$ is a Bessel system for $\mathring{H}^s(\Omega_{i_2}^{(q-1)})$ and $\eta_2^{(q)} \in B\left(\mathring{H}^s(\Omega_{i_2}^{(q-1)}), \mathring{H}^s(\Omega_{\bar{i}}^{(q)})\right)$, we can conclude that $\eta_2^{(q)}(\boldsymbol{\mathcal{F}}_{i_2}^{s,(q-1)})$ is a Bessel system for $\mathring{H}^s(\Omega_{\bar{i}}^{(q)})$, cf. Proposition 2.14 (i). Hence, $\boldsymbol{\mathcal{F}}_{\bar{i}}^{s,(q)} = \Xi^{s,(q)} \cup \eta_2^{(q)}(\boldsymbol{\mathcal{F}}_{i_2}^{s,(q-1)})$ is a union of two Bessel systems and therefore a Bessel system for $\mathring{H}^s(\Omega_{\bar{i}}^{(q)})$, cf. Proposition 2.13 (i).

Since $E_1^{(q)}(\boldsymbol{\mathcal{R}}_{i_1}^{s,(q-1)}) \subset \Xi^{s,(q)}$ and $\boldsymbol{\mathcal{R}}_{i_2}^{s,(q-1)} \subset \boldsymbol{\mathcal{F}}_{i_2}^{s,(q-1)}$, we conclude that $\boldsymbol{\mathcal{R}}_{\bar{i}}^{s,(q)} \subset \boldsymbol{\mathcal{F}}_{\bar{i}}^{s,(q)}$. For $0 \leq i \leq N$, $\boldsymbol{\mathcal{R}}_i^{s,(0)}$ is a Riesz basis for $\mathring{H}^s(\Omega_i^{(0)})$. Furthermore $E^{(q)} = [E_1^{(q)} \quad \eta_2^{(q)}] \in B\Big(\prod_{l=1}^2 \mathring{H}^s(\Omega_{i_l}^{(q-1)}), \mathring{H}^s(\Omega_{\bar{i}}^{(q)})\Big)$ as defined in Proposition 6.9 is boundedly invertible. Thus, we conclude by induction that $\boldsymbol{\mathcal{R}}_{\bar{i}}^{s,(q)} = E^{(q)}(\boldsymbol{\mathcal{R}}_{i_1}^{s,(q-1)}, \boldsymbol{\mathcal{R}}_{i_2}^{s,(q-1)})$ is a Riesz basis for $\mathring{H}^s(\Omega_{\bar{i}}^{(q)})$, cf. Proposition 2.14 (iii) . Hence, $\boldsymbol{\mathcal{F}}_{\bar{i}}^{s,(q)}$ as a Bessel system which contains a Riesz basis is a frame for $\mathring{H}^s(\Omega_{\bar{i}}^{(q)})$, cf. Proposition 2.13 (iii). Especially $\boldsymbol{\mathcal{F}}^s = \boldsymbol{\mathcal{F}}_N^{s,(N)}$ is a frame for $H_0^s(\Omega) = \mathring{H}^s(\Omega_N^{(N)})$. □

6.2.3 Application to the quarklet case

Now, we want to apply the general machinery as outlined in the previous subsections to the quarklet frames on cubes as constructed in Section 6.1. In order to do this, two basic ingredients have to be provided: suitable one dimensional extension operators G_1, cf. Proposition 6.12 that induce the multidimensional extension operators $E_1^{(q)}$, and the additional Bessel systems $\Xi^{s,(q)}$, cf. (6.2.3). In particular, this has to be done in a way that characteristic properties of quarklets like vanishing moments and locality are preserved.

Construction of scale-dependent extension operators

In this part, we repeat the construction of a scale-dependent extension operator as outlined in [20, Subsection 5.1]. Although it does not play a role in the practical application in PDEs, we do cover the dual side since it is of theoretical interest for the study of convergence rates, whose verification is one of the mid to long term goals of the quarklet approach.

For $\vec{\sigma} = (\sigma_0, \sigma_1) \in \{0, \lfloor s + 1/2 \rfloor\}^2$, $s \in [0, m - \frac{1}{2}) \setminus (\mathbb{N}_0 + \{\frac{1}{2}\})$, let us recall from Section 3.2 the pair of dual one-dimensional Primbs wavelet Riesz bases for $L_2(0,1)$

$$\Psi^B_{L_2(0,1),\vec{\sigma}} = \{\psi_\lambda^{\vec{\sigma}} : \lambda \in \nabla_{\vec{\sigma}}^B\}, \quad \tilde{\Psi}^B_{L_2(0,1),\vec{\sigma}} = \{\tilde{\psi}_\lambda^{\vec{\sigma}} : \lambda \in \nabla_{\vec{\sigma}}^B\},$$

where $\tilde{\Psi}^B_{L_2(0,1),\vec{\sigma}}$ is the dual Riesz basis with complementary boundary conditions, cf. Remark 3.15. There exists an $\tilde{s} \in [0, \infty) \setminus (\mathbb{N}_0 + \{\frac{1}{2}\})$ such that the following necessary technical properties are satisfied, cf. [20, Section 3,5]:

($\mathcal{W}_1$) $\{2^{-j\tilde{s}} \tilde{\psi}_\lambda^{\vec{\sigma}} : \lambda \in \nabla_{\vec{\sigma}}^B\}$ is a Riesz basis for $H^{\tilde{s}}(0,1)$, and for some $\mathbb{N} \ni k > s$,

($\mathcal{W}_2$) $|\langle \tilde{\psi}_\lambda^{\vec{\sigma}}, u \rangle_{L_2(0,1)}| \lesssim 2^{-jk} \|u\|_{H^k(\operatorname{supp} \tilde{\psi}_\lambda^{\vec{\sigma}})}$ $(u \in H^k(0,1) \cap H^s_{\vec{\sigma}}(0,1),\ \lambda \in \nabla_{\vec{\sigma}}^B)$,

($\mathcal{W}_3$) $$\begin{aligned} 1 > \rho \ :=& \ \sup_{\lambda \in \nabla_{\vec{\sigma}}^B} 2^j \max(\operatorname{diam} \operatorname{supp} \tilde{\psi}_\lambda^{\vec{\sigma}}, \operatorname{diam} \operatorname{supp} \psi_\lambda^{\vec{\sigma}}) \\ \eqsim& \ \inf_{\lambda \in \nabla_{\vec{\sigma}}^B} 2^j \max(\operatorname{diam} \operatorname{supp} \tilde{\psi}_\lambda^{\vec{\sigma}}, \operatorname{diam} \operatorname{supp} \psi_\lambda^{\vec{\sigma}}), \end{aligned}$$

($\mathcal{W}_4$) $\sup_{i,k \in \mathbb{N}_0} \#\{\lambda \in \nabla_{\vec{\sigma}}^B : j = i \wedge [k2^{-i}, (k+1)2^{-i}] \cap (\operatorname{supp} \tilde{\psi}_\lambda^{\vec{\sigma}} \cup \operatorname{supp} \psi_\lambda^{\vec{\sigma}}) \neq \emptyset\} < \infty$.

($\mathcal{W}_5$) $V_i^{\vec{\sigma}} := \operatorname{span}\{\psi_\lambda^{\vec{\sigma}} : \lambda \in \nabla_{\vec{\sigma}}^B, j \leq i\} = V_i^{\vec{0}} \cap H^s_{\vec{\sigma}}(0,1)$,

($\mathcal{W}_6$) $\nabla^B_{\vec\sigma}$ can be disjointedly decomposed into three sets $\nabla^{B,(L)}_{\sigma_0}$, $\nabla^{B,(I)}$, $\nabla^{B,(R)}_{\sigma_1,}$ such that

(i) $\sup_{\lambda\in\nabla^{B,(L)}_{\sigma_0},\, x\in\operatorname{supp}\psi^{\vec\sigma}_\lambda} 2^j|x| \lesssim \rho, \qquad \sup_{\lambda\in\nabla^{B,(R)}_{\sigma_1},\, x\in\operatorname{supp}\psi^{\vec\sigma}_\lambda} 2^j|1-x| \lesssim \rho,$

(ii) for $\lambda \in \nabla^{B,(I)}$, $\psi^{\vec\sigma}_\lambda = \psi^{\vec 0}_\lambda$, $\tilde\psi^{\vec\sigma}_\lambda = \tilde\psi^{\vec 0}_\lambda$, and the extensions of $\psi^{\vec 0}_\lambda$ and $\tilde\psi^{\vec 0}_\lambda$ by zero are in $H^s(\mathbb{R})$ and $L_2(\mathbb{R})$, respectively.

$$(\mathcal{W}_7)\quad \begin{cases} \operatorname{span}\{\psi^{\vec 0}_\lambda(1-\cdot) : \lambda\in\nabla^{B,(I)},\, j=i\} = \operatorname{span}\{\psi^{\vec 0}_\lambda : \lambda\in\nabla^{B,(I)},\, j=i\}, \\ \operatorname{span}\{\psi^{(\sigma_0,\sigma_1)}_\lambda(1-\cdot) : \lambda\in\nabla^{B,(L)}_{\sigma_0},\, j=i\} = \operatorname{span}\{\psi^{(\sigma_1,\sigma_0)}_\lambda : \lambda\in\nabla^{B,(R)}_{\sigma_1},\, j=i\}, \end{cases}$$

$$(\mathcal{W}_8)\quad \begin{cases} \psi^{\vec\sigma}_\lambda(2^l\cdot) \in \operatorname{span}\{\psi^{\vec\sigma}_\mu : \mu\in\nabla^{B,(L)}_{\sigma_0}\} & (l\in\mathbb{N}_0,\, \lambda\in\nabla^{B,(L)}_{\sigma_0}), \\ \psi^{\vec 0}_\lambda(2^l\cdot) \in \operatorname{span}\{\psi^{\vec 0}_\mu : \mu\in\nabla^{B,(I)}\} & (l\in\mathbb{N}_0,\, \lambda\in\nabla^{B,(I)}). \end{cases}$$

Let us first consider the simple *reflection*

$$\begin{aligned} (\breve G_1 v)(x) &:= v(x) \quad x\in(0,1), \\ (\breve G_1 v)(-x) &:= v(x) \quad x\in(0,1), \end{aligned} \tag{6.2.4}$$

for any $v\in L_2(0,1)$. Obviously, we have

$$\begin{aligned} &\breve G_1 \in B\left(L_2(0,1), L_2(-1,1)\right) \\ &\breve G_1 \in B\left(H^s(0,1), H^s(-1,1)\right), \end{aligned} \tag{6.2.5}$$

for $s < 3/2$.

Remark 6.14. The use of the reflection operator has certain advantages and drawbacks. On the one hand, the reflection preserves the vanishing moment properties of the underlying frame elements, which is a central ingredient for compression estimates, see Section 7.3. Moreover, the reflection possesses a moderate operator norm.

On the other hand, it is clear that the reflection idea only works for Sobolev spaces H^s, $s < 3/2$, i.e., the resulting numerical schemes are restricted to second order elliptic equations. This bottleneck could be clearly avoided by using, e.g., higher order Hestenes extension operators. However, in recent studies, it has turned out that the norm of a Hestenes extension operator grows fast with respect to its order parameter. Moreover, it is not a priori clear if the vanishing moments are preserved. For this reason, we stick with the simple reflection operator.

Let η_1 and η_2 denote the extensions by zero of functions on $(0,1)$ or on $(-1,0)$ to functions on $(-1,1)$, with R_1 and R_2 denoting their adjoints. With a univariate extension $\breve G_1$ as in (6.2.4) at hand, the obvious approach is to define $E_1^{(q)}$ according to Proposition 6.12 with $G_1 = \breve G_1$. A problem with the choice $G_1 = \breve G_1$ is that generally it does *not* imply the desirable property $\operatorname{diam}(\operatorname{supp} G_1 u) \lesssim \operatorname{diam}(\operatorname{supp} u)$. Indeed, think of the application of the reflection to a function u with a small support that is not located near the interface.

To solve this and the corresponding problem for the adjoint extension, following [20], we apply our construction using the modified, *scale-dependent* univariate extension operator

$$G_1 : u \mapsto \sum_{\lambda \in \nabla_0^{B,(L)}} \langle u, \tilde{\psi}_\lambda^{\vec{0}} \rangle_{L_2(0,1)} \breve{G}_1 \psi_\lambda^{\vec{0}} + \sum_{\lambda \in \nabla^{B,(I)} \cup \nabla_0^{B,(R)}} \langle u, \tilde{\psi}_\lambda^{\vec{0}} \rangle_{L_2(0,1)} \eta_1 \psi_\lambda^{\vec{0}}. \tag{6.2.6}$$

So this operator reflects only wavelets that are supported near the interface. A proof of the following proposition can be found in [20, Proposition 5.2].

Proposition 6.15. *For $\vec{\sigma} \in \{0, \lfloor s + \frac{1}{2} \rfloor\}^2$, the scale-dependent extension G_1 from (6.2.6) satisfies*

$$G_1 \psi_\mu^{\vec{\sigma}} = \begin{cases} \eta_1 \psi_\mu^{\vec{\sigma}}, & \mu \in \nabla^{B,(I)} \cup \nabla_{\sigma_1}^{B,(R)}, \\ \breve{G}_1 \psi_\mu^{\vec{\sigma}}, & \mu \in \nabla_{\sigma_0}^{B,(L)}. \end{cases} \tag{6.2.7}$$

The resulting adjoint extension $G_2 := (\mathrm{Id} - \eta_1 G_1^*)\eta_2$ satisfies

$$G_2(\tilde{\psi}_\mu^{\vec{\sigma}}(1 + \cdot)) = \begin{cases} \eta_2(\tilde{\psi}_\mu^{\vec{\sigma}}(1 + \cdot)), & \mu \in \nabla^{B,(I)} \cup \nabla_{\sigma_0}^{B,(L)}, \\ \breve{G}_2(\tilde{\psi}_\mu^{\vec{\sigma}}(1 + \cdot)), & \mu \in \nabla_{\sigma_1}^{B,(R)}. \end{cases} \tag{6.2.8}$$

We have $G_1 \in B\left(L_2(0,1), L_2(-1,1)\right)$, and $G_1 \in B\left(H^s(0,1), H^s_{(\lfloor s+\frac{1}{2} \rfloor, 0)}(-1,1)\right)$, for $s < 3/2$.

Finally, for $\mu \in \nabla_{\vec{\sigma}}$, it holds that

$$\begin{aligned} &\mathrm{diam}(\mathrm{supp}\, G_1 \psi_\mu^{\vec{\sigma}}) \lesssim \mathrm{diam}(\mathrm{supp}\, \psi_\mu^{\vec{\sigma}}), \\ &\mathrm{diam}(\mathrm{supp}\, G_2 \tilde{\psi}_\mu^{\vec{\sigma}}) \lesssim \mathrm{diam}(\mathrm{supp}\, \tilde{\psi}_\mu^{\vec{\sigma}}). \end{aligned}$$

Remark 6.16. In general, it is not possible to divide the univariate quarklet sets in such parts that statements similar to (6.2.7) and (6.2.8) hold. This can be explained as follows: since the univariate wavelets build a Riesz basis for a Sobolev space on the unit interval, every quarklet can be decomposed into wavelet elements. For quarklets near the boundary, it is not guaranteed that the participating wavelets of these decomposition lie exclusively in $\nabla^{B,(I)} \cup \nabla_{\sigma_1}^{B,(R)}$ or in $\nabla_{\sigma_0}^{B,(L)}$. Thus, it could happen that one part of the decomposition would be reflected and another part would be extended by zero. This would destroy the vanishing moments of the extended quarklets. Moreover, the wavelet decompositions of the quarklets have to be computed for every single quarklet, which is possible in theory but in practice very time-consuming. This is the reason why we use another approach with Bessel systems, which was already introduced in Subsection 6.2.2 and is carried out further in the following.

The Bessel systems $\Xi^{s,(q)}$

For the univariate quarklet frame $\Psi_{L_2(0,1),\vec{\sigma}}$ for $L_2(0,1)$ we can specify a *non-canonical* dual frame, cf. (2.1.10), if we augment the dual Riesz basis of the univariate wavelet basis $\Psi^B_{L_2(0,1),\vec{\sigma}}$, with zero functions:

$$\tilde{\Psi}_{L_2(0,1),\vec{\sigma}} := \{\tilde{\psi}^{\vec{\sigma}}_\lambda : \lambda \in \nabla_{\vec{\sigma}}\}, \quad \tilde{\psi}^{\vec{\sigma}}_\lambda :\equiv 0, \text{ for } \lambda \in \nabla_{\vec{\sigma}} \setminus \nabla^B_{\vec{\sigma}}. \tag{6.2.9}$$

It is obvious that $\tilde{\Psi}_{L_2(0,1),\vec{\sigma}}$ is a dual frame of $\Psi_{L_2(0,1),\vec{\sigma}}$, since

$$\sum_{\lambda\in\nabla_{\vec{\sigma}}} \langle f, \tilde{\psi}^{\vec{\sigma}}_\lambda\rangle_{L_2(0,1)}\psi^{\vec{\sigma}}_\lambda = \sum_{\lambda\in\nabla^B_{\vec{\sigma}}} \langle f, \tilde{\psi}^{\vec{\sigma}}_\lambda\rangle_{L_2(0,1)}\psi^{\vec{\sigma}}_\lambda = f, \quad \text{for all } f \in L_2(0,1).$$

With this dual frame at hand, $(\mathcal{W}_1)$-$(\mathcal{W}_4)$ also hold true if we replace $\nabla^B_{\vec{\sigma}}$ with $\nabla_{\vec{\sigma}}$. Moreover, it is possible to construct $\nabla^{(L)}_{\sigma_0} \supset \nabla^{B,(L)}_{\sigma_0}$, $\nabla^{(I)} \supset \nabla^{B,(I)}$, $\nabla^{(R)}_{\sigma_1,} \supset \nabla^{B,(R)}_{\sigma_1,}$, such that $\nabla_{\vec{\sigma}} = \nabla^{(L)}_{\sigma_0} \dot\cup \nabla^{(I)} \dot\cup \nabla^{(R)}_{\sigma_1}$, and

(i) $\sup_{\lambda\in\nabla^{(L)}_{\sigma_0},\, x\in\operatorname{supp}\psi^{\vec{\sigma}}_\lambda} 2^j|x| \lesssim \rho, \quad \sup_{\lambda\in\nabla^{(R)}_{\sigma_1},\, x\in\operatorname{supp}\psi^{\vec{\sigma}}_\lambda} 2^j|1-x| \lesssim \rho,$

(ii) for $\lambda \in \nabla^{(I)}$, $\psi^{\vec{\sigma}}_\lambda = \psi^{\vec{0}}_\lambda$, $\tilde{\psi}^{\vec{\sigma}}_\lambda = \tilde{\psi}^{\vec{0}}_\lambda$, and the extensions of $\psi^{\vec{0}}_\lambda$ and $\tilde{\psi}^{\vec{0}}_\lambda$ by zero are in $H^s(\mathbb{R})$ and $L_2(\mathbb{R})$, respectively,

cf. $(\mathcal{W}_6)$.

Now, let us consider the quarkonial tensor frame $\boldsymbol{\Psi}_{L_2(\Box),\boldsymbol{\sigma}}$ for $L_2(\Box)$. Given cubes $\{\Box_0, \dots, \Box_N\}$ with $\Box_j := \tau_j + \Box$, $\tau_j \in \mathbb{Z}^d$, $j = 0, \dots, N$, cf. Subsection 6.2.1, we immediately get quarklet frames for $L_2(\Box_j)$ by

$$\boldsymbol{\Psi}_j := \boldsymbol{\Psi}_{L_2(\Box),\boldsymbol{\sigma}}(\cdot - \tau_j),$$

which have all the properties we required from the abstract frames $\boldsymbol{\mathcal{F}}_j$ in Subsection 6.2.2. The inherent Riesz bases are

$$\boldsymbol{\Psi}^B_j := \boldsymbol{\Psi}^B_{L_2(\Box),\boldsymbol{\sigma}}(\cdot - \tau_j).$$

Let $s \in [0,\infty) \setminus \{\mathbb{N}_0 + \frac{1}{2}\}$. For $q = 0, \dots, N$, $i = q, \dots, N$, we define the sets $\boldsymbol{\Psi}^{s,(q)}_i$ and $\boldsymbol{\Psi}^{B,s,(q)}_i$ similar to (6.2.3) and (6.2.2), respectively. With these definition at hand, for $q = 1, \dots, N$, we further define $\boldsymbol{\Psi}^{s,(q-1)}_{i_1,L}$ as the subset of functions $f \in \boldsymbol{\Psi}^{s,(q-1)}_{i_1}$ with the following properties:

(i) the support of f intersected with $(0,1) \times \breve{J}$ is not empty,

(ii) the cube of origin $\Box_i$ of f lies in the neighborhood of $\{0\} \times \breve{J}$, i.e., for all $\varepsilon > 0$: $\operatorname{diam}(\Box_i, \{0\} \times \breve{J}) < \varepsilon$,

(iii) the first Cartesian index of f restricted to its cube of origin is contained in $\nabla^{(L)}_0$.

With $\boldsymbol{\Psi}^{s,(q-1)}_{i_1,R} := \boldsymbol{\Psi}^{s,(q-1)}_{i_1} \setminus \boldsymbol{\Psi}^{s,(q-1)}_{i_1,L}$ we denote the complementary subset. Now, we are ready to define the sets $\boldsymbol{\Xi}^{s,(q)}$, cf. (6.2.3), as

$$\boldsymbol{\Xi}^{s,(q)} := \breve{E}^{(q)}_1(\boldsymbol{\Psi}^{s,(q-1)}_{i_1,L}) \cup \eta^{(q)}_1(\boldsymbol{\Psi}^{s,(q-1)}_{i_1,R}), \tag{6.2.10}$$

where $\breve{E}^{(q)}_1$, $q = 1, \dots, N$, are the operators corresponding to the simple reflection $\breve{G}_1$. The proof of the following proposition, which states the Bessel property of $\boldsymbol{\Xi}^{s,(q)}$, again relies on some of the statements about frames and operators of Section 2.3.

Proposition 6.17. *For $q = 1, \dots, N$, the set $\Xi^{0,(q)}$ defined in* (6.2.10) *is a Bessel system for $L_2(\Omega_{\bar{i}}^{(q)})$ and $\Xi^{s,(q)}$ a Bessel system for $\mathring{H}^s(\Omega_{\bar{i}}^{(q)})$, $0 < s < 3/2$, $s \neq \frac{1}{2}$. Also, we have $E_1^{(q)}(\mathbf{\Psi}_{i_1}^{B,s,(q-1)}) \subset \Xi^{s,(q)}$.*

Proof. Both $\mathbf{\Psi}_{i_1,L}^{0,(q-1)}$ and $\mathbf{\Psi}_{i_1,R}^{0,(q-1)}$ are subsets of the frame $\mathbf{\Psi}_{i_1}^{0,(q-1)}$ for $L_2(\Omega_{i_1}^{(q-1)})$. Hence, they are Bessel systems for $L_2(\Omega_{i_1}^{(q-1)})$. Since both $\breve{E}_1^{(q)}$ and $\eta_1^{(q)}$ are bounded operators from $L_2(\Omega_{i_1}^{(q-1)})$ to $L_2(\Omega_{\bar{i}}^{(q)})$, the images $\breve{E}_1^{(q)}(\mathbf{\Psi}_{i_1,L}^{0,(q-1)})$ and $\eta_1^{(q)}(\mathbf{\Psi}_{i_1,R}^{0,(q-1)})$ are Bessel systems for $L_2(\Omega_{\bar{i}}^{(q)})$, cf. Proposition 2.14 (i). For the renormalized versions we have to take care of the boundary conditions and the smoothness of the functions. For $s < 3/2$, it is $\breve{G}_1 \in B\left(H^s_{(0,\lfloor s+\frac{1}{2}\rfloor)}(0,1), H^s_0(-1,1)\right)$. Since the first Cartesian component of $\mathbf{\Psi}_{i_1,L}^{s,(q-1)}$ is in $H^s_{(0,\lfloor s+\frac{1}{2}\rfloor)}(0,1)$ the image of $\mathbf{\Psi}_{i_1,L}^{s,(q-1)}$ under $\breve{E}_1^{(q)}$ is bounded in $\mathring{H}^s(\Omega_{\bar{i}}^{(q)})$ and therefore a Bessel system for $\mathring{H}^s(\Omega_{\bar{i}}^{(q)})$, cf. Proposition 2.14 (i). For the zero extension part we have $\eta_1 \in B\left(H^s_{(\lfloor s+\frac{1}{2}\rfloor,0)}(0,1), H^s_{(\lfloor s+\frac{1}{2}\rfloor,0)}(-1,1)\right)$. The first Cartesian component of $\mathbf{\Psi}_{i_1,R}^{s,(q-1)}$ is in $H^s_{(\lfloor s+\frac{1}{2}\rfloor,0)}(0,1)$ and therefore the image of $\mathbf{\Psi}_{i_1,R}^{s,(q-1)}$ under $\eta_1^{(q)}$ is also a Bessel system for $\mathring{H}^s(\Omega_{\bar{i}}^{(q)})$. The relation $E_1^{(q)}(\mathbf{\Psi}_{i_1}^{B,s,(q-1)}) \subset \Xi^{s,(q)}$ follows directly from (6.2.7) and (6.2.10) and the way how the sets $\mathbf{\Psi}_{i_1,L}^{s,(q-1)}$ and $\mathbf{\Psi}_{i_1,R}^{s,(q-1)}$ are defined. □

The main results

It remains to choose the index sets $\nabla_{\sigma_0}^{B,(L)}, \nabla^{B,(I)}, \nabla_{\sigma_1}^{B,(R)}$ and $\nabla_{\sigma_0}^{(L)}, \nabla^{(I)}, \nabla_{\sigma_1}^{(R)}$ appropriately. It is sufficient to specify the boundary index sets. Let us assume that $m \geq 3$. From [90, Sections 3.3, 4.7] we deduce that the index sets for which either the primal or dual wavelets depend on the incorporated boundary conditions are

$$\nabla_{\sigma_0}^{B,(L)} := \{(0,j,k) \in \nabla_{\vec{\sigma}} : k \in \nabla_{j,\sigma_0}^{(L)}\}, \quad \nabla_{\sigma_1}^{B,(R)} := \{(0,j,k) \in \nabla_{\vec{\sigma}} : k \in \nabla_{j,\sigma_1}^{(R)}\},$$

with

$$\nabla_{j,\sigma_0}^{(L)} = \begin{cases} \{0, \dots, \frac{m+\tilde{m}-4}{2}\}, & j \geq j_0, \\ \{-m+1+\operatorname{sgn}\sigma_0, \cdots, \tilde{m}-2\}, & j = j_0 - 1, \end{cases}$$

and

$$\nabla_{j,\sigma_1}^{(R)} = \begin{cases} \{2^j - \frac{m+\tilde{m}-2}{2}, \dots, 2^j - 1\}, & j \geq j_0, \\ \{2^j - m - \tilde{m} + 2, \dots, 2^j - 1 - \operatorname{sgn}\sigma_1\}, & j = j_0 - 1, \end{cases}$$

cf. (3.2.26). For the selection of the quarklet index sets we have more freedom. We decide to reflect as few as possible quarklets. This leads to the index sets

$$\nabla_{\sigma_0}^{(L)} := \{(p,j,k) \in \nabla_{\vec{\sigma}} : k \in \nabla_{p,j,\sigma_0}^{(L)}\}, \quad \nabla_{\sigma_1}^{(R)} := \{(p,j,k) \in \nabla_{\vec{\sigma}} : k \in \nabla_{p,j,\sigma_1}^{(R)}\}$$

with

$$\nabla^{(L)}_{p,j,\sigma_0} := \begin{cases} \nabla^{(L)}_{j,\sigma_0}, & p=0, \\ \{0+\operatorname{sgn}\sigma_0,\dots,0\}, & p>0, j\geq j_0, \\ \{-m+1+\operatorname{sgn}\sigma_0,\cdots,-m+1\}, & p>0, j=j_0-1, \end{cases}$$

and

$$\nabla^{(R)}_{p,j,\sigma_1} := \begin{cases} \nabla^{(R)}_{j,\sigma_1}, & p=0, \\ \{2^j-1,\dots,2^j-1-\operatorname{sgn}\sigma_1\}, & p>0, \end{cases} \quad j\geq j_0.$$

Remark 6.18. For $m=2$, slight adaptations of the index sets are necessary due to the different construction of the dual wavelets, cf. [90, Section 4.7] for details.

In order to identify individual quarklets from the collections constructed by the applications of the extension operators, we have to introduce some more notations. For $q=0,\dots,N$, we set the index sets

$$\begin{aligned} &\boldsymbol{\nabla}^{(0)}_i := \boldsymbol{\nabla}_{\boldsymbol{\sigma}(i)} \times \{i\} \text{ and, for } q>0, \\ &\boldsymbol{\nabla}^{(q)}_i := \begin{cases} \boldsymbol{\nabla}^{(q-1)}_{i_1} \cup \boldsymbol{\nabla}^{(q-1)}_{i_2}, & i=\bar{i}, \\ \boldsymbol{\nabla}^{(q-1)}_{\hat{i}}, & i\in\{q,\dots,N\}\setminus\{\bar{i}\} \wedge \Omega^{(q)}_i = \Omega^{(q-1)}_{\hat{i}}. \end{cases} \end{aligned} \tag{6.2.11}$$

We define the quarklets on the domains $\Omega^{(q)}_i$ as

$$\boldsymbol{\psi}^{(0,i)}_{\boldsymbol{\lambda},i} := \boldsymbol{\psi}^{\boldsymbol{\sigma}(i)}_{\boldsymbol{\lambda}}(\cdot-\tau_i), \tag{6.2.12}$$

and, for $q>0$,

$$\boldsymbol{\psi}^{(q,i)}_{\boldsymbol{\lambda},n} := \begin{cases} \left.\begin{cases} \breve{E}^{(q)}_1 \boldsymbol{\psi}^{(q-1,i_1)}_{\boldsymbol{\lambda},n}, & (\boldsymbol{\lambda},n)\in\boldsymbol{\nabla}^{(q-1)}_{i_1,L}, \\ \eta^{(q)}_1 \boldsymbol{\psi}^{(q-1,i_1)}_{\boldsymbol{\lambda},n}, & (\boldsymbol{\lambda},n)\in\boldsymbol{\nabla}^{(q-1)}_{i_1,R}, \\ \eta^{(q)}_2 \boldsymbol{\psi}^{(q-1,i_2)}_{\boldsymbol{\lambda},n}, & (\boldsymbol{\lambda},n)\in\boldsymbol{\nabla}^{(q-1)}_{i_2}, \end{cases}\right\} & i=\bar{i}, \\ \boldsymbol{\psi}^{(q-1,\hat{i})}_{\boldsymbol{\lambda},n}, & i\in\{q,\dots,N\}\setminus\{\bar{i}\} \text{ and } \Omega^{(q)}_i = \Omega^{(q-1)}_{\hat{i}}. \end{cases} \tag{6.2.13}$$

The index $n=0,\dots,N$ indicates the cube $\square_n$ where the quarklet stems from. The subsets $\boldsymbol{\nabla}^{(q-1)}_{i_1,L}$ and $\boldsymbol{\nabla}^{(q-1)}_{i_1,R}$ are defined according to $\boldsymbol{\Psi}^{s,(q-1)}_{i_1,L}$ and $\boldsymbol{\Psi}^{s,(q-1)}_{i_1,R}$, cf. the previous part about Bessel systems. With this notations at hand we can establish the following theorem, which is the first main result of this section.

Theorem 6.19. *Let $\Psi_{L_2(0,1),\vec{\sigma}}$ denote a quarklet system of order $m\geq 2$, $\tilde{m}$ vanishing moments, $\frac{\tilde{m}}{m}$ sufficiently big and $m+\tilde{m}$ even, as constructed in Theorem 5.8. Furthermore, let $\Omega\in\mathbb{R}^d$ be a bounded domain that can be decomposed into cubes $\square_i$, $i=0,\dots,N$. If we choose weights $w^{H^s}_{\boldsymbol{\lambda}}$ as in* (6.1.20)*, the system*

$$\boldsymbol{\Psi}_{H^s_0(\Omega)} := \left\{ (w^{H^s}_{\boldsymbol{\lambda}})^{-1}\boldsymbol{\psi}_{\boldsymbol{\alpha}} : \boldsymbol{\alpha}=(\boldsymbol{\lambda},n)\in\boldsymbol{\nabla} \right\}, \quad \delta_1>0,\, \delta_2>1, \quad \boldsymbol{\nabla} := \boldsymbol{\nabla}^{(N)}_N, \tag{6.2.14}$$

cf. (6.2.11)*, with $\boldsymbol{\psi}_{\boldsymbol{\alpha}} := \boldsymbol{\psi}^{(N,N)}_{\boldsymbol{\lambda},n}$, cf.* (6.2.13)*, is a frame for $H^s_0(\Omega)$, $0\leq s<\frac{3}{2}$, $s\neq\frac{1}{2}$.*

$\boldsymbol{p} = (1,1)$, $\boldsymbol{j} = (3,3)$, $\boldsymbol{k} = (0,5)$

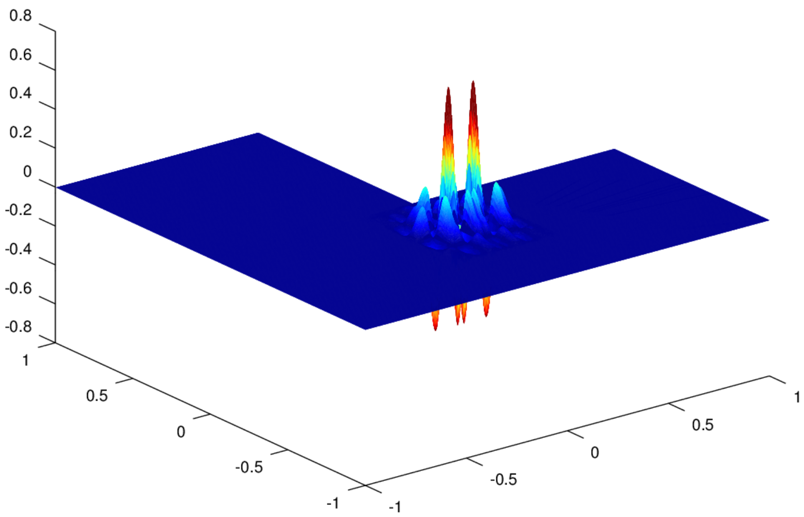

$\boldsymbol{p} = (3,0)$, $\boldsymbol{j} = (3,2)$, $\boldsymbol{k} = (3,-2)$

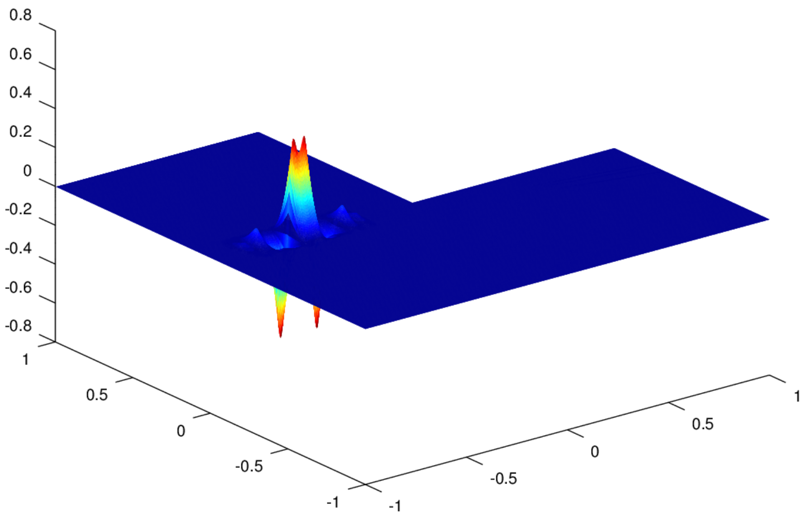

Figure 6.6: Unweighted extended quarklets $\boldsymbol{\psi}_{\boldsymbol{\alpha}}$ on the L-shaped domain with support at the interfaces $\{0\} \times (-1,0)$ and $(-1,0) \times \{0\}$, respectively.

In Figure 6.6, we give a visualization of two unweighted quarklets on the L-shaped domain. They are chosen in a way such that their support is located near an interface. Hence, the effect of the extension operator becomes visible.

Our construction procedure even gives rise to a Gelfand frame for the Gelfand triple $(H_0^s(\Omega), L_2(\Omega), H^{-s}(\Omega))$, cf. Section 2.4. Let us observe that in more detail. Similar to the construction that leads to a frame for $H_0^s(\Omega)$, we obtain a frame for $L_2(\Omega)$,

$$\mathbf{\Psi}_{L_2(\Omega)} := \left\{ (w_{\boldsymbol{\lambda}}^{L_2})^{-1} \boldsymbol{\psi}_{\boldsymbol{\alpha}} : \boldsymbol{\alpha} = (\boldsymbol{\lambda}, n) \in \boldsymbol{\nabla} \right\}, \quad \delta_1 > 0, \tag{6.2.15}$$

cf. (6.1.18) for the weights $w_{\boldsymbol{\lambda}}^{L_2}$. This frame contains a Riesz basis for $L_2(\Omega)$,

$$\mathbf{\Psi}_{L_2(\Omega)}^B := \left\{ \boldsymbol{\psi}_{\boldsymbol{\alpha}} : \boldsymbol{\alpha} \in \boldsymbol{\nabla}^B \right\},$$

where $\boldsymbol{\nabla}^B$ denotes the subset of $\boldsymbol{\nabla}$ that corresponds to wavelets, i.e., all the polynomial coefficients are zero. The weights $w_{\boldsymbol{\lambda}}^{L_2}$ have been dropped since they only depend on the polynomial coefficients. We identify $L_2(\Omega)$ with its dual space and denote with

$$\tilde{\mathbf{\Psi}}_{L_2(\Omega)}^B := \left\{ \tilde{\boldsymbol{\psi}}_{\boldsymbol{\alpha}} : \boldsymbol{\alpha} \in \boldsymbol{\nabla}^B \right\}$$

the dual Riesz basis of $\mathbf{\Psi}_{L_2(\Omega)}^B$. We refer to [20, Proposition 4.9] for more details on how to construct the dual basis. Defining $\tilde{\boldsymbol{\psi}}_{\boldsymbol{\alpha}} :\equiv 0$ for $\boldsymbol{\alpha} \in \boldsymbol{\nabla} \setminus \boldsymbol{\nabla}^B$ we obtain a non-canonical dual frame for $\mathbf{\Psi}_{L_2(\Omega)}$,

$$\tilde{\mathbf{\Psi}}_{L_2(\Omega)} := \left\{ \tilde{\boldsymbol{\psi}}_{\boldsymbol{\alpha}} : \boldsymbol{\alpha} = (\boldsymbol{\lambda}, n) \in \boldsymbol{\nabla} \right\}. \tag{6.2.16}$$

The rescaled version

$$\tilde{\mathbf{\Psi}}_{H^{-s}(\Omega)} := \left\{ \left(\sum_{i=1}^d 4^{sj_i} \right)^{1/2} \tilde{\boldsymbol{\psi}}_{\boldsymbol{\alpha}} : \boldsymbol{\alpha} = (\boldsymbol{\lambda}, n) \in \boldsymbol{\nabla} \right\} \tag{6.2.17}$$

is a non-canonical dual frame for $\mathbf{\Psi}_{H_0^s(\Omega)}$. Hence, $\mathbf{\Psi}_{L_2(\Omega)}$ is a Gelfand frame for $(H_0^s(\Omega), L_2(\Omega), H^{-s}(\Omega))$ with the weight matrix

$$\begin{aligned} D &= \operatorname{diag}(w_{\boldsymbol{\lambda}}^{H^s} / w_{\boldsymbol{\lambda}}^{L_2})_{\boldsymbol{\alpha}=(\boldsymbol{\lambda},n)\in\boldsymbol{\nabla}} \\ &= \operatorname{diag}\left(\left(\sum_{i=1}^d (p_i+1)^{4s+\delta_2} 4^{sj_i} \right)^{1/2} \right)_{\boldsymbol{\alpha}=((\boldsymbol{p},\boldsymbol{j},\boldsymbol{k}),n)\in\boldsymbol{\nabla}}, \end{aligned} \tag{6.2.18}$$

cf. Definition 2.15.

Moreover, the construction of quarklet frames can be extended to more general domains. To be more precise, assume we have a domain $\hat{\Omega}$ that can be decomposed into cubes $\square_i$, $i = 0, \ldots, N$, and another domain Ω which is the image of $\hat{\Omega}$ under a homeomorphism κ. We define the *pull-back*

$$\kappa^* : H_0^s(\Omega) \to H_0^s(\hat{\Omega}), \quad w \mapsto \kappa^* w = w \circ \kappa$$

and its inverse κ^{-*}, the *push-forward*

$$\kappa^{-*} : H_0^s(\hat{\Omega}) \to H_0^s(\Omega), \quad v \mapsto \kappa^{-*}v = v \circ \kappa^{-1}.$$

Then, $\mathbf{\Psi}_{H_0^s(\Omega)} := \kappa^{-*}\mathbf{\Psi}_{H_0^s(\hat{\Omega})}$ is a frame for $H_0^s(\Omega)$, $0 \le s < \frac{3}{2}$. If κ^* is additionally a boundedly invertible mapping from $L_2(\Omega) \to L_2(\hat{\Omega})$ we obtain in a completely analogous way a frame

$$\mathbf{\Psi}_{L_2(\Omega)} := \kappa^{-*}\mathbf{\Psi}_{L_2(\hat{\Omega})} \tag{6.2.19}$$

for $L_2(\Omega)$. A dual frame for $L_2(\Omega)$ is acquired by

$$\tilde{\mathbf{\Psi}}_{L_2(\Omega)} := |\det D\kappa^{-1}|\kappa^{-*}\tilde{\mathbf{\Psi}}_{L_2(\hat{\Omega})}, \tag{6.2.20}$$

which renormalized is a frame for $H^{-s}(\Omega)$. Hence, $\mathbf{\Psi}_{L_2(\Omega)}$ is a Gelfand frame for the Gelfand triple $(H_0^s(\Omega), L_2(\Omega), H^{-s}(\Omega))$. We repeat the latter observations in the following main theorem, which encapsulates the whole construction process of quarklet frames on general bounded domains.

Theorem 6.20. *Let $\Psi_{L_2(0,1),\vec{\sigma}}$ denote a quarklet system of order $m \ge 2$, $\tilde{m}$ vanishing moments, $\frac{\tilde{m}}{m}$ sufficiently big and $m + \tilde{m}$ even, as constructed in Theorem 5.8. Furthermore, let $\Omega \in \mathbb{R}^d$ be a bounded domain that is the image under a homeomorphism κ of another bounded domain $\hat{\Omega} \in \mathbb{R}^d$ that can be decomposed into cubes $\square_i$, $i = 0, \dots, N$. Let κ^* be boundedly invertible as a mapping both from $L_2(\Omega)$ to $L_2(\hat{\Omega})$ and from $H_0^s(\Omega)$ to $H_0^s(\hat{\Omega})$, $0 < s < 3/2$, $s \ne \frac{1}{2}$. Then, $\mathbf{\Psi}_{L_2(\Omega)}$ as defined in* (6.2.19) *is a Gelfand frame for the Gelfand triple $(H_0^s(\Omega), L_2(\Omega), H^{-s}(\Omega))$, cf. Definition 2.15, with the dual frame $\tilde{\mathbf{\Psi}}_{L_2(\Omega)}$ as defined in* (6.2.20) *and the weight matrix D as defined in* (6.2.18).

Chapter 7

Adaptive Iterative Solution of Discretized Problems

In this chapter, we introduce an implementable adaptive frame scheme based on quarklets. For a better understanding of its mechanics, we now give a short recapitulation of the evolution of adaptive wavelet schemes.

The scientific breakthrough for adaptive wavelet methods for solving linear operator equations was achieved in the two papers [31] and [32] by Cohen, Dahmen and DeVore. For the first time ever, they were able to construct adaptive methods based on wavelet Riesz bases with provable optimal convergences rates, i.e., the schemes realized asymptotically the convergence rate of the best N-term wavelet approximation. However, this means that these methods outperform their non-adaptive counterparts if the solution of the operator equation has a lacking Sobolev regularity, e.g., due to singularities. These singularities of the solution are typically induced by a non-smooth right-hand side or by corners and edges if you consider the operator equation to be a boundary value problem on a non-smooth domain. In these cases, non-adaptive methods can only compete if a priori knowledge of the solution and its singularities is used to select the linear approximation spaces. While this is possible for some simple model examples, such an a priori selection is not feasible for more general problems. Adaptive methods, on the other hand, find the approximate solutions solely by utilizing information acquired in the course of the solution process.

Both methods in [31] and [32] use a wavelet discretization to transfer the operator equation to an infinite-dimensional matrix-vector equation, cf. Section 2.5. In [31], this equation is solved by a Galerkin method. The idea behind this method is to select a finite submatrix in every iteration step and solve the resulting finite equation. The adaptivity enters into how the submatrices are selected at each iteration.

In [32], an adaptive Richardson iteration is used to solve the matrix-vector equation. In contrast to the Galerkin method, no proper submatrices enter the routine. Instead, in each iteration step the entire matrix is applied to vectors with only finitely many non-trivial entries. Since the matrix is biinfinite, the matrix-vector multiplication can only be performed up to some accuracy. This accuracy is dynamically updated in each iteration step, whereby the whole adaptivity of the scheme lies in this process.

The numerical efficiency of both algorithms relies on fast matrix-vector multiplications, which can be realized if the stiffness matrix of the operator with respect to the wavelet basis is close to a sparse matrix. If a matrix satisfies this property, we call it *quasi-sparse* or *compressible*. It has been shown that for a large class of operators and suitable wavelet bases, the corresponding stiffness matrices are indeed quasi-sparse.

A natural idea is to extend the two methods just described to the case of wavelet frames. However, for a redundant frame, the occurring stiffness matrix has a non-trivial kernel. Consequently, the condition numbers of submatrices in a Galerkin method can be arbitrarily large, which makes this approach infeasible.

In [97], Stevenson introduced a generalization to wavelet frames of the adaptive Richardson iteration. Under certain extra conditions, he was able to prove optimal convergence rates also in this setting. Again, a quasi-sparse structure of the stiffness matrix is necessary. For wavelets that have sufficiently many vanishing moments and smoothness this could be verified. Although the construction in [97] was initially designed for wavelet frames stemming from overlapping domain decompositions, an application to quarklet frames is possible as long as the corresponding stiffness matrices are quasi-sparse. Let us mention that also other adaptive frame methods, e.g., an adaptive steepest descent method (see [43]), which in general converges faster than a Richardson iteration, can principally be applied to quarklet frames. However, our predominating goal is to construct an adaptive quarklet algorithm with optimal convergence order. For simplicity, we confine the analysis to the easiest algorithm.

The structure of this chapter is the following: In Section 7.1, we reconstruct the adaptive Richardson iteration from [97], introduce the concept of asymptotical optimality and show that under certain assumptions, an adaptive Richardson iteration based on quarklets fits into this concept. Thereupon, in Section 7.2, we establish the necessary building blocks for an adaptive quarklet scheme. Finally, Theorem 7.12 in Section 7.3 states another main result of this thesis, namely, the compressibility of the stiffness matrix for the Poisson equation in quarklet coordinates, which is crucial for a well-performing adaptive scheme.

7.1 The inexact Richardson iteration

The aim of this chapter is to present an adaptive scheme to solve elliptic operator equations

$$\mathcal{L}u = f, \tag{7.1.1}$$

with $\mathcal{L} : H_0^t(\Omega) \to H^{-t}(\Omega)$, $u \in H_0^t(\Omega)$, $f \in H^{-t}(\Omega)$, $t \in \mathbb{N}_0$. This is done in a general fashion without explicitly assuming that we work with quarklet frames. Instead, we assume to have available a Gelfand frame. Hence, also other classes of frames, e.g., aggregated wavelet frames, cf. [42], fit into this framework.

In Section 2.5, we have seen how a discretization of (7.1.1) with respect to a Gelfand frame leads to a matrix-vector equation $\mathbf{Au} = \mathbf{f}$, cf. (2.5.4), with a symmetric, positive semidefinite matrix $\mathbf{A}$. To solve the latter, we consider the exact *damped Richardson iteration*

$$\mathbf{u}^{(0)} := 0, \qquad \mathbf{u}^{(i+1)} := \mathbf{u}^{(i)} - \omega(\mathbf{A}\mathbf{u}^{(i)} - \mathbf{f}), \quad i = 0, 1, \dots. \tag{7.1.2}$$

with a relaxation parameter $\omega > 0$. Let $\lambda_{\max}$ be the maximal eigenvalue of $\mathbf{A}$ and $0 < \omega < 2/\lambda_{\max}$. With $\mathbf{Q}$ the orthogonal projector onto $\operatorname{ran}(\mathbf{A})$, cf. Lemma 2.19, a countable index set $\mathcal{I}$ and an arbitrary solution $\mathbf{u}$ to (2.5.4), it can be shown that

$$||\mathbf{Q}(\mathbf{u} - \mathbf{u}^{(i+1)})||_{\ell_2(\mathcal{I})} \leq \rho ||\mathbf{Q}(\mathbf{u} - \mathbf{u}^{(i)})||_{\ell_2(\mathcal{I})},$$

where $\rho := ||(\mathbf{id} - \omega\mathbf{A})|_{\operatorname{ran}\mathbf{A}}||_{\mathscr{L}(\ell_2(\mathcal{I}))} < 1$. Hence, the algorithm converges in $\ell_2(\mathcal{I})$ to a solution of (2.5.4). We can even say more; since $\mathbf{u}^{(0)}, \mathbf{f} \in \operatorname{ran}(\mathbf{A})$, it is $\mathbf{u}^{(i)} \in \operatorname{ran}(\mathbf{A})$ and therefore the algorithm converges to the solution $\mathbf{Q}\mathbf{u} \in \operatorname{ran}(\mathbf{A})$ of (2.5.4), which is unique in $\operatorname{ran}(\mathbf{A})$, cf. Lemma 2.19. The best performance is obtained if we choose $\omega = 2/(\lambda_{\max} + \lambda_{\min}^{+})$, where $\lambda_{\min}^{+} := 1/||\mathbf{A}|_{\operatorname{ran}\mathbf{A}}^{-1}||_{\mathscr{L}(\ell_2(\mathcal{I}))}$.

In an actual implementation of the Richardson iteration it is impossible to handle either the generally infinite vector $\mathbf{f}$ or the matrix-vector-multiplication with a biinfinite matrix $\mathbf{A}$. This makes an approximation of these ingredients inevitable. We assume the existence of the following routines:

- **APPLY**$[\mathbf{A}, \mathbf{v}, \varepsilon] \to \mathbf{w}_\varepsilon$. Determines, for a finitely supported vector $\mathbf{v} \in \ell_2(\mathcal{I})$ and an $\varepsilon > 0$, a finitely supported $\mathbf{w}_\varepsilon \in \ell_2(\mathcal{I})$ with

  $$||\mathbf{A}\mathbf{v} - \mathbf{w}_\varepsilon||_{\ell_2(\mathcal{I})} \leq \varepsilon.$$

- **RHS**$[\mathbf{f}, \varepsilon] \to \mathbf{f}_\varepsilon$. Determines a finitely supported vector $\mathbf{f}_\varepsilon$ with

  $$||\mathbf{f} - \mathbf{f}_\varepsilon||_{\ell_2(\mathcal{I})} \leq \varepsilon.$$

- **COARSE**$[\mathbf{v}, \varepsilon] \to \mathbf{v}_\varepsilon$. Determines, for a finitely supported vector $\mathbf{v} \in \ell_2(\mathcal{I})$ and an $\varepsilon > 0$, a finitely supported $\mathbf{v}_\varepsilon \in \ell_2(\mathcal{I})$ by replacing all but N coefficients of $\mathbf{v}$ by zeros such that

  $$||\mathbf{v} - \mathbf{v}_\varepsilon||_{\ell_2(\mathcal{I})} \leq \varepsilon, \tag{7.1.3}$$

  whereas N is a at most a constant multiple of the minimal value of N for which (7.1.3) is valid.

While **APPLY** and **RHS** realize the aforementioned approximations of the matrix-vector-multiplication and the right-hand-side, respectively, the purpose of the routine **COARSE** is to balance the work and the accuracy of the whole algorithm.

With these three routines at hand, we formulate the inexact damped Richardson iteration.

Algorithm 1. $\mathbf{SOLVE}[\mathbf{A}, \mathbf{f}, \varepsilon] \to \mathbf{u}_\varepsilon$:

% *Let* $\theta < 1/3$ *and* $K \in \mathbb{N}$ *be fixed such that* $3\rho^K < \theta$.
% $i := 0$, $\mathbf{u}^{(0)} := 0$, $\varepsilon_0 := \|(\mathbf{A}|_{\mathrm{ran}(\mathbf{A})})^{-1}\|_{\mathscr{L}(\ell_2(\mathcal{I}))}\|\mathbf{f}\|_{\ell_2(\mathcal{I})}$
`while` $\varepsilon_i > \varepsilon$ `do`
  $i := i + 1$
  $\varepsilon_i := 3\rho^K \varepsilon_{i-1}/\theta$
  $\mathbf{f}^{(i)} := \mathbf{RHS}[\mathbf{f}, \frac{\theta\varepsilon_i}{6\omega K}]$
  $\mathbf{v}^{(i,0)} := \mathbf{u}^{(i-1)}$
  `for` $j = 1, \ldots K$ `do`
    $\mathbf{v}^{(i,j)} := \mathbf{v}^{(i,j-1)} - \omega(\mathbf{APPLY}[\mathbf{A}, \mathbf{v}^{(i,j-1)}, \frac{\theta\varepsilon_i}{6\omega K}] - \mathbf{f}^{(i)})$
  `endfor`
  $\mathbf{u}^{(i)} := \mathbf{COARSE}[\mathbf{v}^{(i,K)}, (1-\theta)\varepsilon_i]$
`enddo`
$\mathbf{u}_\varepsilon := \mathbf{u}^{(i)}$

The following proposition, cf. [97, Proposition 2.1], states the convergence of Algorithm 1.

Proposition 7.1. *Let* $\mathbf{u} \in \ell_2(\mathcal{I})$ *be some solution to* $\mathbf{A}\mathbf{u} = \mathbf{f}$. *Then, the vectors* $\mathbf{u}^{(i)}$ *produced in* $\mathbf{SOLVE}[\mathbf{A}, \mathbf{f}, \varepsilon] \to \mathbf{u}_\varepsilon$ *satisfy*

$$||\mathbf{Q}(\mathbf{u} - \mathbf{u}_i)||_{\ell_2(\mathcal{I})} \leq \varepsilon_i, \quad i = 0, 1, \ldots,$$

and so, in particular, $||\mathbf{Q}(\mathbf{u} - \mathbf{u}_\varepsilon)||_{\ell_2(\mathcal{I})} \leq \varepsilon$.

Optimality

To get a benchmark for the convergence rate of an algorithm, we introduce the concept of N-term approximation in $\ell_2(\mathcal{I})$. For $N \in \mathbb{N}_0$, we denote by

$$\Sigma_N := \{\mathbf{c} \in \ell_2(\mathcal{I}) : \#\{\lambda \in \mathcal{I} : c_\lambda \neq 0\} \leq N\}$$

the non-linear subspace of all the vectors in $\ell_2(\mathcal{I})$ with at most N non-trivial entries. For $\mathbf{v} \in \ell_2(\mathcal{I})$, a *best* N*-term approximation* is given by a vector

$$\mathbf{v}_N := \underset{\mathbf{w} \in \Sigma_N}{\arg\min} ||\mathbf{v} - \mathbf{w}||_{\ell_2(\mathcal{I})},$$

which minimizes the approximation error $||\mathbf{v} - \mathbf{w}||_{\ell_2(\mathcal{I})}$ over all vectors $\mathbf{w} \in \Sigma_N$. The error of the best N-term approximation is denoted by

$$\sigma_N(\mathbf{v}) := ||\mathbf{v} - \mathbf{v}_N||_{\ell_2(\mathcal{I})}, \quad \mathbf{v} \in \ell_2(\mathcal{I}).$$

It is easy to see that a best N-term approximation of a vector $\mathbf{v} \in \ell_2(\mathcal{I})$ is obtained by replacing all but the N biggest entries in modulus of $\mathbf{v}$ by zero. In general, $\mathbf{v}_N$ is not unique.

Given an $s > 0$, the approximation spaces

$$\mathcal{A}^s(\mathcal{I}) := \{\mathbf{v} \in \ell_2(\mathcal{I}) \ : \ ||\mathbf{v}||_{\mathcal{A}^s(\mathcal{I})} := \sup_{N \in \mathbb{N}_0} (N+1)^s \sigma_N(\mathbf{v}) < \infty\} \tag{7.1.4}$$

consist of all the vectors in $\ell_2(\mathcal{I})$ that can be approximated with a rate s by vectors in Σ_N. The approximation spaces can be characterized by so-called *weak ℓ_τ spaces*. Given some $0 < \tau < 2$, these are defined by

$$\ell_\tau^w(\mathcal{I}) := \{\mathbf{v} \in \ell_2(\mathcal{I}) : |\mathbf{v}|_{\ell_\tau^w(\mathcal{I})} := \sup_{k \in \mathbb{N}} k^{1/\tau} \gamma_k(\mathbf{v}) < \infty\}, \tag{7.1.5}$$

where $\gamma_k(\mathbf{v})$ denotes the k-th largest entry in modulus of $\mathbf{v}$. The name weak ℓ_2 is justified by the embeddings

$$\ell_\tau \hookrightarrow \ell_\tau^w \hookrightarrow \ell_{\tau+\delta}, \quad \delta \in (0, 2-\tau].$$

We define a quasi-norm on $\ell_\tau^w(\mathcal{I})$ by

$$||\mathbf{v}||_{\ell_\tau^w(\mathcal{I})} := ||\mathbf{v}||_{\ell_2(\mathcal{I})} + |\mathbf{v}|_{\ell_\tau^w(\mathcal{I})}.$$

It satisfies the triangle equality only up to a constant:

$$||\mathbf{v} + \mathbf{w}||_{\ell_\tau^w(\mathcal{I})} \leq C(||\mathbf{v}||_{\ell_\tau^w(\mathcal{I})} + ||\mathbf{w}||_{\ell_\tau^w(\mathcal{I})}),$$

with $C = C(\tau) > 0$ depending on τ only when τ tends to zero. The following result states an equivalence relation between $\mathcal{A}^s(\mathcal{I})$ and $\ell_\tau^w(\mathcal{I})$. For a proof, we refer to [64, Section 5].

Proposition 7.2. *For a given $s > 0$, let $\tau = (s + \frac{1}{2})^{-1}$. Then, it holds*

$$||\mathbf{v}||_{\mathcal{A}^s(\mathcal{I})} \simeq ||\mathbf{v}||_{\ell_\tau^w(\mathcal{I})},$$

with constants depending on τ only when τ tends to zero.

Since we have introduced the approximation and weak ℓ_τ spaces, we are able to define what we understand by an optimal algorithm.

Definition 7.3. Let $\mathcal{F} = \{f_\lambda\}_{\lambda \in \mathcal{I}}$ be a Gelfand frame for $(H_0^t(\Omega), L_2(\Omega), H^{-t}(\Omega))$, $t \in \mathbb{N}_0$, and $\mathcal{G} = D^{-1}\mathcal{F}$. Moreover, we assume that for an $s > 0$ the solution $u \in H_0^t(\Omega)$ of the operator equation (7.1.1) has a representation $u = F_{\mathcal{G}}\mathbf{u}$, cf. (2.1.2), (2.4.4), with $\mathbf{u} \in \ell_\tau^w(\mathcal{I})$, $\tau = (s+\frac{1}{2})^{-1}$. We call a numerical algorithm *(asymptotically) optimal* if for any $\varepsilon > 0$ it produces a $\mathbf{u}_\varepsilon \in \ell_2(\mathcal{I})$ such that

$$||u - F_{\mathcal{G}}\mathbf{u}_\varepsilon||_{H^t(\Omega)} \leq C_1\varepsilon, \quad \text{and} \quad \#\operatorname{supp}\mathbf{u}_\varepsilon \leq C_2 \varepsilon^{-1/s} |\mathbf{u}|_{\ell_\tau^w(\mathcal{I})}^{1/s}, \tag{7.1.6}$$

with constants $C_1, C_2 > 0$, where the number of operations and storage locations to compute $\mathbf{u}_\varepsilon$ is also bounded by a multiple of $\varepsilon^{-1/s}|\mathbf{u}|_{\ell_\tau^w(\mathcal{I})}^{1/s}$.

In other words, a numerical algorithm is called optimal if it asymptotically reproduces the convergence rate of the best N-term approximation.

To ensure that Algorithm 1 is optimal, we have to assume certain additional conditions on the routines **APPLY**, **RHS**, **COARSE** and the orthogonal projector $\mathbf{Q}$. To this end, we have to introduce some concepts. We point them out in the following.

We call the routine **APPLY** s^**-admissible*, if for each $s \in (0, s^*)$, $\tau = (s + \frac{1}{2})^{-1}$, for all $\varepsilon > 0$ and finitely supported vectors $\mathbf{v} \in \ell_2(\mathcal{I})$, with $\mathbf{w}_\varepsilon = \mathbf{APPLY}[\mathbf{A}, \mathbf{v}, \varepsilon]$ the following properties are valid:

($\mathcal{A}_1$) $\# \operatorname{supp} \mathbf{w}_\varepsilon \leq C \varepsilon^{-1/s} |\mathbf{v}|^{1/s}_{\ell^w_\tau(\mathcal{I})}, \quad C > 0;$

($\mathcal{A}_2$) the number of arithmetic operations used to compute $\mathbf{w}_\varepsilon$ is bounded by a fixed multiple of $\varepsilon^{-1/s} |\mathbf{v}|^{1/s}_{\ell^w_\tau(\mathcal{I})} + \# \operatorname{supp} \mathbf{v}$.

In Section 7.2, we point out how to construct a suitable **APPLY** routine. Clearly, whether the **APPLY** routine can be arranged in this way depends on the properties of the system matrix $\mathbf{A}$. We see that s^*-admissibility of the **APPLY** routine can be guaranteed if $\mathbf{A}$ is s^*-computable, cf. Definition 7.8.

The **RHS** routine is called s^**-optimal* if for each $s \in (0, s^*)$, $\tau = (s + \frac{1}{2})^{-1}$, for all $\varepsilon > 0$ and $\mathbf{f} \in \ell_2(\mathcal{I})$, $\mathbf{f}_\varepsilon = \mathbf{RHS}[\mathbf{f}, \varepsilon]$ satisfies the following:

($\mathcal{R}_1$) $\# \operatorname{supp} \mathbf{f}_\varepsilon \leq C \varepsilon^{-1/s} |\mathbf{f}|^{1/s}_{\ell^w_\tau(\mathcal{I})}, \quad C > 0;$

($\mathcal{R}_2$) the number of arithmetic operations used to compute $\mathbf{f}_\varepsilon$ is bounded by a fixed multiple of $\varepsilon^{-1/s} |\mathbf{f}|^{1/s}_{\ell^w_\tau(\mathcal{I})}$.

The practical realization of an appropriate **RHS** routine heavily depends on the structure of the particular right-hand side f in (7.1.1). If f is sufficiently smooth, a standard approach is to approximate the most relevant entries of $\mathbf{f}$ by numerical integration. To predict the location of the large coefficients efficiently, a priori information on the smooth and singular parts of f is used. In the following, we just make the assumption, that there exists a routine **RHS** which fulfils the requirements.

Furthermore, we assume that for all $\varepsilon > 0$ and $\mathbf{v} \in \ell_2(\mathcal{I})$, $\mathbf{v}_\varepsilon = \mathbf{COARSE}[\mathbf{v}, \varepsilon]$ satisfies the following:

($\mathcal{C}_1$) $\# \operatorname{supp} \mathbf{v}_\varepsilon \leq C \inf\{N \in \mathbb{N}_0 : \sigma_N(\mathbf{v}) \leq \varepsilon\}, \quad C > 0;$

($\mathcal{C}_2$) the number of arithmetic operations used to compute $\mathbf{v}_\varepsilon$ is bounded by a fixed multiple of $\# \operatorname{supp} \mathbf{v} + \log(\varepsilon^{-1} ||\mathbf{v}||_{\ell_2(\mathcal{I})})$.

In the exact damped Richardson iteration, the iterates $\mathbf{u}^{(i)}$ are always part of $\operatorname{ran}(\mathbf{A})$. Therefore, the scheme converges to the unique solution $\mathbf{Qu} \in \operatorname{ran}(\mathbf{A})$. However, in an inexact iteration step it is possible that the iterate has components in $\ker(\mathbf{A})$. The inexact scheme still converges – but in general, the approximate solution is of type $\mathbf{Qu} + \mathbf{v}$, $\mathbf{0} \neq \mathbf{v} \in \ker(\mathbf{A})$. Parts of the iterates in $\ker(\mathbf{A})$ do not get reduced in subsequent iteration steps. While this does not affect the convergence of the scheme, it can really hamper the performance of the **APPLY** routine. In fact, components in $\ker(\mathbf{A})$ could lead to an unbounded growth of the ℓ^w_τ-norms of the iterates, making the requirements on an s^*-admissible **APPLY** obsolete. Hence, to have an efficient inexact Richardson scheme, it is necessary to control the kernel contributions to the iterates. In fact, the latter is manageable if

$$\mathbf{Q} : \ell^w_\tau(\mathcal{I}) \to \ell^w_\tau(\mathcal{I})$$

is a bounded operator for $\tau = (s + \frac{1}{2})^{-1}$, $s \in (0, s^*)$. We give some comments later on, under which conditions one can guarantee the boundedness of $\mathbf{Q}$. Let us assume for a moment that it holds true as well as the previously formulated conditions on the various routines. Then, we can state the optimality of Algorithm 1 in the following theorem, cf. [97, Theorem 3.12].

Theorem 7.4. *For some $s^* > 0$, assume that the* **APPLY** *routine is s^*-admissible, the* **RHS** *routine is s^*-optimal, and the* **COARSE** *routine fulfils $(\mathcal{C}_1)$, $(\mathcal{C}_2)$. Moreover, for some $s \in (0, s^*)$, with $\tau = (s + \frac{1}{2})^{-1/2}$, let $\mathbf{Au} = \mathbf{f}$ have a solution $\mathbf{u} \in \ell^w_\tau(\mathcal{I})$. In addition, for some $\check{s} \in (s, s^*)$, with $\check{\tau} = (\check{s} + \frac{1}{2})^{-1/2}$, let $\mathbf{Q} : \ell^w_{\check{\tau}}(\mathcal{I}) \to \ell^w_{\check{\tau}}(\mathcal{I})$ be a bounded operator. Under these conditions, and if the parameter K in Algorithm 1 is sufficiently large – sufficient is*

$$3\rho^K < \theta \min\{1, [C \, |\mathbf{I}_\mathcal{I} - \mathbf{Q}|_{\ell^w_{\check{\tau}}(\mathcal{I}) \to \ell^w_{\check{\tau}}(\mathcal{I})}]^{s/(\check{s}-s)}\},$$

where $C = C(\check{\tau}) > 0$ – then, Algorithm 1 is asymptotically optimal.

Let us briefly discuss the boundedness of the operator $\mathbf{Q}$ in a weak ℓ_τ space. Interpreted as a matrix, the latter can be written as

$$\begin{aligned} \mathbf{Q} &= \{\langle S_\mathcal{G}^{-1} g_\lambda, g_\mu \rangle_{H^{-t}(\Omega) \times H^t_0(\Omega)}\}_{\lambda,\mu \in \mathcal{I}} \\ &= \{d_\mu^{-1} \langle S_\mathcal{G}^{-1} g_\lambda, f_\mu \rangle_{H^{-t}(\Omega) \times H^t_0(\Omega)}\}_{\lambda,\mu \in \mathcal{I}}. \end{aligned} \tag{7.1.7}$$

As already mentioned in Section 2.1, it is often difficult to determine the inverse frame operator $\mathcal{S}_\mathcal{G}^{-1}$, and therewith, the canonical dual frame $S_\mathcal{G}^{-1}\mathcal{G}$. Therefore, the question if $\mathbf{Q}$ is a bounded operator on certain weak ℓ_τ spaces can not be answered in general. For wavelets, only for the very special case $t = 0$, cf. (7.1.1), and additional conditions on the wavelets, the boundedness of $\mathbf{Q}$ could be verified. See [97, Subsection 4.3] for details. In particular for the quarklet case, the canonical dual frames are not explicitly known. Hence, another approach is necessary to guarantee optimality.

The following algorithm is a modification of Algorithm 1. In there, it is assumed to have available a bounded operator $\mathbf{P} : \ell_2(\mathcal{I}) \to \ell_2(\mathcal{I})$ with $\ker(\mathbf{P}) = \ker(\mathbf{A})$. After a fixed amount of iterations, we apply the operator $\mathbf{P}$ to the current iteration. In this way, we prevent the part of the iterates in $\ker(\mathbf{A})$ from piling up too much. As a consequence, the ℓ^w_τ-norm of the iterates stays low, which guarantees an efficient **APPLY** routine.

The matrix-vector multiplication with $\mathbf{P}$ is also executed via the **APPLY** routine. Therefore, for an optimal performance of the scheme, we have to assume that $\mathbf{P}$ allows for an s^*-admissible **APPLY** routine for some $s^* > 0$.

Algorithm 2. MOD_SOLVE$[\mathbf{A}, \mathbf{u}, \varepsilon] \to \mathbf{u}_\varepsilon$:

% Let $\theta < 1/3$ and $K \in \mathbb{N}$ be fixed such that $3\rho^K \|\mathbf{P}\|_{\mathscr{L}(\ell_2(\mathcal{I}))} < \theta$.
% $i := 0$, $\mathbf{u}^{(0)} := 0$, $\varepsilon_0 := \|\mathbf{P}\|_{\mathscr{L}(\ell_2(\mathcal{I}))} \|(\mathbf{A}|_{\mathrm{ran}(\mathbf{A})})^{-1}\|_{\mathscr{L}(\ell_2(\mathcal{I}))} \|\mathbf{f}\|_{\ell_2(\mathcal{I})}$
`while` $\varepsilon_i > \varepsilon$ `do`
  $i := i + 1$
  $\varepsilon_i := 3\rho^K \|\mathbf{P}\|_{\mathscr{L}(\ell_2(\mathcal{I}))}\, \varepsilon_{i-1}/\theta$
  $\mathbf{v}^{(i,0)} := \mathbf{u}^{(i-1)}$
  `for` $j = 1, \dots K$ `do`
    $\mathbf{v}^{(i,j)} := \mathbf{v}^{(i,j-1)} - \omega(\mathbf{APPLY}[\mathbf{A}, \mathbf{v}^{(i,j-1)}, \frac{\rho^j \varepsilon_{i-1}}{2\omega K}] - \mathbf{RHS}[\mathbf{f}, \frac{\rho^j \varepsilon_{i-1}}{2\omega K}])$
  `endfor`
  $\mathbf{z}^{(i)} := \mathbf{APPLY}[\mathbf{P}, \mathbf{v}^{(i,K)}, \frac{\theta \varepsilon_i}{3}]$
  $\mathbf{u}^{(i)} := \mathbf{COARSE}[\mathbf{z}^{(i)}, (1-\theta)\varepsilon_i]$
`enddo`
$\mathbf{u}_\varepsilon := \mathbf{u}^{(i)}$

The next theorem, cf. [97, Theorem 3.11], states the optimality of Algorithm 2.

Theorem 7.5. *For some $s^* > 0$, assume that the* **APPLY** *routine is s^*-admissible for both* **A** *and* **P***, the* **RHS** *routine is s^*-optimal, and the* **COARSE** *routine fulfils $(\mathcal{C}_1)$, $(\mathcal{C}_2)$. Moreover, for some $s \in (0, s^*)$, with $\tau = (s + \frac{1}{2})^{-1/2}$, let $\mathbf{Au} = \mathbf{f}$ have a solution $\mathbf{u} \in \ell_\tau^w$. Then, Algorithm 2 is asymptotically optimal.*

An appropriate operator **P** in matrix representation is given by

$$\mathbf{P} = \{d_\mu^{-1} \langle \tilde{g}_\lambda, f_\mu \rangle_{H^{-t}(\Omega) \times H_0^t(\Omega)}\}_{\lambda,\mu \in \mathcal{I}}, \tag{7.1.8}$$

where $\tilde{\mathcal{G}} = \{\tilde{g}_\lambda\}_{\lambda \in \mathcal{I}}$ is an arbitrary dual frame of $\mathcal{G}$.

Proposition 7.6. *The biinfinite matrix* **P** *as defined in* (7.1.8) *represents a bounded operator $\mathbf{P} : \ell_2(\mathcal{I}) \to \ell_2(\mathcal{I})$ with $\ker(\mathbf{P}) = \ker(\mathbf{A})$. We have $\mathbf{P} = \mathbf{Q}$ if and even if the dual frame $\tilde{\mathcal{G}}$ coincides with the canonical dual frame $S_{\mathcal{G}}^{-1}\mathcal{G}$.*

Proof. Obviously, it holds the relation $\mathbf{P} = \tilde{F}_{\mathcal{G}}^* F_{\mathcal{G}}$, where $\tilde{F}_{\mathcal{G}}^*$ is the analysis operator of the dual frame $\tilde{\mathcal{G}}$. Hence, **P** as a composition of bounded operators $F_{\mathcal{G}} : \ell_2(\mathcal{I}) \to H_0^t(\Omega)$ and $\tilde{F}_{\mathcal{G}}^* : H_0^t(\Omega) \to \ell_2(\mathcal{I})$ is bounded from $\ell_2(\mathcal{I})$ to $\ell_2(\mathcal{I})$. Since any dual frame of $\mathcal{G}$ is a frame itself for $H^{-t}(\Omega)$, the dual analysis operator $\tilde{F}_{\mathcal{G}}^*$ is injective and consequently it is $\ker(\mathbf{P}) = \ker(F_{\mathcal{G}})$. From $\ker(F_{\mathcal{G}}) = TD^{-1}$, cf. (2.4.4), and $\ker(TD^{-1}) = \ker(\mathbf{A})$, cf. Lemma 2.18, we finally deduce $\ker(\mathbf{P}) = \ker(\mathbf{A})$.

The remaining part of the proposition immediately follows by the matrix representations (7.1.7), (7.1.8) of the operators **P** and **Q**, respectively. □

Remark 7.7. Proposition 7.6 generalizes Proposition 4.5 of [109]. There, $\mathbf{P}$ was constructed with respect to an aggregated wavelet frame and a particular non-canonical dual frame.

7.2 Building blocks

In this section, we give concrete realizations of the various routines that we introduced in Section 7.1. Moreover, we introduce the concept of computability and compressibility of biinfinite matrices. Finally, we point out how to construct the operator $\mathbf{P}$ in the case of quarklet frames.

We already mentioned in Section 7.1 that in order to have an s^*-admissible **APPLY** routine, the involved matrices need to have certain properties. In the following, we see that if the matrices are s^*-computable, then, the construction of a suitable **APPLY** routine is feasible. Roughly speaking, s^*-computability means that a matrix can be approximated up to a certain order by sparse matrices in a linear amount of time. Let us specify this in the following definition.

Definition 7.8. For an $s^* > 0$, a biinfinite bounded matrix $\mathbf{A} : \ell_2(\mathcal{I}) \to \ell_2(\mathcal{I})$ is called *s^*-compressible*, if for each $J \in \mathbb{N}_0$ there exists a biinfinite matrix $\mathbf{A}_J : \ell_2(\mathcal{I}) \to \ell_2(\mathcal{I})$, created by dropping entries in $\mathbf{A}$, with a number of non-zero entries in each row and column of order 2^J, and

$$||\mathbf{A} - \mathbf{A}_J||_{\mathscr{L}(\ell_2(\mathcal{I}))} \leq C2^{-Js} =: C_J, \tag{7.2.1}$$

with a constant $C > 0$ and $s \in (0, s^*)$. If, moreover, every entry in $\mathbf{A}_J$ can be computed at unit costs, we call $\mathbf{A}$ *s^*-computable*.

Assuming that $\mathbf{A}$ is s^*-computable, we display the following realization of the inexact matrix-vector multiplication, cf. [97, Subsection 3.2].

$\mathbf{APPLY}[\mathbf{A}, \mathbf{v}, \varepsilon] \to \mathbf{w}_\varepsilon$:

- $q := \lceil \log((\#\operatorname{supp}\mathbf{v})^{1/2}\|\mathbf{v}\|_{\ell_2(\mathcal{I})}\|\mathbf{A}\|_{\mathscr{L}(\ell_2(\mathcal{I}))}2/\varepsilon)\rceil$.
- *Divide the elements of* $\mathbf{v}$ *into sets* $V_0, \dots, V_q$*, where for* $0 \leq i \leq q-1$*,* V_i *contains the elements with modulus in* $(2^{-i-1}\|\mathbf{v}\|_{\ell_2(\mathcal{I})}, 2^{-i}\|\mathbf{v}\|_{\ell_2(\mathcal{I})}]$*, and possible remaining elements are put into* V_q*.*
- *For* $k = 0, 1, \dots,$ *generate vectors* $\mathbf{v}_{[k]}$ *by subsequently extracting* $2^k - \lfloor 2^{k-1} \rfloor$ *elements from* $\bigcup_i V_i$*, starting from* V_0 *and when it is empty continuing with* V_1 *and so forth, until for some* $k = \ell$ *either* $\bigcup_i V_i$ *becomes empty or*

$$\|\mathbf{A}\|_{\mathscr{L}(\ell_2(\mathcal{I}))}\Big\|\mathbf{v} - \sum_{k=0}^{\ell}\mathbf{v}_{[k]}\Big\|_{\ell_2(\mathcal{I})} \leq \varepsilon/2. \tag{7.2.2}$$

In both cases $\mathbf{v}_{[\ell]}$ *may contain less than* $2^\ell - \lfloor 2^{\ell-1} \rfloor$ *elements.*

- *Compute the smallest $J \geq \ell$ such that*

$$\sum_{k=0}^{\ell} C_{J-k} \|\mathbf{v}_{[k]}\|_{\ell_2(\mathcal{I})} \leq \varepsilon/2, \tag{7.2.3}$$

  cf. (7.2.1) *for the constants C_{J-k}.*

- *For $k = 0, \ldots, \ell$, compute the non-zero entries in the matrices $\mathbf{A}_{J-k}$ which have a column index in common with one of the entries of $\mathbf{v}_{[k]}$, and compute*

$$\mathbf{w}_\varepsilon := \sum_{k=0}^{\ell} \mathbf{A}_{J-k} \mathbf{v}_{[k]}. \tag{7.2.4}$$

The just presented **APPLY** routine makes heavy use of a so called *bucket sort*, i.e., the elements of $\mathbf{v}$ do not get completely sorted by their modulus but elements in some range of modulus are put into a particular bucket V_i. The reasoning behind this is that a sorting by modulus cannot be implemented in linear time. It would require the order of $(\#\operatorname{supp}\mathbf{v}) \times \log(\#\operatorname{supp}\mathbf{v})$ operations. With the application of a bucket sort, which was developed in [8, 83], the log-factor can be avoided.

It can be deduced from (7.2.4) that the accuracy with which a column of $\mathbf{A}$ is approximated depends on the size in modulus of the corresponding entry of $\mathbf{v}$. This is what makes the **APPLY** routine and as a result the whole algorithm *adaptive*. In the following Proposition we state the s^*-admissibility of the **APPLY** routine. For a proof we refer to [97, Proposition 3.8].

Proposition 7.9. *For an $s^* > 0$, let $\mathbf{A}$ be s^*-computable. Then,* $\mathbf{APPLY}[\mathbf{A}, \cdot, \cdot]$ *is s^*-admissible.*

The easiest way to think of an implementation of the **COARSE** routine would be to sort the entries of the incoming vector in modulus and to replace all the entries below a certain threshold to zero. But again, the sorting of the entries would cause the multiplication of the amount of operations with a log-factor. Therefore, we again utilize a bucket sort and obtain the following coarsening strategy, cf. [97, Subsection 3.1].

$\mathbf{COARSE}[\mathbf{v}, \varepsilon] \to \mathbf{v}_\varepsilon$:

- $q := \lceil \log((\#\operatorname{supp}\mathbf{v})^{1/2} \|\mathbf{v}\|_{\ell_2(\mathcal{I})}/\varepsilon) \rceil$.
- *Divide the elements of $\mathbf{v}$ into sets $V_0, \ldots, V_q$, where for $0 \leq i \leq q-1$, V_i contains the elements with modulus in $(2^{-i-1}\|\mathbf{v}\|_{\ell_2(\mathcal{I})}, 2^{-i}\|\mathbf{v}\|_{\ell_2(\mathcal{I})}]$, and possible remaining elements are put into V_q.*
- *Create $\mathbf{v}_\varepsilon$ by extracting elements first from V_0 and when it is empty from V_1 and so forth, until $\|\mathbf{v} - \mathbf{v}_\varepsilon\|_{\ell_2(\mathcal{I})} \leq \varepsilon$.*

The following proposition can also be found in [97, Proposition 3.1].

Proposition 7.10. *For a finitely supported vector* $\mathbf{v} \in \ell_2(\mathcal{I})$ *and an* $\varepsilon > 0$ *the routine* **COARSE** *produces a vector* $\mathbf{v}_\varepsilon$ *such that*

$$||\mathbf{v} - \mathbf{v}_\varepsilon||_{\ell_2(\mathcal{I})} \leq \varepsilon.$$

Moreover, $\mathbf{v}_\varepsilon$ *fulfils the conditions* $(\mathcal{C}_1)$, $(\mathcal{C}_2)$.

Quarklet frames in Algorithm 1 and 2

Up to now in this chapter, we introduced the adaptive Richardson iteration and the concept of optimality for an abstract Gelfand frame. In the sequel, we want to take a closer look at the case that our Gelfand frame of choice is the quarklet frame $\boldsymbol{\Psi}_{L_2(\Omega)}$, cf. (6.2.19), as constructed in Chapter 6.

Upon closer examination, we note that there are only a few spots in the construction process of the adaptive method, where the particular choice of the Gelfand frame needs to be considered. The by far most important point that needs to be assured is the s^*-computability of the stiffness matrix corresponding to the frame and the operator equation at hand. We recall, that a matrix is s^*-computable if it is s^*-compressible and its entries can be calculated at unit costs, cf. Definition 7.8. Section 7.3 is devoted to the verification of s^*-compressibility for quarklet frames.

In practice, to calculate the entries in the stiffness matrix, one uses certain quadrature rules. Since the quarklets are piecewise polynomials, an exact quadrature is possible. But it should be taken into account that for quarklets with a high polynomial degree more quadrature points and hence more operations are necessary to get an exact result. One way to circumvent this issue is to only approximate integrals if functions with high polynomial degrees are involved. Another possibility is to cap the quarklets at a particular polynomial degree $p_{\max}$. This approach does not destroy the frame property and allows to estimate the costs to calculate the entries from above by a constant depending only on $p_{\max}$. Actually, the practical implementations which are tested in Chapter 8 have easier to handle data structures if we only consider quarklets up to a fixed level $j_{\max}$ and polynomial degree $p_{\max}$ and are therefore realized in this manner.

Another concern is the boundedness of $\mathbf{Q}$ on ℓ_τ^w. Since the canonical dual quarklet frames are not explicitly known, we are not able to answer this question. Fortunately, we have available the non-canonical dual frame $\tilde{\boldsymbol{\Psi}}_{H^{-s}(\Omega)}$, cf. (6.2.17). If we apply the latter in the operator $\mathbf{P}$, cf. (7.1.8), we obtain the matrix representation

$$\mathbf{P} = \{d_{\boldsymbol{\beta}}^{-1} \langle d_{\boldsymbol{\alpha}} \tilde{\boldsymbol{\psi}}_{\boldsymbol{\alpha}}, \boldsymbol{\psi}_{\boldsymbol{\beta}} \rangle_{H^{-t}(\Omega) \times H_0^t(\Omega)}\}_{\boldsymbol{\alpha},\boldsymbol{\beta} \in \boldsymbol{\nabla}},$$

where $d_{\boldsymbol{\alpha}}$ is the diagonal entry of the matrix

$$D = \operatorname{diag}\left(\left(\sum_{i=1}^{d} (p_i + 1)^{4s+\delta_2}\, 4^{sj_i}\right)^{1/2}\right)_{\boldsymbol{\alpha}=((\boldsymbol{p},\boldsymbol{j},\boldsymbol{k}),n) \in \boldsymbol{\nabla}},$$

cf. (6.2.18). Since $\tilde{\mathbf{\Psi}}_{H^{-s}(\Omega)}$ only contains dual wavelets and apart from that zero functions, we have

$$\mathbf{P}_{\boldsymbol{\alpha},\boldsymbol{\beta}} = 0, \quad \text{for all } \boldsymbol{\alpha} \in \boldsymbol{\nabla} \setminus \boldsymbol{\nabla}^B,\ \boldsymbol{\beta} \in \boldsymbol{\nabla}. \tag{7.2.5}$$

For Algorithm 2 to be optimal, we have to verify that the biinfinite matrix $\mathbf{P}$ is s^*-computable for a sufficiently large $s^* > 0$. The dual wavelets can be constructed explicitly and the locality, smoothness and vanishing moments both on the primal and dual side lead to a justified hope that s^*-computability of $\mathbf{P}$ is indeed provable. Nevertheless, we do not further investigate in this direction for two reasons.

On the one hand, in [79] the actual application of $\mathbf{P}$ in the Richardson iteration is tested in practice with the result that it does not pay off to apply $\mathbf{P}$ to the iterates after a fixed amount of iterations either in respect to computing time or to the spent amount of degrees of freedom. Furthermore, for all test problems in [79] the Richardson iteration converged with optimal order without an application of $\mathbf{P}$. Therefore, the author comes to the conclusion that for the adaptive Richardson method the usage of $\mathbf{P}$ is not necessary.

On the other hand, because of (7.2.5), an approximate multiplication with $\mathbf{P}$ would remove the amount of the iterate that corresponds to those quarklets which are no wavelets, that is to say, the quarklets that are enriched with polynomials. Obviously, this totally contradicts the idea behind an *hp*-method as it nullifies the effects of the polynomial enrichment. Therefore, the numerical experiments in Chapter 8 are all based on Algorithm 1.

7.3 Compression

The aim of this section is to show that the stiffness matrix of the Poisson equation in multiple spatial dimensions is compressible. Similar results for wavelets and diverse operator equations can be found, e.g., in [53, 98].

For the readers' convenience, we consider the multivariate compression estimates only on the unit cube, i.e. $\Omega = \square$. But let us mention that the results carry over to the case of general domains. On the one hand, in the latter case the amount of cubes where a single quarklet has a non-trivial support is uniformly bounded by a finite number which only depends on the space dimension d. On the other hand, the extension to general domains is done in a way that the vanishing moments of the quarklets are preserved. Hence, the following compression estimates can be immediately transferred to extended quarklets.

The stiffness matrix $\mathbf{A}$ of the Poisson equation corresponds to the bilinear form

$$a(u,v) = \int_{\square} \langle \nabla u(x), \nabla v(x) \rangle \, \mathrm{d}x = \sum_{k=1}^{d} \int_{\square} \frac{\partial u}{\partial x_k}(x) \frac{\partial v}{\partial x_k}(x) \, \mathrm{d}x, \quad u,v \in H_0^1(\Omega), \tag{7.3.1}$$

cf. (1.4.9). Given the quarklet frame $\mathbf{\Psi}_{H_0^1(\square)}$, cf. (6.1.19), the individual entries of the stiffness matrix $\mathbf{A}$ are sums of products of univariate integrals. To be more precise, it holds

$$\begin{aligned} w_{\boldsymbol{\mu}}^{H^1} w_{\boldsymbol{\lambda}}^{H^1} a\left((w_{\boldsymbol{\mu}}^{H^1})^{-1}\boldsymbol{\psi}_{\boldsymbol{\mu}}^{\mathbf{0}}, (w_{\boldsymbol{\lambda}}^{H^1})^{-1}\boldsymbol{\psi}_{\boldsymbol{\lambda}}^{\mathbf{0}}\right) &= \sum_{k=1}^{d} \int_{\square} \frac{\partial \boldsymbol{\psi}_{\boldsymbol{\mu}}^{\mathbf{0}}}{x_k}(x) \frac{\partial \boldsymbol{\psi}_{\boldsymbol{\lambda}}^{\mathbf{0}}}{x_k}(x)\,\mathrm{d}x \\ &= \sum_{k=1}^{d} \left(\int_0^1 \frac{\partial \psi_{\boldsymbol{\mu}(k)}^{\vec{0}}}{\partial x_k}(x_k) \frac{\partial \psi_{\boldsymbol{\lambda}(k)}^{\vec{0}}}{\partial x_k}(x_k)\,\mathrm{d}x_k \right. \\ &\qquad \left. \cdot \prod_{\substack{i=1\\ i\neq k}}^{d} \int_0^1 \psi_{\boldsymbol{\mu}(i)}^{\vec{0}}(x_i) \psi_{\boldsymbol{\lambda}(i)}^{\vec{0}}(x_i)\,\mathrm{d}x_i \right). \end{aligned} \tag{7.3.2}$$

With the one dimensional Gramian and stiffness matrices

$$\mathbf{G} := \left\{ \int_0^1 \psi_\lambda^{\vec{0}}(x) \psi_\mu^{\vec{0}}(x)\,\mathrm{d}x \right\}_{\lambda,\mu\in\nabla_{\vec{0}}}, \quad \mathbf{S} := \left\{ \int_0^1 \frac{\partial \psi_\lambda^{\vec{0}}(\partial x)}{x} \frac{\partial \psi_\mu^{\vec{0}}(x)}{\partial x}\,\mathrm{d}x \right\}_{\lambda,\mu\in\nabla_{\vec{0}}},$$

respectively, and the weight matrix $\mathbf{D} := \operatorname{diag}\left(w_{\boldsymbol{\lambda}}^{H^1}\right)_{\boldsymbol{\lambda}\in\boldsymbol{\nabla_0}}$, cf. (6.1.20), the relation (7.3.2) leads to a representation of the stiffness matrix as a sum of Kronecker products,

$$\mathbf{A} = \mathbf{D}^{-1}(\mathbf{S} \otimes \mathbf{G} \otimes \ldots \otimes \mathbf{G} + \ldots + \mathbf{G} \otimes \ldots \otimes \mathbf{G} \otimes \mathbf{S})\mathbf{D}^{-1}. \tag{7.3.3}$$

Hence, to estimate the compressibility properties of the resulting stiffness matrix of the Poisson equation (7.3.1), we can make use of the inner product estimates of the univariate quarks and quarklets, which we derived in the Propositions 4.16 and 5.6.

To ensure that the results carry over to general domains, we assume general boundary conditions $\boldsymbol{\sigma} \in \{0,1\}^d$.

Proposition 7.11. *Let $m \geq 3$, $d \geq 2$. Let the weighted quarklets $(w_{\boldsymbol{\lambda}}^{H^1})^{-1}\boldsymbol{\psi}_{\boldsymbol{\lambda}}^{\boldsymbol{\sigma}}$, $(w_{\boldsymbol{\lambda}'}^{H^1})^{-1}\boldsymbol{\psi}_{\boldsymbol{\lambda}'}^{\boldsymbol{\sigma}}$, $\boldsymbol{\lambda} := (\boldsymbol{p},\boldsymbol{j},\boldsymbol{k})$, $\boldsymbol{\lambda}' := (\boldsymbol{p}',\boldsymbol{j}',\boldsymbol{k}')$ be defined as in* (6.1.19)*, and the bilinear form a as in* (7.3.1)*. Then, it holds*

$$|a((w_{\boldsymbol{\lambda}}^{H^1})^{-1}\boldsymbol{\psi}_{\boldsymbol{\lambda}}^{\boldsymbol{\sigma}}, (w_{\boldsymbol{\lambda}'}^{H^1})^{-1}\boldsymbol{\psi}_{\boldsymbol{\lambda}'}^{\boldsymbol{\sigma}})| \lesssim \prod_{i=1}^{d} \left(1 + |p_i - p_i'|\right)^{m-2-\delta_1/2} 2^{-|j-j'|(m-3/2)}, \tag{7.3.4}$$

with $\delta_1 > 2m-4$.

Proof. There is nothing to prove if $\operatorname{supp}\boldsymbol{\psi}_{\boldsymbol{\lambda}}^{\boldsymbol{\sigma}} \cap \operatorname{supp}\boldsymbol{\psi}_{\boldsymbol{\lambda}'}^{\boldsymbol{\sigma}} = \emptyset$. Otherwise, with the Kronecker deltas δ_{ir} indicating whether the quarklet itself or its first derivative is concerned, we use the tensor product structure (7.3.2) of the quarklets to obtain

$$a(\boldsymbol{\psi}_{\boldsymbol{\lambda}}^{\boldsymbol{\sigma}}, \boldsymbol{\psi}_{\boldsymbol{\lambda}'}^{\boldsymbol{\sigma}}) = \sum_{i=1}^{d} \prod_{r=1}^{d} \left\langle \left(\psi_{p_r,j_r,k_r}^{\sigma_r}\right)^{(\delta_{ir})}, \left(\psi_{p_r',j_r',k_r'}^{\sigma_r}\right)^{(\delta_{ir})} \right\rangle_{L_2(0,1)}.$$

Applying the estimates (5.3.4) and (5.3.5) leads to

$$
\begin{aligned}
|a(\boldsymbol{\psi}^{\boldsymbol{\sigma}}_{\boldsymbol{\lambda}}, \boldsymbol{\psi}^{\boldsymbol{\sigma}}_{\boldsymbol{\lambda}'})| &\leq \sum_{i=1}^{d} \prod_{r=1}^{d} \Big((p_r+1)(p_r'+1)\Big)^{m-2+\delta_{ir}} 2^{\delta_{ir}(j_r+j_r')} 2^{-|j_r-j_r'|(m-1/2-\delta_{ir})} \\
&\leq \sum_{i=1}^{d} \Big((p_i+1)(p_i'+1)\Big) 2^{j_i+j_i'} \\
&\quad \cdot \prod_{r=1}^{d} \Big((p_r+1)(p_r'+1)\Big)^{m-2} 2^{-|j_r-j_r'|(m-3/2)}.
\end{aligned}
$$

Estimating the weights $w_{\boldsymbol{\lambda}}, w_{\boldsymbol{\lambda}'}$ defined in (6.1.20) by the Cauchy-Schwarz inequality, we obtain

$$
w_{\boldsymbol{\lambda}}^{-1} w_{\boldsymbol{\lambda}'}^{-1} \leq \left(\sum_{i=1}^{d} ((p_i+1)(p_i'+1))^{2+\delta_2/2} 2^{j_i+j_i'}\right)^{-1} \prod_{r=1}^{d} ((p_r+1)(p_r'+1))^{-\delta_1/2}.
$$

Combining the previous estimates, we derive

$$
|a(w_{\boldsymbol{\lambda}}^{-1}\boldsymbol{\psi}^{\boldsymbol{\sigma}}_{\boldsymbol{\lambda}}, w_{\boldsymbol{\lambda}'}^{-1}\boldsymbol{\psi}^{\boldsymbol{\sigma}}_{\boldsymbol{\lambda}'})| \leq \prod_{r=1}^{d} ((p_r+1)(p_r'+1))^{m-2-\delta_1/2} 2^{-|j_r-j_r'|(m-3/2)}.
$$

Choosing $\delta_1 > 2m-4$ and using the relation

$$
(p+1)(p'+1) \geq 1 + |p-p'|, \quad p, p' \in \mathbb{N}_0,
$$

we finally get the claim. □

Now, we are ready to state the s^*-compressibiltiy of the stiffness matrix for the Poisson equation in quarklet coordinates for spatial dimensions $d > 1$. For a one-dimensional compression result, we refer to [47, Theorem 5]. The following theorem and Theorem 6.20 can be regarded as the central theoretical results of this thesis as the combination of both justifies the application of multidimensional quarklets in adaptive frame schemes for the numerical solution of linear elliptic operator equations.

Theorem 7.12. *Let $m \geq 3$, $d \geq 2$. Let $\mathbf{A}$ be the stiffness matrix of the Poisson equation discretized by $\boldsymbol{\Psi}_{H^1_{\Gamma_{\boldsymbol{\sigma}}}(\square)}$ defined in* (6.1.19)*. Furthermore, for $J \in \mathbb{N}_0$, with $\boldsymbol{\lambda} = (\boldsymbol{p}, \boldsymbol{j}, \boldsymbol{k}), \boldsymbol{\lambda}' = (\boldsymbol{p}', \boldsymbol{j}', \boldsymbol{k}') \in \boldsymbol{\nabla}_{\boldsymbol{\sigma}}$, define $\mathbf{A}_J$ by setting all entries from $\mathbf{A}$ to zero that satisfy*

$$
a \log_2\Big(\prod_{i=1}^{d} 1 + |p_i - p_i'|\Big) + b|\boldsymbol{j} - \boldsymbol{j}'| > J, \tag{7.3.5}
$$

where $a, b > 0$. Then, for $\delta_1 > 2m-2$, the maximal number of non-zero entries in each row and column of $\mathbf{A}_J$ is of the order

$$
\Big(J^{2d-2} 2^{\frac{J}{a}} + J^{d-1} 2^{\frac{J}{b}}\Big) \begin{cases} J, & a = b, \\ 1, & \textit{otherwise}. \end{cases} \tag{7.3.6}
$$

Moreover, with $\tau := m - 2 - \frac{\delta_1}{2}$ it holds that

$$\|\mathbf{A} - \mathbf{A}_J\|_{\mathcal{L}(\ell_2(\boldsymbol{\nabla}_{\boldsymbol{\sigma}}))} \lesssim \left(J^{d-1}2^{-(m-2)\frac{J}{b}} + J^{2d-2}2^{(1+\tau)\frac{J}{a}}\right) \begin{cases} J, & \frac{a}{b} = -\frac{1+\tau}{m-2}, \\ 1, & \textit{otherwise.} \end{cases} \tag{7.3.7}$$

In particular, $\mathbf{A}$ is s^*-compressible with

$$s^* := \min\{a, b\} \min\{\frac{-1-\tau}{a}, \frac{m-2}{b}\}. \tag{7.3.8}$$

Remark 7.13. In the compression estimate (7.3.8), the exponential factors do not depend on the spatial dimension d. In this sense, quarklet frames provide dimension independent compression rates. For fixed m, τ, in (7.3.8), the optimal choices of a, b yield rates

$$s^* = \begin{cases} -(1+\tau), & \frac{a}{b} \in [-\frac{1+\tau}{m-2}, 1), \\ m-2, & \frac{a}{b} \in [1, -\frac{1+\tau}{m-2}]. \end{cases}$$

The proof of Theorem 7.12 is quite technical. In the course of the proof, we use the following facts:

(i) Let $K \in \mathbb{N}$, $t \in \mathbb{R}_+$. Then,

$$\sum_{n=1}^{K} n^{-t} \leq 1 + \int_1^K x^{-t} \mathrm{d}x \lesssim \begin{cases} K^{1-t}, & t < 1, \\ 1 + \ln(K), & t = 1, \\ 1, & t > 1. \end{cases} \tag{7.3.9}$$

(ii) Let $K \in \mathbb{N}$, $t > 1$. Then,

$$\sum_{n=K}^{\infty} n^{-t} \leq K^{-t} + \int_K^{\infty} x^{-t} \mathrm{d}x \lesssim K^{1-t}. \tag{7.3.10}$$

(iii) Let $r \in \mathbb{N}$, $t \in \mathbb{R}_+$, $L_0 \in \mathbb{N}_0$ and $L_1 := \max\{L_0, r/t - 1\}$. Then,

$$\begin{aligned} \sum_{n=L_0}^{\infty} (1+n)^r e^{-tn} &\lesssim (1+L_1)^r e^{-tL_1} + \int_{L_1}^{\infty} (1+x)^r e^{-tx} \mathrm{d}x \\ &\lesssim (1+L_1)^r e^{-tL_1}. \end{aligned} \tag{7.3.11}$$

Proof of Theorem 7.12. First, we estimate the number of non-trivial entries, i.e., (7.3.6). To simplify the notation we assume $j_0 = 0$ for the minimal level in each coordinate of the quarklet frame $\boldsymbol{\Psi}_{H^1_{\Gamma_{\boldsymbol{\sigma}}}(\square)}$.

Let $\boldsymbol{\lambda} \in \boldsymbol{\nabla}_{\boldsymbol{\sigma}}$ be fixed. The number of $\boldsymbol{\lambda}' \in \boldsymbol{\nabla}_{\boldsymbol{\sigma}}$ with fixed $\boldsymbol{p}'$ that fulfil $\mathrm{supp}\boldsymbol{\psi}^{\boldsymbol{\sigma}}_{\boldsymbol{\lambda}} \cap \mathrm{supp}\boldsymbol{\psi}^{\boldsymbol{\sigma}}_{\boldsymbol{\lambda}'} \neq \emptyset$ is of the order $\prod_{i=1}^{d} \max\{1, 2^{j_i'-j_i}\} \leq 2^{|\boldsymbol{j}-\boldsymbol{j}'|}$. Furthermore,

$$|\{\boldsymbol{j} \in \mathbb{N}_0^d : |\boldsymbol{j}| = l\}| = \binom{l+d-1}{l} \lesssim (1+l)^{d-1}$$

with a constant depending on d holds. Together, this implies that the number of entries in the λ-th row of $\mathbf{A}_J$ is bounded by

$$\begin{aligned}
&\sum_{\substack{\boldsymbol{p}'\in\mathbb{N}_0^d \\ \prod_{i=1}^d 1+|p_i-p_i'|\leq 2^{\frac{J}{a}}}} \sum_{l=0}^{\lfloor \frac{J}{b}-\frac{a}{b}\log_2(\prod_{i=1}^d 1+|p_i-p_i'|)\rfloor} \sum_{\substack{\boldsymbol{j}'\in\mathbb{N}_0^d \\ |\boldsymbol{j}-\boldsymbol{j}'|=l}} 2^{|\boldsymbol{j}-\boldsymbol{j}'|} \\
\leq &\sum_{\substack{\boldsymbol{p}''\in\mathbb{N}^d \\ \prod_{i=1}^d p_i''\leq 2^{\frac{J}{a}}}} \sum_{l=0}^{\lfloor \frac{J}{b}-\frac{a}{b}\log_2(\prod_{i=1}^d p_i'')\rfloor} \binom{l+d-1}{l} 2^l.
\end{aligned}$$

In the latter term, $\binom{l+d-1}{l}$ can be estimated from above by $\left(1+\frac{J}{b}\right)^{d-1}$. Hence,

$$\begin{aligned}
&\sum_{\substack{\boldsymbol{p}'\in\mathbb{N}_0^d \\ \prod_{i=1}^d 1+|p_i-p_i'|\leq 2^{\frac{J}{a}}}} \sum_{l=0}^{\lfloor \frac{J}{b}-\frac{a}{b}\log_2(\prod_{i=1}^d 1+|p_i-p_i'|)\rfloor} \sum_{\substack{\boldsymbol{j}'\in\mathbb{N}_0^d \\ |\boldsymbol{j}-\boldsymbol{j}'|=l}} 2^{|\boldsymbol{j}-\boldsymbol{j}'|} \\
\lesssim &\left(\frac{J}{b}\right)^{d-1} 2^{\frac{J}{b}} \sum_{\substack{\boldsymbol{p}''\in\mathbb{N}^d \\ \prod_{i=1}^d p_i''\leq 2^{\frac{J}{a}}}} \left(\prod_{i=1}^d p_i''\right)^{-\frac{a}{b}}.
\end{aligned} \tag{7.3.12}$$

We separate the last component of $\boldsymbol{p}''$ to obtain

$$\sum_{\substack{\boldsymbol{p}''\in\mathbb{N}^d \\ \prod_{i=1}^d p_i''\leq 2^{\frac{J}{a}}}} \left(\prod_{i=1}^d p_i''\right)^{-\frac{a}{b}} = \sum_{\substack{\boldsymbol{p}''\in\mathbb{N}^{d-1} \\ \prod_{i=1}^{d-1} p_i''\leq 2^{\frac{J}{a}}}} \sum_{p_d''=1}^{2^{\frac{J}{a}}\left(\prod_{i=1}^{d-1} p_i''\right)^{-1}} \left(\prod_{i=1}^d p_i''\right)^{-\frac{a}{b}}.$$

Applying (7.3.9) d times with $K = 2^{J/a}$, $t = \frac{a}{b}$ leads to

$$\begin{aligned}
&\sum_{\substack{\boldsymbol{p}''\in\mathbb{N}^d\\ \prod_{i=1}^d p_i''\le 2^{\frac{J}{a}}}} \Big(\prod_{i=1}^d p_i''\Big)^{-\frac{a}{b}} \\
&\lesssim \sum_{\substack{\boldsymbol{p}''\in\mathbb{N}^{d-1}\\ \prod_{i=1}^{d-1} p_i''\le 2^{\frac{J}{a}}}} \begin{cases} 2^{\frac{J}{a}(1-\frac{a}{b})}\Big(\prod_{i=1}^{d-1} p_i''\Big)^{-1}, & a<b,\\ \Big(1+\frac{J}{a}-\ln(\prod_{i=1}^{d-1} p_i'')\Big)\Big(\prod_{i=1}^{d-1} p_i''\Big)^{-1}, & a=b,\\ \Big(\prod_{i=1}^{d-1} p_i''\Big)^{-1}, & a>b,\end{cases} \qquad (7.3.13)\\
&\lesssim \begin{cases} 2^{\frac{J}{a}(1-\frac{a}{b})}\Big(1+\frac{J}{a}\Big)^{d-1}, & a<b,\\ \Big(1+\frac{J}{a}\Big)^{d}, & a=b,\\ 1, & a>b.\end{cases}
\end{aligned}$$

Finally, by the last estimate, (7.3.12) can be further estimated by

$$\sum_{\substack{\boldsymbol{p}''\in\mathbb{N}^d\\ \prod_{i=1}^d p_i''\le 2^{\frac{J}{a}}}} \Big(\frac{J}{b}\Big)^{d-1} 2^{\frac{J}{b}}\Big(\prod_{i=1}^d p_i''\Big)^{-\frac{a}{b}} \lesssim \begin{cases} \Big(\frac{J}{b}\Big)^{d-1}2^{\frac{J}{a}}\Big(1+\frac{J}{a}\Big)^{d-1}, & a<b,\\ \Big(\frac{J}{b}\Big)^{d-1}2^{\frac{J}{b}}\Big(1+\frac{J}{a}\Big)^{d}, & a=b,\\ \Big(\frac{J}{b}\Big)^{d-1}2^{\frac{J}{b}}, & a>b,\end{cases}$$

which implies (7.3.6).

Next, we derive the compression result (7.3.7). As a standard tool for such estimates we employ the Schur lemma. It states that

$$\begin{aligned}
&\sup_{\boldsymbol{\lambda}\in\boldsymbol{\nabla}_{\boldsymbol{\sigma}}} w_{\boldsymbol{\lambda}}^{-1} \sum_{\boldsymbol{\lambda}'\in\boldsymbol{\nabla}_{\boldsymbol{\sigma}}} |(\mathbf{A})_{\boldsymbol{\lambda},\boldsymbol{\lambda}'} - (\mathbf{A}_J)_{\boldsymbol{\lambda},\boldsymbol{\lambda}'}| w_{\boldsymbol{\lambda}'} \le C,\\
&\sup_{\boldsymbol{\lambda}'\in\boldsymbol{\nabla}_{\boldsymbol{\sigma}}} w_{\boldsymbol{\lambda}'}^{-1} \sum_{\boldsymbol{\lambda}\in\boldsymbol{\nabla}_{\boldsymbol{\sigma}}} |(\mathbf{A})_{\boldsymbol{\lambda},\boldsymbol{\lambda}'} - (\mathbf{A}_J)_{\boldsymbol{\lambda},\boldsymbol{\lambda}'}| w_{\boldsymbol{\lambda}} \le C,
\end{aligned}$$

with weights $w_{\boldsymbol{\lambda}} > 0$, $\boldsymbol{\lambda} \in \boldsymbol{\nabla}_{\boldsymbol{\sigma}}$ and $C > 0$, implies $\|\mathbf{A} - \mathbf{A}_J\|_{\mathcal{L}(\ell_2(\boldsymbol{\nabla}_{\boldsymbol{\sigma}}))} \le C$. The symmetry of $\mathbf{A} - \mathbf{A}_J$ implies that it is sufficient to estimate $\sup_{\boldsymbol{\lambda}\in\boldsymbol{\nabla}_{\boldsymbol{\sigma}}} \alpha_{\boldsymbol{\lambda}}$, where

$$\alpha_{\boldsymbol{\lambda}} := w_{\boldsymbol{\lambda}}^{-1} \sum_{\boldsymbol{\lambda}'\in\boldsymbol{\nabla}_{\boldsymbol{\sigma}}} |(\mathbf{A})_{\boldsymbol{\lambda},\boldsymbol{\lambda}'} - (\mathbf{A}_J)_{\boldsymbol{\lambda},\boldsymbol{\lambda}'}| w_{\boldsymbol{\lambda}'}.$$

We choose weights of the form $w_{\boldsymbol{\lambda}} = 2^{-|\boldsymbol{j}|/2}$. In particular, it holds that

$$\prod_{i=1}^d \max\{1, 2^{j_i'-j_i}\}(2^{-|\boldsymbol{j}|/2})^{-1}2^{-|\boldsymbol{j}'|/2} = 2^{|\boldsymbol{j}-\boldsymbol{j}'|/2}.$$

Therefore, our choice for $w_{\boldsymbol{\lambda}}$, the cut-off rule (7.3.5), together with the decay of the bilinear form (7.3.4), the definition of $x_0(\boldsymbol{p}') := \lceil b^{-1}(J - a\log_2(\prod_{i=1}^d 1 + |p_i - p_i'|))\rceil$

and $\tau = m - 2 - \frac{\delta_1}{2}$ yield

$$\alpha_\lambda \lesssim \sum_{\boldsymbol{p}' \in \mathbb{N}_0^d} \Big(\prod_{i=1}^{d} \Big(1 + |p_i - p_i'|\Big)^\tau \Big) \sum_{l=\max\{0, x_0(\boldsymbol{p}')\}}^{\infty} \sum_{\substack{\boldsymbol{j}' \in \mathbb{N}_0^d \\ |\boldsymbol{j}-\boldsymbol{j}'|=l}} 2^{-|\boldsymbol{j}-\boldsymbol{j}'|(m-2)}.$$

Estimating the sum involving $\boldsymbol{j}'$ leads to

$$\alpha_\lambda \lesssim \sum_{\boldsymbol{p}' \in \mathbb{N}_0^d} \Big(\prod_{i=1}^{d} \Big(1 + |p_i - p_i'|\Big)^\tau \Big) \sum_{l=\max\{0, x_0(\boldsymbol{p}')\}}^{\infty} 2^{-l(m-2)}(1+l)^{d-1}. \tag{7.3.14}$$

Applying (7.3.11) with $L_0 = \max\{0, x_0(\boldsymbol{p}')\}$, $r = d-1$, $t = \ln(2)(m-2)$ and $L_1 = x_1(\boldsymbol{p}') := \max\{0, x_0(\boldsymbol{p}'), \frac{d-1}{\ln(2)(m-2)} - 1\}$, yields

$$\begin{aligned}
\alpha_\lambda &\lesssim \sum_{\boldsymbol{p}' \in \mathbb{N}_0^d} \Big(\prod_{i=1}^{d} \Big(1 + |p_i - p_i'|\Big)^\tau \Big)(1 + x_1(\boldsymbol{p}'))^{d-1} 2^{-(m-2)x_1(\boldsymbol{p}')} \\
&\lesssim \sum_{\substack{\boldsymbol{p}' \in \mathbb{N}_0^d \\ x_0(\boldsymbol{p}') \le \max\{0, -1 + \frac{d-1}{\ln(2)(m-2)}\}}} \prod_{i=1}^{d} \Big(1 + |p_i - p_i'|\Big)^\tau \\
&\quad + \sum_{\substack{\boldsymbol{p}' \in \mathbb{N}_0^d \\ x_0(\boldsymbol{p}') > \max\{0, -1 + \frac{d-1}{\ln(2)(m-2)}\}}} \prod_{i=1}^{d} \Big(1 + |p_i - p_i'|\Big)^\tau (1 + x_0(\boldsymbol{p}'))^{d-1} 2^{-(m-2)x_0(\boldsymbol{p}')}.
\end{aligned} \tag{7.3.15}$$

First, we have a closer look at the first sum of (7.3.15). By splitting the sum and setting $x := (J - b\max\{0, \frac{d-1}{\ln(2)(m-2)} - 1\})/a$, we get

$$\begin{aligned}
&\sum_{\substack{\boldsymbol{p}' \in \mathbb{N}_0^d \\ x_0(\boldsymbol{p}') \le \max\{0, -1 + \frac{d-1}{\ln(2)(m-2)}\}}} \prod_{i=1}^{d} \Big(1 + |p_i - p_i'|\Big)^\tau \\
&= \sum_{\substack{\boldsymbol{p}' \in \mathbb{N}_0^d \\ \log_2(\prod_{i=1}^{d} 1 + |p_i - p_i'|) \ge x}} \prod_{i=1}^{d} (1 + |p_i - p_i'|)^\tau \\
&= \sum_{\boldsymbol{p}' \in \mathbb{N}_0^{d-1}} \prod_{i=1}^{d-1} (1 + |p_i - p_i'|)^\tau \sum_{\substack{p_d' \in \mathbb{N}_0 \\ \log_2(1 + |p_d - p_d'|) \ge x - \log_2(\prod_{i=1}^{d-1} 1 + |p_i - p_i'|)}} (1 + |p_d - p_d'|)^\tau.
\end{aligned}$$

Consequently, by applying (7.3.10) with $t=-\tau$, $K=2^{x-\log_2(\prod_{i=1}^d 1+|p_i-p_i'|)}$ we get

$$\sum_{\substack{\boldsymbol{p}'\in\mathbb{N}_0^d\\ x_0(\boldsymbol{p}')\le\max\{0,-1+\frac{d-1}{\ln(2)(m-2)}\}}}\prod_{i=1}^d(1+|p_i-p_i'|)^\tau$$
$$\lesssim \sum_{\boldsymbol{p}'\in\mathbb{N}_0^{d-1}}\prod_{i=1}^{d-1}(1+|p_i-p_i'|)^\tau \min\{1,2^{(1+\tau)(x-\log_2(\prod_{i=1}^{d-1}1+|p_i-p_i'|))}\}$$
$$\lesssim \sum_{\substack{\boldsymbol{p}'\in\mathbb{N}_0^{d-1}\\ \log_2(\prod_{i=1}^{d-1}1+|p_i-p_i'|)\ge x}}\prod_{i=1}^{d-1}(1+|p_i-p_i'|)^\tau$$
$$+\sum_{\substack{\boldsymbol{p}'\in\mathbb{N}_0^{d-1}\\ \log_2(\prod_{i=1}^{d-1}1+|p_i-p_i'|)< x}}\prod_{i=1}^{d-1}(1+|p_i-p_i'|)^{-1}2^{(1+\tau)x}.$$

It follows by induction and with an estimate similar as in (7.3.13), that

$$\sum_{\substack{\boldsymbol{p}'\in\mathbb{N}_0^d\\ x_0(\boldsymbol{p}')\le\max\{0,-1+\frac{d-1}{\ln(2)(m-2)}\}}}\prod_{i=1}^d(1+|p_i-p_i'|)^\tau\lesssim 2^{(1+\tau)x}(1+x)^{d-1}. \tag{7.3.16}$$

For the second sum, with the definition of $x_0(\boldsymbol{p}')$, we obtain

$$\sum_{\substack{\boldsymbol{p}'\in\mathbb{N}_0^d\\ x_0(\boldsymbol{p}')>\max\{0,-1+\frac{d-1}{\ln(2)(m-2)}\}}}\prod_{i=1}^d\Big(1+|p_i-p_i'|\Big)^\tau(1+x_0(\boldsymbol{p}'))^{d-1}2^{-(m-2)x_0(\boldsymbol{p}')}$$
$$\le \sum_{\substack{\boldsymbol{p}'\in\mathbb{N}_0^d\\ x_0(p')\ge\frac{J}{a}-x}}\prod_{i=1}^d\Big(1+|p_i-p_i'|\Big)^\tau\Big(1+\frac{J}{b}-\frac{a}{b}\log_2\Big(\prod_{i=1}^d 1+|p_i-p_i'|\Big)\Big)^{d-1}$$
$$\cdot\, 2^{-(m-2)\left(\frac{J}{b}-\frac{a}{b}\log_2(\prod_{i=1}^d 1+|p_i-p_i'|)\right)}.$$

We further estimate

$$\sum_{\substack{\boldsymbol{p}'\in\mathbb{N}_0^d\\ x_0(\boldsymbol{p}')>\max\{0,-1+\frac{d-1}{\ln(2)(m-2)}\}}}\prod_{i=1}^d\Big(1+|p_i-p_i'|\Big)^\tau(1+x_0(\boldsymbol{p}'))^{d-1}2^{-(m-2)x_0(\boldsymbol{p}')}$$
$$\le\Big(1+\frac{J}{b}\Big)^{d-1}2^{-(m-2)\frac{J}{b}}\sum_{\substack{\boldsymbol{p}'\in\mathbb{N}_0^d\\ \log_2\prod_{i=1}^{d-1}1+|p_i-p_i'|\le x}}\prod_{i=1}^d\Big(1+|p_i-p_i'|\Big)^{\tau+(m-2)\frac{a}{b}}.$$

Similar estimates as in (7.3.13) imply

$$
\begin{aligned}
&\sum_{\substack{\boldsymbol{p}'\in\mathbb{N}_0^d\\ x_0(\boldsymbol{p}')>\max\{0,-1+\frac{d-1}{\ln(2)(m-2)}\}}} \prod_{i=1}^{d}\Big(1+|p_i-p_i'|\Big)^{\tau}(1+x_0(\boldsymbol{p}'))^{d-1}2^{-(m-2)x_0(\boldsymbol{p}')}\\
&\lesssim \Big(1+\frac{J}{b}\Big)^{d-1}2^{-(m-2)\frac{J}{b}}\begin{cases}2^{(1+\tau+(m-2)\frac{a}{b})x}(1+x)^{d-1}, & \tau+(m-2)\frac{a}{b}>-1,\\ (1+x)^d, & \tau+(m-2)\frac{a}{b}=-1,\\ 1, & \tau+(m-2)\frac{a}{b}<-1,\end{cases}\\
&\lesssim \left(\Big(1+\frac{J}{b}\Big)^{d-1}2^{-(m-2)\frac{J}{b}}+\Big(1+\frac{J}{b}\Big)^{d-1}\Big(1+\frac{J}{a}\Big)^{d-1}2^{(1+\tau)\frac{J}{a}}\right)\\
&\quad\cdot\begin{cases}(1+\frac{J}{a}), & \tau+(m-2)\frac{a}{b}=-1,\\ 1, & \text{otherwise}.\end{cases}
\end{aligned}
\tag{7.3.17}
$$

Finally, combining (7.3.15) - (7.3.17) yields (7.3.7). □

Chapter 8

Numerical Experiments

In this chapter, we test the adaptive quarklet frame algorithm as presented in Chapter 7 for the Poisson equation on several domains in one and two spatial dimensions. The aim is to verify the convergence of the scheme, as it has been stated in Proposition 7.1, in practice. Furthermore, we want to study the convergence rates of the various problems. Also, the qualitative behaviour of the quarklet coefficients is of particular interest to us as we want to figure out how much the quarklets on different levels and polynomial degrees contribute to the approximated solutions. The test examples are chosen in a way that, on the one hand, they fit into the quarklet approach and, on the other hand, we have a certain comparability to other typical test problems for adaptive algorithms, see, e.g., [41,43,77,80,92,109]. Let us mention that the example on the L-shaped domain was already tested in [44].

8.1 The Poisson equation on the unit interval

As a model problem on the unit interval, we consider the variational formulation of the Poisson equation with homogeneous Dirichlet boundary conditions

$$\int_0^1 \langle \nabla u(x), \nabla v(x) \rangle \,\mathrm{d}x = f(v), \quad u, v \in H_0^1(0,1),\ f \in H^{-1}(0,1), \tag{8.1.1}$$

cf. (1.4.4) and Example 1.3. We choose the right-hand side as the functional $f(v) := 4v(\frac{1}{2}) + \int_0^1 g(x)v(x)\,\mathrm{d}x$ with

$$g(x) := -9\pi^2 \sin(3\pi x) - 4.$$

Straight calculation leads to the solution

$$u(x) = -\sin(3\pi x) + \begin{cases} 2x^2, & x \in [0, \frac{1}{2}), \\ 2(1-x)^2, & x \in [\frac{1}{2}, 1], \end{cases} \tag{8.1.2}$$

which is depicted in Figure 8.1.

This is a classical test problem for adaptive wavelet schemes, which was also examined, e.g., in [43,80,92,109] . The reason for this is that the solution has a slightly

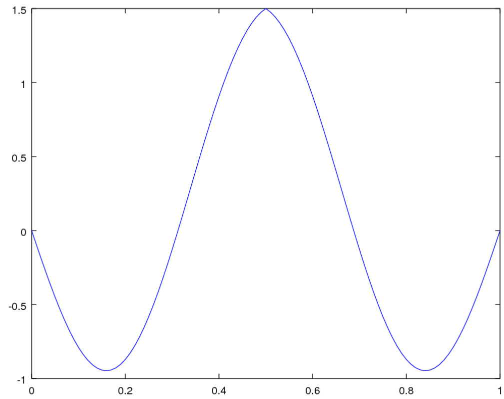

Figure 8.1: Exact solution of the one-dimensional test problem (8.1.1).

higher Besov than Sobolev regularity due to the singularity at $x = \frac{1}{2}$. Since the Besov regularity determines the order of convergence for optimal adaptive wavelet schemes, they outperform uniform schemes, whose convergence order is governed by the Sobolev regularity. Particularly for the test problem at hand, the rate of convergence for the adaptive wavelet schemes is only limited by the order of the wavelets.

For the adaptive quarklet scheme, we do know that it should perform at least as good as an adaptive wavelet scheme based on the underlying Primbs wavelet Riesz basis. Hence, the convergence order of the underlying wavelet basis serves as a lower bound for the convergence order of the quarklet scheme. By now, we do not know how to describe an upper bound for the convergence order. To get an upper bound, one has to answer the following question: how do the function spaces look like, which contain the functions that can be approximated by an N-term quarklet approximation at a certain order. If the solution of an operator equation is part of this function space, then, the convergence order of the best-N-term quarklet approximation is the benchmark for an optimal adaptive quarklet scheme. Regarding this, the quarklet scheme has an advantage over a wavelet scheme if the convergence rate of the best-N-term quarklet approximation to the solution is higher than the rate of the best-N-term wavelet approximation.

Although we do not have an answer yet to the theoretical question, we do have some hope that our scheme is well-suited to the problem (8.1.1). This is due to the shape of the solution (8.1.2). The smooth sinusoidal part should be depicted well by the smooth quarklets of high polynomial order on low levels, whereas quarklets on a high level should reproduce the singularity.

We test Algorithm 1 with the quarklet frame $\Psi_{H_0^1(0,1)}$ with order $m = 3$, $\tilde{m} = 3$ vanishing moments and the weight parameters $\delta_1 = 6$, $\delta_2 = 2$, cf. Theorem 5.9. The minimal quarklet level appears to be $j_0 = 3$. As usual, we assign the level $j_0 - 1 = 2$ to the quarks. With the designated parameters, a certain compressibility of the stiffness matrix is guaranteed by Theorem 7.12.

For performance reasons, we made slight adaptations to Algorithm 1 for both the one and two-dimensional tests. The main change is the call of the **COARSE** routine after any call of the routine **APPLY**. By doing this, we prevent a rapidly growing number of degrees of freedom. However, with this additional coarsening, the thresholding after the inner loop can be omitted. Furthermore, we assume $||\mathbf{A}||_{\mathscr{L}(\ell_2(\mathcal{I}))} = ||\mathbf{A}|_{\operatorname{ran}\mathbf{A}}^{-1}||_{\mathscr{L}(\ell_2(\mathcal{I}))} = 1$, although this is maybe too optimistic. Similar adaptations have been made, e.g., in [80, 109] where they turned out to be uncritical.

On the left-hand side of Figure 8.2, we plotted the residual error $||\mathbf{A}\mathbf{u}^{(i)} - \mathbf{f}||_{\ell_2(\nabla)}$ versus the degrees of freedom of the iterates $\mathbf{u}^{(i)}$ in double logarithmic scale. The residual error serves as an upper bound for the $H^1(0,1)$-norm of the continuous residual due to the norm equivalence $||\mathbf{A}\mathbf{u}^{(i)} - \mathbf{f}||_{\ell_2(\nabla)} \sim ||F_{\Psi_{H_0^1(0,1)}}\mathbf{u}^{(i)} - u||_{H^1(0,1)}$, where $F_{\Psi_{H_0^1(0,1)}}$ is the synthesis operator of the frame $\Psi_{H_0^1(0,1)}$, cf. (2.1.2). On the right-hand side, the degrees of freedom of $\mathbf{u}^{(i)}$ are substituted by the spent CPU time. A convergence rate of approximately $s = 2$ can be deduced with respect to both the degrees of freedom and the CPU time. However, for the CPU time this rate appears after an initial phase.

If we take a look at the quarklet coefficients in Figure 8.3, we assess the predicted behaviour. For polynomial order $p > 0$ we have large entries in modulus on the quark level and on the low quarklet levels representing the sinusoidal part. The singular part is represented by the high level quarklets in the region. This phenomenon is visible for all polynomial orders, but the quarklets for $p = 0$ seem to have the biggest impact.

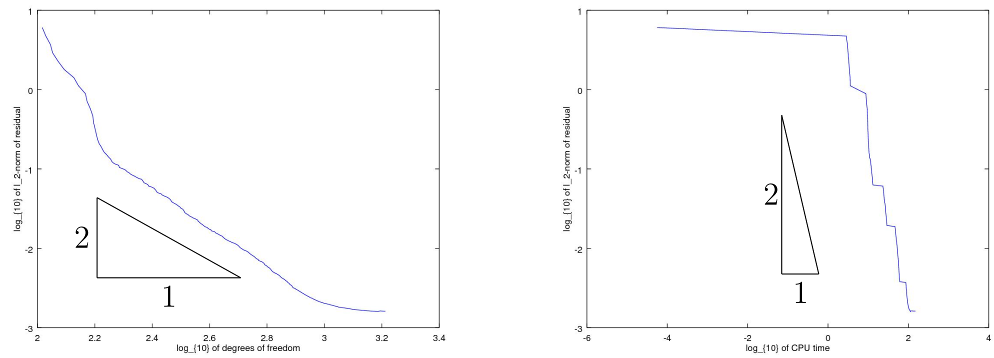

Figure 8.2: Adaptive error asymptotics for the test problem on the unit interval with respect to the amount of degrees of freedom (left) and the CPU time (right).

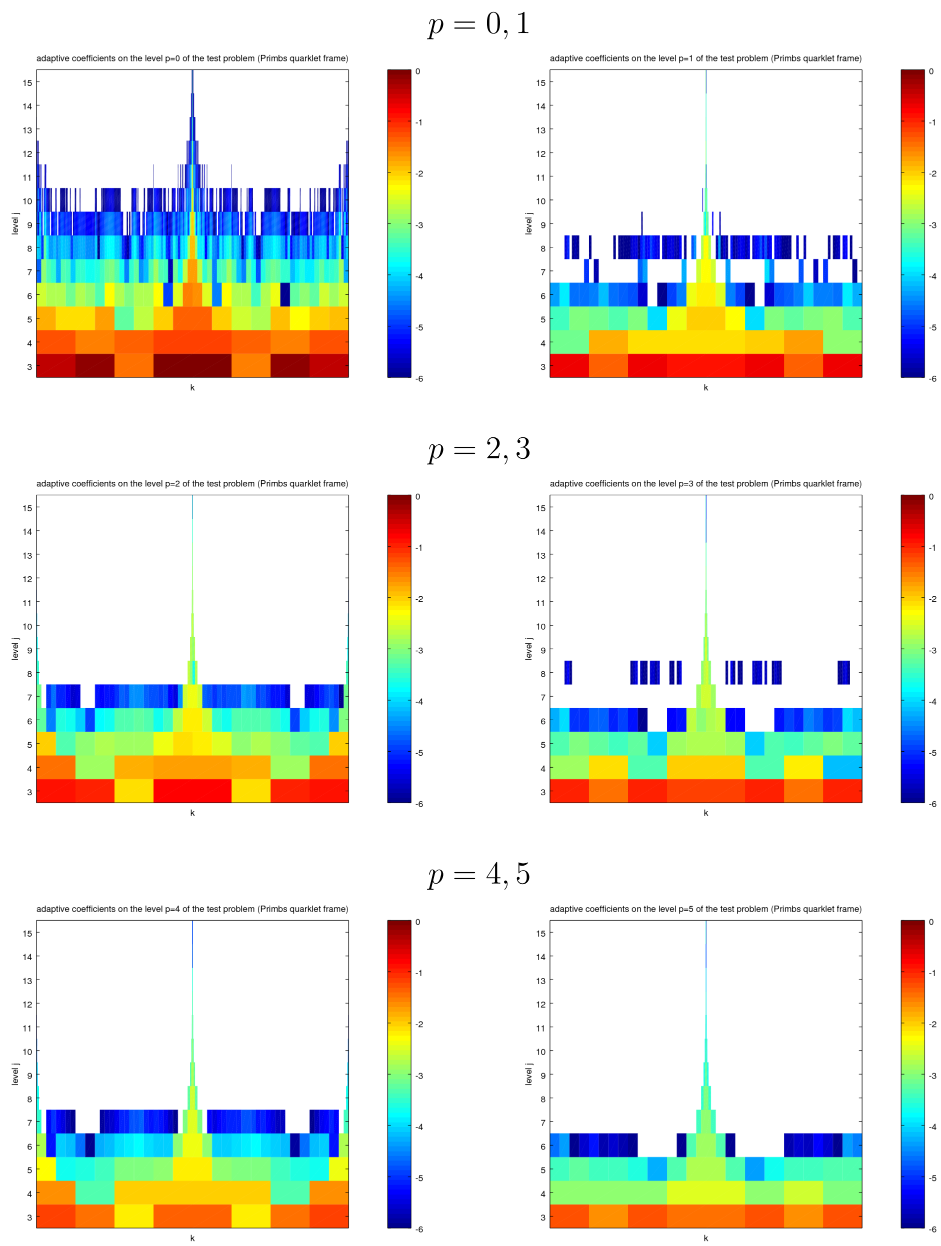

Figure 8.3: Distribution of the quarklet coefficients for the approximate solution of the one dimensional test problem for different polynomial orders. Line-by-line: $p = 0, \ldots, 5$.

8.2 The Poisson equation in two-dimensional bounded domains

For the numerical experiments in two spatial dimensions we consider the Poisson equation with homogeneous Dirichlet boundary conditions on diverse bounded domains $\Omega \subset \mathbb{R}^2$. In this case, the variational formulation of the problem, cf. (1.4.4), is given by

$$a(u,v) = f(v), \quad u, v \in H_0^1(\Omega),\, f \in H^{-1}(\Omega), \tag{8.2.1}$$

where the bilinear form $a : H_0^1(\Omega) \times H_0^1(\Omega) \mapsto \mathbb{R}$ can be written as

$$a(u,v) = \sum_{k=1}^{2} \int_{\Omega} \frac{\partial u}{\partial x_k}(x) \frac{\partial v}{\partial x_k}(x)\, \mathrm{d}x.$$

cf. Example 1.3. We pick the examples in a way that the occurring domains can be decomposed into non-overlapping cubes. Hence, they fit into the construction process as outlined in Section 4.2. Throughout this section, we fix the parameters $m = 3$, $\tilde{m} = 3$, $\delta_1 = 6$, $\delta_2 = 2$, for the quarklet frame $\mathbf{\Psi}_{H^s_{\Gamma_{\boldsymbol{\sigma}}}(\square)}$ on the unit cube with $\boldsymbol{\sigma} \in (\{0,1\}^2)^2$, cf. Theorem 6.6. Again, the compressibility of the stiffness matrix with respect to the Poisson equation and the quarklet frame is a consequence of Theorem 7.12. Furthermore, we choose $\omega = 0.5$ as the relaxation parameter in all three examples.

As a result of the chosen order m and vanishing moments $\tilde{m}$ the minimal quarklet level is $\boldsymbol{j}_0 = (3,3)$. We allocate multivariate quarks to the level $(2,2)$. The levels $(j_1, 2)$, $(2, j_2)$ with $j_1, j_2 \geq 3$ belong to multivariate quarklets which are a tensor product of a univariate quark and a univariate quarklet.

L-shaped domain

The first two-dimensional test example is the Poisson equation on the L-shaped domain $\Omega = (-1,1)^2 \setminus [0,1)^2$. The latter is a prominent test domain for adaptive algorithms, since the reentrant corner induces certain singular solutions, see, e.g., [72], that have to be resolved by the numerical method under investigation. To obtain a quarklet frame for Ω we split the domain as explained in Section 6.2, into the subdomains $\Omega_0^{(0)} = \{(-1,0)\} + (0,1)^2$, $\Omega_1^{(0)} = \{(-1,-1)\} + (0,1)^2$ and $\Omega_2^{(0)} = \{(0,-1)\} + (0,1)^2$. These subdomains with their incorporated boundary conditions are depicted in Figure 8.4. The arrows indicate the direction of the non-trivial extension. The order in which the extension are executed is irrelevant. By proceeding this way, conditions $(\mathcal{D}_1)$-$(\mathcal{D}_5)$, cf. Subsection 6.2.1, are fulfilled.

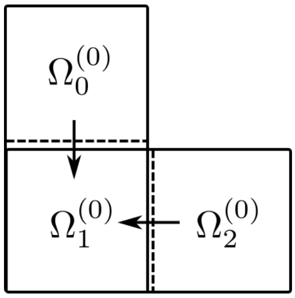

Figure 8.4: Extension process for the L-shaped domain. Dotted lines indicate free boundary conditions, straight lines indicate zero boundary conditions.

We equip the subdomains $\Omega_0^{(0)}$, $\Omega_1^{(0)}$ and $\Omega_2^{(0)}$ with the frames

$$\begin{aligned} \mathbf{\Psi}_0 &= \mathbf{\Psi}_{H^s_{\Gamma_{\boldsymbol{\sigma}_0}}(\square)}\left(\cdot + \begin{pmatrix}1\\0\end{pmatrix}\right), & \boldsymbol{\sigma}_0 &= (1,1)\times(0,1),\\ \mathbf{\Psi}_1 &= \mathbf{\Psi}_{H^s_{\Gamma_{\boldsymbol{\sigma}_1}}(\square)}\left(\cdot + \begin{pmatrix}1\\1\end{pmatrix}\right), & \boldsymbol{\sigma}_1 &= (1,1)\times(1,1),\\ \mathbf{\Psi}_2 &= \mathbf{\Psi}_{H^s_{\Gamma_{\boldsymbol{\sigma}_2}}(\square)}\left(\cdot + \begin{pmatrix}0\\1\end{pmatrix}\right), & \boldsymbol{\sigma}_2 &= (0,1)\times(1,1), \end{aligned}$$

respectively. To obtain a quarklet frame for $H_0^1(\Omega)$ we extend $\mathbf{\Psi}_0$ and $\mathbf{\Psi}_2$ as described in Section 6.2. Essentially, this corresponds to reflecting those quarklets that do not vanish at the boundaries at the dotted lines in Figure 8.4. After that, we take the union of the two resulting sets of functions with $\mathbf{\Psi}_1$. We choose the right-hand side in (8.2.1) in such a way that the exact the solution is the sum of $\sin(2\pi x)\sin(2\pi y)$, $(x,y)\in\Omega$ and the singularity function

$$\mathcal{S}(r,\theta) := 5\zeta(r)r^{2/3}\sin\left(\frac{2}{3}\theta\right), \tag{8.2.2}$$

with (r,θ) denoting polar coordinates with respect to the reentrant corner at the origin, and where ζ is a smooth truncation function on $[0,1]$, which is identically 1 on $[0,r_0]$ and 0 on $[r_1,1]$, for some $0 < r_0 < r_1 < 1$, see again [72] for details. In Figure 8.5, the exact solution and the right-hand side of the test problem are depicted.

Singularity functions of the form (8.2.2) are typical examples of functions that have a very high Besov regularity but a very limited L_2-Sobolev smoothness due to the strong gradient at the reentrant corner. Therefore, for this kind of solution it can be expected that adaptive (h-)algorithms outperform classical uniform schemes. We refer, e.g., to [37, 41] for a detailed discussion of these relationships.

We also expect that the very smooth sinusoidal part of the solution can be very well approximated by piecewise polynomials of high order. Therefore, our test example is contained in the class of problems for which we expect a strong performance of adaptive quarklet schemes.

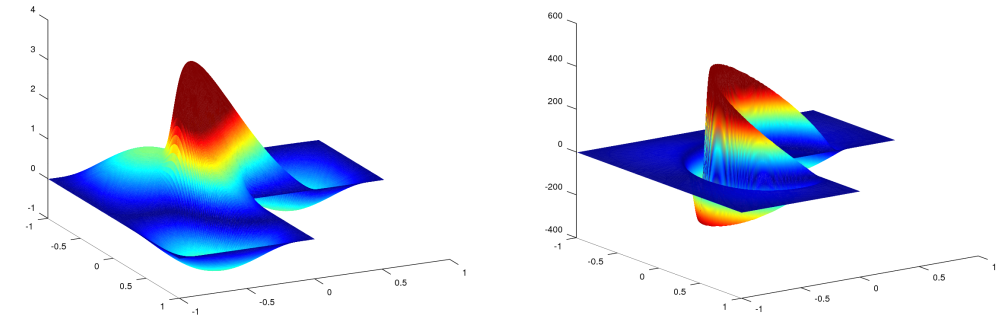

Figure 8.5: Exact solution and right-hand-side of the test problem on the L-shaped domain.

To solve the problem numerically we use again Algorithm 1. In Figure 8.6 one observes the ℓ_2-norm of the residual $\mathbf{Au}^{(j)} - \mathbf{F}$ plotted against the degrees of freedom of the approximates $\mathbf{u}^{(j)}$ and against the spent CPU time. We see that the algorithm is convergent with convergence order $\mathcal{O}(N^{-2})$. In [41] an adaptive wavelet frame approach based on overlapping domain decompositions was used to solve a similar problem. Since the singularity function (8.2.2) has arbitrary high Besov regularity, the convergence order of adaptive wavelet schemes only depends on the order of the underlying spline system. For $m = 3$, one gets, after an initial phase, the approximation rate $\mathcal{O}(N^{-1})$, see again [41, Subsection 6.2] for details. If we compare this to our approach, we see that the adaptive quarklet schemes outperform the adaptive wavelet schemes in terms of degrees of freedom.

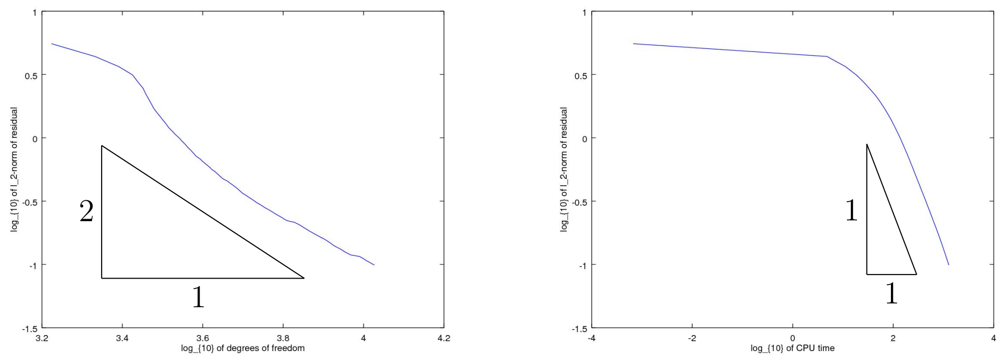

Figure 8.6: Adaptive error asymptotics for the test problem on the L-shaped domain with respect to the amount of degrees of freedom (left) and the CPU time (right).

Figure 8.6 also shows that the CPU time that is currently needed might be im-proved. This observation indicates that maybe the compression estimates outlined in Section 7.3 are still suboptimal. Refined compression estimates based, e.g., on second compression ideas (see [93]) will be the topic of further research.

Figure 8.7 illustrates two approximations to the solution of the test example after 10 and 100 iterations, respectively. The characteristics of the exact solution are clearly visible after only 10 iterations, while the absolute pointwise values in particular at the singularity are considerably smaller in comparison to the exact solution, cf. Figure 8.5. After 100 iterations, however, also the quantitative behaviour of the approximation comes very close to the exact solution.

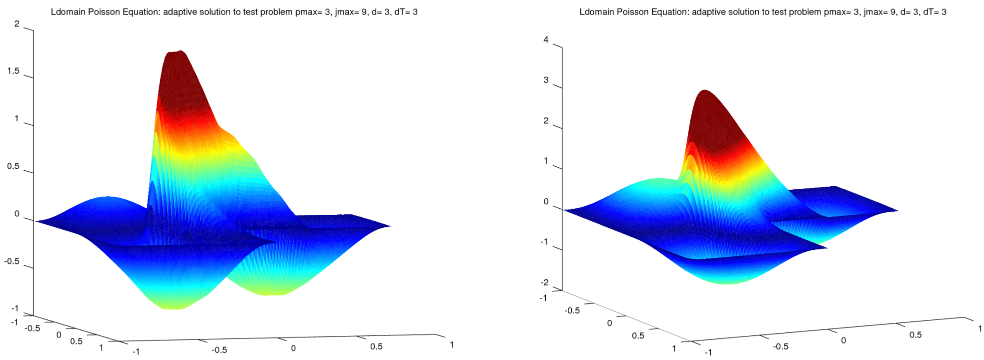

Figure 8.7: Approximate adaptive solution of the test problem on the L-shaped domain after 10 (left) and 100 (right) iterations.

In Figures 8.8 - 8.10 the distribution of selected coefficients $\mathbf{u} = \{u_{\boldsymbol{\alpha}}\}_{\boldsymbol{\alpha}\in\nabla}$ of the approximate solution $\sum_{\boldsymbol{\alpha}\in\nabla} u_{\boldsymbol{\alpha}}(\boldsymbol{w}_{\boldsymbol{\alpha}}^{H^1})^{-1}\boldsymbol{\psi}_{\boldsymbol{\alpha}}$ are plotted with respect to their modulus in logarithmic scale. In every single figure, the coefficients for one fixed level $\boldsymbol{j}$ are plotted, with $|\boldsymbol{p}|$ increasing in vertical direction. We can see that qualitatively the distribution of the coefficients behaves as expected in the sense that for low levels $\boldsymbol{j}$ frame elements with higher polynomial degree are requested to reproduce the smooth part of the solution. On the higher level $\boldsymbol{j} = (4,4)$ the demand for high polynomial quarklets ceases. In particular, for $|\boldsymbol{p}| > 3$ no non-zero coefficient emerges in the expansion of the approximate solution.

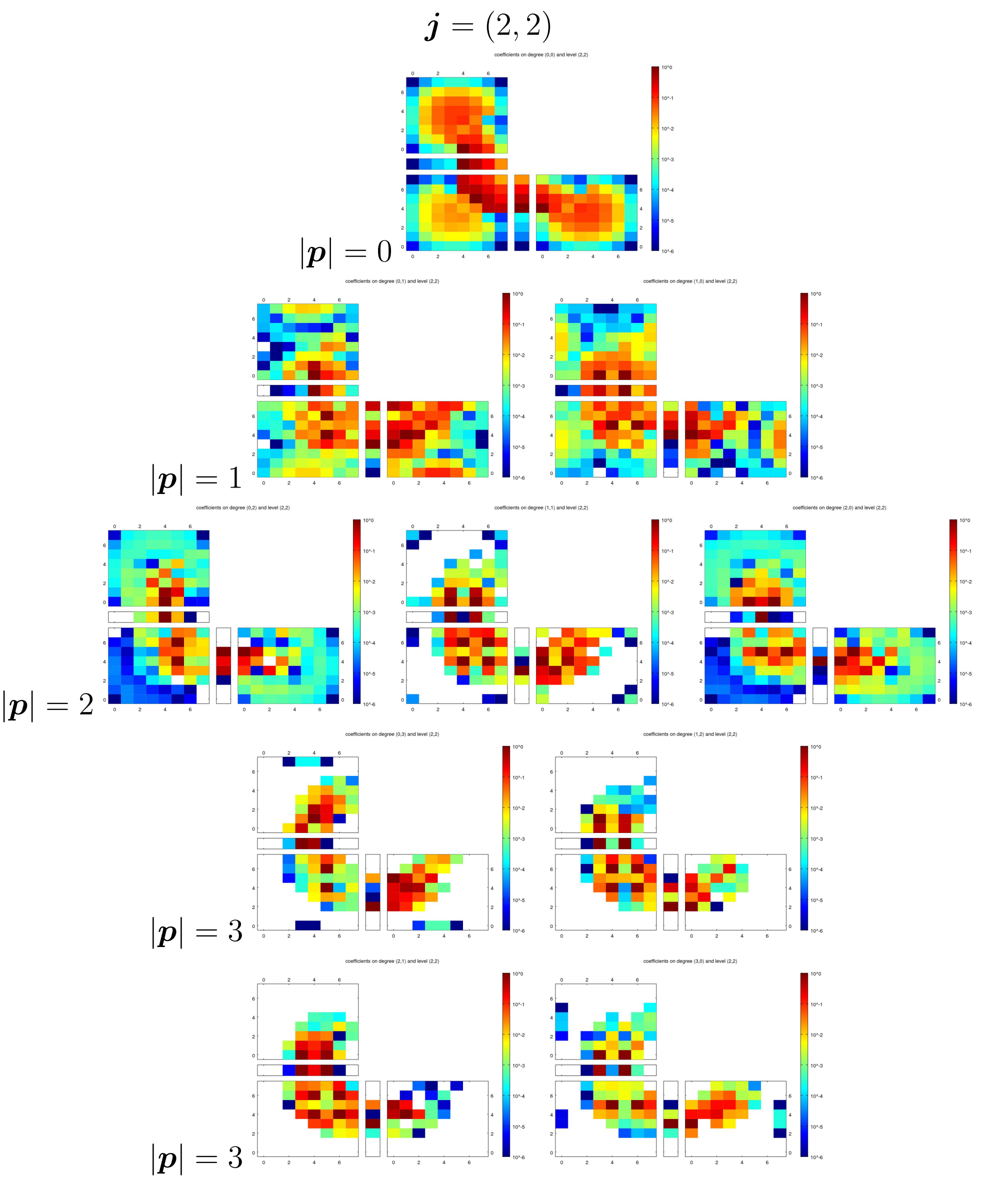

Figure 8.8: Coefficients of the approximate solution to the test problem on the L-shaped domain for the quark level $\boldsymbol{j} = (2, 2)$.

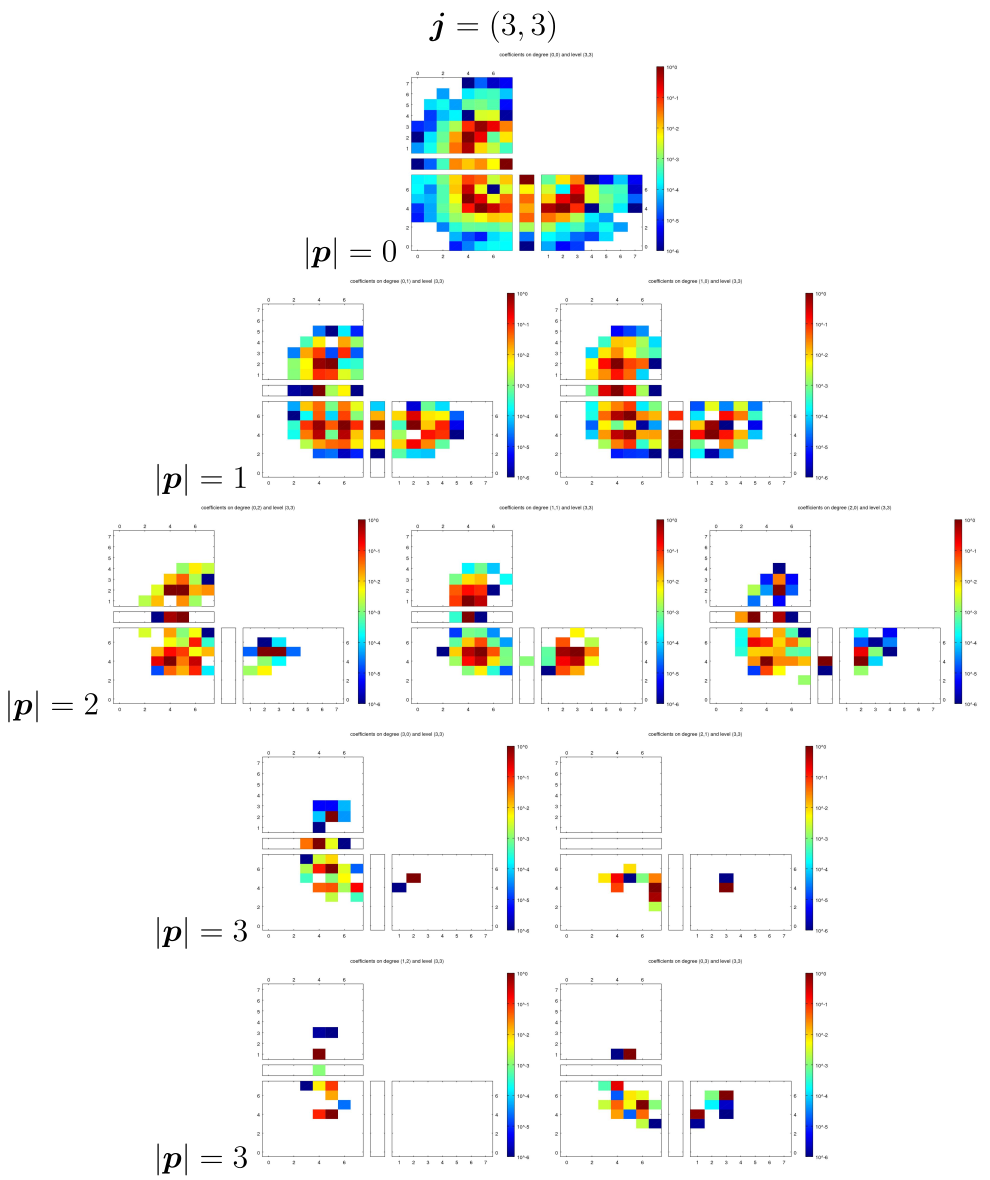

Figure 8.9: Coefficients of the approximate solution to the test problem on the L-shaped domain for the lowest quarklet level $\boldsymbol{j} = (3,3)$.

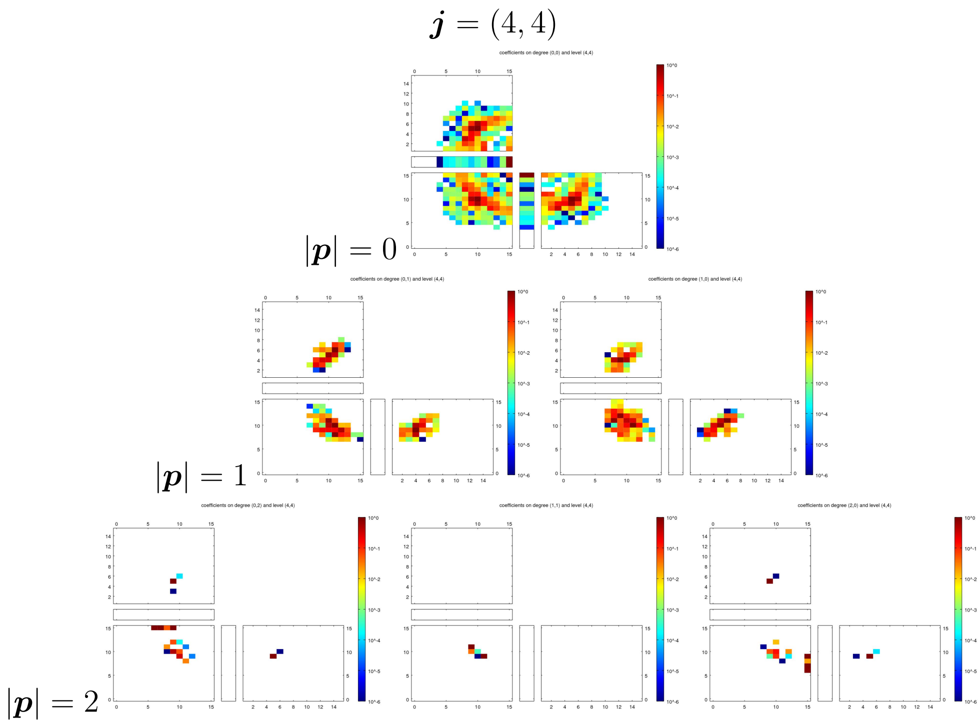

Figure 8.10: Coefficients of the approximate solution to the test problem on the L-shaped domain for the quarklet level $\boldsymbol{j} = (4, 4)$.

Ring-shaped domain

We now consider a second two-dimensional test example. Our aim is to show that we are not restricted to the standard test case of the L-shaped domain but are able to reproduce the results also on more general domains. Therefore, we decided to take the ring-shaped $\Omega = (-1,2)^2 \setminus [0,1]^2$ as our domain of choice. Similar to the L-shaped domain, it has reentrant corners which lead to singularities of the solution of operator equations, which are usually resolved well by adaptive methods.

We choose the quarklet frames on the respective subcubes $\Omega_i^{(0)}$, cf. Figure 8.11, as

$$\mathbf{\Psi}_0 = \mathbf{\Psi}_{H^s_{\Gamma_{\boldsymbol{\sigma}_0}}(\square)}\left(\cdot + \begin{pmatrix}1\\1\end{pmatrix}\right), \qquad \mathbf{\Psi}_1 = \mathbf{\Psi}_{H^s_{\Gamma_{\boldsymbol{\sigma}_1}}(\square)}\left(\cdot + \begin{pmatrix}0\\1\end{pmatrix}\right),$$
$$\mathbf{\Psi}_2 = \mathbf{\Psi}_{H^s_{\Gamma_{\boldsymbol{\sigma}_2}}(\square)}\left(\cdot + \begin{pmatrix}-1\\1\end{pmatrix}\right), \qquad \mathbf{\Psi}_3 = \mathbf{\Psi}_{H^s_{\Gamma_{\boldsymbol{\sigma}_3}}(\square)}\left(\cdot + \begin{pmatrix}-1\\0\end{pmatrix}\right),$$
$$\mathbf{\Psi}_4 = \mathbf{\Psi}_{H^s_{\Gamma_{\boldsymbol{\sigma}_4}}(\square)}\left(\cdot + \begin{pmatrix}-1\\-1\end{pmatrix}\right), \qquad \mathbf{\Psi}_5 = \mathbf{\Psi}_{H^s_{\Gamma_{\boldsymbol{\sigma}_5}}(\square)}\left(\cdot + \begin{pmatrix}0\\-1\end{pmatrix}\right),$$
$$\mathbf{\Psi}_6 = \mathbf{\Psi}_{H^s_{\Gamma_{\boldsymbol{\sigma}_6}}(\square)}\left(\cdot + \begin{pmatrix}1\\-1\end{pmatrix}\right), \qquad \mathbf{\Psi}_7 = \mathbf{\Psi}_{H^s_{\Gamma_{\boldsymbol{\sigma}_7}}(\square)}\left(\cdot + \begin{pmatrix}1\\0\end{pmatrix}\right),$$

with the boundary conditions

$$\boldsymbol{\sigma}_i = \begin{cases} (1,1)\times(1,1), & i \in \{0,2,4,6\},\\ (0,0)\times(1,1), & i \in \{1,5\},\\ (1,1)\times(0,0), & i \in \{3,7\}, \end{cases}$$

By extending the frames $\mathbf{\Psi}_1$, $\mathbf{\Psi}_3$, $\mathbf{\Psi}_5$, $\mathbf{\Psi}_7$ as depicted in Figure 8.11, the conditions $(\mathcal{D}_1)$-$(\mathcal{D}_5)$, cf. Subsection 6.2.1, are fulfilled and we end up with a quarklet frame for $H^1_0(\Omega)$. As for the case of the L-shaped domain, the order in which the different extensions are made is irrelevant. See Section 6.2 for details on the extension process.

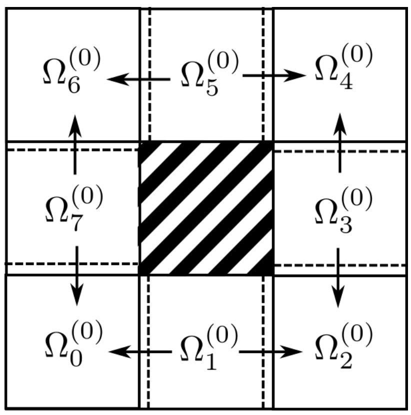

Figure 8.11: Extension process for the ring-shaped domain. Dotted lines indicate free boundary conditions, straight lines indicate zero boundary conditions. The arrows point at the direction of the nontrivial extension.

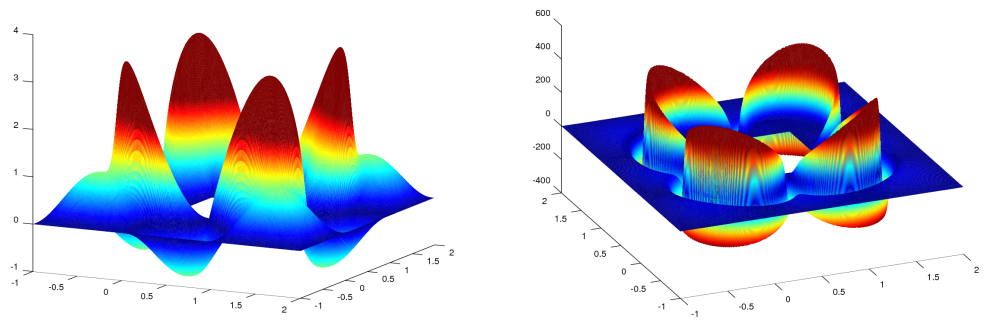

Figure 8.12: Exact solution (left) and right-hand-side (right) of the test problem on the ring-shaped domain.

We choose the right-hand side in (8.2.1) such that the exact solution is given by the sum of $\sin(2\pi x)\sin(2\pi y)$, $(x,y) \in \Omega$, and four singularity functions (8.2.2) situated around each of the reentrant corners. In Figure 8.12, the exact solution and the corresponding right-hand side are depicted. A similar test example without the sinusoidal part was investigated, e.g., in [109, Subsection 7.2.3]. There, for aggregated wavelet frames of the same order and vanishing moments as in here, an adaptive Schwarz method produced a convergence rate of order $s = 1$.

From Figure 8.13 we take again a convergence rate of $s = 2$ with respect to the amount of active indices in the quarklet expansion of the approximations. Hence, we outperform a classical wavelet frame algorithm also in this case. Furthermore, with the slower convergence with respect to the CPU time, we note the same effect as for the test example on the L-shaped domain.

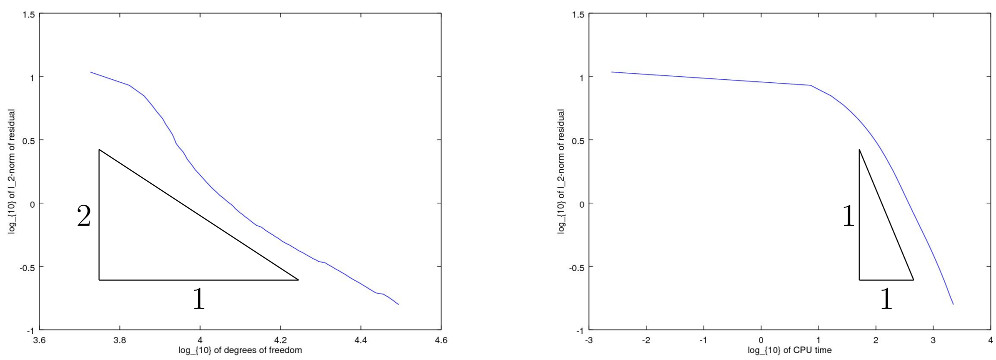

Figure 8.13: Adaptive error asymptotics for the test problem on the ring-shaped domain with respect to the amount of degrees of freedom (left) and the CPU time (right).

The illustrations in Figure 8.14 of two iterates of the adaptive algorithm and in Figures 8.15 - 8.17 of selected quarklet coefficients once again punctuate the consistency of the adaptive quarklet method as analogous phenomena in comparison to the L-shaped domain example can be deduced, cf. the explanations at the end of the first part of this section.

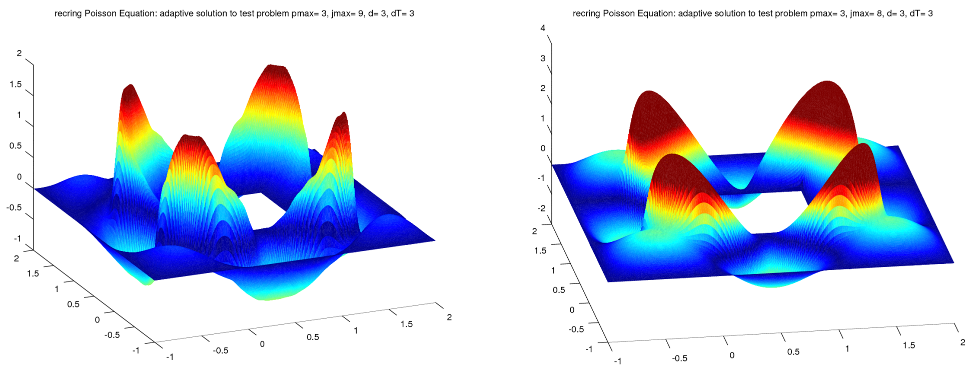

Figure 8.14: Approximate adaptive solution of the test problem on the ring-shaped domain after 10 (left) and 100 (right) iterations.

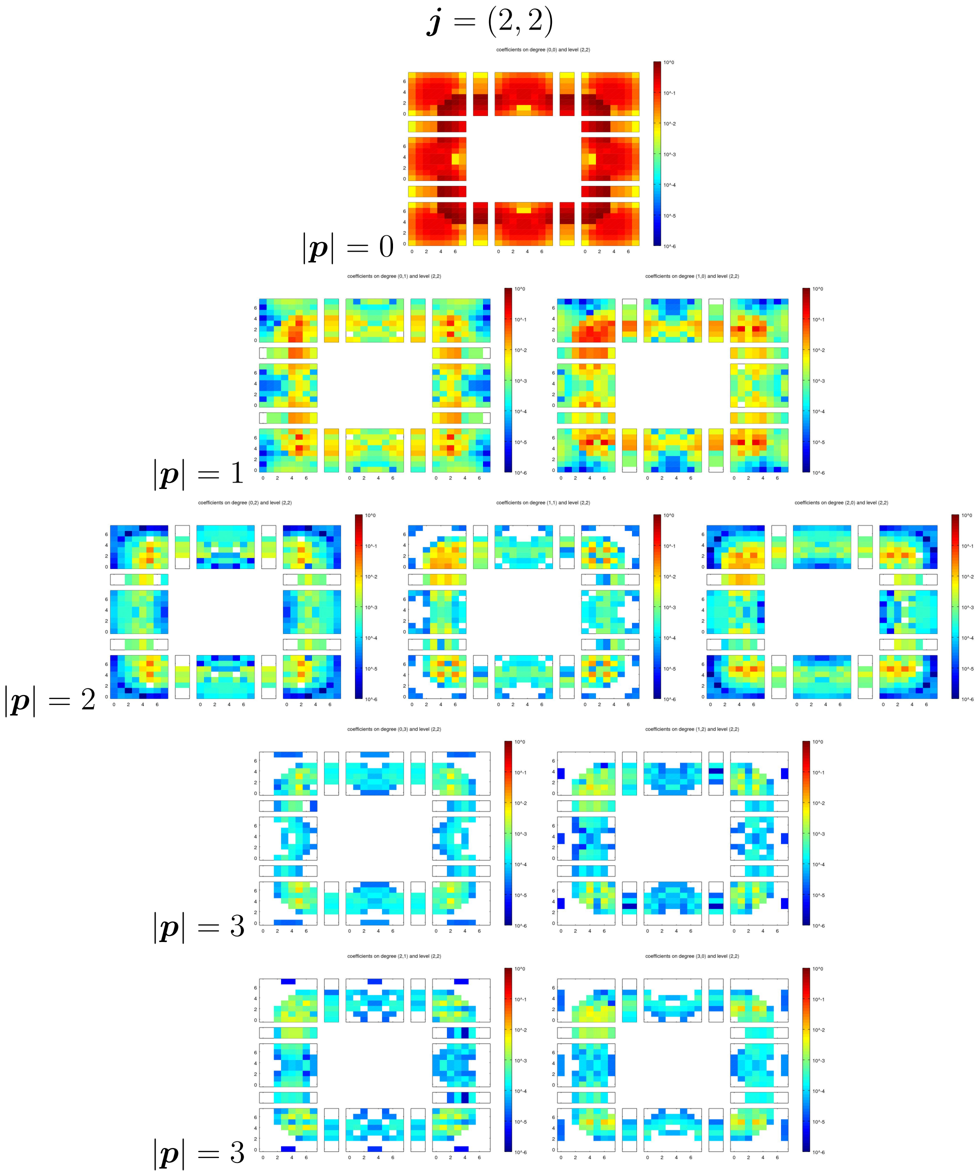

Figure 8.15: Coefficients of the approximate solution to the test problem on the ring-shaped domain for the quark level $\boldsymbol{j} = (2,2)$.

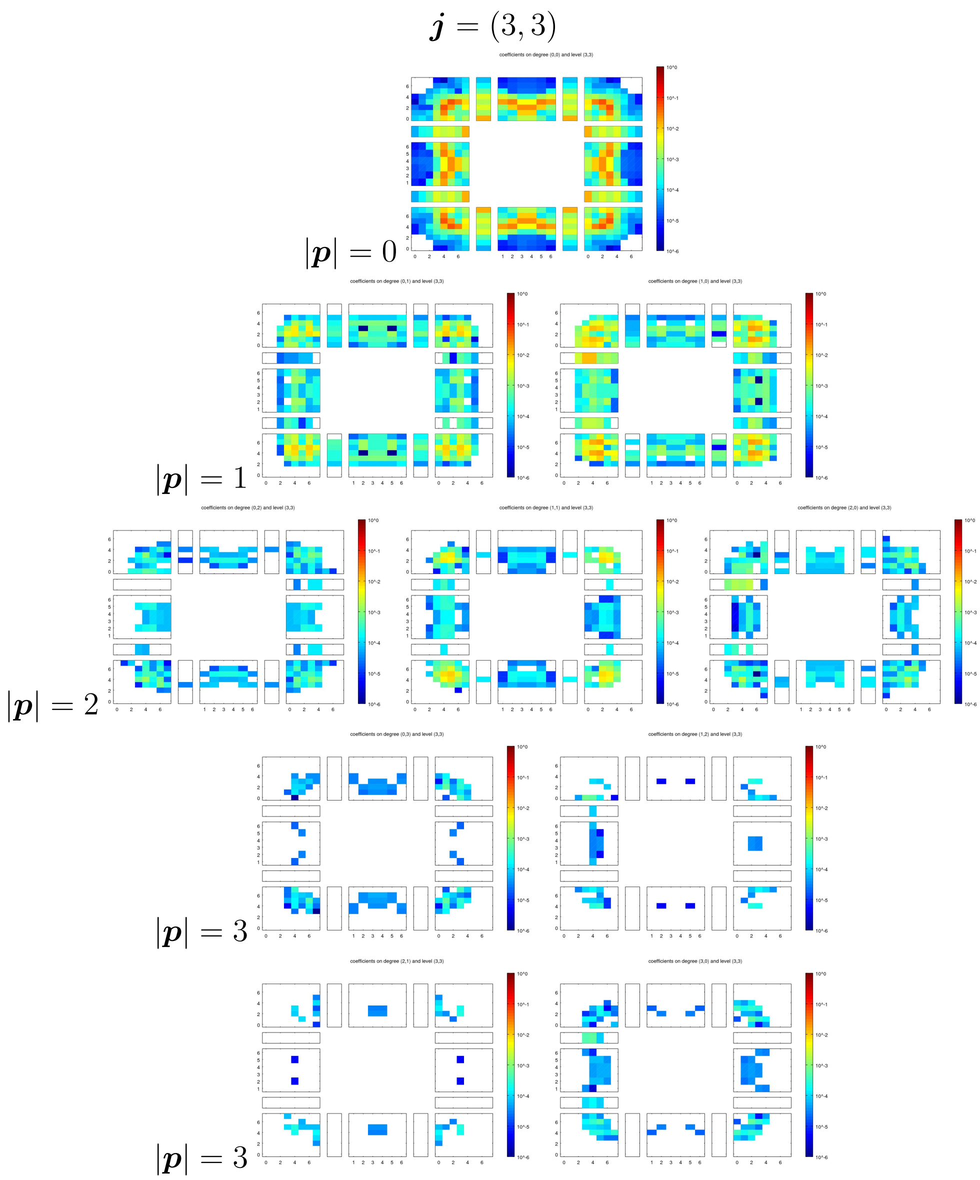

Figure 8.16: Coefficients of the approximate solution to the test problem on the ring-shaped domain for the lowest quarklet level $\boldsymbol{j} = (3,3)$.

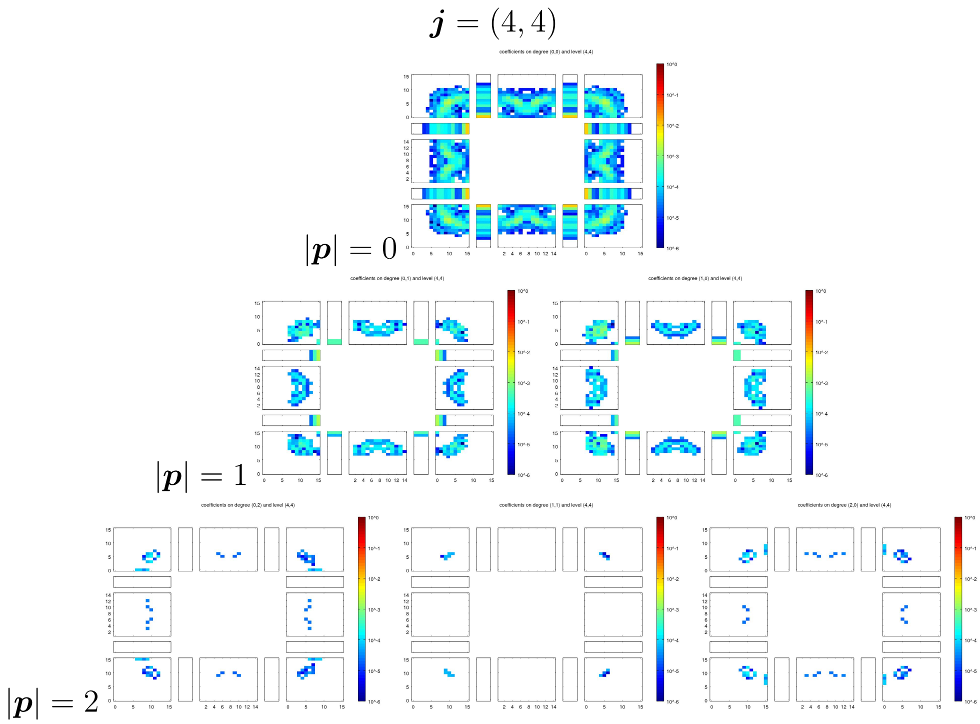

Figure 8.17: Coefficients of the approximate solution to the test problem on the ring-shaped domain for the quarklet level $\boldsymbol{j} = (4, 4)$.

Slit domain

As the third and last two-dimensional test example we consider the Poisson equation on the slit domain $\Omega = (-1, 1)^2 \backslash \{0\} \times (0, 1)$. In distinction to the first two multivariate test domains, the slit domain is not Lipschitz. Although we expected throughout this thesis Ω to be a Lipschitz domain it is possible to define Sobolev spaces also for more general domains, see [1] for details. However, the whole theory for the solution of PDEs is based on the Lipschitz property of the domain. For example, the weak formulation of a PDE, partial integration or the trace operator, cf. (1.3.12) rely on the Lipschitz property. Nevertheless, the practical results we display confirm that Algorithm 1 converges also in this particular case.

We decompose Ω into four non-overlapping subcubes $\Omega_0^{(0)} = (-1, 0) \times (0, 1)$, $\Omega_1^{(0)} = (-1, 0) \times (-1, 0)$, $\Omega_2^{(0)} = (0, 1) \times (-1, 0)$ and $\Omega_3^{(0)} = (0, 1) \times (0, 1)$, cf. Figure 8.18, and choose the quarklet frames on the respective subcubes as

$$\begin{aligned}
\mathbf{\Psi}_0 &= \mathbf{\Psi}_{H^s_{\Gamma_{\boldsymbol{\sigma}_0}}(\square)}\left(\cdot + \begin{pmatrix}1\\0\end{pmatrix}\right), & \boldsymbol{\sigma}_0 &= (1,1)\times(0,1),\\
\mathbf{\Psi}_1 &= \mathbf{\Psi}_{H^s_{\Gamma_{\boldsymbol{\sigma}_1}}(\square)}\left(\cdot + \begin{pmatrix}1\\1\end{pmatrix}\right), & \boldsymbol{\sigma}_1 &= (1,1)\times(1,1),\\
\mathbf{\Psi}_2 &= \mathbf{\Psi}_{H^s_{\Gamma_{\boldsymbol{\sigma}_2}}(\square)}\left(\cdot + \begin{pmatrix}0\\1\end{pmatrix}\right), & \boldsymbol{\sigma}_2 &= (0,1)\times(1,1),\\
\mathbf{\Psi}_3 &= \mathbf{\Psi}_{H^s_{\Gamma_{\boldsymbol{\sigma}_3}}(\square)}, & \boldsymbol{\sigma}_3 &= (1,1)\times(0,1).
\end{aligned}$$

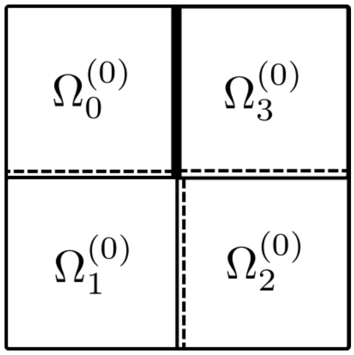

Figure 8.18: The initial decomposition of the slit domain into subcubes.

Thereupon, we extend the frames $\mathbf{\Psi}_0$, $\mathbf{\Psi}_2$ and $\mathbf{\Psi}_3$ as depicted in Figure 8.19. In this case, the order of extensions is relevant to ensure that the conditions $(\mathcal{D}_1)$-$(\mathcal{D}_5)$, cf. Subsection 6.2.1, are not violated.

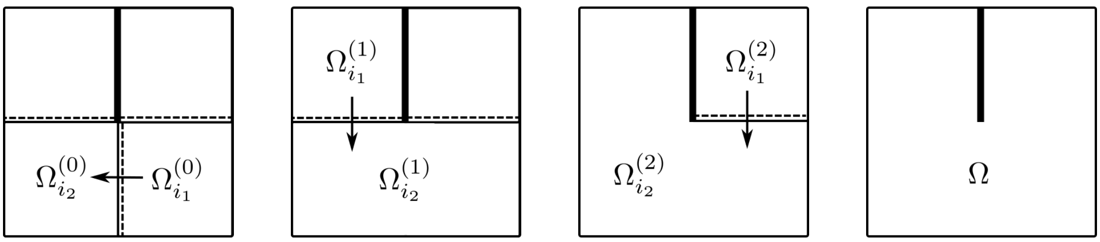

Figure 8.19: Successive extension process for the slit domain. Dotted lines indicate free boundary conditions, straight lines indicate zero boundary conditions.

Again, the test example is constructed in a way that the exact solution of the Poisson equation is given by a sum of $\sin(2\pi x)\sin(2\pi y)$, $(x, y) \in \Omega$ and a singularity function. In this particular case, the latter differs in comparison the other two-dimensional test examples due to the reason that it does not surround a reentrant corner but a slit. Hence, we have the representation

$$\mathcal{S}^*(r,\theta) := 5\zeta(r)r^{1/2}\sin\left(\frac{1}{2}\theta\right). \tag{8.2.3}$$

For more details about the parameters in (8.2.3), take a look at the explanations after (8.2.2).

The exact solution and right-hand side of the example are displayed in Figure 8.20. Once again, the algorithm exhibits the same convergence rates as in the previous test cases, see Figure 8.21.

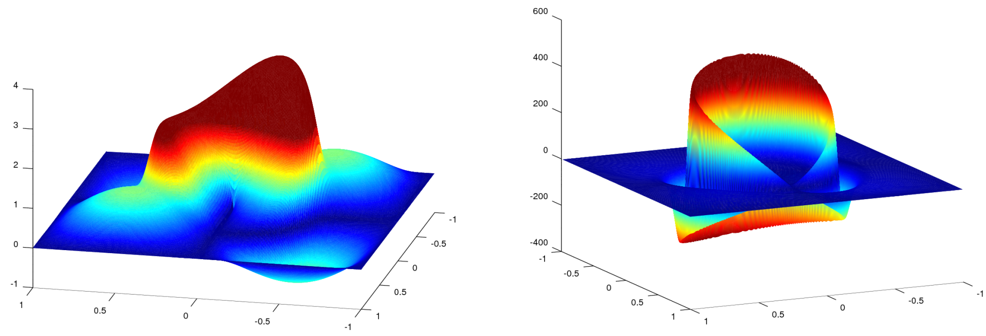

Figure 8.20: Exact solution (left) and right-hand side (right) of the test problem on the slit domain.

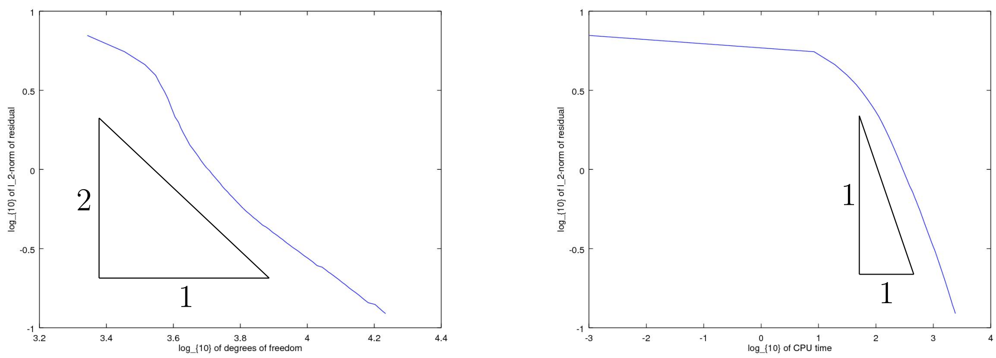

Figure 8.21: Adaptive error asymptotics for the test problem on the slit domain with respect to the amount of degrees of freedom (left) and the CPU time (right).

The qualitative properties of the exact solution is already notable for the 10th iterate, whereas after 100 iterations also the absolute accordance is evident, cf. Figure 8.22. The distribution of the quarklet coefficients is depicted in the Figures 8.23 - 8.25. In contrast to the previous examples in this section, there are active coefficients for $\boldsymbol{j} = (4, 4)$, $|\boldsymbol{p}| = 4$, cf. Figure 8.25. However, their amount and size in modulus are negligible. Apart from that, the same characteristics as in the earlier tests occur.

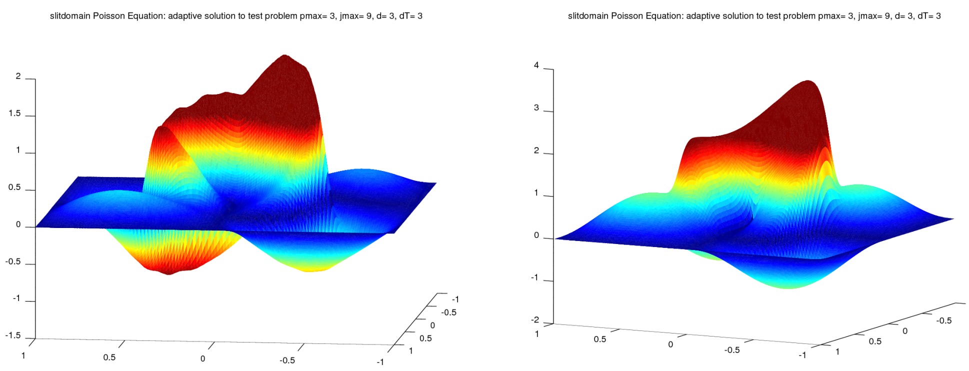

Figure 8.22: Approximate adaptive solution of the test problem on the slit domain after 10 (left) and 100 (right) iterations.

Let us shortly summarize the numerical results. In every single example, the convergence of the adaptive quarklet scheme has been confirmed. Although we do not have any theoretical results about the convergence rates to expect so far, we have observed a very consistent behaviour in all test cases. Especially in the two-dimensional experiments, we have been able to outperform classical adaptive wavelet algorithms, which justifies the application of quarklets in adaptive schemes and gives hope that in the future, also theoretically, higher convergence rates for specific test problems can be confirmed. The multivariate experiments have also exhibited that there is still some work to do to close the gap between the convergence rates with respect to the CPU time and the degrees of freedom. In general, this should be possible. Qualitatively, the share of high polynomial quarklets in the expansions of the iterative solutions has been clearly recognizable, which indicates that they also have contributed to the good quantitative performance of the adaptive quarklet scheme.

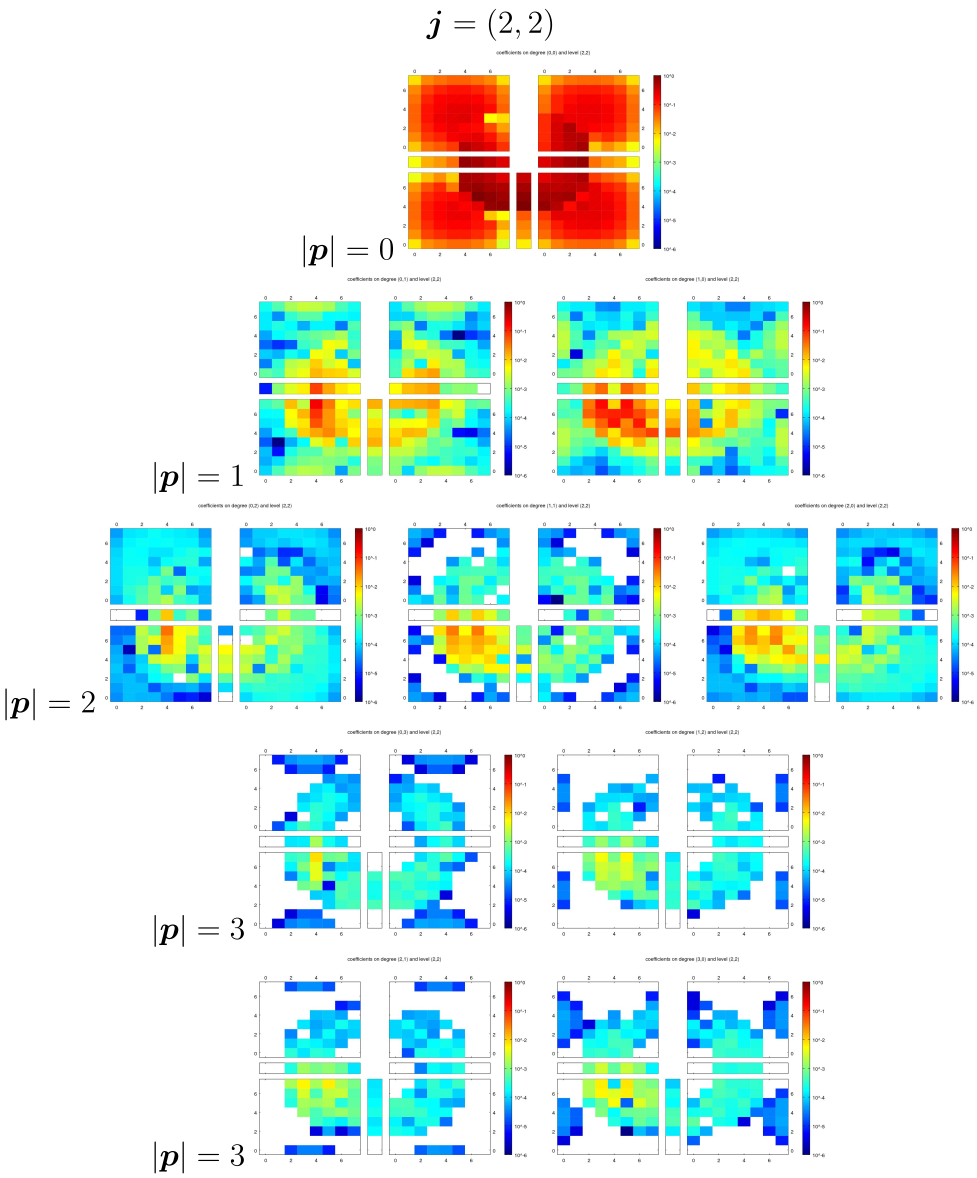

Figure 8.23: Coefficients of the approximate solution to the test problem on the slit domain for the quark level $\boldsymbol{j} = (2, 2)$.

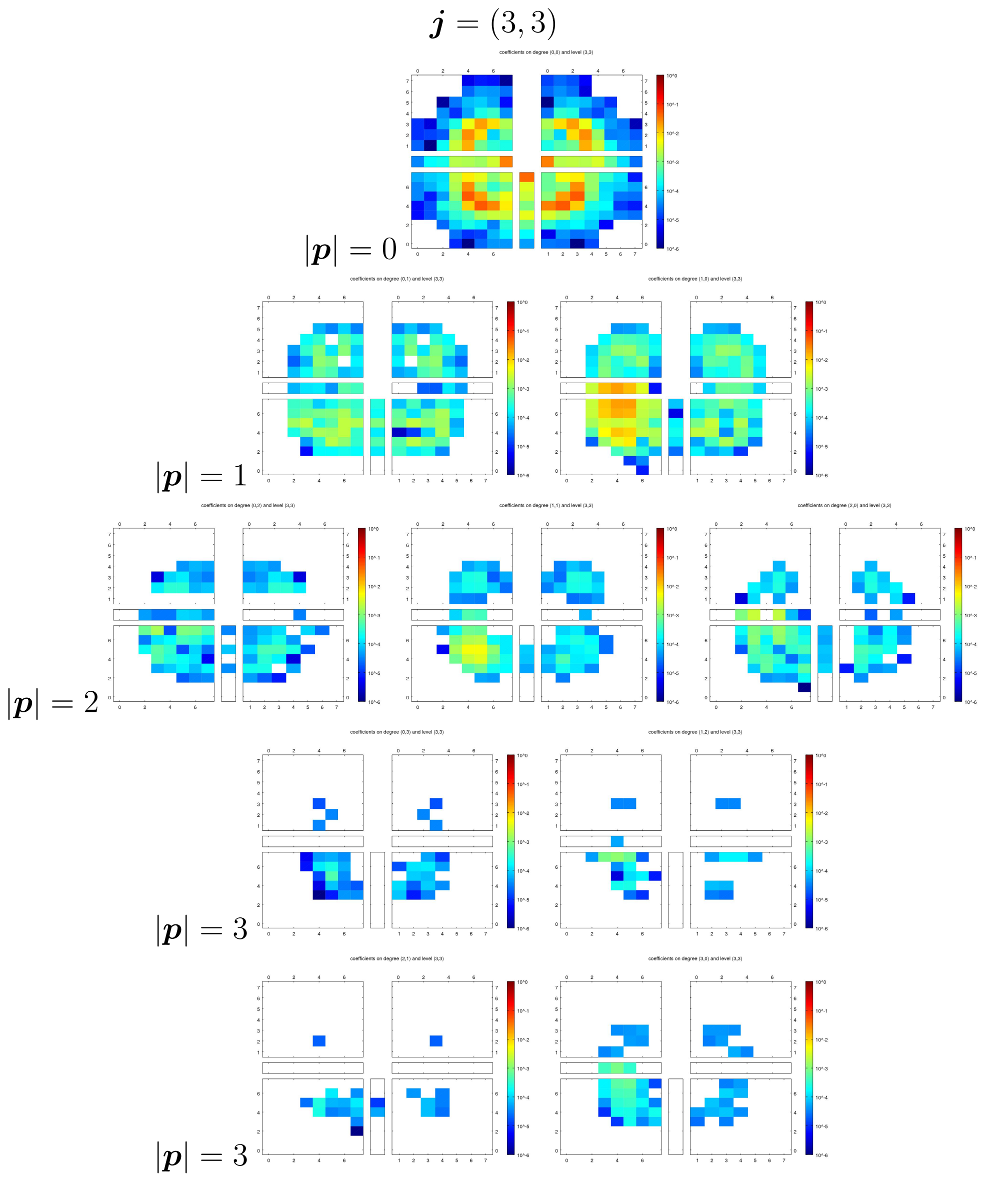

Figure 8.24: Coefficients of the approximate solution to the test problem on the slit domain for the lowest quarklet level $\boldsymbol{j} = (3, 3)$.

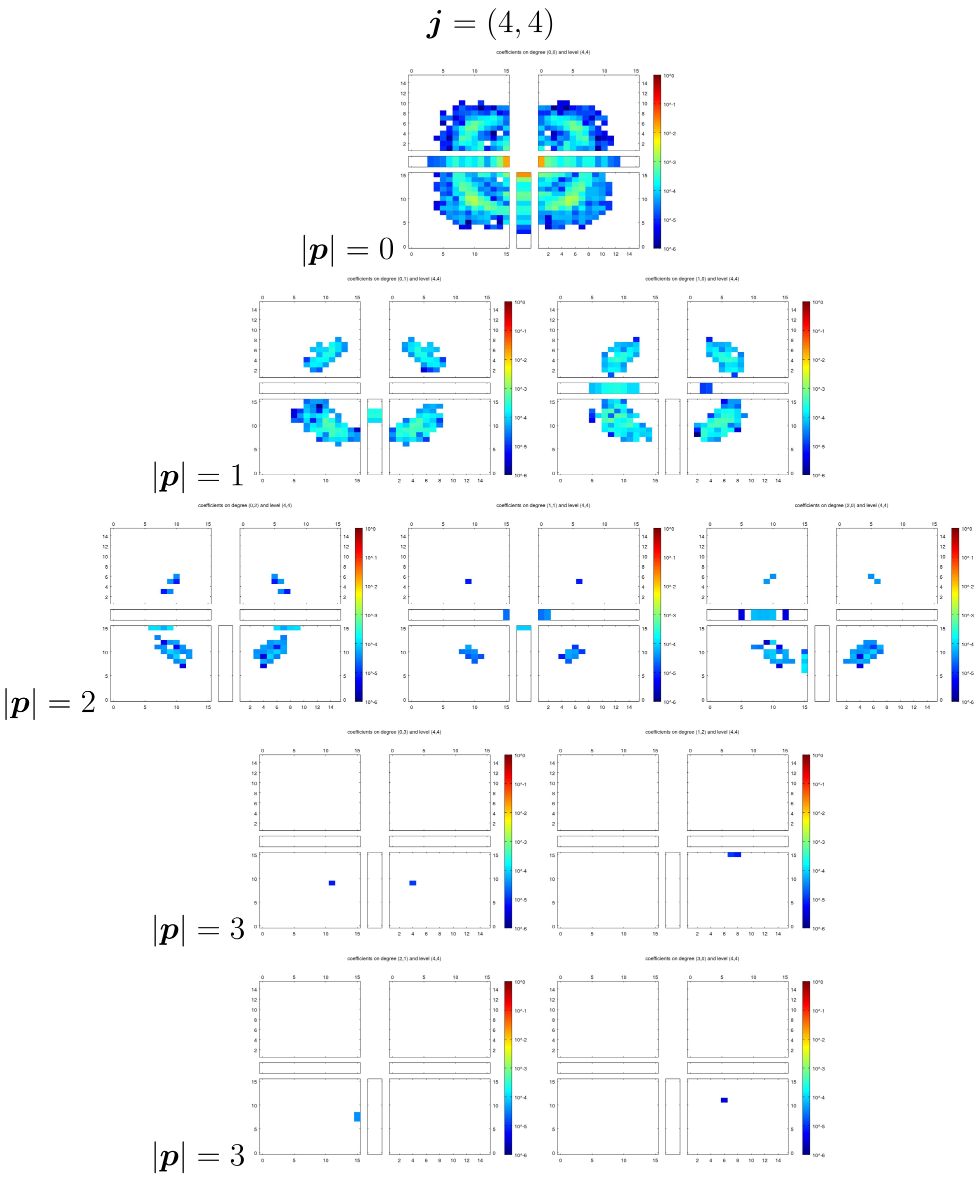

Figure 8.25: Coefficients of the approximate solution to the test problem on the slit domain for the quarklet level $\boldsymbol{j} = (4, 4)$.

Conclusion and Outlook

In this thesis, we have developed quarklets, a new class of smooth, localized functions with vanishing moments. We have shown how to derive quarklet frames for Lebesgue and Sobolev spaces in multiple spatial dimensions and applied them to solve elliptic operator equations. For that purpose, we have collected all the building blocks for a well-known adaptive frame scheme and combined the latter with quarklet frames. Several tests have been made to study the convergence of the scheme.

Let us now discuss the results in more detail. In particular, we want to take a look at the tasks (T1) to (T3) as outlined in the introduction and see how they have been addressed. The chapters 4 to 6 have been devoted to task (T1), the construction of quarklet frames in one and in multiple spatial dimensions. The main results in one dimensions are the theorems 4.15 and 5.9, which state the frame property for Sobolev spaces on the real line and the unit interval, respectively. In Chapter 6, Theorem 6.20 has given a very satisfying result regarding multidimensional quarklet frames. It states that quarklets lead to Gelfand frames for the Gelfand triple $(H_0^s(\Omega), L_2(\Omega), H^{-s}(\Omega))$ for a certain range $s \in \mathbb{R}_+$, on very general bounded domains $\Omega \in \mathbb{R}^d$. In addition, the construction could be executed in a way that all quarklets have a certain amount of vanishing moments. Hence, task (T1) can be considered accomplished.

In Chapter 7, we have turned our attention to task (T2), the design of a convergent adaptive quarklet frame scheme for linear elliptic operator equations. Proceeding from an inexact adaptive Richardson iteration, we have shown that all the building blocks could be adjusted to work with quarklets. The main challenge has been the verification of the compressibility of the stiffness matrix in quarklet coordinates. In Theorem 7.12, we have provided a compression result for the stiffness matrix of the Poisson equation in multiple dimensions. As this is a prototypical example, the proof concepts for the compression for other linear elliptic equations can be expected to be very similar. Due to the tensor approach, the proven compression rates are independent of the spatial dimension. Under certain assumptions, for instance, that the optimal convergence rate is not higher than the compression rate, we have even been able to prove the asymptotical optimality of the scheme. Up to now, we have not used second compression ideas (cf. [98]), i.e., the exploitation of the piecewise polynomial structure of the quarklets to achieve higher compression rates. However, all in all, we have largely solved task (T2).

The last remaining task, (T3), the practical implementation and numerical experiments in one and two spatial dimensions of the adaptive quarklet frame scheme, has been addressed in Chapter 8. The adaptive solution of the Poisson equation has been tested on several domains. Special attention has been paid to domains with reentrant corners, as they lead to solutions with singularities. The convergence of the scheme could be verified for every single test problem. Moreover, the convergence rates with respect to the degrees of freedom have appeared to be very promising as they outperformed convergence rates of other well-known adaptive wavelet schemes. The slower convergence with respect to the runtime possibly is a consequence of the not yet optimal compression rate. There seems to be room for improvement in this field. For future works, numerical tests with linear elliptic operator equations other than the Poisson equation could be of interest. Furthermore, it would be interesting to see how the scheme reacts on various kinds of right-hand-sides. Nevertheless, task (T3) has been solved as well.

As the quarklet approach is still in its infancy, there are plenty of goals to be achieved in future work. An almost completely uninvestigated field is the approximation theory with respect to quarklets. By this we mean how well certain functions can be approximated with linear combinations of quarklets. The only thing in this context we know by now is the obvious fact that the best N-term quarklet approximation to any function is at least as good as the best N-term wavelet approximation of the underlying wavelet basis. A very interesting question is if there are functions for which quarklets outperform wavelets in the sense of a better N-term approximation. And if so, can these functions be characterized in terms of belonging to a certain function space? Is it possible to show an equivalence between an approximation space and a function space as it is the case for wavelets and Besov spaces?

Since adaptive quarklet schemes are a kind of *hp*-method, there is some hope that it is possible to show exponential convergences rates for the best N-term approximation for certain functions. This would definitely mean a breakthrough of the quarklet method. If exponential convergence can be shown, the next challenging task will be the design of an adaptive scheme that realizes this particular rate. As we have seen that the convergence rate of an adaptive scheme is governed by the compression rate of the respective stiffness matrix, the verification of exponential compression rates is at the heart of a successive algorithm. To this end, it might be necessary to modify the construction of the quarklets. The vanishing moment property of the quarklets play a crucial role in this context. For the current construction, we were able to prove that the quarklets maintain the vanishing moment property of the underlying wavelets. In comparison to the quarkonial approach, cf. [50], [104], this can be considered as a huge development. However, in order to really achieve exponential convergence results, we do not get around the fact that we need an increasing amount of vanishing moments for increasing polynomial degrees of the quarklets. One way out of this, which deserves closer attention, could be to use more involved polynomials for the enrichment of the wavelets. A promising approach seems to be the application of orthogonal polynomials in this context. In fact, it is relatively easy to show that we get functions with an increasing amount of vanishing moments with this attempt. However, there is still a lot of analysis to be done to examine if it is able to construct frames for Sobolev spaces with these kind of functions.

Another idea to get rapidly converging algorithms is to use some kind of regularization in the iteration process. This approach, which is widely used in the compressed sensing area, penalizes approximations with a large ℓ_1-norm. It is well-known that in this way the algorithm is forced to produce a sparse approximation of the solution. Examples where this approach was used to find sparse atomic decompositions in terms of localized functions as wavelets and shearlets can be found, e.g., in [48], [59]. Since quarklet frames are highly redundant, regularization could really make sense in this context. The fewer amount of entries in the stiffness matrix, which need to be calculated during the successive iteration steps, could save a lot of computing time. However, the verification of certain convergence rates for adaptive algorithms with regularization has not been considered by now such that there is some analysis to be done first.

In [20], it was shown that the tensor approach with non-overlapping domain decompositions leads to convergence rates which are independent of the spatial dimension. Based on the latter fact, the application of quarklets in operator equations in multiple spatial dimensions seems to be potentially fruitful and should be considered in the future. Moreover, quarklets can be applied to other types of operator equations, e.g., of parabolic type. Considering the latter, one has to ensure that quarklets lead to frames for Sobolev spaces of negative order. Such results are available for wavelets and in principle a transfer to quarklets should be feasible.

Let us finish by saying that quarklets seem to have a lot of future potential and it is going to be exciting to see where the journey will take them.

Appendix

In the appendix, we provide the proof of Proposition 5.2. In order to do this, we start with an auxiliary result about the extremal points of boundary quarks.

Lemma A.1. *Let $1 \leq k \leq m-1$ and $\varphi_{p,0,-m+k}$ a left boundary quark. For every $p \geq (m-1)(k-1)$, the unique extremal point of $\varphi_{p,0,-m+k}$ is located at*

$$\hat{x} = \frac{kp}{p+m-1}. \tag{A.1}$$

Proof. Let $x \in \mathbb{R}$. At first, we have a look at the leftmost quark, i.e., $k=1$:

$$\varphi_{p,0,-m+1}(x) = \left(\frac{x}{-m+1+m}\right)^p B^m_{0,-m+1}(x) = x^p B^m_{0,-m+1}(x).$$

Using the differentiation rules and the recursive form of the B-splines, cf. [94, Thm. 4.15, 4.16], we derive

$$\begin{aligned}
\varphi'_{p,0,-m+1}(x) &= px^{p-1}B^m_{0,-m+1}(x) + x^p B^{m\prime}_{0,-m+1}(x)\\
&= px^{p-1}B^m_{0,-m+1}(x) - x^p(m-1)B^{m-1}_{0,-m+2}(x)\\
&= px^{p-1}\frac{t_1 - x}{t_1 - t_{-m+2}}B^{m-1}_{0,-m+2}(x) - x^p(m-1)B^{m-1}_{0,-m+2}(x)\\
&= x^{p-1}\left(p(1-x) - x(m-1)\right)B^{m-1}_{0,-m+2}(x).
\end{aligned}$$

We obtain the critical points $x=0$, where the B-spline and also the quark is zero, and $\hat{x} = \frac{p}{p+m-1}$, where $|\varphi_{p,0,-m+1}|$ attends its maximum. Now, assume $m \geq 3$, $k \geq 2$ and $\varphi_{p,0,-m+k}$ to be the k-th left boundary quark.:

$$\varphi_{p,0,-m+k}(x) = \left(\frac{x}{-m+k+m}\right)^p B^m_{0,-m+k}(x) = k^{-p}x^p B^m_{0,-m+k}(x).$$

The support of $\varphi_{p,0,-m+k}$ is the interval $[0,k]$. In the first step, we show that $\varphi_{p,0,-m+k}$ is monotonically increasing on $[0,k-1]$. For the first derivative, we estimate

$$\begin{aligned}
\varphi'_{p,0,-m+k}(x) &= k^{-p}px^{p-1}B^m_{0,-m+k}(x) + k^{-p}x^p B^{m\prime}_{0,-m+k}(x)\\
&= k^{-p}x^{p-1}\left(pB^m_{0,-m+k}(x) + xB^{m\prime}_{0,-m+k}(x)\right)\\
&\geq k^{-p}x^{p-1}\left(pB^m_{0,-m+k}(x) - \left|xB^{m\prime}_{0,-m+k}(x)\right|\right).
\end{aligned}$$

Again, we use the differentiation rules and recursion to derive

$$\begin{aligned}\varphi'_{p,0,-m+k}(x) &\geq k^{-p}x^{p-1}\left(pB^m_{0,-m+k}(x) - \left|x(m-1)\left(\frac{B^{m-1}_{0,-m+k}(x)}{k-1} - \frac{B^{m-1}_{0,-m+k+1}(x)}{k}\right)\right|\right)\\ &\geq k^{-p}x^{p-1}\left(pB^m_{0,-m+k}(x) - x(m-1)\left(\frac{B^{m-1}_{0,-m+k}(x)}{k-1} + \frac{B^{m-1}_{0,-m+k+1}(x)}{k}\right)\right).\end{aligned}$$

For $x \in [0,1]$, it holds $k - x \geq x$, which yields

$$\begin{aligned}\varphi'_{p,0,-m+k}(x) &\geq k^{-p}x^{p-1}\\ &\cdot\left(pB^m_{0,-m+k}(x) - (m-1)\left(\frac{x}{k-1}B^{m-1}_{0,-m+k}(x) + \frac{k-x}{k}B^{m-1}_{0,-m+k+1}(x)\right)\right)\\ &= k^{-p}x^{p-1}\left(pB^m_{0,-m+k}(x) - (m-1)B^m_{0,-m+k}(x)\right)\\ &= k^{-p}x^{p-1}\left(p-(m-1)\right)B^m_{0,-m+k}(x).\end{aligned}$$

Hence, the derivative is non-negative on $[0,1]$ if $p \geq m-1$. For $x \in [1, k-1]$, it trivially holds $x \geq 1$ and $k - x \geq 1$. It follows

$$\begin{aligned}\varphi'_{p,0,-m+k}(x) &\geq k^{-p}x^{p-1}\left(pB^m_{0,-m+k}(x) - x\left|B^{m\prime}_{0,-m+k}(x)\right|\right)\\ &\geq k^{-p}x^{p-1}\left(pB^m_{0,-m+k}(x) - (k-1)\left|B^{m\prime}_{0,-m+k}(x)\right|\right)\\ &= k^{-p}x^{p-1}\\ &\cdot\left(pB^m_{0,-m+k}(x) - (k-1)\left|(m-1)\left(\frac{B^{m-1}_{0,-m+k}(x)}{k-1} - \frac{B^{m-1}_{0,-m+k+1}(x)}{k}\right)\right|\right).\end{aligned}$$

By the above considerations, we can further estimate

$$\begin{aligned}&\varphi'_{p,0,-m+k}(x)\\ &\geq k^{-p}x^{p-1}\left(pB^m_{0,-m+k}(x) - (k-1)(m-1)\left|\frac{1}{k-1}B^{m-1}_{0,-m+k}(x) - \frac{1}{k}B^{m-1}_{0,-m+k+1}(x)\right|\right)\\ &\geq k^{-p}x^{p-1}\left(pB^m_{0,-m+k}(x) - (k-1)(m-1)\left(\frac{1}{k-1}B^{m-1}_{0,-m+k}(x) + \frac{1}{k}B^{m-1}_{0,-m+k+1}(x)\right)\right)\\ &\geq k^{-p}x^{p-1}\\ &\cdot\left(pB^m_{0,-m+k}(x) - (k-1)(m-1)\left(\frac{x}{k-1}B^{m-1}_{0,-m+k}(x) + \frac{k-x}{k}B^{m-1}_{0,-m+k+1}(x)\right)\right).\end{aligned}$$

By the recursive relation of B-splines, we get

$$\begin{aligned}\varphi'_{p,0,-m+k}(x) &\geq k^{-p}x^{p-1}\left(pB^m_{0,-m+k}(x) - (k-1)(m-1)B^m_{0,-m+k}(x)\right)\\ &= k^{-p}x^{p-1}\left(p-(k-1)(m-1)\right)B^m_{0,-m+k}(x).\end{aligned}$$

Finally, we can conclude that for $p \geq (m-1)(k-1)$ the derivative is non-negative on $[1, k-1]$. So all extremal points are located in $[k-1, k]$, where we can compute an explicit form of $\varphi_{p,0,-m+k}$. To do this, we first compute the explicit form of $B^d_{0,-m+k}$. By definition and the recursion for divided differences, we get:

$$\begin{aligned}
B^m_{0,-m+k}(x) &= (t^0_k - t^0_{-m+k})\,(\cdot - x)^{m-1}_+[t^0_{-m+k},\dots,t^0_k] \\
&= \frac{k}{k}\Big((\cdot - x)^{m-1}_+[t^0_{-m+k+1},\dots,t^0_k] - (\cdot - x)^{m-1}_+[t^0_{-m+k},\dots,t^0_{k-1}]\Big) \\
&= (\cdot - x)^{m-1}_+[t^0_{-m+k+1},\dots,t^0_k].
\end{aligned}$$

The latter divided difference vanishes because of $x \geq k-1$. On the interval $[0,k-1]$, the truncated polynomial $(\cdot - x)^{m-1}_+$ is zero. Hence, all of the coefficients of the interpolating polynomial are zero. By repeating this argument $(m-k-1)$ times, we obtain

$$B^m_{0,-m+k}(x) = k^{-1-(m-k-1)}(\cdot - x)^{m-1}_+[1,\dots,k].$$

Further $(k-1)$-times iteration gives

$$B^m_{0,-m+k}(x) = k^{-m+k}\frac{1}{(k-1)!}(\cdot - x)^{m-1}_+[k].$$

We end up with

$$B^d_{0,-m+k}|_{[k-1,k]}(x) = k^{-m+k}\frac{1}{(k-1)!}(k-x)^{m-1}.$$

With this representation, we compute the derivative $\varphi'_{p,0,-m+k}$ on $[k-1,k]$:

$$\begin{aligned}
\varphi'_{p,0,-m+k}(x) &= k^{-p}px^{p-1}B^m_{0,-m+k}(x) + k^{-p}x^pB^{m\prime}_{0,-m+k}(x) \\
&= k^{-p}x^{p-1} \\
&\cdot\left(pk^{-m+k}\frac{1}{(k-1)!}(k-x)^{m-1} - xk^{-m+k}\frac{1}{(k-1)!}(m-1)(k-x)^{m-2}\right) \\
&= k^{-p-m+k}x^{p-1}\frac{1}{(k-1)!}\Big((k-x)^{m-2}(p(k-x) - x(m-1)\Big).
\end{aligned}$$

We obtain the critical points $x=0$, $x=k$, where $B^m_{0,-m+k}$ is zero, and $\hat{x} = \frac{kp}{p+m-1}$, where $|\varphi_{p,0,-m+k}|$ attains its maximum. Indeed, $\hat{x}$ lies in $[k-1,k]$ because, on the one hand, we have

$$\hat{x} = \frac{kp}{p+d-1} \leq \frac{kp+k(d-1)}{p+d-1} = \frac{k(p+d-1)}{p+d-1} = k.$$

On the other hand, it holds true that

$$k-1 = k - \frac{k(d-1)}{k(d-1)} = k - \frac{k(d-1)}{(d-1)(k-1)+d-1} \leq k - \frac{k(d-1)}{p+d-1} = \frac{kp}{p+d-1} = \hat{x},$$

and so the claim is proved. □

With Lemma A.1 at hand, we are able to prove Proposition 5.2.

Proposition A.2. *Let $k = 1, \dots, m-1$. For every left boundary quark $\varphi_{p,0,-m+k}$, and $1 \le q \le \infty$, there exist constants $c = c(m,k,q) > 0$, $C = C(m,k,q) > 0$, such that for all $p \ge (m-1)(k-1)$:*

$$c(p+1)^{-(m-1+1/q)} \le ||\varphi_{p,0,-m+k}||_{L_q(\mathbb{R})} \le C(p+1)^{-(m-1+1/q)}. \tag{A.2}$$

Proof. We show (A.2) for the extremal cases $q \in \{1, \infty\}$ and conclude by Hölder's inequality. To derive the upper bound for $q = 1$, we use an integration formula for general B-splines and functions $f \in C^m([t^0_{-m+k}, t^0_k])$, cf. [94, Thm. 4.23]:

$$\int_{t^0_{-m+k}}^{t^0_k} B^m_{0,-m+k}(x) f^{(m)}(x) \,\mathrm{d}x = (t^0_k - t^0_{-m+k})(m-1)! f[t^0_{-m+k}, \dots, t^0_k].$$

Choosing $f(x) := x^{p+m} \frac{1}{(p+m)\cdots(p+1)}$, we obtain

$$\begin{aligned} ||\varphi_{p,0,-m+k}||_{L_1(\mathbb{R})} &= \left(\frac{1}{k}\right)^p \int_{t^0_{-m+k}}^{t^0_k} B^m_{0,-m+k}(x) x^p \,\mathrm{d}x \\ &= \left(\frac{1}{k}\right)^p (k-0)(m-1)!\,(\cdot)^{p+m}[t^0_{-m+k}, \dots, t^0_k] \frac{1}{(p+m)\cdots(p+1)} \\ &\le \left(\frac{1}{k}\right)^{p-1} (m-1)!\,(\cdot)^{p+m}[t^0_{-m+k}, \dots, t^0_k](p+1)^{-m}. \end{aligned}$$

To estimate the divided difference, we use a Leibniz rule with $x^{p+m} = x x^{p+m-1}$, cf. [94, Thm. 2.52]:

$$(\cdot)^{p+m}[t^0_{-m+k}, \dots, t^0_k] = \sum_{i=-k+m}^{k} (\cdot)^1[t^0_{-m+k}, \dots, t^0_i]\,(\cdot)^{p+m-1}[t^0_i, \dots, t^0_k].$$

For the first order polynomial, there remains just one non-trivial summand:

$$\begin{aligned} (\cdot)^{p+m}[t^0_{-m+k}, \dots, t^0_k] &= (\cdot)^1[t^0_{-m+k}]\,(\cdot)^{p+m-1}[t^0_{-m+k}, \dots, t^0_k] \\ &\quad + (\cdot)^1[t^0_{-m+k}, t^0_{-m+k+1}]\,(\cdot)^{p+m-1}[t^0_{-m+k+1}, \dots, t^0_k] \\ &= (\cdot)^{p+m-1}[t^0_{-m+k+1}, \dots, t^0_k]. \end{aligned}$$

Repeating this argument $(d-k)$ times, we get

$$(\cdot)^{p+m}[t_{-m+k}, \dots, t_k] = (\cdot)^{p+k}[t^0_0, \dots, t^0_k].$$

By eliminating the leading zeros, we get equidistant knots and can replace the divided difference by a forward difference, cf. [94, Theorem. 2.57]:

$$\begin{aligned}(\cdot)^{p+m}[t^0_{-m+k}, ..., t^0_k] &= \frac{1}{k!}(\Delta^k(\cdot)^{p+k})(0)\\ &= \frac{1}{k!}\sum_{j=0}^{k}\binom{k}{j}(-1)^{k-j}j^{p+k}\\ &\le \frac{1}{k!}k^p\sum_{j=0}^{k}\binom{k}{j}j^k.\end{aligned}$$

Finally, we get the upper estimate with $C(m,k) = \frac{(m-1)!}{(k-1)!}\sum_{j=0}^{k}\binom{k}{j}j^k$:

$$||\varphi_{p,0,-m+k}||_{L_1(\mathbb{R})} \le C(p+1)^{-m}. \tag{A.3}$$

Now let $q = \infty$. We directly compute

$$\begin{aligned}||\varphi_{p,0,-m+k}||_{L_\infty(\mathbb{R})} &= |\varphi_{p,0,-m+k}(\hat{x})| = k^{-p}\hat{x}^p k^{-m+k}\frac{1}{(k-1)!}(k-\hat{x})^{m-1}\\ &= \frac{k^{-m+k}}{(k-1)!}\left(\frac{p}{p+m-1}\right)^p\left(\frac{k(m-1)}{p+m-1}\right)^{m-1}.\end{aligned}$$

We get the upper estimate with some constant $C(m,k) = \frac{k^{-m+k}}{(k-1)!}(k(m-1))^{m-1}$:

$$||\varphi_{p,0,-m+k}||_{L_\infty(\mathbb{R})} \le C(p+1)^{-(m-1)}. \tag{A.4}$$

For $1 < q < \infty$, an application of Hölder's inequality and (A.3), (A.4) yield

$$\begin{aligned}||\varphi_{p,0,-m+k}||^q_{L_q(\mathbb{R})} &\le ||\varphi_{p,0,-m+k}||^{1/q}_{L_1(\mathbb{R})}||\varphi_{p,0,-m+k}||^{1-1/q}_{L_\infty(\mathbb{R})}\\ &\le C(p+1)^{-(m-1-1/q)},\end{aligned}$$

which proves the upper estimate. Now, we turn over to the lower estimate. Let $q = \infty$. From our previous calculations we directly get the lower estimate with $c(m,k) = \tilde{c}e^{1-m}\frac{k^{-m+k}}{(k-1)!}(k(m-1))^{m-1}$, where $\tilde{c} > 0$ just depends on m:

$$c(p+1)^{-(m-1)} \le ||\varphi_{p,0,-m+k}||_{L_\infty(\mathbb{R})}. \tag{A.5}$$

It remains to show the lower estimate for $q \in \mathbb{N}$. By an elementary estimate, we get

$$\begin{aligned}||\varphi_{p,0,-m+k}||^q_{L_q(\mathbb{R})} &= \int_0^k |\varphi_{p,0,-m+k}(x)|^q \,\mathrm{d}x \ge \int_{k-1}^k |\varphi_{p,0,-m+k}(x)|^q \,\mathrm{d}x\\ &= \int_{k-1}^k \left(\frac{x}{k}\right)^{pq}\left(B^m_{0,-m+k}(x)\right)^q \,\mathrm{d}x\\ &= \int_{k-1}^k \left(\frac{x}{k}\right)^{pq}\left(k^{-m+k}\frac{1}{(k-1)!}(k-x)^{m-1}\right)^q \,\mathrm{d}x.\end{aligned}$$

Substitution leads to

$$\begin{aligned}||\varphi_{p,0,-m+k}||^q_{L_q(\mathbb{R})} &\geq \frac{1}{((k-1)!)^q} k^{(-m+k)q} \int\limits_{k-1}^{k} \left(\frac{x}{k}\right)^{pq} (k-x)^{(m-1)q} \,\mathrm{d}x \\ &= \frac{1}{((k-1)!)^q} k^{(-m+k)q} \int\limits_0^1 \left(\frac{k-y}{k}\right)^{pq} y^{(m-1)q} \,\mathrm{d}y \\ &\geq \frac{1}{((k-1)!)^q} k^{(-m+k)q} \int\limits_0^1 (1-y)^{pq} \, y^{(m-1)q} \,\mathrm{d}y.\end{aligned}$$

By $m(q-1)$-times partial integration, we obtain

$$\begin{aligned}\int\limits_0^1 (1-y)^{pq} y^{(m-1)q} \,\mathrm{d}y &= \frac{(m-1)q}{pq+1} \int\limits_0^1 (1-y)^{pq+1} y^{(m-1)q-1} \,\mathrm{d}y \\ &= \frac{((m-1)q)!}{(pq+1)(pq+2)\cdots(pq+mq-q)} \frac{1}{pq+mq-q+1}.\end{aligned}$$

We go on estimating by

$$\int\limits_0^1 (1-y)^{pq} y^{(m-1)q} \,\mathrm{d}y \geq \frac{((m-1)q)!}{(\tilde{c}(p+1))^{mq-q+1}},$$

where $\tilde{c} > 0$ just depends on m and q. Finally, we get the lower estimate with $c(m,k,q) = \frac{k^{-m+k}}{(k-1)!} \left(\frac{((m-1)q)!}{\tilde{c}}\right)^{1/q}$:

$$||\varphi_{p,0,-m+k}||_{L_q(\mathbb{R})} \geq c(p+1)^{-(m-1+1/q)}. \tag{A.6}$$

For $1 < q < \infty$, we again use Hölder's inequality. First, let $1 < q \leq 2$. Then, by (A.5),(A.6) it follows

$$\begin{aligned}||\varphi_{p,0,-m+k}||^q_{L_q(\mathbb{R})} &\geq ||\varphi_{p,0,-m+k}||^{2/q}_{L_2(\mathbb{R})} ||\varphi_{p,0,-m+k}||^{1-2/q}_{L_\infty(\mathbb{R})} \\ &\geq c(p+1)^{-(m-1-1/q)}.\end{aligned}$$

For $2 \leq q < \infty$, using (A.6) we have

$$\begin{aligned}||\varphi_{p,0,-m+k}||^q_{L_q(\mathbb{R})} &\geq ||\varphi_{p,0,-m+k}||^{2-2/q}_{L_2(\mathbb{R})} ||\varphi_{p,0,-m+k}||^{2/q-1}_{L_1(\mathbb{R})} \\ &\geq c(p+1)^{-(m-1-1/q)},\end{aligned}$$

which completes the proof. □

List of Figures

Bibliography

[1] R. A. Adams and J. F. F. Fournier, *Sobolev Spaces*, Pure Appl. Math., vol. 140, Academic Press, Amsterdam, 2003.

[2] I. Babuska and W. Gui, *The h, p and h-p versions of the finite element method in 1 dimension. Part II. The error analysis of the h- and h-p versions.*, Numerische Mathematik **49** (1986), no. 4, 613–658.

[3] ———, *The h, p and h-p versions of the finite element method in 1 dimension. part III. The adaptive h-p version.*, Numerische Mathematik **49** (1986), no. 4, 659–683.

[4] I. Babuška and E. Rank, *An expert system for the optimal mesh design in the hp-version of the finite element method*, Int. J. Numer. Meth. Engng. **24** (1987), 2087–2106.

[5] I. Babuška and B. Szabó, *Finite Element Analysis*, John Wiley and Sons, 1991.

[6] I. Babuška, B. Szabó, and I. N. Katz, *The p-version of the finite element method*, SIAM Journal of Numerical Analysis **18** (1981), 515–545.

[7] I. Babuška, O. C. Zienkiewicz, J. Gago, and E. R. de A. Oliviera, *Accuracy Estimates and Adaptive Refinements in Finite Element Computations*, John Wiley and Sons, 1986.

[8] A. Barinka, *Fast Computation Tools for Adaptive Wavelet Schemes*, Ph.D. thesis, RWTH Aachen, 2005.

[9] A. Barinka, T. Barsch, P. Charton, A. Cohen, S. Dahlke, W. Dahmen, and K. Urban, *Adaptive wavelet schemes for elliptic problems: Implementation and numerical experiments*, SIAM J. Sci. Comput. **23** (2001), no. 3, 910–939.

[10] J. Bergh and J. Löfström, *Interpolation Spaces*, Grundlehren der mathematischen Wissenschaften, vol. 223, Springer-Verlag, 1976.

[11] P. Binev, *Instance optimality for hp-type approximation*, Oberwolfach reports, vol. 39, 2013, pp. 14–16.

[12] ———, *Tree approximation for hp-adaptivity*, Preprint 2015:07, University of South Carolina, 2015.

[13] P. Binev, W. Dahmen, and R. DeVore, *Adaptive finite element methods with convergence rates*, Numer. Math. **97** (2004), no. 2, 219–268.

[14] C. Canuto, R.H. Nochetto, R. Stevenson, and M. Verani, *High-order adaptive Galerkin methods*, Spectral and High Order Methods for Partial Differential

Equations ICOSAHOM 2014 (M. Berzins, J.S. Hesthaven, and R.M. Kirby, eds.), Lect. Notes Comput. Sci. Eng., no. 106, Springer, 2014, pp. 51–72.

[15] ______, *Convergence and optimality of hp-AFEM*, Numer. Math. **135** (2017), no. 4, 1073–1119.

[16] ______, *On p-robust saturation for hp-AFEM*, Comput. Math. Appl. **73** (2017), no. 9, 2004–2022.

[17] C. Canuto, A. Tabacco, and K. Urban, *The wavelet element method, part I: Construction and analysis*, Appl. Comput. Harmon. Anal. **6** (1999), 1–52.

[18] ______, *The wavelet element method, part II: Realization and additional features in 2D and 3D*, Appl. Comput. Harmon. Anal. **8** (2000), 123–165.

[19] J. M. Carnicer, W. Dahmen, and J. M. Peña, *Local decomposition of refinable spaces and wavelets*, Appl. Comput. Harmon. Anal. **3** (1996), 127–153.

[20] N. Chegini, S. Dahlke, U. Friedrich, and R. Stevenson, *Piecewise tensor product wavelet bases by extensions and approximation rates*, Found. Comput. Math. **82** (2013), 2157–2190.

[21] N. Chegini and R. Stevenson, *The adaptive tensor product wavelet scheme: Sparse matrices and the application to singularly perturbed problems*, IMA J. Numer. Anal **32** (2012), no. 1, 75–104.

[22] E. W. Cheney and W. A. Light, *Approximation Theory in Tensor Product Spaces*, Lecture Notes in Mathematics: Springer, Berlin, 1985.

[23] O. Christensen, *Frames and Bases, an Inroductory Course*, Birkhäuser, Basel, 2008.

[24] ______, *An Introduction to Frames and Riesz Bases*, Birkhäuser, Basel, 2016.

[25] C. K. Chui, *An Introduction to Wavelets*, Academic Press, Boston, 1992.

[26] C. K. Chui and J. Z. Wang, *A cardinal spline approach to wavelets*, Proc. Amer. Math. Soc. **113** (1991), 785–793.

[27] ______, *On compactly supported spline wavelets and the duality principle*, Trans. Amer. Math. Soc. **330** (1992), 903–915.

[28] ______, *An analysis of cardinal spline-wavelets*, J. Approx. Theory **72** (1993), 54–68.

[29] P. Cioica, S. Dahlke, and F. Eckhardt, *Besov regularity for the stationary Navier-Stokes equation on bounded Lipschitz domains*, Appl. Anal. **97** (2018), no. 3, 177–199.

[30] A. Cohen, *Numerical Analysis of Wavelet Methods*, Studies in Mathematics and its Applications, vol. 32, North-Holland, Amsterdam, 2003.

[31] A. Cohen, W. Dahmen, and R. DeVore, *Adaptive wavelet methods for elliptic operator equations – Convergence rates*, Math. Comput. **70** (2001), no. 233, 27–75.

[32] ———, *Adaptive wavelet methods II: Beyond the elliptic case*, Found. Comput. Math. **2** (2002), no. 3, 203–245.

[33] ———, *Adaptive wavelet schemes for nonlinear variational problems*, SIAM J. Numer. Anal. **41** (2003), no. 5, 1785–1823.

[34] A. Cohen, I. Daubechies, and J.-C. Feauveau, *Biorthogonal bases of compactly supported wavelets*, Commun. Pure Appl. Math. **45** (1992), 485–560.

[35] A. Cohen, I. Daubechies, and P. Vial, *Wavelets on the interval and fast wavelet transforms*, Appl. Comput. Harmon. Anal. **1** (1993), 54–81.

[36] S. Dahlke, *Besov regularity for elliptic boundary value problems on polygonal domains*, Applied Mathematics Letters **12** (1999), 31–38.

[37] S. Dahlke, W. Dahmen, and R. DeVore, *Nonlinear approximation and adaptive techniques for solving elliptic operator equations*, Multiscale Wavelet Methods for Partial Differential Equations (W. Dahmen, A. Kurdila, and P. Oswald, eds.), Academic Press, San Diego, 1997, pp. 237–283.

[38] S. Dahlke, W. Dahmen, R. Hochmuth, and R. Schneider, *Stable multiscale bases and local error estimation for elliptic problems*, Appl. Numer. Math. **23** (1997), no. 1, 21–48.

[39] S. Dahlke, W. Dahmen, and K. Urban, *Adaptive wavelet methods for saddle point problems — Optimal convergence rates*, SIAM J. Numer. Anal. **40** (2002), no. 4, 1230–1262.

[40] S. Dahlke, L. Diening, C. Hartmann, , B. Scharf, and M. Weimar, *Besov regularity of solutions to the p-Poisson equation*, Nonlinear Anal. **130** (2016), 298–329.

[41] S. Dahlke, M. Fornasier, M. Primbs, T. Raasch, and M. Werner, *Nonlinear and adaptive frame approximation schemes for elliptic PDEs: Theory and numerical experiments*, Numer. Methods Partial Differ. Equations **25** (2009), no. 6, 1366–1401.

[42] S. Dahlke, M. Fornasier, and T. Raasch, *Adaptive frame methods for elliptic operator equations*, Adv. Comput. Math. **27** (2007), no. 1, 27–63.

[43] S. Dahlke, M. Fornasier, T. Raasch, R. Stevenson, and M. Werner, *Adaptive frame methods for elliptic operator equations: The steepest descent approach*, IMA J. Numer. Anal. **27** (2007), no. 4, 717–740.

[44] S. Dahlke, U. Friedrich, P. Keding, T. Raasch, and A. Sieber, *Adaptive quarkonial domain decomposition methods for elliptic partial differential equations*, Bericht 2018–1, Philipps Universität Marburg, 2018.

[45] S. Dahlke, H. Harbrecht, M. Utzinger, and M. Weimar, *Adaptive wavelet BEM for boundary integral equations: Theory and numerical experiments*, Numerical Functional Analysis and Optimization **39** (2018), no. 2, 208–232.

[46] S. Dahlke, R. Hochmuth, and K. Urban, *Adaptive wavelet methods for saddle point problems*, M2AN Math. Model. Numer. Anal. **34** (2000), 1003–1022.

[47] S. Dahlke, P. Keding, and T. Raasch, *Quarkonial frames with compression properties*, Calcolo **54** (2017), no. 3, 823–855.

[48] S. Dahlke, G. Kutyniok, G. Steidl, and G. Teschke, *Shearlet coorbit spaces and associated Banach frames.*, Appl. Comput. Harmon. Anal. **27** (2009), no. 2, 195–214.

[49] S. Dahlke, D. Lellek, S. H. Lui, and R. Stevenson, *Adaptive wavelet Schwarz methods for the Navier-Stokes equation*, Numerical Functional Analysis and Optimization **37** (2016), no. 10, 1213–1234.

[50] S. Dahlke, P. Oswald, and T. Raasch, *A note on quarkonial systems and multilevel partition of unity methods*, Mathematische Nachrichten **286** (2013), 600–613.

[51] S. Dahlke and W. Sickel, *On Besov regularity of solutions to nonlinear elliptic partial differential equations.*, Rev. Mat. Complut. **26** (2013), no. 1, 115–145.

[52] W. Dahmen, *Stability of multiscale transformations*, J. Fourier Anal. Appl. **4** (1996), 341–362.

[53] ———, *Wavelet and multiscale methods for operator equations*, Acta Numerica **6** (1997), 55–228.

[54] W. Dahmen, A. Kunoth, and K. Urban, *Biorthogonal spline-wavelets on the interval — Stability and moment conditions*, Appl. Comput. Harmon. Anal. **6** (1999), 132–196.

[55] W. Dahmen and C. A. Micchelli, *Banded matrices with banded inverses, II: Locally finite decomposition of spline spaces*, Constr. Approx. **9** (1993), 263–281.

[56] W. Dahmen and R. Schneider, *Wavelets with complementary boundary conditions — Function spaces on the cube*, Result. Math. **34** (1998), no. 3–4, 255–293.

[57] ———, *Composite wavelet bases for operator equations*, Math. Comput. **68** (1999), 1533–1567.

[58] I. Daubechies, *Ten Lectures on Wavelets*, CBMS–NSF Regional Conference Series in Applied Math., vol. 61, SIAM, Philadelphia, 1992.

[59] I. Daubechies, M. Defrise, and C. De Mol, *An iterative thresholding algorithm for linear inverse problems with a sparsity constraint*, Commun. Pure Appl. Math. **57** (2004), no. 11, 1413–1457.

[60] M. Dauge, *Singularities of corner problems and problems of corner singularities*, ESAIM **6** (1999), 19–40.

[61] M. Dauge and R. Stevenson, *Sparse tensor product wavelet approximation of singular functions*, SIAM J. Math. Anal. **42** (2010), no. 5, 2203–2228.

[62] C. de Boor, *A Practical Guide to Splines*, revised ed., Applied Mathematical Sciences, vol. 27, Springer, New York, 2001.

[63] L. Demkowicz, O. Hardy, J. T. Oden, W. Rachowicz, and T. A. Westermann, *Toward a universal h-p adaptive finite element strategy*, Computer Methods in Applied Mechanics and Engineering **77** (1989), no. 1, 79–212.

[64] R. DeVore, *Nonlinear approximation*, Acta Numerica **7** (1998), 51–150.

[65] R. DeVore and G.G. Lorentz, *Constructive Approximation*, Springer, Berlin, 1998.

[66] T. J. Dijkema, *Adaptive Tensor Product Wavelet Methods for Solving PDEs*, Ph.D. thesis, Utrecht University, 2009.

[67] F. Eckhardt, *Besov regularity for the Stokes and the Navier-Stokes system in polyhedral domains*, ZAMM **95** (2015), no. 11, 1161–1173.

[68] T. Gantumur, *An optimal adaptive wavelet method for nonsymmetric and indefinite elliptic problems*, J. Comput. Appl. Math. **211** (2008), no. 1, 90–102.

[69] T. Gantumur, H. Harbrecht, and R. Stevenson, *An optimal adaptive wavelet method without coarsening of the iterands*, Math. Comput. **76** (2007), no. 258, 615–629.

[70] M. Griebel and P. Oswald, *Tensor product type subspace splittings and multilevel iterative methods for anisotropic problems*, ACMA **4** (1995), 171–206.

[71] P. Grisvard, *Singularities in Boundary Value Problems*, Research Notes in Applied Mathematics, Springer, Berlin-Heidelberg, 1992.

[72] ———, *Elliptic Problems in Nonsmooth Domains*, SIAM, New York, 2011.

[73] K.-H. Gröchenig, *Foundations of Time–Frequency Analysis*, Birkhäuser, Boston-Basel-Berlin, 2001.

[74] A. Haar, *Zur Theorie der orthogonalen Funktionensysteme*, Math. Annalen **69** (1910), 331–371.

[75] W. Hackbusch, *Elliptic Differential Equations: Theory and Numerical Treatment*, 2nd ed., Springer, Berlin, 2010.

[76] D. D. Haroske and H. Triebel, *Distributions, Sobolev Spaces, Elliptic Equations*, European Mathematical Society, Zürich, 2008.

[77] J. Kappei, *Adaptive Frame Methods for Nonlinear Elliptic Problems*, Ph.D. thesis, Philipps-Universität Marburg, 2011.

[78] V.I. Kolyada and A.K. Lerner, *On limiting embeddings of Besov spaces*, Stud. Math. **171** (2005), no. 1, 1–13.

[79] D. Lellek, *Adaptive Frame-Verfahren für elliptische Operatorgleichungen: Verfeinerungen und neue Strategien*, Diplomarbeit, Philipps-Universität Marburg, 2010.

[80] ———, *Adaptive Wavelet Schwarz Methods for Nonlinear Elliptic Partial Differential Equations*, Ph.D. thesis, Philipps-Universität Marburg, 2015.

[81] S. Mallat, *Multiresolution approximation and wavelet orthonormal bases of* $L_2(\mathbb{R}^d)$, Trans. Amer. Math. Soc. **315** (1989), 69–87.

[82] ______, *A Wavelet Tour of Signal Processing*, 2nd ed., Academic Press, San Diego, 1999.

[83] A. Metselaar, *Handling Wavelet Expansions in Numerical Analysis*, Ph.D. thesis, University of Twente, 2002.

[84] Y. Meyer, *Ondelettes et opérateurs I: Ondelettes*, Actualités Mathématiques, Hermann, Paris, 1990.

[85] ______, *Wavelets and Operators*, Cambridge Studies in Advanced Mathematics, vol. 37, Cambridge University Press, Cambridge, 1992.

[86] M. S. Mommer and R. Stevenson, *A goal-oriented adaptive finite element method with convergence rates.*, SIAM J. Numer. Anal. **47** (2009), no. 2, 861–886.

[87] P. Morin, R. H. Nochetto, and K. G. Siebert, *Convergence of adaptive finite element methods*, SIAM Rev. **44** (2002), no. 4, 631–658.

[88] R. H. Nochetto and A. Veeser, *Primer of adaptive finite element methods*, pp. 125–225, Springer, Berlin-Heidelberg, 2012.

[89] P. Oswald, *Stable space splittings and fusion frames*, Proceedings of SPIE San Diego Volume 7446: Wavelets XIII (V. Goyal, M. Papadakis, D. Van de Ville, eds.), 2009.

[90] M. Primbs, *Stabile biorthogonale Spline-Waveletbasen auf dem Intervall*, Ph.D. thesis, Universität Duisburg-Essen, 2006.

[91] M. Primbs, *New stable biorthogonal spline-wavelets on the interval*, Results in Mathematics **57** (2010), no. 1, 121–162.

[92] T. Raasch, *Adaptive Wavelet and Frame Schemes for Elliptic and Parabolic Equations*, Ph.D. thesis, Philipps-Universität Marburg, 2007.

[93] R. Schneider, *Multiskalen- und Wavelet-Matrixkompression. Analysisbasierte Methoden zur effizienten Lösung großer vollbesetzter Gleichungssysteme*, Habilitationsschrift, TH Darmstadt, 1995.

[94] L. L. Schumaker, *Spline functions : Basic theory*, Cambridge University Press, 2007.

[95] C. Schwab, *p- and hp-Finite Element Methods. Theory and Applications in Solid and Fluid Mechanics*, Clarendon Press, Oxford, 1998.

[96] A. Sieber, *Adaptive Quarklet-Verfahren für Dirichlet Randwertprobleme*, Master's thesis, Philipps-Universität Marburg, 2017.

[97] R. Stevenson, *Adaptive solution of operator equations using wavelet frames*, SIAM J. Numer. Anal. **41** (2003), no. 3, 1074–1100.

[98] ———, *On the compressibility of operators in wavelet coordinates*, SIAM J. Math. Anal. **35** (2004), no. 5, 1110–1132.

[99] ———, *Optimality of a standard adaptive finite element method.*, Found. Comput. Math. **7** (2007), no. 2, 245–269.

[100] ———, *Adaptive wavelet methods for solving operator equations: an overview.*, DeVore, Ronald (ed.) et al., Multiscale, nonlinear and adaptive approximation. Dedicated to Wolfgang Dahmen on the occasion of his 60th birthday. Springer, Berlin, 2009, pp. 543–597.

[101] R. Stevenson and M. Werner, *A multiplicative Schwarz adaptive wavelet method for elliptic boundary value problems*, Math. Comput. **78** (2009), no. 266, 619–644.

[102] J.-O. Strömberg, *A modified Franklin system and higher-order spline systems on $\mathbb{R}^d$ as unconditional bases for Hardy spaces*, Harmonic analysis, Conf. in Honor A. Zygmund, Chicago, 1983, pp. 475–494.

[103] H. Triebel, *Theory of Function Spaces*, Birkhäuser, Basel, 1983.

[104] ———, *Theory of Function Spaces II*, Birkhäuser, Basel, 1992.

[105] ———, *Fractals and Spectra related to Fourier Analysis and Function Spaces*, Birkhäuser, Basel, 1997.

[106] ———, *The Structure of Functions*, Birkhäuser, Basel, 2001.

[107] K. Urban, *Wavelets in Numerical Simulation. Problem Adapted Construction and Applications.*, Lecture Notes in Computational Science and Engineering, vol. 22, Springer, Berlin, 2002.

[108] R. Verfürth, *A Review of A Posteriori Eerror Estimation and Adaptive Mesh-Refinement Techniques*, Wiley-Teubner, Chichester, UK, 1996.

[109] M. Werner, *Adaptive Wavelet Frame Domain Decomposition Methods for Elliptic Operators*, Ph.D. thesis, Philipps-Universität Marburg, 2009.

[110] P. Wojtaszczyk, *A Mathematical Introduction to Wavelets*, Cambridge University Press, Cambridge, 1997.